Nitrogen Use Efficiency in *Brassica napus*

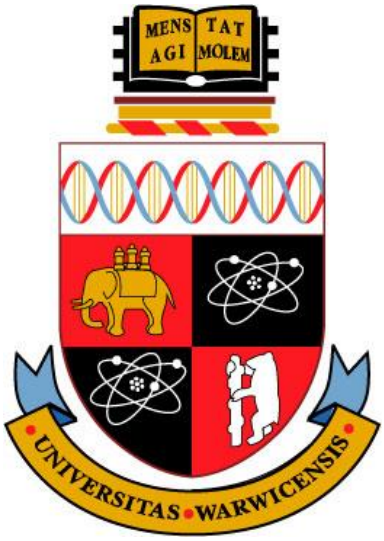

A thesis submitted for the Degree of

Doctor of Philosophy

by

Hussein Gherli, BSc, MSc

School of Life Sciences, University of Warwick
United Kingdom

July 2017

Table of Contents

List of Figures

List of Tables

List of Abbreviations

ABC	Ammonium bicarbonate
AFLP	Amplified fragment length polymorphism
AHDB	Agriculture and Horticulture Development Board
AMT	Ammonium transporter
ANOVA	Analysis of variance
APS	Adenosine phosphosulphate
ATP	Adenosine triphosphate
ATs	Multi-affinity transport system protein
βME	β-mercaptoethanol
CID	Collision-induced dissociation
cM	centiMorgan
CV	Coefficient of variation
DF	Deflowering - removal of flowers
DH	Doubled haploid
DNA	Deoxyribonucleic acid
DP	Depodding, removal of pods
DTT	Dithiothreitol
DW	Dried weight
EDTA	Ethylenediaminetetraacetic acid
EEA	European Environment Agency
ESI	Electrospray ionisation
FASP	Filter aided sample preparation
FDR	False discovery rate
FIA	Flow injection analysis
FLC	Flowering Locus C
FT	Flowering time
FW	Fresh weight
FWHM	Full width at half maximum height of peak
GAPDH	Glyceraldehyde-3-phospate dehydrogenase

GDH	Glutamate dehydrogenase
GHG	Greenhouse gas
GOGAT	Glutamate-oxoglutarate aminotransferase
GS	Growth stage
HAT	High affinity transport system protein
HPLC	High performance liquid chromatography
IAA	Iodoacetamide
ICP-OES	Inductively coupled plasma optical emission spectrometry
IM	Interval mapping
LAT	Low affinity transport system protein
LC	Liquid chromatography
LG	Linkage group
LOD	Limit of detection
LOD	Logarithm of odds (base 10)
LS	Lateral main stem
LSD	Least significant difference
MALDI	Matrix-assisted laser desorption ionisation
MFH	Main inflorescence height
Mha	Million hectares
MQM	Multiple QTL mapping
MS	Mass spectrometry
m/z	Mass to charge ratio
NB	Mumber of branches
NiR	Mitrite reductase
NIT2	Indole-3-acetonitrile nitrilase
NPB	Number of pods on the branches
NPMF	Number of pods on the MF
NR	Nitrate reductase
NRT	Nitrate transporter
NSP	Number of seed per pod
NUE	Nitrogen use efficiency
NVZ	Nitrate vulnerable zone

OAS	O-acetyl serine
OASTL	O-acetyl serine thiol lyase
OSR	Oilseed rape
PAGE	Polyacrylamide gel electrophoresis
PAPS	Phosphoadenosine phosphosulphate
PH	Plant height
Pht1	Phosphate transporter 1
Pi	Inorganic phosphate
PMF	Peptide mass fingerprint
PMSF	Phenyly-methyl-sulphonyl fluoride
pQTL	Protein QTL
Q	Quadrupole
QRT-PCR	Quantitative reverse transcription polymerase chain reaction
QTL	Quantitative trait locus/loci
r	Correlation coefficient
RFLP	Restriction fragment length polymorphism
RIL	Recombinant inbred line
RNA	Ribonucleic acid
SD	Standard deviation
SDS	Sodium dodecylsuphate
SEM	Standard error of the mean
SHB	Stem height to the first branch
SHP	Stem height to the first pod
SLAF	Specific locus amplified fragment
SNP	Single nucleotide polymorphism
TFA	trifluoroacetic acid
TNDH	Tapidor DH and Ningyou 7 mapping population
TNP	Total number of pods
TOF	Time of flight
VSP	vegetative storage protein
W	Shapiro-Wilks test for normality

Acknowledgments

Firstly, I would like to express my gratitude to both my supervisors, Dr Guy Barker and Dr Graham Teakle. I thank you for both for your advice, guidance and endless support you have given me throughout my PhD. I also thank you for your patience and encouragement during the preparation of this thesis.

Secondly, I would like to acknowledge the Syrian Government as my funding body as without their financial sponsorship, both my PhD and MSc degrees would not have been feasible. In the proteomics department of Life Sciences at the University of Warwick, I would also like to thank Dr Sue Slade, Dr Alex Jones and Dr Cleidiane Zampronio for their proteomics advice, support and numerous discussions. I also thank Matthew Mitchel for his advice, suggestions and discussions on mineral analysis. Thanks to all the members of the Barker research group. I enjoyed all the enjoyable times we shared both in the office or chatting away in the lab. I won't forget Lab C.46 anytime soon!

I would also like to thank all the friends I have been privileged to meet over my years at the University of Warwick. Being far from home is difficult during the stresses of the PhD, but the friends I made here made me realise I am not the only one suffering! Thanks for all your kind support and friendship both now and in the years to come.

Finally, I would like to thank my family back home. To my mother and father who have always encouraged my education. To my brothers and sisters, whom I have missed, I thank you for your reassurance and guidance when I needed it. Last but not least a very special thank you to my fiancée Jenny.

Declaration

I hereby declare that the work contained in this thesis is the original work of the author, except where specific reference is made to other sources, with the nature and extent of the author's contribution indicated (as appropriate) where work was based on collaborative research. The work was undertaken at the School of Life Sciences, University of Warwick between October 2011 and June 2016 and has not been submitted, in whole or in part, for any other degree, diploma or other qualification.

Hussein Gherli

July 2017

Abstract

The aim of this project was to enhance our knowledge of how nitrogen is transported and utilised within *Brassica napus* through the use of proteomics, phenotyping and genetic mapping. It highlights the importance of looking at all possible plant tissues to determine the mechanisms underlying seven macronutrients (N, P, Mg, Ca, S and Na) and five micronutrients (B, Cu, Fe, Mn and Zn) accumulation, since differences were observed between different tissues. Significant amount of mineral elements were found to remain in both the stem and roots at harvest, which in turn, highlights the inefficient mechanisms applied by some plants in the way they redistribute and utilise minerals such as N, P, K and S. Large genotypic differences in minerals concentration was found between different accessions of *B. napus,* ranging from 1.48-fold for Ca in the bottom of the stem to 20-fold for Na in top of the stem at maturity. Genotypes were identified that differed significantly from one another in relation to mineral concentration in the stem and root at harvest or in both. Differences were observed in the parents of the TN mapping population allowing a QTL approach to be adopted. Complex network of relationships between minerals were observed within and between tissues, and found to be dependent on the tissue and the growth stage. The strongest significant positive correlations ($0.91 > r > 0.71$) were between Ca/P, S/Ca and N/Ca in taproot, Ca/Mg in stem, and Mg/P and N/S in seed.

A significant source of N is that stored within proteins. Several proteins were shown to be accumulated significantly in the top part of the plants especially in the senescing silique walls and the stem adjacent to them. Putative vegetative storage proteins, VSPs, were identified in these tissues and we have suggested that these could be associated with N remobilisation. Development of a screening methodology based on these proteins through which quantitative analysis could be performed on a proteomic based experiment has been successfully developed which will allow the identification of QTLs associated with the N remobilisation and utilisation in plants.

These finding could assist plant breeders in developing varieties with enhanced mineral utilisation efficiency. Such developments will eventually lead to significant benefits both economically and socially worldwide as they should lead to increased abilities to enhance crop yields of oilseed rape while lowering the fertiliser requirements.

Chapter 1 General Introduction

1.1 Oilseed rape (*Brassica napus* L.)

Oilseed rape (OSR, *Brassica napus* L), also referred to as rapeseed, rape or canola, is an important crop in the Brassicaceae family (formally the Cruciferae family) it is considered a major source of both oil and fat for human nutrition. The meal remaining after oil extraction is also a valuable source of nutrients essential for animal feed. More than 173 million tons (Mt) of vegetable oil was produced worldwide in 2014, of which approximately 15 % was credited as rapeseed oil (FAOSTAT, 2017).

1.1.1 *B. napus* origin

Throughout the globe, four *Brassica* species are widely grown as oilseed crops. These include (1) *Brassica napus* (Swede rape), (2) *Brassica juncea* (Indian mustard), (3) *Brassica carinata* (Ethiopian mustard) and (4) *Brassica rapa* (Turnip rape). Three of these species are the result of hybridisations between the diploid species of *Brassica rapa* (A, n=10), *Brassica nigra* (B, n=8) and *Brassica oleracea* (C, n=9) (summarised in Figure 1.1). The resulting hybrids are amphidiploids and are *Brassica juncea* (AB, n=18), *Brassica napus* (AC, n=19) and *Brassica carinata* (BC, n=17) (Bunting, 1984; Downey and Rimmer, 1993). All these species are grown specifically for oilseed in different regions, they are then grouped using the terminology of oilseed rape or rapeseed.

Brassica juncea is widely cultivated in India and some regions of China. *Brassica carinata* is cultivated in North East of Africa. The winter varieties of *Brassica napus* are the most commonly cultivated oilseed crop in both Europe and China. Interestingly, cultivation of the summer varieties of *B.rapa* is limited to cooler climates such as Canada and northern regions of Europe. In contrast, the spring

varieties of *B. napus* are cultivated in both cold and warm climates. Specifically, spring oilseed rape is grown in Canada where the growing season is restricted to the summer due to the severe cold during the winter, whereas spring oilseed rape is grown in the milder winter season in Australia because the summer is too hot and dry.

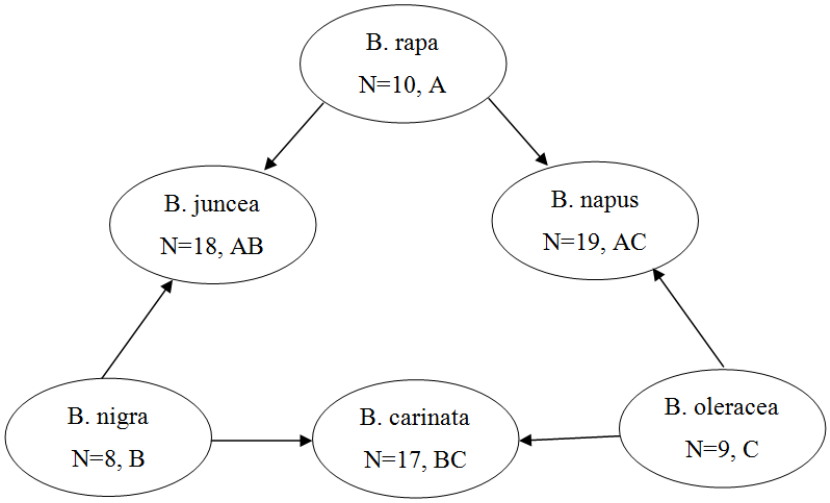

Figure 1.1 Genetic relationship between four *Brassica* species.

Brassica napus is an amphidiploid (AC, n =19) derived from the cross between *Brassica rapa* and *oleracea*.

1.1.2 Oilseed rape production area

The global area of OSR has increased from approximately 10 million hectares (Mha) in the 1960s to more than 35 Mha in 2014. Of the total production area worldwide 22.6 % was grown in Canada in 2014, followed by India 20 %, China 18.3 %, Australia 7.6 %, France 4.2 %, Germany 4 %, Poland 2.7 %, UK 1.9 % and USA 1.8 %, Table 1.1.

Table 1.1 Global production area of OSR during last two decades (ten thousands hectares).

	1980	1985	1990	1995	2000	2005	2010	2014
World	1099	1472	1761	2382	2584	2769	3223	3576
Canada	208	278	253	527	486	518	685	807
India	347	399	497	606	603	732	558	720
China	284	449	550	691	749	728	737	655
Australia	2	7	7	38	146	97	170	272
France	39	47	68	86	119	123	146	150
Germany	26	41	72	97	108	134	146	139
Poland	32	47	50	61	44	55	95	95
UK	9	30	39	44	40	59	64	68
USA	0	0	3	17	61	45	58	63

(FAOSTAT, 2017)

1.1.3 Oilseed rape yield trends

OSR yield is calculated on the weight of the seed at a standardised 90 g/kg (9 %) moisture content. The yield of OSR seeds varies considerably throughout the world. Since the year 2000, the average yield of OSR has been around 3 tonnes/hectares (t/ha) in the United Kingdom (Figure 1.2), France and Germany, 2.4 t/ha in Poland, and between 1.0 - 1.6 t/ha in Australia, Canada, India and China. The average yield increase per year has been relatively constant since the middle of sixties in countries such as China, India, Canada and Germany, with reported average annual increases in yield of 30, 15, 14 and 39 kg/ha respectively.

On the other hand, until the middle of 1980s countries such as Australia, UK, France, and Poland demonstrated an average annual increase in yield between 28 to 65 kg/ha. However, after 1985 there has been no significant increase in yield in these countries.

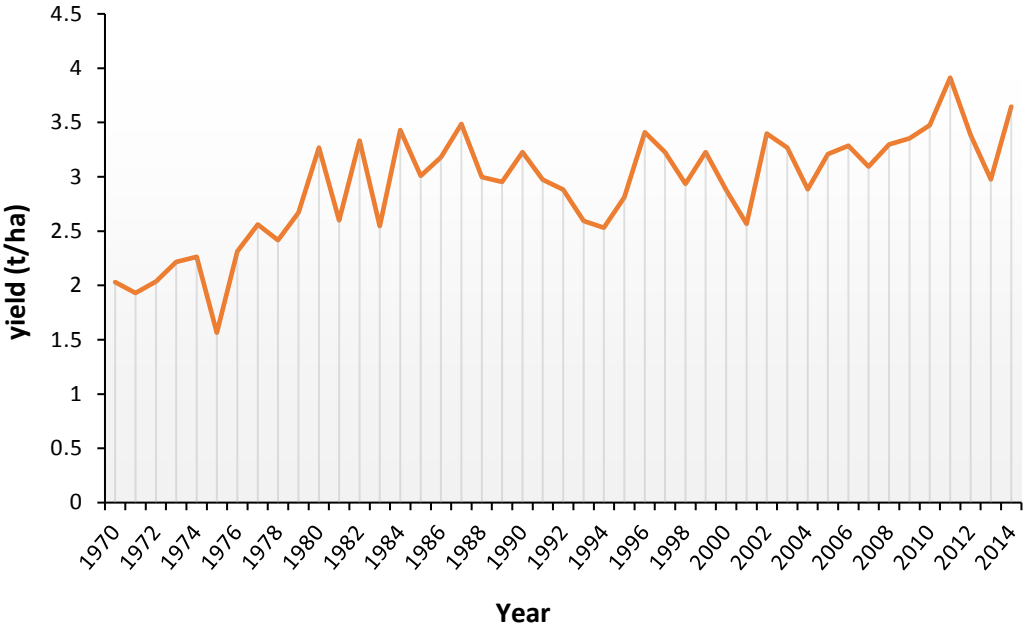

Figure 1.2 OSR yield trends in the UK.

Graph illustrates the steady incline in OSR yield observed over the last two decades (FAOSTAT, 2017).

Figure 1.2 shows that rapeseed yield in the UK has remained constant at 3-3.5 t/ha in recent years. However, the potential yield of rapeseed in the UK could be 6.5 t/ha , through production of *ca.* 130,000 seeds/m^2 and extending the seed filling to last for a period of 46 days (Berry and Spink, 2006). This lack of increase in the yield of OSR could be due to 1) lack of genetic improvement; 2) the potential yield has reached its limit and 3) alternations in crop management. The first two points are unlikely to be a contributing factor for the halt in OSR yield in the UK due to the introduction of new varieties of oilseed rape each year. The measured yield potential of the best varieties reported in the recent AHDB OSR Recommended List trial yields for the years 2013-2017 range from 4.6 - 6 t/ha (AHDB, 2017). When cultivated under optimum growing conditions, they caused a yearly increase of 62 kg/ha between the end of the 1970s to 2005. Rather, a combination of varying crop management practices has been attributed

to the stable OSR yield. These practices include 1) shorter rotations (faster rotations for more profitable outcome), 2) minimal cultivation (opposed to ploughing), 3) less sulphur and nitrogen fertiliser and 4) reduced fungicide application. Prior to 1970, the majority of plants received an adequate amount of sulphur dioxide (SO_2) from the environment. However, due to restrictions on highly reactive gaseous emissions, the emission of sulphur oxides was reported by the European Environment Agency (EEA) to decrease by *ca.* 74 % between the years 1990 to 2011 (EEA, 2016). Brassica crops require a minimum of *ca.* 30 kg of sulphur/ha for efficient plant metabolism, in part due to the requirement of the sulphur-containing glucosinolate compounds produced by brassicas. Despite the large decrease of sulphur, farmers appear slow to supplement their crops with the appropriate quantity of S fertiliser.

1.1.4 Importance of OSR crop

Approximately 85 % of the harvested seeds of OSR are subjected to oil extraction process which yields 40 – 45 % oil, rendering it an important cultivated crop in the UK. Rapeseed oil is rich source of unsaturated fatty acids of which oleic acid compose the majority with approximately 60 %, only olive oil having a greater proportion with about 73 %. After oil extraction, the remainder of the product, known as meal, contains high content of protein up to 32 – 40 %. Once subject to heat treatment to remove toxic components such as glucosinolates, this secondary product can be used as animal feed. A further 10 % of the oilseed rape yield is exported and the remaining yield (5 %) is used for other uses such as production of biodiesel (Twining and Clarke, 2009; Weightman *et al.*, 2010). The total production of rapeseed oil in 2014 worldwide is *ca.* 26 Mt and in Europe is *ca.* 10.8 Mt, which makes it the third most important source

of vegetable oil worldwide after oil palm (57.3 Mt) and soybean (45.7 Mt) and the second in Europe behind sunflower (12.1 Mt) (FAOSTAT, 2017).

In the UK, oilseed rape is grown as a valuable break crop within the cereal crop rotation. Additionally, OSR is grown as a catch crop due to its ability to absorb N from the soil during Autumn and early Winter. It is readily able to decrease the leaching of nitrate from the arable crops. Moreover, important ecologically, oilseed crop provides a nesting place for birds and a considerable amount of early pollen for bees (Weightman *et al.*, 2010). As with all higher plants, both the growth and production of OSR is dependent on the availability of several mineral elements. Therefore, a brief introduction to the essential elements and their available mineral forms that plants absorb from the soil solution is discussed below.

1.2 Minerals acquisition, transport and assimilation

Derived from both the air and water, plants uptake Carbon (C), Hydrogen (H_2) and Oxygen (O_2). However, to maintain their growth and complete their lifecycles, plants require an additional 14 essential mineral elements from the soil solution (Barker and Pilbeam, 2007; Kirkby, 2012). Depending on their relative concentrations in plant tissues, these minerals are categorised into two groups, macronutrients and micronutrients. Macronutrients are accumulated in relatively large quantities by plant tissues (up to 0.1% and more of the dried weight, DW) and include Nitrogen (N), Phosphorus (P), Potassium (K), Magnesium (Mg), Calcium (Ca) and Sulphur (S). In contrast, micronutrients, are absorbed at smaller concentrations in plant tissues (<0.01 % of the DW) and include Copper (Cu), Manganese (Mn), Boron (B), Iron (Fe) and

Zinc (Zn). In addition, plants obtain beneficial, but non-essential elements such as Sodium (Na) (Barker and Pilbeam, 2007; White and Brown, 2010).

Plant roots absorb P from the soil solution primarily in the form of dihydrogen phosphate ($H_2PO_4^-$) and secondarily in the form of hydrogen phosphate (HPO_4^{-2}) (Sánchez-Calderón *et al.*, 2010). S is primarily taken up in the form of sulphate (SO_4^2) from the soil solution, but plants can also absorb sulphur dioxide (SO_2) or hydrogen sulphide (H_2S) from the atmosphere (Leustek *et al.*, 2000). B is absorbed in the form of boric acid (H_3BO_3) from the soil solution (Miwa and Fujiwara, 2010); K, Mg, Ca, Mn and Na are taken up in the form of their ions K^+, Mg^{2+}, Ca^{2+}, Mn^{2+} and Na^+ from the soil solution (Barker and Pilbeam, 2007; Marschner, 2012b), while Cu, Fe and Zn are taken up either as their ions Cu^{2+}, Fe^{2+}/Fe^{3+} and Zn^{+2}, or as chelates (Barker and Pilbeam, 2007; Broadley *et al.*, 2007). Given the importance of P, K, S and N required for both plant growth and development, these primary mineral elements will be discussed in greater detail including nutrient uptake, distribution and assimilation within the plant.

1.2.1 Phosphorus

Phosphorus (P) is a major component of nucleic acids, phospholipids and adenosine triphosphate (ATP). Thereby, it is not surprising that after N, P is the second most important macronutrient for plant growth. During the vegetative growth of the plant, *ca.* 3 – 5 mg/g DW of P is required for optimum growth. P concentrations ≥ 10 mg/g DW can induce P plant toxicity (Lambers *et al.*, 2010).

Despite a high concentration of P in the soil, often it is present in unavailable forms for plant uptake. For example, approximately 20 – 80 % of P in the soil is present as

phytic acid (organic, unavailable form) (Richardson and Simpson, 2011). The remainder, P_i (inorganic, available form) is present which rarely exceeds 8 µM and can be significantly reduced (< 1 µM) in highly weathered, sandy and alkaline soils (Holford, 1997). Plants have developed efficient mechanisms to adequately regulate the concentration of P. Under reduced soil P concentrations, the plant initiates additional root growth and translocates stored P from older leaves and vacuoles. In contrast, when the concentration of P is too high, it is converted to phytic acid. The form of P_i can vary depending on the pH. At physiological pH of 7.2, it exists as the monovalent $H_2PO_4^-$ anion, whereas lowering the pH generates HPO_4^{2-} anions. Studies have shown that the greatest uptake of P_i occurred in the pH range of 5.0 – 6.0, suggesting $H_2PO_4^{2-}$ is the most dominate form of P_i uptake (Furihata *et al.*, 1992).

The P_i concentration in the apoplast is *ca.* 2 µM, in contrast to the cytosol where it is present in the range of 5 – 17 mM (Mimura, 2001). Overcoming this large electrochemical gradient ensures the transport of phosphate anions from the soil into the root cells requires a high-affinity and energy driven transport mechanism. This mechanism is mediated by a variety of proteins affiliated to Pht1 family of plant phosphate transporters. These proteins usually consist of 520 – 550 amino acids and are approximately 60 kDa in size. Northern blot analysis studies have identified that the *Pht1* genes are expressed in the roots (Nussaume *et al.*, 2011). Additionally, to maintain the cytosolic concentration of P_i, P_i stored in the vacuoles (which can reach up to 120 mM) can aid in maintaining the P_i homeostasis within plants. Transport of P_i via internal plant components occurs via the tonoplast membrane. However, this molecular mechanism of internal P_i transport has yet to be elucidated. Phosphate acts as a structural scaffold in nucleic acids, linking the ribonucleoside bases forming

macromolecules. The acidic nature of both deoxyribonucleic acid (DNA) and ribonucleic acid (RNA) can be attributed to phosphorus. Essential for the growth of new cells and transferring genetic information from one cell to another, an adequate supply of P is necessary (Sánchez-Calderón *et al.*, 2010; Hawkesford *et al.*, 2012).

1.2.2 Potassium

For optimal plant growth, plants require a large quantity of potassium ca. 20 – 50 g/kg in vegetative tissues. Potassium, a univalent cation (K^+), is the most prominent cation in the cytosol. The uptake of K^+ is highly selective and its transport is mediated by integral membrane ion transporter channels (White, 2012b, a). Potassium possesses various roles within the plant, depending on its location. For example, it maintains the pH between 7 and 8 in both the cytosol and chloroplasts due to its high concentration (100 – 200 mM), rendering an optimum pH for enzyme reactions. The roles of K^+ are influenced by its concentration. Abnormal influx or efflux of K^+ can inhibit these roles and lead to metabolic disorders within the plant. For example, enzymes are often dependent on or stimulated by K^+ (Suelter, 1970). For protein activation, the univalent cation induces a conformational change. This regularly occurs at a K^+ salt concentration of ca. 100 - 150 mM, which is the optimum pH of protein hydration. Moreover, this agrees with the K^+ concentration in the cytosol. Under temporary K-deficiency the cytosolic [K^+] is maintained whilst the vacuolar [K^+] is decreased (Walker *et al.*, 1996). However, plants subjected to prolonged K-deficiency; result in a decrease in the cytosolic [K^+]. The consequences of which result in inhibition of cytosolic enzymes and fluctuating cytosolic pH (Hawkesford *et al.*, 2012). Changes in enzyme activity directly affect the metabolite pattern, leading to increase in soluble carbohydrates, reduction in sugars and decrease in amino acids and pyruvate

(Armengaud *et al.*, 2009). K^+ is also a key component in activation of membrane-attached proton-pumping ATPases (White, 2012b). For protein synthesis, higher concentrations of K^+ are required in contrast to enzyme activation. It has been reported that K^+ participates in numerous steps of the translation process (Hawkesford *et al.*, 2012).

As already mentioned, the uptake and transport of K^+ throughout the plant is mediated by high-affinity ion channels. The varying arrangement of genes results in transporters possessing different properties, such as functional, regulatory and tissue-specificity. The K^+ ion channels (which are similar to Ca^{2+}) are voltage-regulated and control the influx and efflux of K^+. Additionally, these channels are influenced by the plant response to both biotic and abiotic stresses. In contrast to Ca^{2+}, K^+ behaves directly as solutes leading to changes in the osmotic and membrane potential (Lebaudy *et al.*, 2007).

Additional important functions of K^+, include its role in cell extension and osmoregulation. A large vacuole expanding to ca. 80 – 90 % of the total cell volume is formed during cell extension. Numerous factors are required for cell extension such as 1) loosening of the cell wall, 2) synthesis and deposit of new wall components and 3) solute accumulation to generate appropriate osmotic potential for turgor pressure. K^+ behaving as a solute is often attributed to cell extension in most plants. It acts by stabilising the pH in the cytoplasm and apoplast whilst increasing the osmotic potential in the vacuoles (Hawkesford *et al.*, 2012) Potassium is also involved in the role of loading of sucrose and transport of photosynthates from source to sink in phloem transport (White, 2012a). During this process K^+ maintains a high pH and contributes to the osmotic potential of the sieve tubes of the phloem. The role of K^+ was

established by work performed by Cakmak *et al.* (1994) on both K-sufficient and K-deficient plants.

Thereby, the array of processes in which K^+ is involved demonstrates it importance in plant metabolism. Inadequate K supply can influence the composition and nutritional benefits of plants and fruits. K deficiency can be easily observed by retarded plant growth.

1.2.3 Sulphur

Although atmospheric sulphur dioxide (SO_2) can be absorbed and used by the aerial components of plants (Eichert and Fernández, 2012), sulphate is the most abundant form absorbed by the roots (White, 2012a). Sulphate is present as the divalent anion (SO_4^{2-}) at physiological pH. Similar to N assimilation, SO_4^{2-} assimilation requires reduction prior to S incorporation into amino acids, proteins and enzymes. However, SO_4^{2-} can also be directly incorporated into organic structures such as sulpholipids (Hawkesford *et al.*, 2012).

The uptake of S from the soil into the root cells is mediated by high-affinity H^+ cell transporters. Whereas, low affinity transporters are responsible for the transport of S across the plasma membrane, in the remobilisation and storage from the vacuoles across the tonoplast. Interestingly, the transport and reduction of S in chloroplasts has yet to be elucidated (Hawkesford and De Kok, 2006).

The first step of S assimilation involves the activation of SO_4^{2-} by the enzyme ATP sulphurylase. ATP sulphurylase catalyses the substitution of two phosphate groups of the ATP by the sulphuryl group. This generates adenosine phosphosulphate (APS) and pyrophosphate. APS then functions as a substrate for either the formation of sulphate

esters or sulphate reduction. In an ATP-dependent reaction, the enzyme APS kinase catalyses the formation of phosphoadenine phosphosulphate (PAPS). The resultant activated sulphate binds with a hydroxyl (OH) group, forming a sulphate ester (Saito, 2004).

Alternatively, for sulphate reduction the APS is reduced to sulphite (SO_3^{2-}) mediated by two electrons from glutathione and the enzyme APS reductase. Then occurring primarily in the chloroplast, SO_3^{2-} is reduced to sulphite (S^{2-}) via six electrons from ferredoxin catalysed by the enzyme sulphite reductase. By the action of the enzyme *O*-acetylserine (thiol) lyase (OASTL), the formed sulphite is converted to *O*-acetylserine (OAS) (Kopriva, 2006). The first product of SO_4^{2-} assimilation is cysteine which then behaves as precursor for all subsequent organic compounds containing reduced S (Nikiforova *et al.*, 2004). Sulphur is also present in the other amino acids methionine (Met), and thereby constituents of proteins, and in the antioxidant glutathione (GSH). Often it acts as a structural component (R_1-C-S-C-R_2) or functional group (R-SH) involved in metabolic processes. The uptake and assimilation of sulphate is regulated by 1) regulation of the sulphate transporters, 2) modulate the activity of enzyme responsible for SO_4^{2-} reduction and 3) control the availability of APS as a substrate (Vauclare *et al.*, 2002).

Glucosinolates are a product of secondary metabolism and are relevant for agriculture as they play an important role in pest defence in brassicas. They are biologically inactive and stored in the vacuoles but when the cells are damaged, they are released and undergo hydrolysis mediated by the enzyme myrosinase. This results in the release of glucose, sulphate and biologically active volatile compounds (McCully *et al.*, 2008). In S-deficient plants, under S demands, the glucosinolates are converted by

myrosinase and re-introduced into the S assimilation pathway (Hawkesford *et al.*, 2012).

Limited quantities of cysteine and methionine inhibit protein synthesis and decrease the concentration of chlorophyll in the leaves. The reduction in S amino acids possesses a direct implication on the nutritional quality of the resulting crop (Arora and Luchra, 1970; Hawkesford *et al.*, 2012). Plants require between 0.1 – 0.5 % of the dry weight of sulphur for optimal growth. However, this requirement varies between crop plants, decreasing in the order of Cruiferae (11 – 17 g/kg), > Legumniosae (2.5 – 3.0 g/kg), and > Gramineae (1.8 – 1.9 g/kg), with values depicting the concentration of S in their seeds (Hawkesford *et al.*, 2012).

1.2.4 Nitrogen

Plants absorb N from the soil solution in mineral forms such as nitrate (NO_3^-) and ammonium (NH_4^+) which are reduced to form amino acids in the vegetative tissue (Hawkesford *et al.*, 2012). In addition, plants can also absorb N in organic forms such as amino acids, peptides, proteins and urea (Miller and Cramer, 2004; Näsholm *et al.*, 2009). NO_3^- and NH_4^+ uptake into plant roots involves multi-affinity transporter systems (ATs) proteins such as the high-affinity (HATs) and low-affinity (LATs). At low external concentrations (< 0.5 mM) of NO_3^- and NH_4^+, the uptake operates by the HATs, whereas the LATs operate at higher concentration (> 0.5 mM) (Hawkesford *et al.*, 2012). In fertilised soil, nitrate is present in excess (1 - 5 mM) compared to ammonium (20 – 200 µM). This excess can be attributed to the higher mobility of nitrate than ammonium, rendering it more available to plants as reported Miller and Cramer (2005). Several NO_3^- and NH_4^+ transporter proteins have been identified and

characterised, in particular, the genes belong to the NRT (nitrate transporter), AMT (ammonium transporter) and CLC (chloride channel) families. For example, two types NO_3^- transporters belong to the NRT1 and NRT2 families has been identified to be involved in NO_3^- acquisition by the plant root system. Transporters of the NRT1 family are LATs, except for NRT1.1 which possesses a dual affinity. There are 53 *AtNRT1* genes in *A. thaliana*, of which only *AtNRT1.1* and *AtNRT1*.2 known to mediate $NO3^-$ transport into roots (Tsay *et al.*, 2007). However, studies showed that these two genes expressed in different location in roots. *AtNRT1.1* expressed primarily in the epidermal cells of the root tip and in the cortex and endodermis of the mature regions of roots (Huang *et al.*, 1996), while *AtNRT1*.2 found to be primarily expressed only in root hairs and the epidermal cells of both young and more mature roots (Huang *et al.*, 1999). In comparison, there are only seven *AtNRT2* genes belonging to the NRT2 family which are considered as HATs, of which only two genes; *AtNRT2.1* and *AtNRT2.2* are involved in NO_3^- transport into roots (Tsay *et al.*, 2007). Following its uptake form the soil soliton into the root system, NO_3^- will be then transported via different NRT members and located within different plant tissues. For example, NRT1.5 is located in the plasma membrane and encoded by the *AtNRT1.5* gene in *A. thaliana.* This gene is expressed in the pericyclic cells of the root near the xylem which found to be mediating the long-distance NO_3^- transport from the root to the shoot (Lin *et al.*, 2008).

Similar to the reduction and assimilation of CO_2 in photosynthesis, the uptake and assimilation of N is tightly regulated. The NO_3^- assimilation pathway is a multi-step reaction. It requires two key enzymes in order to assimilate NO_3^- into organic compounds. Firstly, nitrate reductase (NR) a cytosolic enzyme catalyses the two-

electron reduction of NO_3^- to nitrite (NO_2^-). The resulting NO_2^- is translocated to the chloroplast and via nitrite reductase (NiR), the second enzyme of the pathway, is reduced to ammonium (NH_4^+) as shown in Figure 1.3.

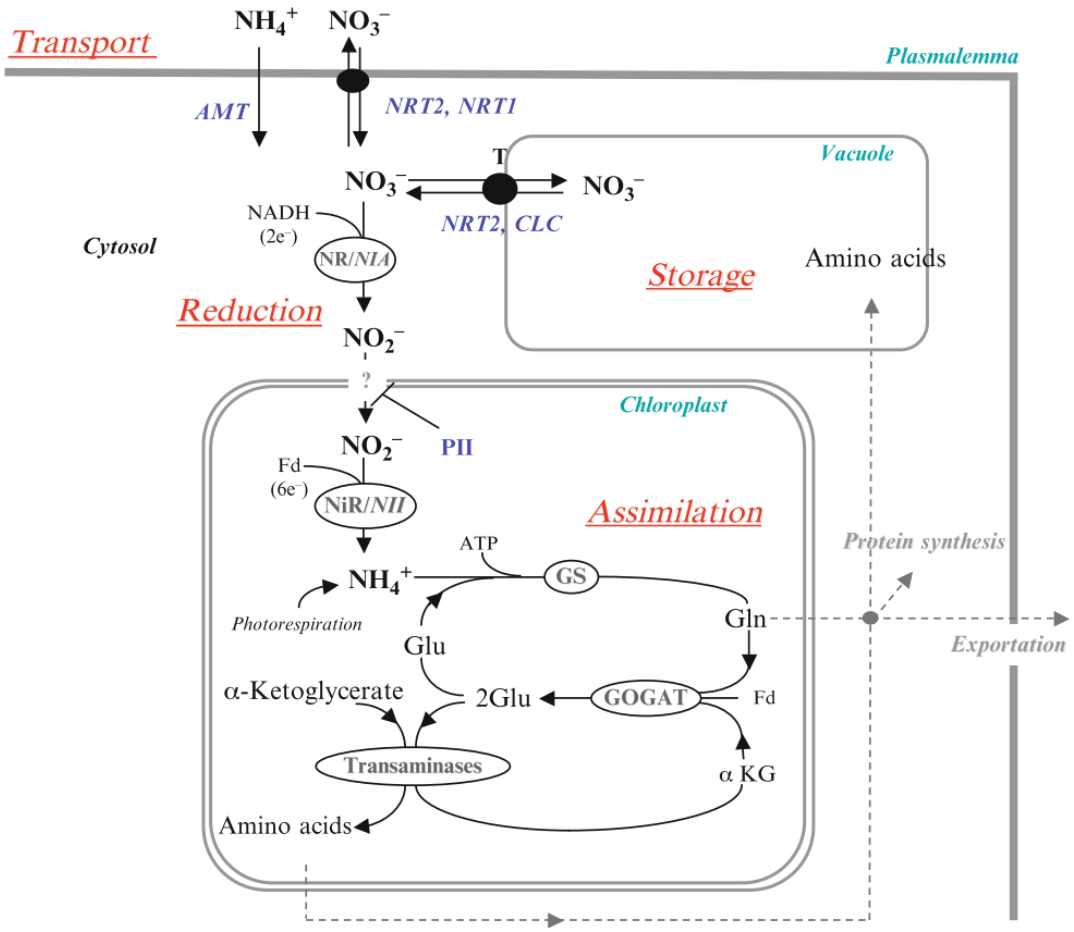

Figure 1.3 Nitrogen assimilation pathways in plants.

The transport, storage, reduction and assimilation pathway(s) of both NO_3^- and NH_4^+. Both NO_3^- and NH_4^+ are facilitated by protein transporters (NRT2, NRT1 and AMT) to enter the cytosol of the cell to be stored in the vacuole or subject to reduction to be assimilated to amino acids. This figure is adopted from Daniel-Vedele *et al.* (2010).

Interestingly, despite being present at lower concentration, NH_4^+ is the preferred source of N in plants and its accumulation occurs at high rates. However, it is toxic at high concentrations meaning that the assimilation of NH_4^+ needs to be performed

immediately upon absorption. For several years, ammonium assimilation was believed to be mediated by the enzyme glutamate dehydrogenase (GDH). However, additional studies have revealed that GDH also releases ammonium during senescence (Labboun *et al.*, 2009).

Regardless of NH_4^+ being accumulated from nitrate reduction or directly absorbed from the soil, the assimilation is mediated by two enzymes. These include both glutamine synthetase (GS) and glutamine-oxoglutarate aminotransferase (GOGAT). The amino acid glutamate behaves as an acceptor for ammonium, generating glutamine. Predominately occurring in the plastids of plants, the second enzyme, GOGAT catalyses the transfer of the amide ($-NH_2$) group from glutamine to 2-oxoglutarate (a product from the tricarboxylic acid cycle). This forms two molecules of glutamate (Glass *et al.*, 2002; Daniel-Vedele *et al.*, 2010). One glutamate molecule maintains the ammonium assimilation cycle, whereas the second glutamate molecule is translocated from the assimilation site and used for the biosynthesis of proteins. An overview into the role and importance of N-base fertiliser within OSR plants as well as N uptake, remobilisation and use efficiency is provided.

1.3 Nitrogen within OSR plants

1.3.1 Importance of N fertiliser and its application time

Nitrogen is an essential macronutrient for plant growth and development. Plants require a large amount of N to provide a typical vegetative growth. Being an essential constituent of amino and nucleic acids, plant hormones, chlorophyll and coenzymes (Hawkesford *et al.*, 2012), N plays such an important role in plant metabolism. However, the limited natural availability of N in the soil leads to negative impacts on

plant metabolism and development (Epstein and Bloom, 2005) such as reduction in leaf area and plant content of chlorophyll. This inevitably reduces the rate of photosynthesis and the quantity of derived products thus reducing plant biomass as well as decreasing the oil and protein yield (Tegeder and Rentsch, 2010). It has well been documented in OSR crop that N availability is immensely associated with the increase in number of leaf per plant (Svečnjak and Rengel, 2006b), leaf area and chlorophyll content (Ogunlela *et al.*, 1989), number of siliques per plant (Svečnjak and Rengel, 2006b) and seed yield (Rathke *et al.*, 2005; Schulte auf˙m Erley *et al.*, 2011; Koeslin-Findeklee and Horst, 2016). Therefore to maximise OSR yield it is necessary to supply supplementary N in fertilisers. The Defra RB209 Fertiliser Manual (Defra, 2010) details the recommended application rates, depending on the residual soil Nitrogen supply levels. However, much of central UK is ecologically at risk of excess nitrate applications, especially with leaching into water supplies, and are covered by nitrate vulnerable zones (NVZs) to protect them. In NVZs the applications of N is governed by further restrictions, detailed in (Defra and EA, 2016).

In order to achieve an optimum yield of 3 to 3.5 t/ha in the UK (Berry and Spink, 2006), OSR plants require large amount of N fertiliser - more than 200 kg/ha is recommended (Weightman *et al.*, 2010). Nonetheless, the determining factor relies on the timing of fertilisation to the soil (Gombert *et al.*, 2010) so as to prevent wasting the fertiliser when plants capacity to acquire N is at a low level in order to improve N uptake efficiency. According to soil N availability, the main quantity of N-based fertiliser is applied in spring when plant growth increases rapidly until middle of flowering when most of the added N should be absorbed by plants. Given plants have

the capacity to absorb ca. 3 kg N/ha per day until flowering time, no single addition greater than 100 kg/ha is recommended (Berry *et al.*, 2014).

1.3.2 Nitrogen uptake

N absorption by the root system is dependent on several factors such as soil moisture and thermal condition, root architecture and the volume of soil investigated by the roots, and the soil N availability and form which regulate the transporters activity of NO_3^- and NH_4^+ (Xu *et al.*, 2012). A range of studies were performed to investigate the relationship between plant root growth and N absorption at different plant development and growth stages, focused on significance of the root length over root biomass to increase N uptake efficiency in OSR (Kamh *et al.*, 2005; Schulte auf'm Erley *et al.*, 2007; Berry *et al.*, 2010a). However, due to the energetic cost of root growth, alternative approaches which strike a balance between N absorption activity and metabolic cost are more favourable. Increasing fine roots density, the abundance of aerenchyma tissue within the root cortex, and root-mycorrhiza association can be efficient strategies to increase N absorption efficiency (White *et al.*, 2013; Lynch, 2015).

As it has been described previously, plant absorption of NO_3^- and NH_4^+ into the roots is mediated by members of the transporter families. However, the rates of absorption differs according to the plant growth stage. In *B. napus* L., it has been shown that NO_3^- uptake increases from the beginning of stem extension until the onset of flowering, whereas little uptake of NO_3^- occurred during the pods filling stages (Rossato *et al.*, 2001; Malagoli *et al.*, 2004; Zhang *et al.*, 2010; Ulas *et al.*, 2013). nevertheless, as demonstrated by Malagoli *et al.* (2005a) N acquisition continued at a

high rate after the beginning of the seed development stage; GS 6.1 seeds expanding, particularly within highly N efficient genotypes at low level of N supply Horst *et al.* (2003).

In the study of Berry *et al.* (2010b), it has been shown that the most critical time of N uptake in OSR life cycle is after plants flowering. Moreover, the proportion of N obtained at this stage is a major factor influencing the determination of the genotypic variation in seeds yield of OSR crop. In the same study, it was also reported that every new addition of one kg/ha of N during the flowering time contributed to an increase of 16 kg/ha in seeds yield.

1.3.3 Nitrogen utilisation and remobilisation

A considerable portion of the total leaves N (2 - 2.5 % of the dry weight) is returned to the soil with dead leaves dropped at different plant development stages, especially at a low degree of light intensity and temperature (Dejoux *et al.*, 2000). Furthermore, it has been shown by Rossato *et al.* (2001) that 15 % of the total plant N is sent back to the soil by dead leaves dropped before the seed development stages, in contrast to 26 % residual N in stem and root system at seed maturity. Hirel *et al.* (2007) also illustrated that a large portion (~ 40 %) of the total N absorbed during the vegetative growth is returned to the soil with falling leaves. Nevertheless, different studies have shown that the loss of N associated with stem and taproot at harvest is significantly larger than leaves (McGrath and Zhao, 1996; Ulas *et al.*, 2013; Koeslin-Findeklee and Horst, 2016). For example, the quantity of N loss with stem at maturity was >2.5-fold than with leaves (Ulas *et al.*, 2013).

Despite the high capacity of *B. napus* plants to obtain N from the soil, OSR cultivated in the field, as it is reported in many studies (Schjoerring *et al.*, 1995; Rossato *et al.*, 2001; Chamorro *et al.*, 2002; Zhang *et al.*, 2010), has a very low level of N uptake in plants when calculated as the total plant N content divided by the applied amount of N. The quantity of N remobilised from the vegetative organs to the siliques does not exceed 45 to 67 % regardless of the added quantity of N to the plant through the soil.

Under deficient N environment (no added N), more than 56 % of the shoot N content is stored in the stem and the rest in leaves at the onset of flowering (Ulas *et al.*, 2013). In contrast, approximately 30 – 40 % of the total N of the plant canopy was located in pod walls at the end of flowering stage (Schjoerring *et al.*, 1995). The vegetative parts of plant (stem, taproot and leaves) are crucial components in supplying the N during seed development stages (Rossato *et al.*, 2001; Malagoli *et al.*, 2005a; Ulas *et al.*, 2013). As demonstrated by Malagoli *et al.* (2005a) and Gombert *et al.* (2010) over 70 % of the total pods N recovered from the vegetative organs, of which 8 – 16 % is derived from taproot, 22 % from the flowerings parts, 34 – 47 % from stem, and 36 % from leaves. The greatest portion of N remobilised to seeds is obtained during the stem extension stage of plant growth (Zhang *et al.*, 2010; Ulas *et al.*, 2013). Berry *et al.* (2010b) demonstrated that the amount of N remobilised from stem ranged from 10 to 42 kg N/ha (37 – 67 % of stem N) between plant flowering and seed maturity among 10 genotypes at limited N availability, and significantly associated with N harvest index. Aforementioned, these studies indicate that inefficiency of OSR plants in remobilising N and there is room to exploit the natural variation to increase it.

1.3.4 Nitrogen Use Efficiency

Nitrogen use efficiency is defined as dry mass produced/unit of available nitrogen absorbed from the soil (Hirose, 2011). N use efficiency can be further split into Nitrogen uptake efficiency and Nitrogen utilisation efficiency, relating to the efficiency of N absorbed and efficiency to convert absorbed N to yield, respectively. Despite the high capacity of *B. napus* plants to obtain N from the soil, particularly before flowering, OSR has an innate low N Use Efficiency (Sylvester-Bradley and Kindred, 2009; Sieling and Kage, 2010), of less than 10 kg dry matter/kg N, compared to 69, 31, 27, 25 and 21 for sugar beet, triticale, winter oats, winter wheat and malting spring barley, respectively (Sylvester-Bradley and Kindred, 2009). As previously reported this is primarily due to confluence of two factors; an inadequate efficiency of N remobilisation from the vegetative tissues to the siliques as previously described (Malagoli *et al.*, 2005a; Gombert *et al.*, 2006; Koeslin-Findeklee and Horst, 2016) as well as low N uptake, in particular, post-flowering N uptake (Berry *et al.*, 2010b). Interestingly, several field studies under limiting N fertiliser conditions have reported on an increased association between N uptake efficiency and N use efficiency compared to N utilisation efficiency (Berry *et al.*, 2010b; Schulte auf'm Erley *et al.*, 2011; Kessel *et al.*, 2012; Nyikako *et al.*, 2014).

Interestingly, despite the volume of work done to date in addressing N use efficiency in OSR, at present no OSR varieties have been released publicly with improved performance for this trait (Bouchet *et al.*, 2014). Oilseed rape breeders develop new varieties to perform well on the AHDB Recommended List, the primary source of validated information from which growers select the varieties to use. However, the Recommended List trials are performed under standard high fertiliser input conditions,

which does not provide breeders with an incentive to develop varieties with improved N use efficiency. Furthermore, the same identical OSR genotypes may respond differently under low supply of N. Thereby, it is necessary to breed and test OSR varieties under low quantities of N to identity both the plant characteristics and traits which would best suit a limited N environment (Berry *et al.*, 2010b; Schulte auf˙m Erley *et al.*, 2011). In the study by Schulte auf˙m Erley *et al.* (2011), they investigated traits contributing to N Use Efficiency among 17 genotypes of *B. napus* under both low and high N availability. From their results, they concluded that N uptake was more important to plant seed yield with reduced N supply. While N utilisation trait was more important with increased N supply. In comparison, Nyikako *et al.* (2014) who investigated genetic variation in N uptake and utilisation efficiency among 56 genotypes (54 segregating double haploid lines in addition to two parental cultivars) under field condition at contrasting N availability, reported that both N uptake and utilisation associated significantly with plant seed yield under limited N supply. Surprisingly, there was no association between N utilisation and seed yield at high N supply. It is possible now to utilise the large genetic differences in N use efficiency among numerous varieties of OSR that reported in several studies in different countries such as in the UK among 10 genotypes (Berry *et al.*, 2010b), in Germany among 12 (Horst *et al.*, 2003), 17 (Schulte auf˙m Erley *et al.*, 2011), 36 (Kessel *et al.*, 2012) and 56 genotypes (Nyikako *et al.*, 2014), in France among 10 genotypes (Girondé *et al.*, 2015), in China among eight genotypes (Zhang *et al.*, 2010; Lee *et al.*, 2015) and in Australia among 12 contrasting N efficient genotypes (Balint and Rengel, 2008). Reducing N fertiliser while preserving high level of OSR seed yield , it would

certainly be of great importance for sustainable crop production and food security in the future (Bouchet *et al.*, 2016).

It has been reported that an increase in N Use Efficiency of 7.2 kg DS/kg N accompanied with a reduction in N fertiliser requirement of about 49 kg/ha might be achieved by breeders, this could be achieved through: I. Reduction of N concentration remaining in stem and pod wall at harvest by 0.4 %, II. Increasing the plant capacity to absorb N after flowering by 20 kg/ha, III. Increase the density of root length to 1 cm/cm^3 in the first 100 cm of the soil depth (Berry *et al.*, 2010a). Using his simulation model on N dynamics in OSR plants grown in the field to improve N Use Efficiency, Malagoli *et al.* (2005b) showed that a possible improvement of 15 % in N content or harvested seed could be achieved by optimising the mechanism by which N mobilise from the vegetative tissues to the siliques during seed filling phases as well as reducing concentration of the remaining N in falling leaves. The benefit of increasing the value of N Use Efficiency is not limited to plant breeders but can impact the global economy, for example through a reduction in the emissions of greenhouse gas (GHG) as well as in the amount of nitrate leaching to the water body is also of great importance.

1.3.5 Environmental impact of N fertilisers

The total production of N fertiliser increased worldwide from 85.3 Mio t in 2002 to 113.3 Mio t in 2014 (FAOSTAT, 2017). The use of N fertilisers can lead to a number of environmental problems. The first is that manufacture of N fertilisers initially makes use of the Haber-Bosch process to fix gaseous N_2 to form ammonia. This process requires high temperatures and pressures and consumes a large amount of energy.

Actually, over 1 % of the energy produced in the world is used in this process (Smith, 2002) which means that N fertiliser has a very high carbon footprint.

Secondly, only about 60 % of the N fertiliser applied to OSR is taken up by the crop. The remainder can either leach into streams and rivers where it can cause eutrophication, hence the NVZs, or it is broken down by soil microorganisms to produce nitrous oxide (N_2O) (Butterbach-Bahl *et al.*, 2013). This is a potent greenhouse gas with a global warming potential of 298 times compared to CO_2. It has been reported that GHG emissions averaged 1080 kg CO_2 equivalent associated with a production of optimal yield (3.2 t/ha) of OSR under the standard OSR crop inputs in the UK, including fertilisers, seeds, pesticides and fuel (Weightman *et al.*, 2010; Berry *et al.*, 2011), N fertiliser is responsible for more than 79 % of these GHG emissions (Mahmuti *et al.*, 2009). In total, N fertiliser application accounts for more than 50 % of the total energy use in crop production (Woods *et al.*, 2010).

1.3.6 Financial contribution of fertiliser

Achieving a typical seed yield of 3.5 t/ha, OSR plants demand high requirements of the main nutrients, for example an average of 200 kg/h for N, 48 kg/ha for P, 80 kg/h for K and 30 kg/ha for S. Moreover, every increase of 0.5 t/h in yield up to 4.5 t/ha is accompanied with a further addition of 30, 7 and 6 kg/ha of N, P and K, respectively, as recommended in the Fertiliser Manual, RB209 (Defra, 2010). Needless to say, fertiliser application is the major financial and energy cost in OSR production which attributed to more than 66 % of the total variable cost in 2009 (Weightman *et al.*, 2010). The increase in fossilised fuel prices which is the primary feedstock during the N fixation process, further increases the N-base fertiliser cost. Thereby, efficient use

of fertiliser and in particular N, will undoubtedly increase the profitability of OSR. Aforementioned, enhancement of N Use Efficiency, is in important target for plant breeders (Berry *et al.*, 2010b) as it can increase profitability of OSR production either through greater seed production or by a cost reduction of N-based fertiliser. Reducing the amount of N fertiliser input to OSR is cost-effective for famers and supported by environmental concerns.

Since restrictions on cultivation of genetically modified crops have been applied in many countries in the world, exploring the natural genotypic variation is of great interest for plant breeders to improve minerals use efficiency. One of the main approaches to explore such natural variation in several crops is using Quantitative Trait Loci (QTL) analysis (Hawkesford *et al.*, 2014). This analysis requires a segregating population obtained from the cross between two parental genotypes by which a genetic map is generated. Using this linkage map in addition to phenotypic traits can lead to the identification of genomic regions associated with these traits. Throughout this thesis, QTL analysis has been used to identify QTLs related to yield, yield related traits and proteomic traits that contribute to N storage and remobilisation. For this reason, a brief description to quantitative traits, mapping population and QTLs related to several traits in OSR is provided.

1.4 Quantitative Trait Loci

1.4.1 Introduction to Quantitative traits

Numerous relevant agricultural characteristics such as grain yield, quality and disease resistance are regulated by multiple genes and referred to as quantitative traits. Quantitative Trait Loci (QTL) are defined as the regions in the genome comprised of

the genes associated with a specific quantitative trait. QTL determines positions of the DNA which are in close proximity to the gene of interest. The design of molecular markers in the 1980s enhanced the opportunity to identify and select for QTL (Collard *et al.*, 2005).

The function of molecular markers is to demonstrate genetic variances, known as polymorphisms, between organisms or species. These molecular markers occupy specific positions within the chromosome called "loci". Markers closely located near the gene of interest are said to be linked to the gene and are often referred to as "gene tags", while at larger distances from the target gene the markers are referred to as "signs or flags" (Collard *et al.*, 2005). Different markers are available to use for QTL identification: 1) morphological, 2) enzymes and 3) molecular markers, and each marker is utilised to determine specific traits such as phenotypic, enzyme differences and variation sites in DNA, respectively. In plant genome studies an array of DNA markers are available, such as SNP (single-nucleotide polymorphism), RFLP (restriction fragment length polymorphism), AFLP (amplified fragment length polymorphism), and SSR (single sequence repeats) (Semagn *et al.*, 2006; Collard and Mackill, 2008).

Due to their abundance, DNA markers are widely used. Their use may be attributed to them being unaffected by environmental factors (compared to morphological and enzyme markers). There are three main laboratory applications for DNA markers to distinguish genetic differences between individuals of the same or different species, as classified by Gupta *et al.* (1999) These include 1) hybridisation-based (e.g. RFLP), 2) polymerase chain reaction (e.g. AFLP, SSR) and 3) DNA-based sequence (SNP)

(Gupta *et al.*, 1999). One of the primary application of these markers is to produce genetic mapping.

1.4.2 Mapping population and linkage map

A major use of molecular markers in agricultural studies has been in the assembly of linkage maps for segregating populations generated from crosses between two parent plants that have differing properties. These maps have been exploited to locate the chromosomal regions possessing genes which are responsible for the traits. Linkage maps illustrate the locus and relative genetic distances between the molecular markers along chromosomes. The construction of linkage maps and performing QTL-analysis to isolate genomic regions linked with traits is known as QTL-mapping (Mohan *et al.*, 1997). There are an array of benefits associated with QTL analysis including but not limited to 1) identification of traits affected by the environment e.g. salinity, nutrient availability and drought, 2) test trait associations, 3) determination of genes to clone (Salvi and Tuberosa, 2005).

Rather than using recombinant inbred lines (RILs), which are time consuming to make, the use of doubled haploid (DH) line populations has become common for genetic analysis in brassicas. Through the induction of chromosome doubling, DH populations are grown by regenerated plants. This can be achieved either through anther culture or microspore culture. The latter technique offers reduced contamination between the pollen microspores and the diploid anther wall. Being homozygous, DH populations can be multiplied and reproduced without any genetic variability. In plant studies, this is a great benefit rendering the possibility to replicate trials in both various locations and in different years. Another benefit of DH

populations is their short acquisition times to produce a functional population. DH populations are predominately used in mapping chromosomes and identification of genetic markers (Forster *et al.*, 2007). The mapping population used in the present study was produced from the F1 cross between two contrasting parental genotypes belonging to different geographical locations by microspore culture (Qiu *et al.*, 2006). Tapidor DH, the female genotype, is a European winter variety which has a high requirement of vernalisation, a low seed content of erucic acid and glucosinolates (Qiu *et al.*, 2006), and characterised as a B-inefficient cultivar (Liu *et al.*, 2009a). In contrast, Ningyou 7, the male genotype, is a Chinese semi-winter variety with a low requirement of vernalisation, a high seed content of erucic acid and glucosinolates (Qiu *et al.*, 2006), and is characterised as a B-efficient cultivar (Liu *et al.*, 2009a). The population is thereby referred to as TNDH mapping population from which a total of 202 DH segregating lines were produced in 2002. A linkage map of 19 linkage groups (LGs) was generated with an average interval of *ca.* 3.02 cM between adjacent markers. This mapping population has been initially used to identify QTLs associated with seed content of oil and erucic acid under field conditions (Qiu *et al.*, 2006). Several mapping populations have been developed in *B. napus* and different plant species such as *Arabidopsis thaliana*, wheat (*Triticum aestivum* L.) and maize (*Zea mays* L.) to map several agronomic quantitative traits and identify the genomic region associated with them as the initial step to determine and characterise the related genes.

1.4.3 QTLs for several traits in OSR

QTL analysis using multiple segregation populations is a powerful approach for dissecting complex agronomical traits in plants. QTLs have been mapped for numerous traits in *B. napus* including yield and yield related traits, oil, erucic acid and

glucosinolates content, flowering time, abiotic stress, and resistance to diseases. However, a limited number have been mapped for mineral use efficiency.

1.4.3.1 Seed yield and yield related traits

Seed yield is very complex trait that is influenced by several yield components, mainly; seed and pod number per m^2 , seed number per pod, number of branches per plant and individual seed weight (Berry and Spink, 2006). The seed yield and harvest index (seed dry matter/total plant dry matter) have been the primary target for plant breeders for years, as key steps for improved N use efficiency. However, these are limited to analysis at the end of the crop life cycle. As such they possess additional factors such as plant growth, abiotic and biotic stresses which contribute to the overall N use efficiency (Bouchet *et al.*, 2016). Many QTLs for yield and yield related traits have been previously mapped in *B. napus*. Quijada *et al.* (2006) and Radoev *et al.* (2008) identified several genomic regions associated with seed yield and its component using DH populations and their testcrosses populations in Canada and Germany, respectively. In the study of Shi *et al.* (2009), they investigated QTLs associated with yield traits using the TNDH population and a reconstructed F2 population grown in the field under 10 distinct environments in China. They found 85 QTLs associated with seed yield which explained 2.2 – 33.5 % of the phenotypic variation of which four were major QTLs, 159 QTLs associated with seed weight of which four were major, 50 associated with pod number, 87 associated with plant height and 70 with branch number. However, a significant interaction between genotype and environment was observed. In the study by Zhou *et al.* (2014), they integrated 1960 QTLs associated with 13 different yield and yield related traits which were previously identified in 15 distinct studies published between 1999 – 2012. 142 conserved QTLs

was found among these different segregating populations and environments, in addition 25 loci were characterised as multifunctional loci where each locus regulated at least two traits. Further comparative genomic analysis with *A. thaliana* identified 80 brassica genes, underlying yield and yield related QTL these were homologous to 61 genes of *A. thaliana* due to the triplicated nature of the brassica genome and *B. napus*'s amphidiploid composition. 69 of these genes were determined to be localised on the A genome where the LG A07 carried the greatest number of genes of 11 in comparison with nine other LGs.

1.4.3.2 Seed oil content and quality, and glucosinolates content

OSR is cultivated primarily for its rich seed in oil content. The preference to develop genotypes with a very low erucic acid concentration and relatively low glucosinolates content, was for many years a major focus for plant breeders. Many studies have been involved in the identification of QTLs associated with oil content. Qiu *et al.* (2006) used the TNDH population under field conditions and detected a QTL on the LG A08 at two distinct environments in China and two growing seasons. Delourme *et al.* (2006), used two DH populations field-grown in France. They detected five QTLs under different environments of which only one on the LG A03 was identified in both populations. Jiang *et al.* (2014), reported a great genotypic variation and identified 41 QTLs in the TNDH population across 15 performed experiments. Other studies have identified genomic regions associated with different aspects that determine the oil quality. A novel QTL was detected for erucic acid content and localised 7 cM away from the most important erucic acid QTL (*FAE1*) on the LG A08 (Cao *et al.*, 2010). 131 genomic regions associated with three unsaturated (oleic, linoleic and linolenic acid) and three saturated fatty acids (palmitic, stearic and arachidic acid), of which

two QTLs on chromosome C3 were associated with all of these fatty acids (Javed *et al.*, 2016). Several QTLs associated with seed glucosinolates content were also identified (Howell *et al.*, 2003; Feng *et al.*, 2012). In a recent study by Huang *et al.* (2016), a QTL was identified, using RILs population derived from two contrasting parents. The glucosinolates content determined by these loci (28 and 60 µmol/g), explained 47.71 % of the phenotypic variation localised on the chromosome A10.

1.4.3.3 QTLs associated with flowering time

Flowering time varies quantitatively among OSR genotypes. This variation is attributed to the complex regulation network of multiple genes controlling flowering time (Long *et al.*, 2007). Therefore, understanding the genetic mechanisms which regulate plant flowering time is of great interest for plant breeders. Flowering time has been previously mapped in *B. napus* germplasm. A number of major QTLs were identified such as the loci on the LG C6 which explained 19.2 – 27.6 % (Delourme *et al.*, 2006), and 26 – 52 % (Long *et al.*, 2007) of the phenotypic variation. A QTL (*BnFLC10*) localised on the LG A10 which was specific to non-vernalisation environments explaining 50 % of the phenotypic variation (Long *et al.*, 2007). Similarly, the *FRI* gene in *A. thaliana*, the *BnaA.FRI.a* has been reported to play a key regulatory function in flowering time of OSR which inhibits floral transition through activation of *BnFLC* (Wang *et al.*, 2011a). A major QTL for flowering time was found to be co-localised with QTLs for seed yield and plant height in a 7.2-cM region on the chromosome A02. Using comparative genomic analysis with *A. thaliana*, this locus was found to include two flowering time related genes, *VIN3* and *ZTL* (Shi *et al.*, 2009). Likewise, in the study by Javed *et al.* (2016), QTL associated with flowering time was identified on the LG A02 near a vernalisation gene, accounting for 43.2 %

of the phenotypic variation. Recently, a major locus explaining 21.7 % of the flowering time variation has been detected on the LG C5 with two genes identified, light regulated *LWD1* and flowering *BHLH1* (ArifUzZaman *et al.*, 2016).

1.4.3.4 QTLs for N use efficiency

Despite the significant effect of N fertilisation on OSR production and in contrast to the previously discussed agronomic traits, few studies have been performed for the identification of loci associated with N use efficiency and its related traits under contrasting N conditions in *B. napus* (Gül, 2003; Miro, 2010; Bouchet *et al.*, 2014). Hence, little is known of the description and function of these identified genomic regions. Using the TNDH segregating population to map several N use efficiency and its related traits under low and adequate N environment over two growing seasons, Miro (2010) reported that 49 – 72 and 44 – 62 QTLs were detected under adequate and limiting N environment, respectively, with significant interactions between genotype and N environment were reported. For example, 10 QTLs for N uptake efficiency were only detected at low N environment and localised mostly on the LG A01, while 7 QTLs for N utilisation efficiency were only identified at high N availability and localised mostly on chromosome C7.

Many QTLs have also been recently identified in the study of Bouchet *et al.* (2014) whom investigated the genetic control of yield and its components under limited and adequate N availability. Moreover, these QTLs were highly stable among N conditions suggesting that no interaction between genotype and N condition occurred. In contrast, a significant interaction between genotype and growing season was reported. One of 11 stable QTLs among both N conditions and growing seasons and localised on chromosome A05 was found to a strong candidate for marker assisted selection.

Likewise, Gül (2003) identified six to eight QTLs associated with yield components under contrasting N availability, respectively, with no interaction between genotype and N environment, contrary to that reported by Miro (2010).

1.4.3.5 Other minerals composition and use efficiency

Minerals acquisition, distribution, accumulation and utilisation are under the control of complex regulatory networks from the moment of absorption until the final metabolites are being utilised by the plant cells (Hawkesford *et al.*, 2012). Thereby, QTL analysis offers a powerful strategy to unravel such complex traits. Liu *et al.* (2009a) unravelled the complexity of shoot composition of seven minerals with QTL analysis using the TNDH mapping population. 18 and 17 QTLs explaining 4.4 – 19 % of the phenotypic variation, were mapped using limited and adequate B supply respectively. Significant interaction between genotype and B environment, in addition to 74 epistatic QTLs were detected. A major QTL associated with P concentration was identified on the LG A01 under both B environments explaining 17.4 and 19 % of the trait variation, where the cultivar Ningyou 7 contributed to the allele accounted for increasing shoot P concentration. Additionally, some mineral QTLs were co-localised, for example, QTLs associated with Ca and Mg on LGs A03, A06 and C8, with P and B on LG A01 and with B and Cu on LG A04. In a different study that a RIL population was used to map QTLs associated with seven seed minerals composition, Ding *et al.* (2010), identified 35 and 45 QTLs under low and normal P supply, respectively, these accounted for 7.8 – 18.1 % of the traits variation. Eight of these QTLs were found to be identified on the same chromosomes in comparison with the study performed by Liu *et al.* (2009a) in which a different mapping population was used. The top of the LG C6 was found to be an important locus responsible for controlling seed minerals

(Ca, Mg, P, Zn and Cu) concentration under adequate P supply. However, these QTLs were detected on different LGs under low N supply and only explained a small proportion of the trait variation. As such these results, could reflect the difficulty of increasing seed composition of minerals under limiting P environment. Using the comparative analysis with *A. thaliana* genome, Liu *et al.* (2009a) and Ding *et al.* (2010) managed to map 26 and 21 orthologous genes involved in ion homeostasis in *B. napus*. These included, for example, different members of each of Mg transporter, P transporter, high-affinity Cu transporter, PAP, YSL, ZIP CAX and CCX family. A recent study used genome wide association to map shoot ionome of 30 day-old seedlings in a diversity set of 509 inbreds. They used an array of 6000 single nucleotide polymorphism (known as SNP), Bus *et al.* (2014) identified 29 significant loci for seven minerals concentration; Ca, Mg, S, Na, Cu, Mn and Zn, of which a locus associated with Cu, Mn and Zn concentration on the LG C3 was detected. Additionally, they identified a 540 kb locus with multiple associations related to Na concentration located on the LG A09 in the vicinity of the gene *SOS1* which encode Na^+/H^+ antiporter that plays an important role in plant Na tolerance through regulating Na acquisition and efflux (Fraile-Escanciano *et al.*, 2010).

Using two different DH mapping populations, Zhao *et al.* (2012) mapped several QTLs for yield and yield related traits and B efficiency under contrasting B conditions. From which a major QTL was identified for both yield and B efficiency on the chromosome A02 mapped to the *AtBE1-2* QTL in *A. thaliana* by comparative analysis. Further *in silico* analysis with *B. rapa* genome, determined that the genes Bra020592 and Bra020595, function as small molecule transporters with potential for improvement B efficiency in *B. napus*. Yang *et al.* (2010) studied the genetic control

of the plant biomass, root morphology and P uptake using an F10 RIL population under contrasting P environments. 62 QTLs were mapped, of which 45 were clustered on only four LGs and integrated into eight unique QTLs by meta-analysis. Two unique significant QTLs were identified to be specific for root and P uptake traits under deficient P environment. Similarly, very significant QTLs associated with lateral root number and density were mapped on the LG A03, while QTL for primary root length were mapped on the LGs A07 and C6 under low P supply using the TNDH population (Shi *et al.*, 2013a). These identified loci have potential to be attributed for the adaptability of *B. napus* to limited P availability. Recently, a major QTL associated for lateral root density was mapped on chromosome C9, accounting for 17.6 % of the phenotypic variation (Zhang *et al.*, 2016b). It is believed that this QTL can play an important role in improving P uptake efficiency.

1.4.4 QTLs for mineral use efficiency and its related traits in different plant species

A vast number of genomic regions associated with mineral use efficiency traits in addition to several architecture, physiological, and yield related traits have been mapped in many plant species. In rice (*Oriza sativa*), a major QTL associated with P uptake 1 (*Pup1*) under P stress was identified and mapped to 150 kb on chromosome 12 including 60 candidate genes (Wissuwa *et al.*, 2002; Chin *et al.*, 2011). Furthermore, using fine mapping, a minor QTL related to heading date (*qHd1*) which possessed pleiotropic effects on yield was mapped to a 95 kb region on chromosome 1 which contained 10 annotated genes (Chen *et al.*, 2014). Recently, using the specific locus amplified fragment sequencing (SLAF-seq) technology to detect polymorphic markers within two bulked DNA pools, both a major QTL and two minor QTLs

associated with rice grain length and weight were mapped to a 350 kb genomic region on chromosome 3. Interestingly, the lines that possessed two out of these three QTLs contributed from one parent which had a significantly greater grain weight (Xu *et al.*, 2015).

Several studies involved in QTL identification in *B. oleracea* associated with shoot mineral composition. For Ca and Mg (Broadley *et al.*, 2008) a 4 cM genomic region on chromosome C9 was found to be highly associated with Ca concentration. (Hammond *et al.*, 2009) found significant QTLs for shoot P content and P use efficiency were mapped on the LGs C3 and C7. (White *et al.*, 2010) identified a major QTL on chromosome C7 which mapped at 62.2 cM under glasshouse environment. Using comparative genomic analysis with *A. thaliana*, this QTL introgression was found to contain four genes assigned as K transporters. In a study by Li *et al.* (2015), clusters of QTL associated with N use efficiency and root architecture traits have been mapped in maize (*Zea mays*). Among them, 13 QTL clusters for N uptake efficiency and 12 for utilisation efficiency were found to be co-localised with QTL clusters associated with root architecture traits. Five of these QTL clusters had direct effects on both traits under low and high N conditions as a result from the performance of backcross population which can be very useful for marker assisted selection breeding to improve N use efficiency in *Z. mays*. Many segregating populations have been used to map various traits including mineral related traits in Arabidopsis. Hence, several QTLs have been identified to date. For example, QTLs were mapped for shoot N (Loudet *et al.*, 2003b), shoot P (Loudet *et al.*, 2003a), shoot minerals; Ca, Mg, K, Zn, Fe and Cadmium (Cd) concentration (Willems *et al.*, 2010). A major QTL related to both Zn and Cd tolerance were mapped and co-localised with HMA4, a member of

the heavy metal transporting ATPase family (Courbot *et al.*, 2007; Willems *et al.*, 2007). QTLs were also mapped for seed minerals content Ca, Mg, K, Mn, Fe, Zn, P, S and Cu using RIL populations (Vreugdenhil *et al.*, 2004; Waters and Grusak, 2008) wherein the strongest QTL was detected for P concentration on the top of the chromosome 3. Confirmation of gene function can be supported through protein analysis. Proteomics can also aid in the discovery of novel QTL.

1.5 Proteomic traits regulated plant development

Before its utilisation within the silique formation N is believed to be primarily stored in the vegetative organs in the form of proteins (Staswick, 1994), from which it can be released by enzymatic degradation of the proteins and transported to the developing reproductive organs (Simpson, 1986; Masclaux-Daubresse *et al.*, 2010). Therefore, many different proteomic traits can be mapped throughout the plant life cycle such as the vegetative storage proteins (VSPs) in addition to their regulations and functions, VSPs will be described in more detail in both *B. napus* and other plant species.

1.5.1 Vegetative storage protein in *B. napus*

Rossato *et al.* (2001) studied N storage and remobilisation in *B.napus* under controlled conditions they showed that a temporary accumulation of N occurred in the taproot of genotype Capitol plants during flowering through accumulation of a 23 kDa protein. This was primarily found to be accumulated in the vacuoles of the cortical root cells surrounding the phloem vessels (Rossato *et al.*, 2002a). It was suggested that this protein could play a role as a vegetative storage protein (VSP) due to its complete hydrolysis during pod development. Furthermore, it was found that growing plants under low temperature, results in delayed flowering as well as a delay in the

accumulation and remobilisation of this putative VSP which supports its role of storage protein (Rossato *et al.*, 2001). It was later found that this protein also behaves as a storage buffer of N mobilised from senescing leaves and its accumulation induced strongly by methyl jasmonate and abscisic acid (Rossato *et al.*, 2002a). A couple of years later, Noquet *et al.* (2004) reported the accumulation of the 23 kDa protein in the taproot of the same variety under field condition. Furthermore, during their investigation into the impact of altering source/sink relationship on the accumulation of the 23 kDa, Noquet *et al.* (2004) found that removal of the stem during the stem elongation stage prevented the accumulation of this protein in taproot. However, the accumulation of this protein was significantly increased in the taproot of deflowered and depodded plants. Little was known of the activity of such protein in *B. napus*. Several VSPs has been previously found in different plant species. However, their role and activity of many of them have been reported.

1.5.2 VSPs in different plant species

It has been previously found that various herbaceous (Staswick, 1994) and woody (Stepien *et al.*, 1994) plant species possesses similar VSPs. These well-characterised VSPs include proteins of 27 (*VSPα*), 29 (*VSPβ*) and 94 kDa in leaves and pods of soybean (*Glycine max* L.) (Wittenbach, 1983; Staswick, 1990; Staswick, 1994), the 29 and 30 kDa proteins known as *AtVSP* and *AtVSP2*, respectively, in *A. thaliana* (Berger *et al.*, 1995), the 32, 19 and 15 kDa (Hendershot and Volenec, 1993; Meuriot *et al.*, 2003) and the ~56 kDa (Gana *et al.*, 1998) found in taproot of alfalfa (*Medicago sativa* L.), the 17.3 kDa detected in stolon and root of white clover (*Trifolium repnes* L.), the 26 kDa found in leafy spurge (*Euphorbia esula* L.) (Cyr and Bewley, 1990), the 32 kDa protein accumulated in the bark of poplar (*Populus deltoids* Bartr. ex

Marsh.) (Coleman *et al.*, 1991) and the 22 kDa (*LcVSP1)* identified in the bark of lychee (*Litchi chinensis*) (Tian *et al.*, 2007).

As such, due to their multiple biological activities VSPs could contribute to numerous roles in different plant tissues. It has been demonstrated that the *G. max VSPα* and *VSPβ* in addition to the *A. thaliana AtVSP* and *AtVSP2* possess acid phosphatase activity (DeWald *et al.*, 1992; Berger *et al.*, 1995), moreover, the *AtVSP2* possessed a role in plant defence as an anti-insect (Liu *et al.*, 2005). Furthermore, β-amylase activity was attributed to the 56 kDa VSP in *M. sativa* (Gana *et al.*, 1998) and class III chitinase activity for the 32 kDa VSP through which plays a role in plant protection against pathogenesis (Avice *et al.*, 2003). In comparison, the *LcVSP1* in lychee (Tian *et al.*, 2007) and the 23 kDa VSP in *Sapindus mukorassi* (Liu *et al.*, 2009b) possessed trypsin inhibition activity. The importance of such proteins as storage proteins can therefore sometimes be overlooked due to their involvement in multiple pathways. Throughout this thesis proteomic traits have been studied such as putative VSP and other proteins that can effect N remobilisation. In order to identify such observed proteins and to further quantify them, tandem mass spectrometry technique was applied. Therefore, an overview into mass spectrometry including the principles, ionisation methods, mass analyser, and protein identification and quantification workflow is provided.

1.6 Mass Spectrometry in proteomic studies

1.6.1 Development

J.J Thompson assembled the first mass spectrometer in 1912 (Finehout and Lee, 2004). Despite an array of spectrometers being developed soon after and some being

awarded the Nobel Prize (Chace, 2003) it was not until the late 1980s in which Mass Spectrometry (MS) became a powerful analytical tool. Determining the amino acid sequence of proteins provides a connection between cell physiology and genetics, as reported by Domon and Aebersold (2006). Refinements in the instrumentation such as improving the sensitivity, resolution and accuracy, led to the diversified uses of MS within the field of life sciences (Chace *et al.*, 2002; Gygi *et al.*, 2002; Mano and Goto, 2003), that essentially replaced the Edman degradation method (Klemm, 1984). Moreover, the attraction to use MS to elucidate structural information of proteins was accelerated by the genome project (Cantor, 2000). The complete analysis of proteins within a tissue or cell, has been coined "Proteomics" (Anderson and Anderson, 1996; Wilkins *et al.*, 1996). However, prior to discussing the use of MS in proteomics, the general concepts of MS will be outlined.

1.6.2 Principles of Mass Spectrometry

In general, the analyte (molecular ion, $M^{+\cdot}$) under investigation is subjected to an ionisation source. This in turn, fragments the molecular ion generating a series of product ions that are separated according to their mass-to-charge (m/z) ratio and plotted against their relative abundance. Thereby, a mass spectrum is a graphical display of ion abundance versus mass-to-charge ratio Figure 1.4 (Hoffmann and Stroobant, 2007a). MS can provide both qualitative (structural) and quantitative (concentration) of the investigated analyte (Domon and Aebersold, 2006; Cox and Mann, 2011).

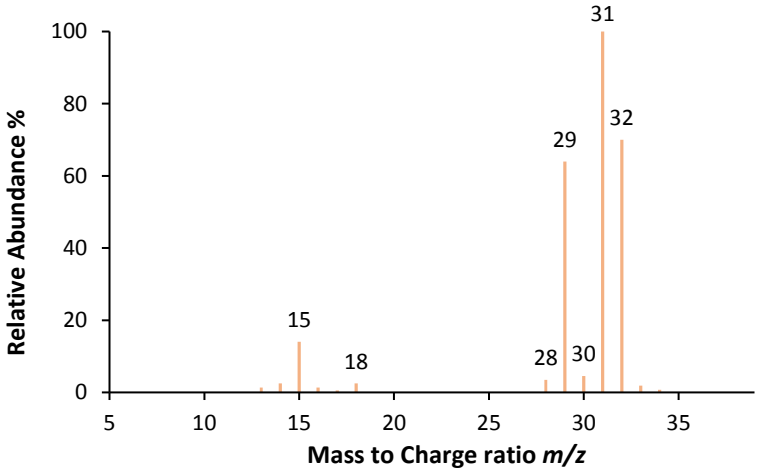

Figure 1.4 Mass spectrum of methanol

The most abundant peak (the base peak) with 31 m/z and relative abundance of 100 %. The other peaks abundance is proportional to the base peak.

1.6.2.1 Ionisation methods

Numerous ionisation methods are available in today's spectrometers (Munson and Field, 1966; Young, 1989). However, Matrix-assisted laser desorption ionisation (MALDI) and Electrospray Ionisation (ESI) are the two most common "soft ionisation" methods that transformed MS (Portolés *et al.*, 2011). The term "soft" relates to the reduced amount of fragmentation associated with these methods. MALDI, as the name refers involves the use of a matrix, typically an organic-based compound possessing 1) a wavelength equivalent to that of the laser pulse and 2) an acidic proton (Hillenkamp *et al.*, 1991). Briefly, the analyte of interest is mixed with the matrix; this mixture is then dried on the MALDI target for a known period of time, after which the laser is powered generating the singly charged analyte ions (Liyanage and Lay, 2006; Hoffmann and Stroobant, 2007b). Although, the final result is proton-transfer to the analyte, the exact mechanism of MALDI is not yet fully understood

(Garcia and Gaskell, 2006). The application of MALDI-MS has been recently reviewed within the field of both virology and clinical microbiology (Cobo, 2013; Fournier *et al.*, 2013).

ESI-MS is more amenable to analysis of biomolecules not suitable to other conventional analytical methods. The only requirement is that the molecule of interest to be analysed possesses a high degree of polarity, to facilitate the attachment of a charge. In ESI, the sample becomes ionised once the inlet stream exits the voltage-applied capillary. This generates a spray of charged droplets that are desolvated as they pass through a series of stages with decreasing pressure (Fenn *et al.*, 1989). A more detailed account of the mechanism of ESI can be located in the review published by Bruins (Bruins, 1998). Unlike MALDI, ESI produces analyte ions multiply charged, thereby expanding the range of masses to be analysed. Additionally, ESI is compatible with online-separation techniques such as high performance liquid-chromatography (HPLC-MS) (Ho *et al.*, 2003). This provides high sample throughput and rapid analysis without compromising data quality. For more complex mixtures, infusion mode or nano-electrospray (nano-ESI) is implemented, a scaled-down version of electrospray. Operating without pumps, with low flow rates and small sample volumes (*ca.* 1 μL) enables complex mixtures to be sequenced (Juraschek *et al.*, 1999).

1.6.3 Mass analyser

The resultant ions can be separated either by a) time-of-flight (TOF-MS), b) quadrupole electric fields or c) selective ejection of ions (Banerjee and Mazumdar, 2012). Mass spectrometers operated by MALDI or ESI ionisation methods, can

possess either of these mass analysers. However, the former two will be the only ones discussed here. MALDI mass spectrometers are typically coupled to a TOF mass analyser. As previously described, after the dried-mixture has been subjected to the laser pulse, the resultant ions are sped up to a fixed amount of kinetic energy and travel down a flight tube. Smaller ions possess a higher velocity and are detected prior to the larger ions. This generates a time-of-flight (TOF) spectrum (Emonet *et al.*, 2010). In comparison, ESI can be coupled with quadrupole (Q) or ion trap analysers. The quadrupole acts a mass filter, which only allows specific ions of particular masses to pass through. To improve the sensitivity and resolution of MS, a series of mass spectrometry was developed. This is referred to as tandem mass spectrometry or MS/MS (Hoffmann, 1996). In this mode, the analyte ions of interest are selected in the first quadrupole, then subjected to fragmentation in the second quadrupole and finally analysed in a TOF device, Q-Q-TOF. MS/MS resultant spectra possess a high degree of accuracy and resolution. There are different fragmentation methods available (Zubarev *et al.*, 1998; Syka *et al.*, 2004; Zubarev, 2006; Han *et al.*, 2008), but collision-induced dissociation (CID) (Shukla and Futrell, 2000) is predominately used in proteomics studies. CID will be explained in more detail in section 1.6.4.1.

For more complex mixtures, commonly encountered in proteomics, the components of tandem MS/MS, TOF and high performance liquid chromatography (HPLC) (McMaster, 2006) have been coupled. The use of HPLC-ESI-MS/MS within the field of proteomics can be attributed to the work performed by Hunt and his colleagues (Hunt *et al.*, 1992; Aebersold and Mann, 2003). Firstly, the analyte of interest is fractioned on an HPLC column. Eluting at different retention times due to the hydrophobicity, each resultant fraction is then subjected to a triple quadrupole mass

spectrometers (QQQ-MS) possessing three quadrupole analysers. These are arranged in a linear configuration as shown in Figure 1.5, where Q1 and Q3 behave as mass analysers, with the intermediate quadrupole (Q2) functioning as a collision cell, as described by (Wink, 2006).

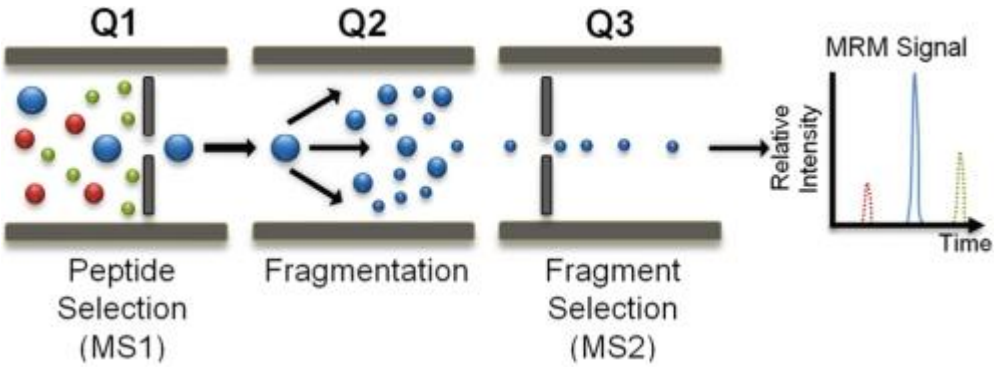

Figure 1.5 Schematic of triple quadrupole (QQQ) mass spectrometer.

The first quadrupole filters specific known ions which fragmented CID in the second quadrupole. The entire fragmented ions are scanned by the third quadrupole to record the relative intensity. Figure adopted from Boja and Rodriguez (2011).

QQQ spectrometers operate on the basis of a precursor/product ion combination. Simply, the precursor ion refers to the major ion produced during ESI, whereas the product ion refers to the ion generated after being subjected to CID. QQQ spectrometers provide four different scanning modes, product, precursor, neutral scans and multiple reaction monitoring. The difference between these modes depend on how the Q1 and Q3 are set (Pitt, 2009). In the product scan mode, the Q1 is fixed and the Q3 is scanned. This is commonly referred to as selected reaction monitoring (SRM). SRM is commonly used in quantification experiments and will be discussed in section 1.6.5. MS-based proteomics could investigate a wide range of materials from a single cell or the entire tissue. However, prior to subjecting peptides for MS analysis, they

must first be correctly prepared. Therefore, an overview of the preparation method used in this thesis is provided, in addition to peptide fragmentation and identification.

1.6.4 Proteomic workflow

The protein of interest is commonly identified from the SDS gel-electrophoresis using Coomassie staining method (Blakesley and Boezi, 1977). The proteins band is cut from the gel first and subjected to protein extraction process. Alternatively, characterisation of the proteins can be performed on the entire mixture of proteins. In both cases, the extracted proteins are enzymatically digested to peptides, most commonly using trypsin (Huynh *et al.*, 2009). This process of analysing proteins based on digested peptides is referred to as "shotgun/bottom-up" proteomics (Wolters *et al.*, 2001; Yates, 2004; Zhang *et al.*, 2013).

For nanoLC-MS, the enzymatically digested peptide mixture is then desalted and concentrated. Extreme caution should be taken to avoid contamination with human keratin(s) (Gaspari and Cuda, 2011). Keratins are digested equivalently to the protein(s) of interest, they will complicate spectra and make it difficult in low abundant samples (Westermeier *et al.*, 2008a). The highly concentrated and salt-free peptide is eluted onto the nano-electrospray needle; a nanoLC reverse-phase column separates the peptides by hydrophobicity, subject to ionisation and transferred to the mass spectrometer for analysis, as summarised in Figure 1.6. NanoLC-MS spectrometers have reported sensitivity at 1 – 10 fmol and even in the low attomole range (Cox *et al.*, 1994). This increased sensitivity can be attributed to the small column diameter and lower flow rates (Mann *et al.*, 2001).

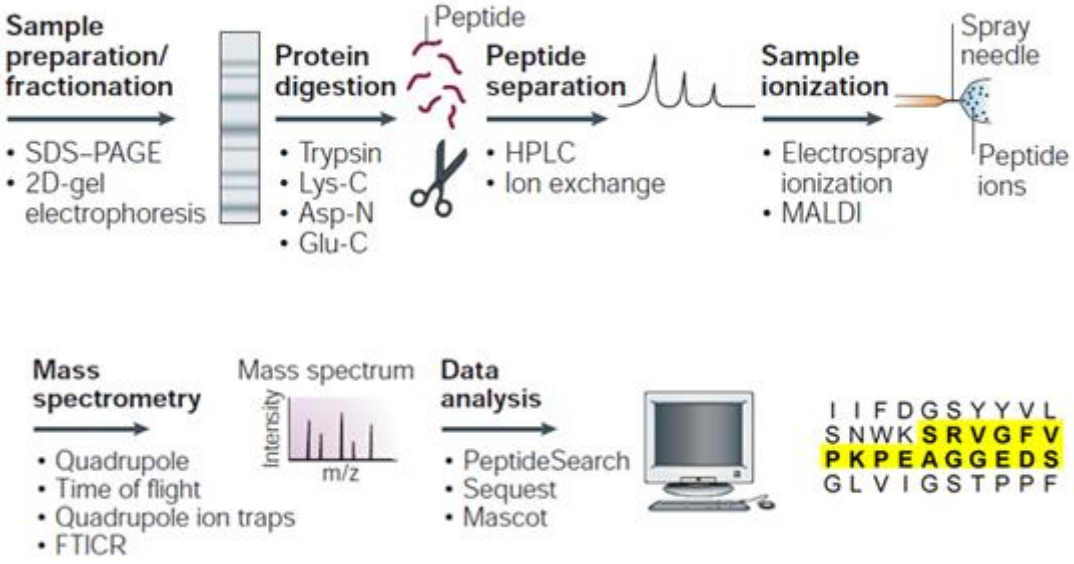

Figure 1.6 Overview of sample preparation and protein analysis and identification.

The extracted proteins are digested by numerous enzymes. The obtained peptides are separated on HPLC column and ionized by means of ESI or MALDI. The ionized fragments ions can be analysed by different type of MS. The final step is to search the generated peptide mass spectra against protein database using one of a wide range of internet database searching tools for the purpose of peptides and proteins identification. This figure adopted form Steen and Mann (2004).

1.6.4.1 Peptide fragmentation

Aforementioned, the product ion (Figure 1.5) is formed from the dissociation of the precursor ion by collision (CID). As shown in Figure 1.7, fragmentation generally occurs at the amide bond forming b and y ions, when the charge is retained by the amino-terminal and carboxyl-terminal fragment, respectively. The subscript Roman numeral refers to the number of residues in the fragment. The nomenclature was first proposed by Roepstorff and Fohlman (1984) and later modified by Johnson *et al.* (1987). Tryptic peptides often carry two or more charges (Steen and Mann, 2004).

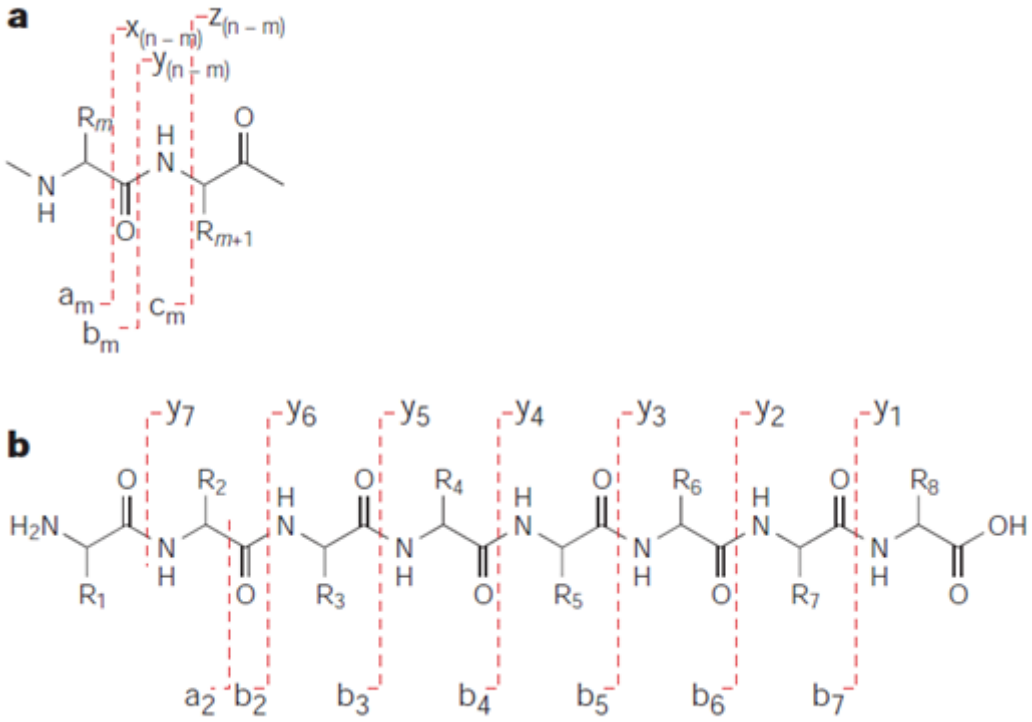

Figure 1.7 Fragmentation pattern of a chemical structure of a peptide subjected to CID by MS/MS.

The b and y ions refer to the charge retained on the amino and carboxyl-terminals, respectively. The Roman numerals refer to the number of residues within the fragment. Figure adopted from Steen and Mann (2004).

The experimentally derived mass spectrum is often referred to as the peptide mass fingerprint (PMF) (Westermeier *et al.*, 2008b). Despite the advances in HPLC-ESI-MS/MS, for peptide sequencing numerous spectra are generated and analysis is often time-consuming and tedious. Thereby, the development of protein databases has sped up protein analysis.

1.6.4.2 Identification by database searching

The databases operate on the concept of correlating the PMF to theoretical mass spectra of proteins cut *in silico*. The confidence level of the match is determined via

various algorithms using mass accuracy and percentage of protein sequence covered (Perkins *et al.*, 1999). As reported by Mann *et al.* (2001) for unequivocal assignment five peptides of the protein and 15 % of the protein requires to be covered (Mann *et al.*, 2001). There is a wide range of internet accessible databases tools, common ones include Mascot (Clauser *et al.*, 1999), MS-Fit (Zhang and Chait, 2000) and Profound (Thiede *et al.*, 2005). Mass spectrometer companies often specify a vendor software as stated by Webhofer and Schrader (2011).

1.6.5 Protein(s) quantification workflow

The colour gradient obtained from gel staining provides a qualitative estimate of the amount of protein(s) present. However, for low abundance protein(s) this method is unsuitable. For more accurate quantification of protein(s) present, alternative quantification methods can be utilised. There are two common HPLC-ESI-MS/MS-based quantification methods; isotope labelling or label-free (Cox and Mann, 2011; Liebler and Zimmerman, 2013; Zhang *et al.*, 2013). Quantification of proteins in isotope labelling is more accurate. However, label free method avoids drawbacks often associated with isotope labelling such as extra sample processing steps, cost of labelling reagents ($H_2{}^{18}O_2$) and inefficient labelling. Isotope labelling was not used in this thesis, for additional information the reader is recommended to the relevant literature (Zhang *et al.*, 2013).

There are two quantification options in the label free method; either the frequency of a particular peptide is measured as the relative abundance or the chromatographic signal intensity is measured. This is commonly performed using selected or multiple reactions monitoring, SRM (Lange *et al.*, 2008; Picotti and Aebersold, 2012) and

MRM (Addona *et al.*, 2009). As described previously in section 1.6.3, this mode can be achieved by setting the Q1 and Q3 quadrupole's of the QQQ mass spectrometer. In SRM mode, Q1 is fixed to detect specific ions of interest to be later subjected to collision in the Q2 component. From the resultant chromatogram of the ion, the intensity of each fragment is used for quantification purposes. This highly selective method is often referred to as targeted analysis (Cox and Mann, 2011; Marx, 2013).

Within SRM analysis, different time acquisitions can be selected or unselected, referred to as scheduled and unscheduled SRM analysis, respectively. Scheduled SRM is more efficient and sensitive, as signals are only acquired during the specified window (Liebler and Zimmerman, 2013). An important development in targeted analysis was the creation of Skyline, an open source platform for both experimental and down-stream data analysis. Skyline offers users an array of rich data to inspect, analyse and deduce their data. This powerful tool in the field of proteomics enables in-depth analysis with statistical function (MacLean *et al.*, 2010).

Of the main advantages of the SRM performed on the QQQ-MS is the significant reduction in noise as a consequence of having the two filtering steps as well as the high sensitivity. However, one of the main disadvantages of using SRM in proteomics-based quantification is the time-consuming process having to establish the appropriate fragment ions, referred to as "transitions", for each targeted peptide in advance (Lange *et al.*, 2008; Gallien *et al.*, 2011; Picotti and Aebersold, 2012; Kinter and Kinter, 2013c).

1.7 The aim of this thesis

This thesis aims to elucidate the mechanisms underlying Nitrogen and minerals mobilisation during seed development stages in *Brassica napus* L. Understanding the pathways involved will lead to the ability to breed for improved minerals use efficiency.

1.7.1 The objectives

The objectives of this thesis are:

- To understand the breadth of the genetic variation in N and other minerals use between various *B. napus* L. cultivars growing in the field under no fertiliser application, through mineral elements analysis of various tissues at different growing stages.
- To identify possible vegetative storage proteins and/or other key genes involved in N remobilisation within two genotypes, Ningyou 7 and Tapidor DH, and to determine if changing the sink/source relationship between two varieties under glasshouse conditions can alter the expression of putative vegetative storage proteins.
- To develop a screening strategy to identify candidate genes underlying Quantitative Trait Loci that control Nitrogen remobilisation in *B. napus*.
- To map QTL associated with yield and yield related traits as well as mineral nutrients related traits in order to improve mineral use efficiency in *B. napus*.

Chapter 2 Variation Underlying Nitrogen Accumulation in *Brassica napus* L.

2.1 Introduction

OSR has been shown to have low N Use Efficiency (Sylvester-Bradley and Kindred, 2009; Sieling and Kage, 2010). This has been attributed to low N uptake rate (Berry *et al.*, 2010b; Schulte auf'm Erley *et al.*, 2011; Ulas *et al.*, 2013) and poor N redistribution (Malagoli *et al.*, 2005a; Koeslin-Findeklee and Horst, 2016). It has been shown by many studies that the amount of N remobilised does not exceed 45 to 70 % regardless of N availability (Rossato *et al.*, 2001; Gombert *et al.*, 2010; Zhang *et al.*, 2010).

It has been shown by Rossato *et al.* (2001) that more than 15 % of the total plant N is sent back to the soil by dead leaves dropped before the seed development stages, in contrast to 26 % residual N in stems and roots at seed maturity. Hirel *et al.* (2007) also confirmed that a large portion of the total N absorbed during the vegetative growth is returned to the soil with falling leaves. Nevertheless, different studies have shown that the loss of N associated with stem and taproot at harvest is massively larger than leaves. Ulas *et al.* (2013) reported that the loss of N associated with stem (33 kg N/ha) was significantly greater than with leaves (13 kg N/ha) in winter OSR varieties grown under field conditions. In contrast, without added N fertiliser, the quantity of N loss from leaves does not exceed 3.5 kg/ha (4.3 % of the total plant N at harvest). Moreover, the study of Koeslin-Findeklee and Horst (2016) revealed that more than 41 % of the total plant N residual at maturity observed within stem (11.8 kg N/ha) and taproot (6.4 kg N/ha) compared to 7.3 % with leaves (3.3 kg N/ha). Similarly, McGrath and Zhao (1996) showed that stem exhibited 35 – 40 % of the total plant N at harvest. The amount of stem residual N was greater in the study of Berry *et al.* (2010b), ranged between 18.5 and 27.9 kg N/ha under low N supply. All of these studies summarise

the inefficiency of the *B. napus* L. vegetative tissues in remobilising N to the pods during seed filling phases as well as the importance of the stem and root as a key storage of N.

Varietal differences in N content have been reported in *B.napus* within harvest seeds among field-grown 36 genotypes (Kessel *et al.*, 2012), 17 genotypes (Schulte auf˙m Erley *et al.*, 2011), 10 genotypes (Berry *et al.*, 2010b) at low N supply, 4 genotypes grown hydroponically at low and high N supply (Svečnjak and Rengel, 2006b) and glasshouse-grown 12 canola genotypes (Balint and Rengel, 2008) as well as within stem N concentration at maturity (Svečnjak and Rengel, 2006b; Balint and Rengel, 2008) and within root residual N concentration (Svečnjak and Rengel, 2006b). However, genotypic differences in stem residual N concentration have not been observed among field-grown and N-efficiency contrasting 4 genotypes (Ulas *et al.*, 2013), in taproot, stem and seeds N concentration at maturity among 2 genotypes at low N supply (Koeslin-Findeklee and Horst, 2016) and in root N composition among 8 genotypes grown on a mixture of soil and perlite under controlled condition at the vegetative growth (Lee *et al.*, 2015).

The interaction between mineral elements within OSR plants have been reported in many studies and within species such as *Arabidopsis thaliana* (Baxter *et al.*, 2012) and *B. napus* (Bus *et al.*, 2014; Thomas *et al.*, 2016). Such associations could be due to shared uptake and regulation pathways or the pleiotropic effects of genes (Bus *et al.*, 2014). This relationship between mineral elements has been demonstrated to be tissue-specific (Buescher *et al.*, 2010; Baxter *et al.*, 2012; Thomas *et al.*, 2016). Strong association between shoot N concentration and shoot P and Mg concentration observed in the study of Broadley *et al.* (2004) across 117 angiosperm species.

Many studies has previously been conducted on *B. napus* in which N content within seeds and stem were investigated, in contrast only a few studies have been performed on root N content. As yet there is no study investigating partitioning between different plant organs such as stem and root nor investigating lateral root N content. It was thought that by sectioning stem and root at two growth stages, it would be possible to monitor closely both N redistribution and N residual concentration within the plant organs. By doing this among a range of *B. napus* genotypes, it would be possible to reduce residual N and hence increasing N use efficiency.

2.2 The aim of this chapter

The aim of this chapter is to quantify N concentration in several plant organs of stem, root and seeds at growth stage 6.2/6.3 and at maturity in a diversity collection of *B. napus* L. genotypes grown in the filed under low level of available N, without addition of fertiliser. Furthermore, to determine the relationships between N and a set of eleven mineral nutrients within the analysed tissues for better understanding of the mechanisms control N accumulation in the plant.

2.3 Material and methods

2.3.1 Low Nitrogen OREGIN field experiment

A field experiment was conducted in Harpenden, UK, at Rothamsted Research (Latitude 51°80'48.93" N, Longitude 0°37'52.31" W and Evaluation of 132 m above sea level) during 2010/2011 growing season as part of the Oilseed Rape Genetic Improvement Network (OREGIN) diversity field trials (Hopkins *et al.*, 2010-2011). The trial included 205 *B.napus* varieties of which 84 winter oilseed rape, 55 spring oilseed rape, 34 Swede and 32 other (fodder rapes/kales, forage) varieties. The trial was sown on the 6th and 13th of September 2010 at 60 seeds/m^2 and grown using residual soil total available N without addition of fertilisers. The soil type was classified as clay-with-flints (Batcombe). The field had been used previously for spring barley. Soil analysis was carried out by Rothamsted Research as part of the trial, where 30-cm soil samples were collected and analysed. The soil content of the total residual available N averaged 22 kg N/ha at the time when the first dose of fertiliser would normally be applied, of which 9 kg/ha were as NO_3^- and 13 kg/ha were as NH_4^+. The average annual air temperature at Rothamsted Research site was 9.7 °C. The total precipitation was 630 mm during the growing season, of which 220 mm were received between February and July. A Randomised Complete Block design using plot layout was used in two replicates, each block measuring 39.75 m x 34.75 m. The varieties were randomised on the plots within each block, 432 plots in total each measuring 1.5 m x 1.8 m were planted. Nets were set up around the field perimeter to protect against rabbits during the early period of establishment, and humming tape and flappers were used to protect against pigeon. Pesticides and fungicides were applied

to control pests and diseases according to the Rothamsted Research standard procedures and when was necessary.

Materials were collected on two occasions from one replicate representing two different growth stages when nitrogen mobilisation was expected to occur. The first stage was the growth stage (GS) of seed development when most seeds appear translucent but have full size named as GS 6.2, and the stage when most seeds are green named as GS 6.3 according to the *B. napus* growth stages code of Sylvester-Bradley and Makepeace (1984), these plants were sampled on 2 June 2011. The second stage was at harvest, with plants sampled on 14 July 2011.

2.3.2 Plant sampling at seed development stage GS 6.2/6.3

Materials were collected from three plants from each of the following 14 varieties of OSR (Canberra, Darmor, FD502, Grizzly, Lioness, Ningyou 7, NK Bravour, PR45-D01, Royal, Sun, Tapidor ADAS, Tapidor DH, Winner and Yudal). The varieties were selected based on LINK project report LK0979 conducted by Berry *et al.* (2011) in which these varieties have shown differences in N uptake and utilisation efficiency. Plants were manually excavated using pickaxe, shovel and trowel. Care was taken to loosen soil some distance from the roots and the roots eased out with as much care as possible. This ensured that the majority of the roots if not all were collected. Plants were transported whole in individual bags to Wellesbourne where they were then processed.

Each plant was divided into seven tissues from roots, stem and seeds as illustrated in Figure 2.1 below. The stem was divided into three sections; the bottom of the stem (Stem B), the middle of the stem (Stem M) and at the top of the stem (Stem T). Plants

roots were washed with deionized water (dH_2O) prior to sectioning. The roots were divided into three sections; lateral roots (L.root), the top of taproot (T.root T) and the bottom of taproot (T.root B). 10 cm of each section, when it is available, was first weighed (fresh weight) then dried in the oven at 60 °C until constant weight was reached and the weight noted (dried weight; DW). Samples were subsequently ground by a machine mill to a size which would pass through a 0.1 cm sieve and subjected to Kjeldahl digestion for estimating total Kjeldahl Nitrogen concentration. The total concentration of other 11 mineral elements P, K, Mg, Mn, Ca, Na S, B, Cu, Fe and Zn were also determined (see Chapter 3).

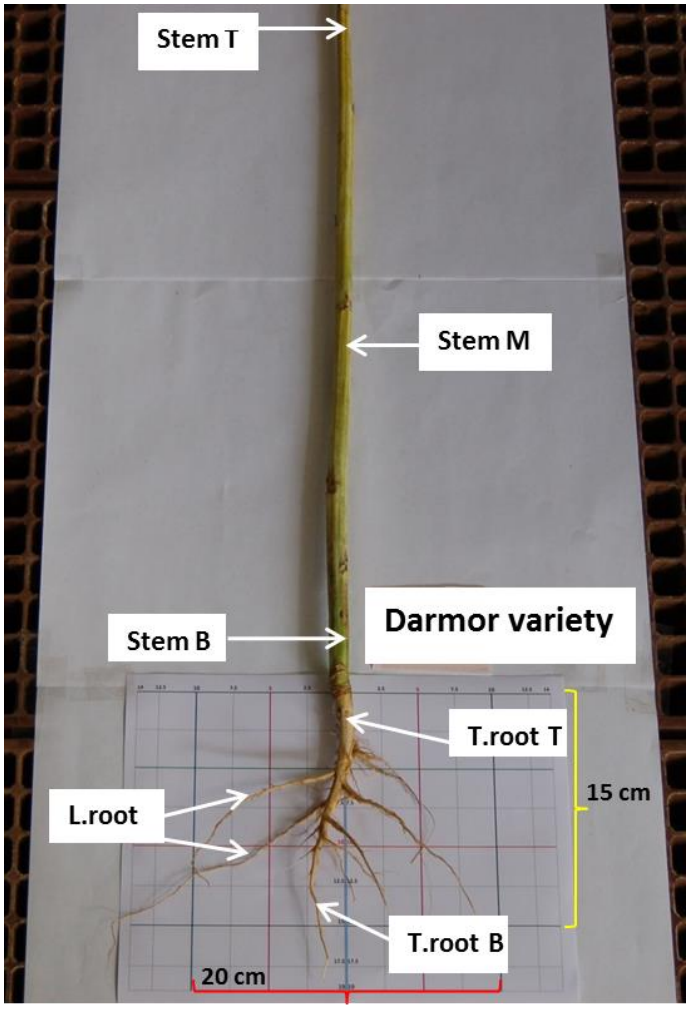

Figure 2.1 Illustration of plant sampling

This picture is of one of the Darmor plants collected. It is used to illustrate the sampling carried out. 10 cm of tissue was sampled from each area. 3 tissue sections were taken from the stem, the bottom of the stem in blue (Stem B), the middle of the stem in red (Stem M) and the top of the stem in green (Stem T). 2 tissue sections from taproot, the top and bottom (T.root T) and (T.root B), respectively. One tissue from Lateral roots (L.root). The scaled white paper underneath the roots is A4 paper (21 x 29.7 cm), and the bigger paper is A3 (29.7 x 42 cm).

2.3.3 Plant sampling at harvest

Similarly, materials from this trial were collected when the plants were due to be harvested. Materials were collected from 30 varieties, 14 OSR varieties as previously

mentioned in section 2.3.2 and an additional 16 OSR varieties. Due to financial limitations, if was not possible to sample all the lines used within the field trial although this would have been the ideal. The additional lines were selected based on further information obtained from Dr Peter Berry and based on their potential for mapping using new populations for example, the varieties TN145, TN172 and Temple were selected for the development of new mapping populations, the varieties Best of All and Vige DH1 were selected as outliers from data obtained on N uptake efficiency in previous OREGIN field trial.

The 30 lines harvested were also selected to represent the 3 distinctive crop types;

I. **Winter OSR:** (Canberra, Darmor, English Giant DH1, FD502, Grizzly, Lioness, Ningyou 7, NK Bravour, PI271451, PR45-D01, Red Russian, Royal, Sun, Tapidor ADAS, Tapidor DH, Temple, TN145, TN172 and Winner).
II. **Spring OSR:** (Cubs Root DH1, Drakkar, Regina II DH1, Stellar DH and Yudal).
III. **Swede:** (Best of All, Drummonds PT, Jaune, Petranova, Turnip Hybrid and Vige DH1).

At harvest, due to the completion of the trial it was possible for us to sample five plants from each variety. These were sampled as described in section 2.3.2 above. Samples were ground by a machine mill to pass through a 0.1 cm sieve and subjected to Kjeldahl digestion for estimating total Kjeldahl Nitrogen concentration. The total concentration of other 11 mineral elements P, K, Mg, Mn, Ca, Na S, B, Cu, Fe and Zn were also determined.

2.3.4 Preparation of Kjeldahl digestion acid

Prior to the process of sample digestion, a catalyst was added to the acid which accelerates the rate of reaction and completeness of converting the N in plant tissue to ammonium sulphate ($(NH_4)_2SO_4$) (Horneck and Miller, 1998). Therefore, 0.5 g of selenium was weighed and transferred to a 1 L conical flask; 500 ml of analytical grade sulphuric acid (H_2SO_4 98%) were added. The flask was heated (swirled every two minutes to prevent the selenium from setting) on a pre-heated hotplate at 85 °C for 20 minutes or until opaque solution became dark green, indicative that the selenium had dissolved. The flask was left overnight to completely cool.

2.3.5 Sample preparation and analysis

All samples were oven-dried at 60 °C for three days until a constant weight showed. Materials were milled to 2 mm by machine mill and oven dried prior to digestion to ensure complete dehydration. Tissue samples (~0.1 g) were placed into a digestion tube containing an anti-bumping granule to which the digestion acid (2 mL) was added and left for 2 h in the fumehood. Operational blank as well as in-house reference material from pooled dried canopy leaves of field-grown *B.napus* cultivar Temple were included in each digestion run. Prior to loading the digestion tubes (57 tubes) into the heating rack, 1 mL of hydrogen peroxide (H_2O_2, 30 % w/w) was added. Digestion tubes were then loaded into the heating rack of the Gerhardt block digestion system and heated at 330°C for 45 m. An additional 1 mL of hydrogen peroxide (H_2O_2, 30 % w/w) was added after the tubes cooled. The tubes were then subjected to 330°C for 30 m, until the solution became clear. Afterwards, reverse osmosis water (R.O. water, 48.6 ml) was added to the tube and mixed well using a WhirliMixer (Fisons,

UK). The solution was then transferred to a scintillation vial. This method was generated by Matthew Mitchell in the mineral analysis laboratory at Warwick Crop Centre (previously known as Warwick HRI) and adopted from Bradstreet (1965); Horneck and Miller (1998) and uses the same standard each time.

For Kjeldahl N, samples were analysed on the flow injection analyser after a 1:100 dilution was performed using FIAstar 5000 Analyzer (supplied by FOSS UK) connected to an auto sampling system (Sampler 5027, FOSS UK). The system is fully controlled by the FIAstar 5000 SoFIA software. After verifying the correct cassette and detector filters, M =590 nm (the wavelength at which all prepared standards and samples are measured), and R=720 nm (the reference standard wavelength for the internal calibration of the instrument) was installed. Using the SoFIA software the ammonium 0-5 mg/L method was selected and the absorbance of the ammonium indicator is checked. The absorbance is adjusted to be in the range of 300 - 500 mAU using dropwise addition of 0.01M sodium hydroxide or 0.01M hydrochloric acid to water depending on the value shown by the indicator. A calibration check is then followed.

The calibration standards were prepared as dilutions (0, 0.5, 1, 2 and 5 mg/L) of 1000 mg/L ammonium-N stock solution, $(NH_4)_2SO_4$. The diluted samples were then moved to 11.5 ml Rohren tubes and placed in the auto sampler and subjected to analysis. During the experimental runs a 1 mg/L calibration check was applied after every 10 samples. 60 samples were analysed in each run and a total of 1394 samples were analysed. The SoFIA software calculated the concentration of ammonium (mg/L) in each sample from which the total Kjeldahl Nitrogen concentration was calculated as

mg/L. the percentage of N in plant tissue was then calculated using the following formula:

$$N\ \% = \frac{\text{N (mg. L}^{-1}) * \text{final diluted volume (ml)}}{\text{dired weight of digested tissue (g)} * 10^4}$$

The principle of this analysis is that a carrier stream of the sample which contains ammonium ions is injected into a stream of sodium hydroxide (NaOH) to form gaseous ammonia. The ammonia gas passes across a gas diffusion membrane into an indicator stream where it will react with an admixture of acid-base indicators. The resulting colour change could be monitored photometrically at 590 nm (Crompton, 2001).

2.3.6 Data analysis

Analysis of Variance (ANOVA) was performed to study the effect of the treatments; crop type, genotype and tissue, and the interaction between them on the concentration of Nitrogen (%DW) at both growth stages; GS 6.2/6.3 and harvest according to the model; [genotype x tissue] at the GS 6.2/6.3, [(croptype/genotype) x tissue] at harvest and [growth stage x variety x tissue] to compare between the two growth stages. TukeyHSD analysis at 1 % significant level was used as a *Post Hoc* test when overall significant differences were observed. The proportion of total and partial variance in N concentration that attributes to each treatment factor was reported as omega squared (ω^2) and partial omega squared (ω^2_p) and calculated following the equations below (Olejnik and Algina, 2000):

$$\omega^2 = \frac{SS_{treatment} - df_{treatment}\ MS_{error}}{SS_{total} + MS_{error}}$$

$$\omega^2_p = \frac{SS_{treatment} - df_{treatment} MS_{error}}{SS_{treatment} + (N - df_{treatment}) MS_{error}}$$

Where *SS* is the sum of squares, *MS* is the mean of squares, *df* is the degree of freedom and *N* is the total number of observations. The variety mean value and standard error of the mean (SEM) were determined where n =3 at GS 6.2/6.3 and n =5 at harvest. Outliers in boxplot are data values that are 1.5 times the interquartile range (1.5 x IQR) from either end of the box. Pearson correlation analysis was conducted to determine the Correlation Coefficient (*r*) and to investigate relationship between the variables (between N and other 11 mineral elements across seven plant tissue types) using genotype means. The linear relationship was examined by Regression Analysis. The equation of line of the best fit ($y = b + ax$) and the coefficient of determination r^2 for simple regression analysis and adjusted R^2 for multiple regression analysis were all determined. All statistical analyses were performed using the R environment for statistical computing and graphics (version 3.3.2, 2016).

2.4 Results

Total Kjeldahl N concentration [N] as a percentage of dried weight, (%DW) have been determined in different plant tissue types of root, stem and seeds during two different time points of plant growth among a number of *Brassica napus* L. accessions (14 and 30 for GS 6.2/6.3 and harvest, respectively) grown under low N supply (no N fertiliser) in a field experiment.

2.4.1 Variation in N concentration at GS 6.2/6.3

The analysis of variance between two subjects (tissue x variety) was conducted and revealed significant differences (P >0.0001) in N concentration between tissues F(6,196) =3022.3 and between varieties F(13,196) =11.4 and there was an interaction between tissue and variety F(78,196) =4.68, P <0.0001. A large proportion of the total and partial variance >96 % in [N] attributed to tissue type, whereas genotype accounted for about 32 % of the partial variance and only 0.7 % of the total variance measured as the partial omega squared and omega squared, respectively. The 14 OSR varieties grown under a low N supply (without N fertiliser) show considerable variation in N concentration of all analysed seven tissues of stem, roots and seeds Figure 2.2 (page 66) during the seed development stage GS 6.2/6.3. As an average across all OSR varieties, it is apparent seeds are the greatest store of N with about 2.6 %DW. The next highest store of N was observed in the bottom of the stem (0.6 %DW) followed by the top of the stem, lateral roots, the middle of the stem, the top of tap root, and finally the bottom of tap root with 0.34, 0.2, 0.15, 0.14 and 0.13 %DW, respectively (Appendix 1, Table 1).

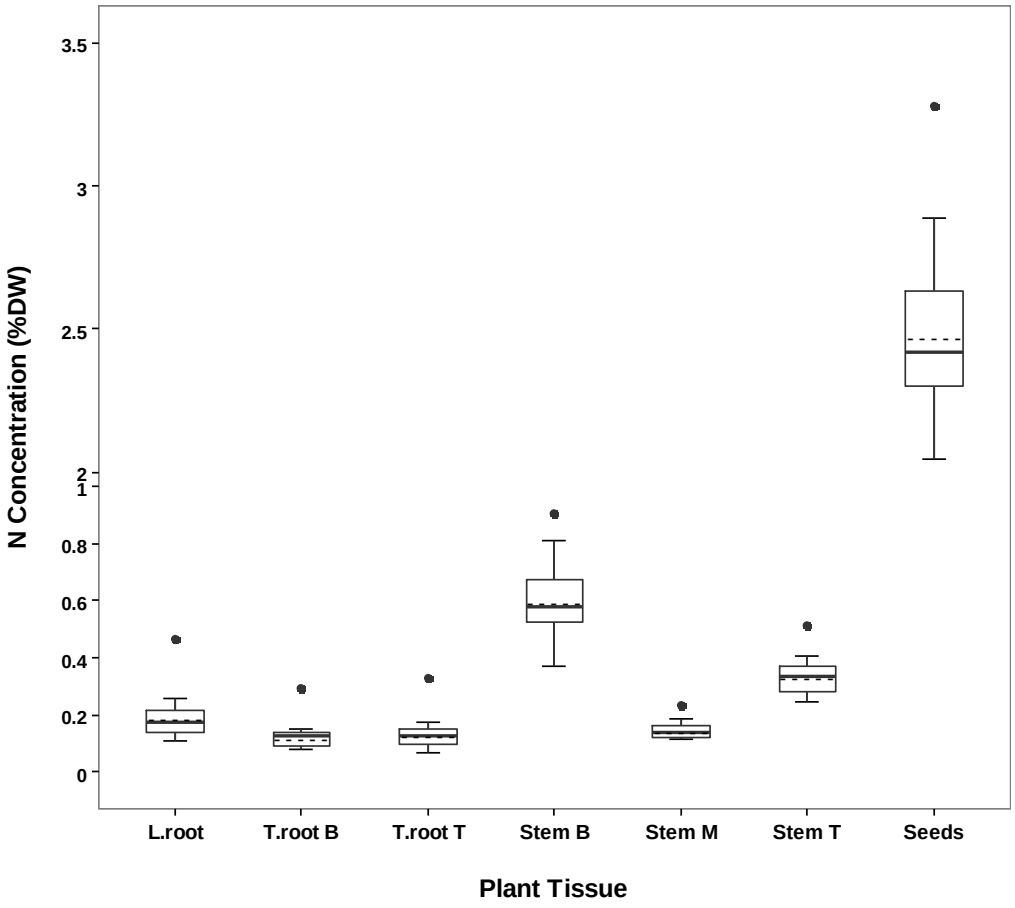

Figure 2.2 Variation in N concentration of different plant tissues among 14 *Brassica napus* L. accessions at the seed development stage GS 6.2/6.3

Varieties were grown at low level of N supply in a field experiment. Total N concentration was measured by Kjeldahl method. Data are the estimated means (n=3) of N concentration in a percentage of dried weight (DW). Plant tissues are lateral roots (L.root), the bottom of taproot (T.root B), the top of taproot (T.root T), the bottom of the stem (Stem B), the middle of the stem (Stem M), the top of the stem (Stem T) and seeds. The lower and upper boundaries of the box represent the 25 and 75 percentiles, respectively. The solid and dashed lines within the box represent the median and mean, respectively. Whiskers closest and farthest to zero represent the smallest and largest non-outliers in the data set, respectively. Circles represent outliers.

There is moderate variation in N content of the bottom of the stem ranged from 0.37 %DW in the Sun variety to about 2.5-fold range in the Tapidor DH and Ningyou 7

varieties. Two-fold range of variation was observed in N content in the middle of the stem within the same genotypes to Stem B Figure 2.2. However, a different pattern of two-fold of variation was observed in the top of the stem where the varieties Ningyou 7 and Darmor are showed the lowest and highest concentration from 0.25 to 0.51 %DW, respectively (Appendix 1, Table 1). During this growth stage the accumulation of N varied substantially between the plant roots and stem, with the roots exhibiting the lowest N concentration. Interestingly, within the different sections of the root itself, the concentration of N also varied. Throughout all 14 OSR varieties, the lateral roots possessed a higher N concentration than the taproot. The Ningyou 7 variety demonstrated the highest N concentration in both the tap root sections as an average, and lateral roots with 0.31 and 0.47 %DW, respectively (Appendix 1, Table 1). The varieties, FD502, Royal and Royal demonstrated the lowest concentration of N with more than 3.6-fold range Figure 2.2 (page 66).

Less than 1.6-fold of variation in seed N concentration was observed Figure 2.2 (page 66) and ranged only from 2.14 to 3.38 %DW in Winner and Ningyou 7, respectively (Appendix 1, Table 1). Significant varietal differences (TukeyHSD, P >0.001) were observed within the bottom of the stem and seeds. However, there were no significant varietal differences within the other tissues which might be related to the small sample size (n =3). Some of these *B.napus* L. accessions behave differently, the accession Ningyou 7 was found to have a high N concentration in stem and roots, and in seeds. In contrast, a lower N concentration was observed in both stem and roots of the variety Sun, but higher in the seeds. These obvious differences in the concentration of N in tap roots, lateral roots and the bottom of the stem could be as a result of N

redistribution from the vegetative organs where N is initially stored to the siliques to supply seeds with the required amount of N during development.

2.4.2 Relation between N and other mineral elements at GS6.2/6.3

To further explore the differences of the N concentration in plant tissues and establishing the relation between N and other 11 mineral elements within and between OSR tissue types, Pearson correlation analysis was conducted on all possible 560 pair-wise combinations of seven N traits and other 77 traits (11 mineral elements and seven tissue types). Out of all possible combination, 86 significant ((P <0.05, df =12) and positive (r >0.53) relationships were reported, of which 22 and 64 were within and between tissues, respectively Figure 2.3. Four strong positive pair-wise relationships observed within all root tissue types between N and S (r =~0.9), Ca (0.57< r <0.92), Mg (0.67< r <0.74) and Zn (0.55< r <0.65); all P <0.05. Furthermore, strong association between N and Cu observed within both taproot tissues (0.77< r <0.84, P <0.005). There was also moderated and significant correlation between N and P within L.root (r =54), but this relationship (r =~0.47) was not significant (P >0.05) within taproot tissues. In addition, only one moderate association found within Stem B between N and Fe (r =56) and very strong within Stem M between N and Zn (r =0.84), whereas four positive correlations found within Stem T; N/P, N/Fe, N/Mg and N/K (0.55< r <0.62). Seeds N concentration correlated strongly with S (r =0.82) and P (r =0.58) Figure 2.3 below. It is appeared that approximately 82 and 84 % of the variation in L.root [N] could be significantly accounted for by its relation to S and Ca, respectively Figure 2.4. However, about 89 % of the variance in [N] could be accounted for by the confluence of both Ca and S concentration (multiple regression analysis, adjusted R^2 =0.89; F(2,11) =51.27; P <0.00001).

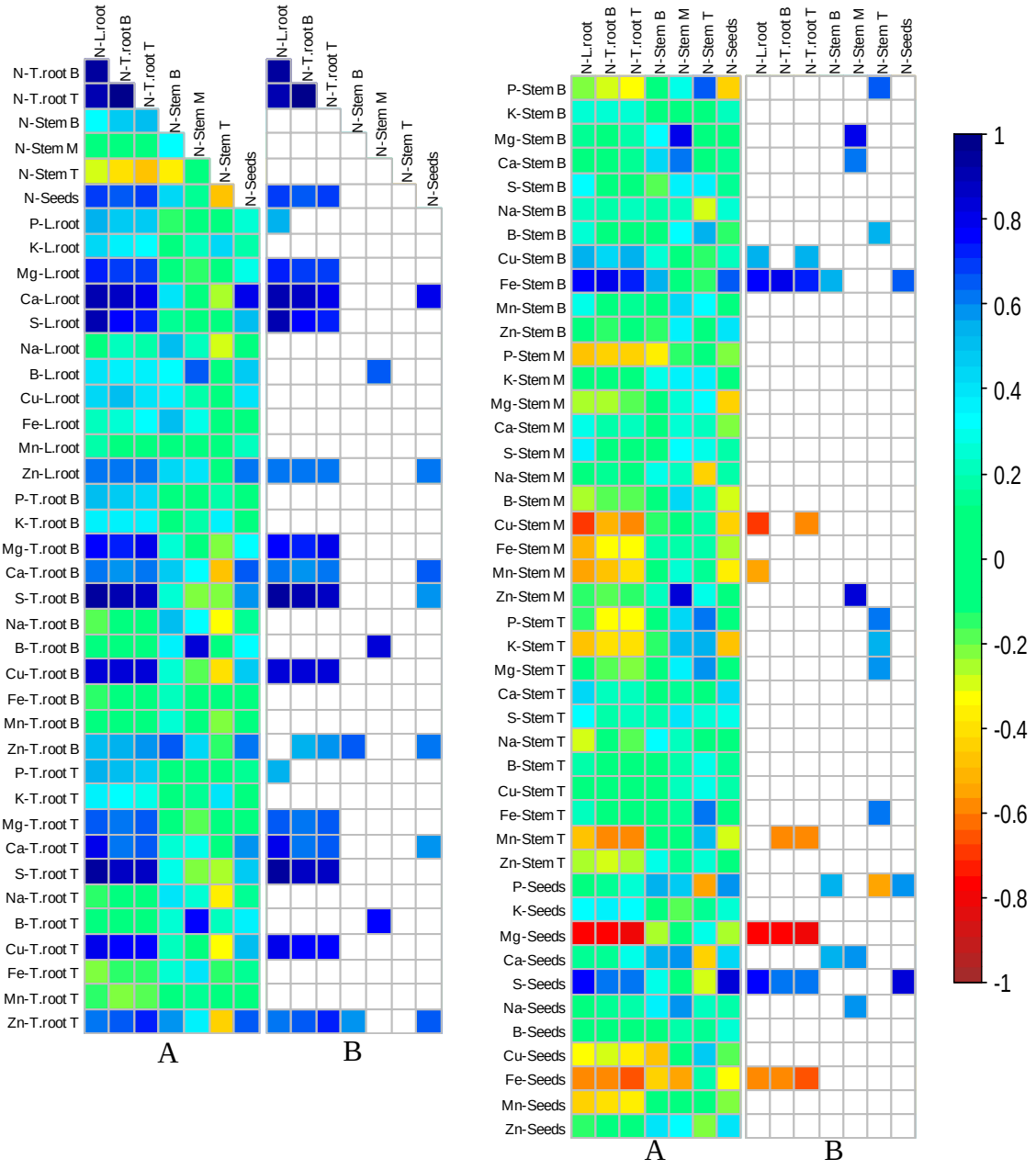

Figure 2.3 Pair-wise correlation analysis between N traits and other 77 traits in 14 *B.napus* genotypes at GS6.2/6.3.

N concentration within seven tissues of root (L.root, T.root B and T.root T), stem (Stem B, M and T) and seeds consist N traits. 11 mineral element concentrations within seven tissues consist 77 traits. (A) Represent all 560 possible pair-wise correlations. (B) Represent only significant correlation (P <0.05). Data used are genotype mean (n =3). Correlation coefficients panel are placed to the right and scaled from -1 (dark brown) to +1 (dark blue).

Furthermore, S and Cu significantly explained about 77 and 60 % of the variation in T.root T [N], respectively, S and P significantly accounted for 67 and 33 % of the variation in seeds N concentration, respectively Figure 2.4 (below). The strongest positive relationships between tissues were in N concentration between all root tissues as well as in [N] and [S] between root tissues ($0.89< r <0.97$); all $P <2.3*10^{-5}$ Figure 2.3 above. Approximately 86 - 94 % of the variance in N concentration is shared between all root tissue types, in contrast to only 43 - 47 % shared variance between seeds [N] and [N] within all root tissue types.

12 significant negative ($P <0.05$, df =12, $r <-0.53$) pair-wise relationships were only found between the above ground tissues, none of these were within tissues. The strongest negative relationships observed between root N concentrations and seeds Mg concentration ($r = \sim -0.78$) Figure 2.3 above. 58 - 61 % of the variation in seeds Mg concentration could explained by its relation to root N concentration. Interestingly, there were a moderated negative correlation between the top of the stem and Stem B, taproot and seeds, however this association was not statistically significant which might be due to the small sample size (n =14).

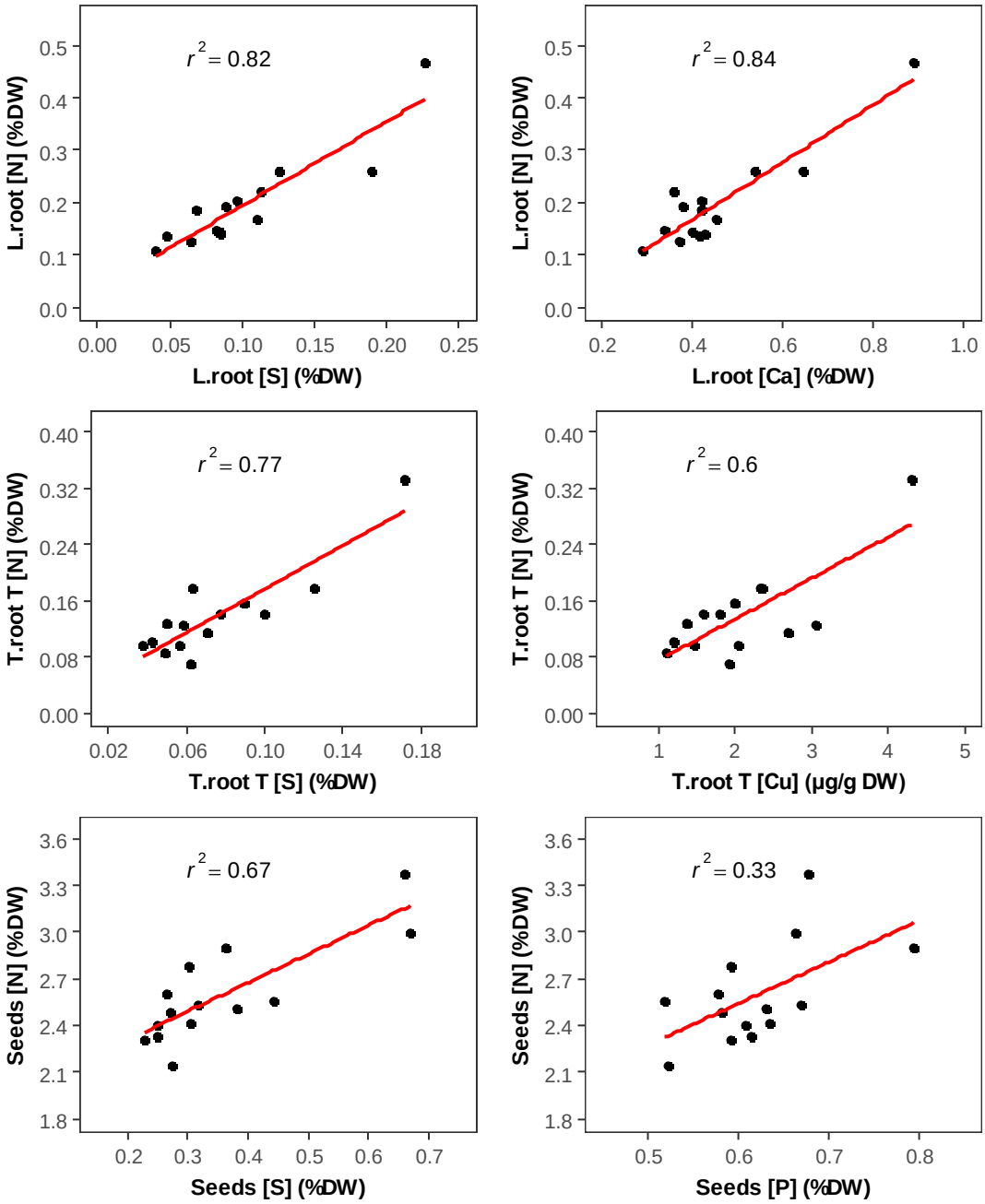

Figure 2.4 Relationship between N concentration and S, Ca, Cu and P concentration within different tissues at GS 6.2/6.3.

Data are the genotype mean (n =3). The red line represents the line of best-fit. Within L.root $y = 0.03 + 1.61x$; r^2 =0.82 (N and S), $y = -0.05 + 0.55x$; r^2 =0.84 (N and Ca); both P <0.0001. Within T.root T $y = 0.02 + 1.54x$; r^2 =0.77 (N and S), $y = 0.02 + 0.06x$; r^2 =0.60 (N and Cu); both P <0.005. Within seeds $y = 1.93 + 1.84x$; r^2 =0.67; P <0.0005 (N and S), $y = 0.94 + 2.67x$; r^2 =0.33; P <0.05 (N and P); all df(1, 12).

On the other hand, the ratio of N and six macronutrients were determined across seven plant tissue types in order to ascertain how N interacts with macronutrients within different plant organ Table 2.1 below. It is appeared that the N to macronutrients ratio differed among tissue types. Seeds possessed the highest ratio across all macronutrients except for K, the highest ratio was found with Stem B. the lowest ratio of N:P and N:Ca reported within Stem B, ratio of N:K and N:S within Stem M, and ration of N:Mg and N:Na within T.root B.

Table 2.1 Ratio of N to six macronutrients (P, K, Mg, Ca, S and Na) within seven tissue types at GS 6.2/6.3.

Data used to determine the ratio of N to other macronutrients are the tissue mean among 14 genotypes of *Brassica napus* at GS 6.2/6.3.

Tissue	N:P	N:K	N:Mg	N:Ca	N:S	N:Na
L.root	0.86	0.20	2.21	0.43	1.94	1.30
T.root B	0.79	0.16	1.60	0.46	1.60	0.63
T.root T	0.78	0.17	2.01	0.47	1.84	0.68
Stem B	0.51	3.45	7.83	0.04	3.88	2.24
Stem M	0.79	0.08	2.03	0.25	0.75	0.82
Stem T	1.79	0.26	5.02	0.34	1.01	10.2
Seeds	4.18	2.49	9.61	7.65	7.29	684

2.4.3 Variation in N concentration at harvest

N concentration was determined as percentage of DW for seven plant tissues on five plants of each of 30 OSR varieties within three crop types. The analysis of variance was conducted according to the model [(croptype/variety) x tissue]. Significant differences in N concentration were revealed between crop type/variety and tissue, as well as significant interaction between them Table 2.2.

Table 2.2 Analysis of Variance for the N concentration at harvest.

ANOVA was conducted according to the model [(croptype/variety) x tissue]. SS is the sum of squares, MS is the mean squares, df is the degree of freedom, F is the variation ratio, and P is the probability. The proportion of total variance represented by omega squared ω^2 and the partial variance estimated by partial omega squared ω^2_p. The colon represents the interaction between factors.

Source of variance	df	SS	MS	F	P value	ω^2_p	ω^2
Croptype	2	0.2507	0.1253	8.0818	3.3E-04	0.013	0.0003
Tissue	6	670.52	111.75	7206.1	0.0E+00	0.976	0.975
Croptype:Variety	27	11.802	0.4371	28.185	7.6E-100	0.404	0.015
Croptype:Tissue	12	2.7954	0.2329	15.021	5.5E-29	0.135	0.004
Croptype:Variety:Tissue	161	38.535	0.2394	15.434	1.7E-171	0.682	0.049
Residuals	873	13.539	0.0155				
Total	1081	737.44					

The largest proportion (>97 %) of the total and partial variance in [N] attributed to tissue type, whereas crop type and croptype/genotype accounted for only 0.03 and 1.55 %, respectively, of the total variance measured as omega squared, and about 1.3 and 4 %, respectively, of the partial variance measured as the partial omega squared. The three crop types varied widely in N concentration between the seven sampled tissues from stem, roots and seeds Figure 2.5.

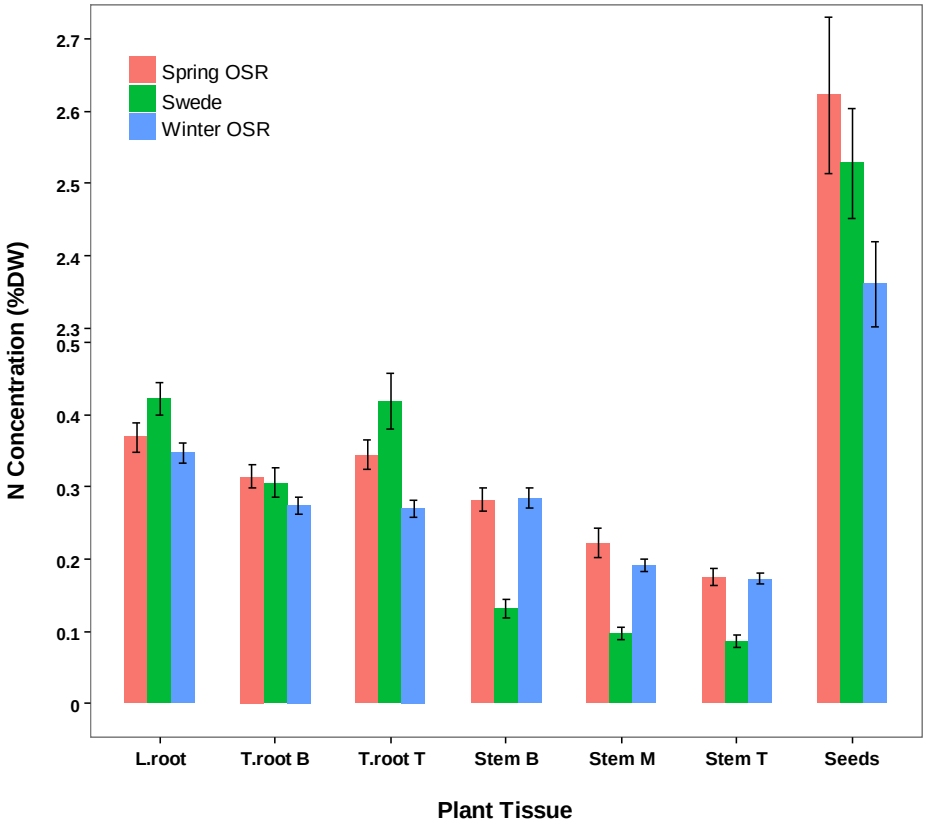

Figure 2.5 Total N concentration of different plant tissues among three crop types (Winter OSR, Swede and Spring OSR) of *Brassica napus* L. at harvest.

Varieties were grown at low level of N supply in a field experiment. Total N concentration (% dried weight, DW) was measured by Kjeldahl method. Data are the estimated crop type means ± the standard error of the mean (SEM) (n=25, 30 and 95 for Swede, Spring OSR and Winter OSR, respectively). Bottom axis shows tissue types described in section 2.3.2 (page 57).

The Swede plants exhibited the lowest [N], about 0.1 %DW in all three stem tissues, in comparison to Winter OSR (0.23 %DW) and Spring OSR (0.25 %DW). Interestingly, [N] in the roots of the Swede plants were approximately 4-fold higher than that of the stem, and possessed the highest concentration compared to the Spring OSR (0.36 %DW) and the Winter OSR (0.3 %DW) possessing the lowest N concentration. The Winter and Spring OSR displayed a similar stem N concentration.

Bottom Stem (Stem B) concentration was higher than the middle and the top of the stem in all three crop types. In a similar way, [N] was higher in the lateral roots than the taproot Figure 2.5 (above). Lateral roots (0.37 %DW) were the second highest in [N] across all varieties after seeds (2.5 %DW), followed by T.root T, T.root B, Stem B, Stem M and Stem T with 0.31, 0.29, 0.25, 0.18 and 0.15 %DW, respectively Figure 2.6 below and (Appendix 1, Table 2).

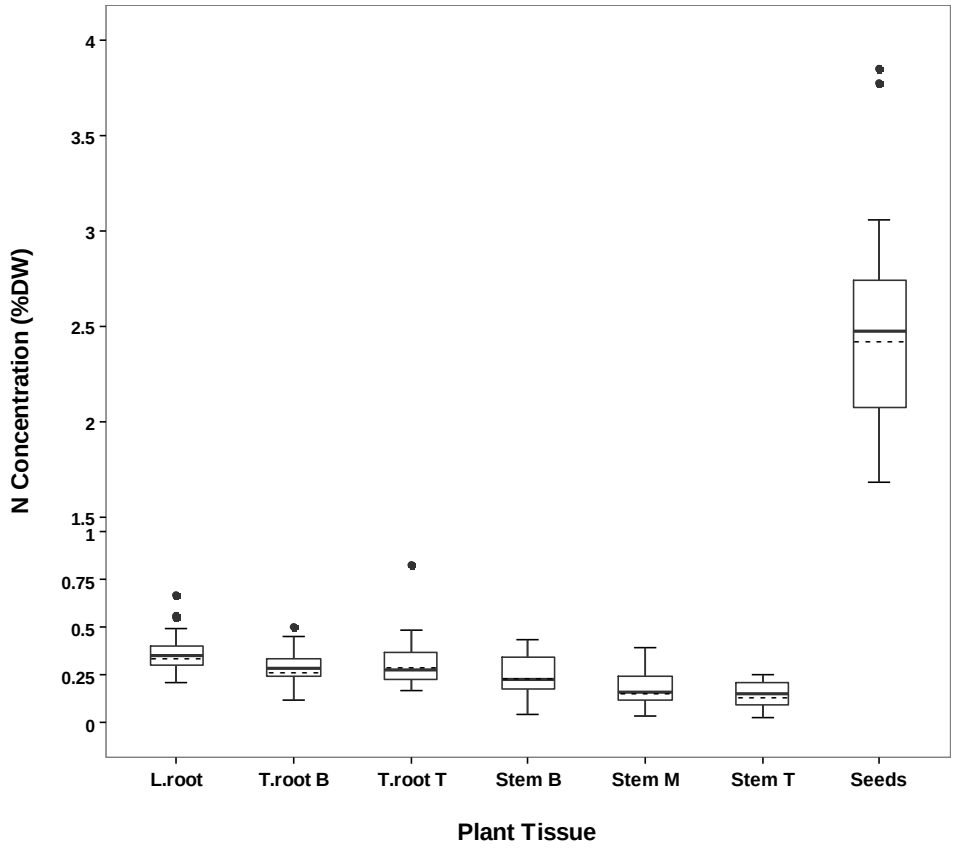

Figure 2.6 Variation in N concentration of different plant tissues among 30 *Brassica napus* L. accessions at harvest.

Varieties were grown at low level of N supply in a field experiment. Total N concentration (% dried weight, DW) was measured by Kjeldahl method. Data are the estimated varieties means (n=5). The lower and upper boundaries of the box represent the 25 and 75 percentiles, respectively. The solid and dashed lines within the box represent the median and mean, respectively. Whiskers closest and farthest to zero represent the smallest and largest non-outliers in the data set, respectively. Circles represent outliers.

The 30 genotypes of *B.napus* L. showed a large amount of variation in [N] over the seven tissues of roots, stem and seeds at harvest Figure 2.6 above. Considerable variation in Stem B [N] was observed and varied 9.5-fold (0.05 - 0.44 %DW between the variety Best of All and Ningyou7, respectively). Stem M [N] also varied about 10-fold (0.04 – 0.4 %DW between the variety Drummonds PT and Yudal, respectively). Moreover, a range of 9-fold in Stem T (0.03 – 0.26 %DW) between the variety Best of All and Tapidor ADAS was observed in Figure 2.6 (page 75). The Table 2 in Appendix 1 shows the averaged N concentration in the seven tissue sections among the 30 genotypes.

Significant varietal differences (TukeyHSD, $P < 0.01$) were observed between the three stem tissues. N concentration in the top of Taproot (T.root T) varied 5-fold (0.17 – 0.83 %DW between the varieties Darmor and Vige DH1, respectively). There was a variation range of 4-fold (0.12 – 0.5 %DW) and 3-fold (0.21 – 0.67 %DW) between the genotypes Temple and Ningyou7 in the bottom of the Taproot (T.root B) and Lateral roots (L.root), respectively Figure 2.6 (page 75). All of these pair comparisons between the varieties (lowest and highest [N]) are significant (TukeyHSD, $P < 0.01$).

The seeds exhibited the largest store of N at this stage with a concentration of 2.5 % of dried weight, and varied by 13-fold compared to the stem [N] and 8-fold compared to the roots [N]. Furthermore, only a rage of 2.3-fold variation detected in Seeds [N] Figure 2.6 (page 75) between the genotypes Temple and Regina II DH1 (1.68 – 3.85 % DW, respectively) with significant varietal differences ((TukeyHSD, $P < 0.01$).

2.4.4 Relation between N and other mineral elements at harvest

Pearson correlation analysis was conducted on all possible 560 pair-wise combinations of seven N traits and other 77 traits (11 mineral elements and seven tissue types) in order to elucidate the factors possibly contributing to these N concentration variations. Out of all possible combination, 97 significant positive relationships (r >0.36, P <0.05, df =28) were reported, of which 36 and 61 observed within and between tissues, respectively. On the other hand, 19 significant negative associations (r <-0.36, P <0.05, df =28) were reported, of which only 3 observed within tissues and 16 observed between tissues Figure 2.7 below.

Six positive associations were found within root tissue types between N concentration and the elements (S, Ca, Mg, Mn, B and Zn) concentration. The strongest correlation was with S (r =0.58) within L.root, and with Ca within both T.root B and T.root T (r =0.59 and 0.85, respectively); all P <0.001. N was also significantly correlated with P and Fe within T.root T (r =0.82 and 0.43, p <0.00001 and 0.05, respectively) and T.root B (r =0.37 and 0.29, P <0.05 and >0.05, respectively). Linear Regression analysis revealed that about 68, 49, 28, 73, 58, 57, 49, 28 and 18 % of the variation in T.root T [N] could be significantly (F(1,28) >6.18, P <0.019) explained by its relation to P, Mn, B (Figure 2.8), Ca, Mg, S, and Fe, respectively. The strongest relationship within all stem tissue types were between N and P (0.52< r <0.61, P <0.005). [P] accounted for 28 – 37 % of the variance in [N] Figure 2.8. Moreover, N was also correlated with Mg, Mn, B and Fe (r =~0.4) within Stem B, and with Mg, B, S and Ca (0.42< r <0.51) within Stem M.

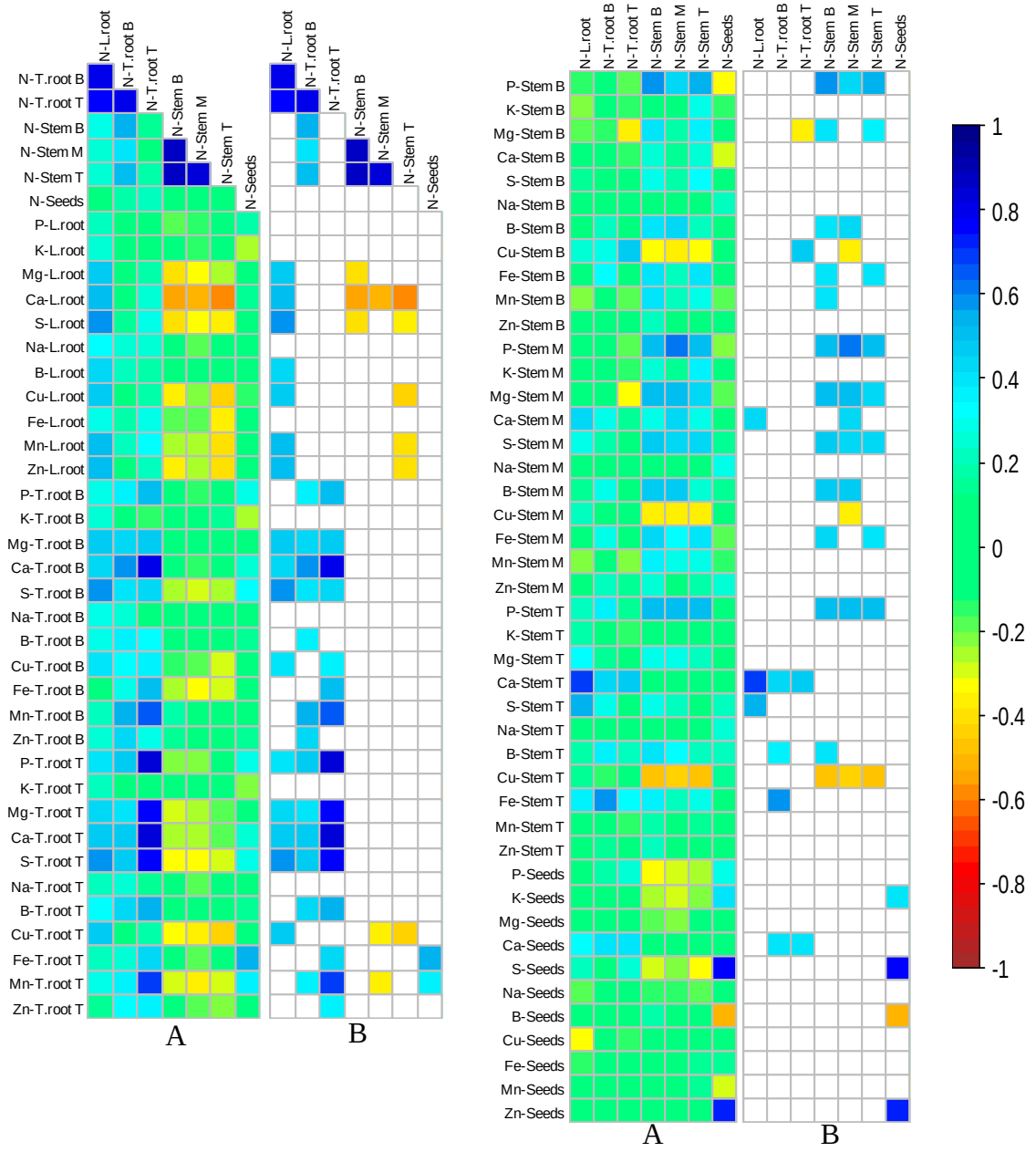

Figure 2.7 Pair-wise correlation analysis between Nitrogen traits and other 77 traits in 30 *B.napus* genotypes at harvest.

N concentration within seven tissues of root (L.root, T.root B and T.root T), stem (Stem B, M and T) and seeds consist N traits. 11 mineral element concentrations within seven tissues consists 77 traits. (A) Represents all 560 possible pair-wise correlations. (B) Represents only significant correlation (P <0.05). Data used are genotype mean (n =5). Correlation coefficients panel are placed to the right and scaled from -1 (dark brown) to +1 (dark blue).

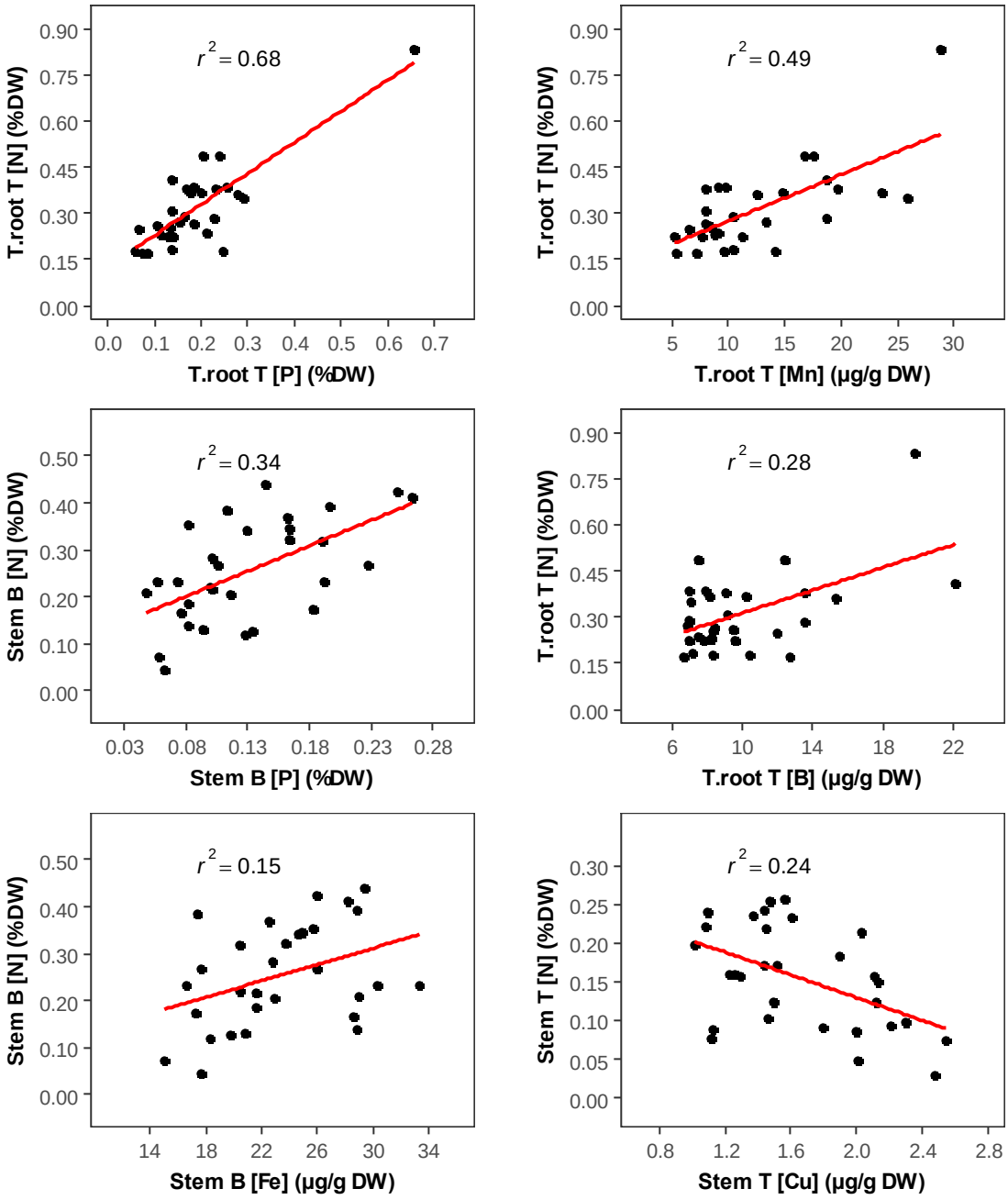

Figure 2.8 Relationship between N concentration and P, Mn, B, Fe and Cu concentration within different tissues at harvest.

Data are the genotype mean (n =5). The red line represents the line of best-fit. Within T.root T $y = 0.13 + 1.01x$; r^2 =0.68 (N and P), $y = 0.12 + 0.02x$; r^2 =0.49 (N and Mn), $y = 0.13 + 0.02x$; r^2 =0.28 (N and B); all P <0.0026. Within Stem B $y = 0.11 + 1.08x$; r^2 =0.34 (N and P), $y = 0.05 + 0.01x$; r^2 =0.15 (N and Fe); both P <0.036. Within Stem T $y = 0.28 - 0.07x$; r^2 =0.24; P <0.006 (N and Cu); all df(1, 28).

A negative relationship existed between N and Cu within all stem tissue types ranged from r =-0.49 (Stem T) to r =-0.32 (Stem B), however it was not significant within Stem B. about 24 % of the variation in Stem T [N] could be explained by its relation to Cu concentration Figure 2.8 above.

The strongest positive relationships within seeds reported between N concentration and S and Z (r =0.75 and 0.72, respectively; P <0.0001). In contrast, negative correlation was existed between N and B within seeds (r =-0.50, P <0.005) Figure 2.7 (Page 78). S, Zn and B accounted significantly for approximately 56, 52 and 25 % (Figure 2.9 below), respectively, of the variance in seeds [N]. Nonetheless, about 72 % of the variation could be explained by the confluence of both S and Zn concentration (multiple regression analysis, adjusted R^2 =0.72; F(2,27) =37.83; P <0.00001).

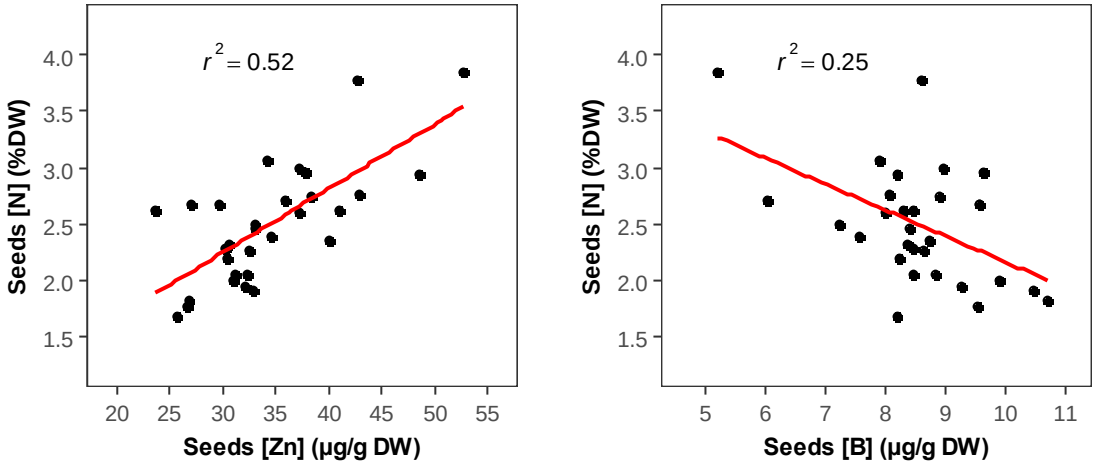

Figure 2.9 Relationship between seed N concentration and Zn and B concentration at harvest.

Data are the genotype mean (n =5). The red line represents the best-fitting line. $y = 0.53 + 0.06x$; r^2 =0.52 (N and Zn), $y = 4.48 - 0.23x$; r^2 =25 (N and B); both P <0.005, df(1, 28).

Furthermore, the strongest positive associations between tissues were unsurprisingly found in [N] between all stem tissue types ($0.82< r <0.88$) as well as between all root tissue types ($0.76< r <0.80$). Approximately 68 - 78 % of the variance in N concentration was significantly ($P <1.7*10^{-6}$) shared between all stem tissue types, and 58 - 64 % shared between all root tissue types. In contrast, the strongest negative relationships between tissues were observed between all stem tissues N concentration and L.root Ca concentration ($-0.50> r >-0.57$, $P <0.0058$). 25 – 33 % of the variance within all stem tissues could be significantly ($P <0.0058$) accounted for by it is relation to L.root [Ca].

On the other hand, ratio of N and six macronutrients were determined across seven plant tissue types in order to identify how N interacts with macronutrients within different plant organ Table 2.3 below. N to macronutrients ratio differed among tissue types, where seeds possessed the highest ratio across all macronutrients. In contrast, the lowest ratio of N:P observed within root tissues and the ration of N:K, N:Mg, N:Ca, N:S and N:Na observed within stem tissues.

Table 2.3 Ratio of N to six macronutrients (P, K, Mg, Ca, S and Na) within seven tissue types at harvest.

Data used to determine the ratio of N to other macronutrients are the tissue mean among 30 genotypes of *Brassica napus* at harvest.

Tissue	N:P	N:K	N:Mg	N:Ca	N:S	N:Na
L.root	1.85	0.34	4.68	0.59	1.99	2.09
T.root B	1.78	0.33	4.56	0.58	1.90	1.72
T.root T	1.70	0.40	5.34	0.59	2.05	1.99
Stem B	1.96	0.15	2.88	0.30	1.15	1.01
Stem M	2.12	0.11	3.27	0.27	0.84	0.91
Stem T	2.64	0.13	3.21	0.24	0.69	1.05
Seeds	3.08	4.17	11.4	5.82	5.56	654

2.4.5 Comparison between two stages GS 6.2/6.3 and harvest

Nitrogen were independently analysed during the growth stage (GS 6.2/6.3) and the harvest. Genotypic variation within tissues and between tissues were studied as well as the relationship between N and other 11 mineral elements. 14 genotypes of *B.napus* L. accessions were shared between the two different stages. Therefore, combining the two stages together to elucidate differences in mineral nutrient concentrations in every tissue was of interest. Across the 14 varieties and the seven analysed tissues there was no significant differences between the two growth stages in N concentration ($F(1,588) = 0.571$, $P > 0.05$). However, there were significant interaction between the growth stage and tissue ($F(5,588) = 61.6$, $P < 0.0001$), and variety ($F(13,588) = 2.3$, $P < 0.01$) according to ANOVA model [stage x tissue x variety].

Not surprisingly, variation in N concentration was observed among seven tissue types and within each tissue between the two stages. it appeared that taproot and lateral roots Figure 2.10 and Stem M Figure 2.11 (B) exhibited the highest N concentration at harvest (0.3, 0.37 and 0.24 %, respectively, across 14 genotypes) compared with the GS 6.2/6.3 stage (0.13, 0.2 and 0.15 % , respectively), whereas N concentration in Stem B (0.34 %) and Stem T (0.2 %) Figure 2.11 (A and C, respectively) were the lowest at maturity in contrast with GS 6.2/6.3 (0.6 and 0.34 %, respectively). Interestingly, some varieties showed little difference between the two stages such as Canberra and Sun within Stem B Figure 2.11 (A), Winner, Darmor and NK Bravour within Stem M Figure 2.11 (B), and Ningyou 7 within Stem T Figure 2.11 (C). The seeds exhibited no differences in N concentration between the GS 6.2/6.3 and harvest stages, however, significant differences were reported between two stages within genotypes; Winner, Royal, Tapidor ADAS and Sun Figure 2.11 (C).

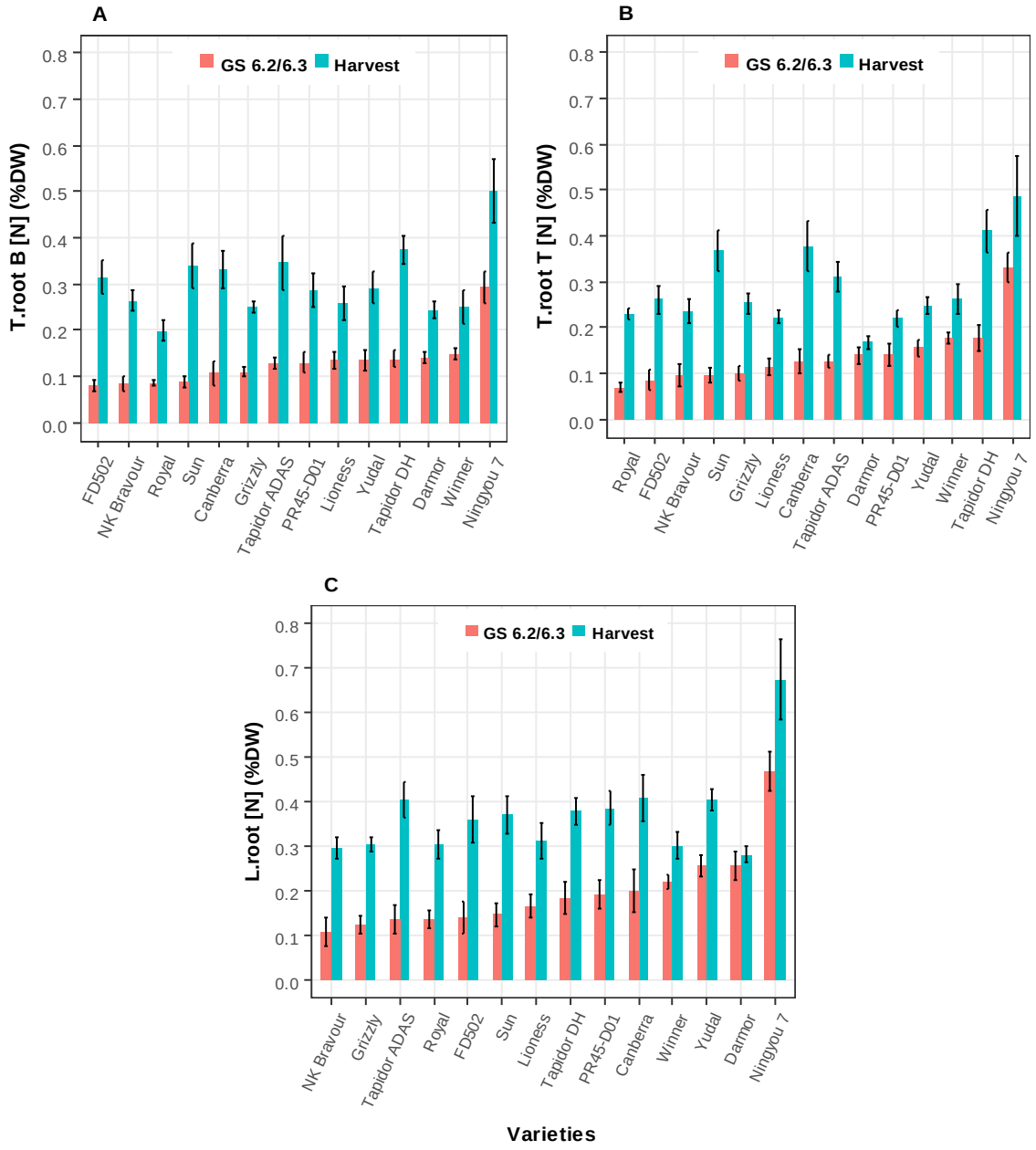

Figure 2.10 Roots N concentration across two growth stages; GS 6.2/6.3 and harvest among 14 *B. napus* L. accessions.

(A) T.root B (B) L.root B (C) L.root. Data are the mean ± SEM (n=3 and n=5 at GS 6.2/6.3 and harvest, respectively). Varieties were sorted into ascending order according to [N] at the GS 6.2/6.3.

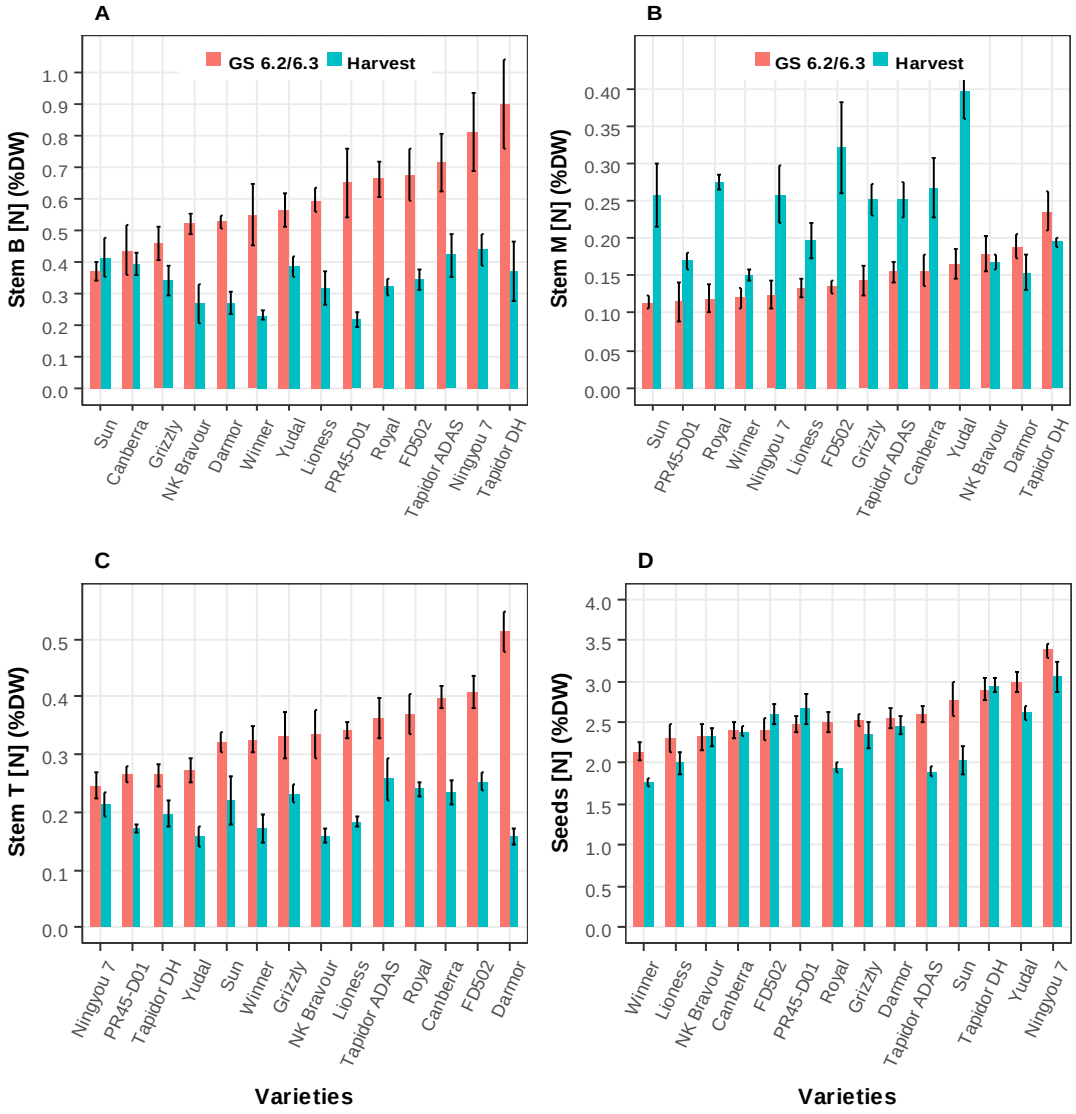

Figure 2.11 Stem and seeds N concentration between two growth stages (GS 6.2/6.3 and harvest) among 14 *B. napus* L. accessions.

(A) Stem B (B) Stem M (C) Stem T and (D) Seeds. Data are the mean ± SEM (n=3 and n=5 at GS 6.2/6.3 and harvest, respectively). Varieties were sorted into ascending order according to [N] at GS6.2/6.3

2.5 Discussion

During this chapter, three *B.napus* plant organs; stem, root and seeds were studied. The stem and root were sectioned into three tissues each. N concentration were

quantified within the seven tissue types during two growth stages of OSR; GS 6.2/6.3 contained 14 genotypes and at harvest contained 30 genotypes grown under field conditions at low N supply. A considerable variation in N concentration was detected between all plant tissues of stem, root and seeds at both plant growth stages and mainly at harvest. The variation in [N] ranged from 1.6-fold (seeds) to 4.8- fold (T.root T) at GS 6.2/6.3 Figure 2.2 (page 66). However, at maturity, variation in [N] ranged from 2.3-fold (seeds) to *ca.*10-fold (Stem B and M) Figure 2.6 (page 75). Smaller scale of variation in mature seeds [N] were reported under limited N availability in previous studies, for instance, a variation of 1.5-fold among field-grown 17 genotypes of OSR (Schulte auf˙m Erley *et al.*, 2011), 1.45-fold among 36 genotypes (Kessel *et al.*, 2012), 1.12-fold among 10 genotypes (Berry *et al.*, 2010b) and 1.14-fold among 12 canola genotypes (Balint and Rengel, 2008). Moreover, only 2-fold of variation was observed in stem N residual (Balint and Rengel, 2008).

N concentration differed significantly among all plant tissue types and decreased at GS 6.2/6.3 in the sequence; seeds >Stem B >Stem T >L.root >Stem M >T.root T >T.root B which is inconsistent with Svečnjak and Rengel (2006a) whom demonstrated that stem N concentration is smaller than root at the rosette stage among 4 canola genotypes regardless N availability. In contrast, N concentration decreased at maturity in the sequence; seeds > L.root > T.root T >T.root B > Stem B >Stem M >Stem T which is consistent with another study of Svečnjak and Rengel (2006b) in which root exhibited higher concentration of N than stem at maturity. Having reported this, the present study interestingly showed that N concentration differed within the plant organs itself. For example, N concentration in the bottom of the stem (Stem B, 0.6 %DW) was significantly about 4.1-fold and 1.8-fold greater than Stem M and Stem

T, respectively, at GS 6.2/6.3, and about 1.4-fold and 1.6-fold higher respectively at harvest. Moreover, lateral root possessed greater [N] than both taproot tissue sections at both growth stages; 1.42- and 1.52-fold at GS 6.2/6.3 in contrast to 1.18- and 1.18-fold at maturity. A difference was also observed between two sections of taproot where the top part (T.root T) had greater N concentration than the lower section (T.root B) of about 1.1-fold across two growth stages. As yet we are not aware of either any previous publication highlighted this finding nor a research group who are doing similar study.

In the study conducted by Berry *et al.* (2010b) who investigated the varietal differences underline N Use Efficiency in 10 Winter OSR genotypes under limited N environment of N fertiliser, N concentration within mature seeds was 2.8 %DW averaged across four experiments and ranged from 2.65 to 2.97 %DW between genotypes Grizzly and Royal, respectively. In the present study, mature seeds [N] averaged 2.26 %DW among the same 10 genotypes and ranged from 1.76 to 2.95 %DW between genotypes Winner and Tapidor DH, respectively.

It is clear that the top parts of plants (Stem T and seeds) possessed high N concentration at the seed development stage (GS 6.2/6.3) and this is possibly due to trends of N translocation into siliques. At maturity, [N] within Stem T and Stem B decreased although N concentration remained relatively high within Stem B, whereas [N] within all root tissues and Stem M increased. These results correspond with several studies investigated N remobilisation such as Malagoli *et al.* (2005a); Tilsner *et al.* (2005); Gombert *et al.* (2006); Sylvester-Bradley and Kindred (2009) whom demonstrated the low efficiency of N redistribution from the vegetative organs to the siliques. Ulas *et al.* (2013) reported that reducing N supply had a significant effect on

the residual amount of stem N at harvest which decreased between 2- and 4-fold according to the applied quantity of N. In the same study, it was concluded that without N supply, the amount of stem N residue averaged *ca.* 5.9 kg N/ha with no genotypic differences among four genotypes and comprised approximately 2-fold of the N loss with leaves. In the study of Berry *et al.* (2010b) which conducted under low N supply, the amount of residual N was higher and ranged from 18.5 to 27.9 kg N/ha. In this chapter, the amount of residual N within Stem B averaged 4.7 kg N/ha where the 10 cm section of Stem B averaged approximately 2.5 g at harvest. However, at a density of 80 plants/m^2, the amount of N residue could exceed 6.1 kg N/ha which is even more than the whole stem residue reported in the study of Ulas *et al.* (2013). Interestingly, the variation ranged between 0.92 kg N/ha for cultivar Best of all and 8.76 kg N/ha for cultivar Ningyou 7.

Swede OSR plants possessed the lowest N concentration averaged 0.13 %DW within Stem B in comparison with Winter and Spring OSR; both, 0.28 %DW at maturity Figure 2.5 (page 74) and (Appendix 1, Table 2). Thus, if it was possible to reduce N concentration in the bottom of the stem by 0.15 %DW to what is averaged in Swede crop, there would be a reduction in residual N of more than 3 Kg N/ha. In contrast, if the reduction in [N] by 0.24 %DW to what is averaged in cultivar Best of All (0.05 %DW), the amount of N loss at maturity could be reduced by more than 4.7 kg N/ha.

Svečnjak and Rengel (2006b) reported than root N concentration at harvest averaged 0.85 %DW among four genotypes of canola at low N supply, which is not in accord with the present study where taproot [N] averaged 0.29 – 0.31 %DW and lateral root 0.37 %DW Figure 2.6 (page 75) and (Appendix 1, Table 2). Furthermore, N concentration within L.root was greater than Stem B at maturity among all crop types.

Moreover, taproot N concentration was higher than Stem B among Spring OSR and Swede, but only similar to Stem B in Winter OSR Figure 2.5 (page 74) and (Appendix 1, Table 2). Root tissues were observed to have greater dry matter than stem tissues, thus the amount of N loss by root would be higher than by stem. The amount of N loss by a taproot section of only 5 g DW would reach 10.8, 13.68 and 16.76 kg N/ha for Winter OSR, Spring OSR and Swede, respectively, according to the averaged N concentration among these three crop types. The genotypic variation ranged between less than 7.4 kg N/ha for cultivars such as Temple, Darmor and TN145, and more than 19.4 kg N/ha for cultivars such as Ningyou 7 and Cubs Roots DH1. Thus, there is large room for reduction in taproot N concertation by 0.14 %DW. Therefore, reducing N loss with taproot by more than 5.7 kg N/ha according to an averaged taproot [N] of 0.31 %DW. Unfortunately, It was not possible to compare the loss of N by stem and leaves through lack of data about leaves. Nevertheless, plant stem contained relatively a high N at maturity compared to plant root.

Genotypic differences have been clearly reported in several studies involved in N dynamics, remobilisation and N Use Efficiency within *B.napus* (Schjoerring *et al.*, 1995; Macdonald *et al.*, 1997; Dreccer *et al.*, 2000; Horst *et al.*, 2003; Malagoli *et al.*, 2005a; Svečnjak and Rengel, 2006a; Berry *et al.*, 2010a; Berry *et al.*, 2010b). In this chapter, the performed experiment also showed a large scale of genotypic differences in N concentration within different plant tissues. Some of these genotypes differed distinctly from one another in relation to N concentration contained in the stem and root at harvest. Of the Winter OSR varieties, Ningyou 7 possessed the highest concentration across all tissue sections, whereas in contrast, Temple exhibited the lowest concentration. Some varieties such as the Swede Best of All and Drummonds

PT showed differences in [N] between stem and roots. The variety Vige DH1 showed an attractive result where [N] was the greatest in taproot and could account approximately for 2-fold [N] within taproot of cultivar Ningyou 7. It has previously been observed that the cultivars Vige DH1 and Best of All were an outliers in a previous OREGIN field experiment investigating N Uptake Efficiency.

11 mineral nutrient concentrations had been quantified in addition to N within every plant tissue types at two growth stages. The relationships among these mineral concentration were evaluated by analysis of correlation. Interestingly, all pair-wise correlations between N and other nutrient concentrations were positive within all root tissues at GS 6.2/6.3 Figure 2.3 (page 69) and at maturity Figure 2.7 (page 78). Moreover, most of the pair-wise relationships (40 out of 47) within above ground tissues were also positive. This results can suggest that there are shared pathways involved in uptake and assimilation of the correlated nutrients, or pleiotropic gene effects among those associated nutrients (Bus *et al.*, 2014). However, the relationships between N and other mineral nutrients in the present study were not consistent across plant tissues. For example, N/S and N/Zn were strongly correlated within only all root tissues and seeds, and N/Ca were strongly associated within only all root tissues. In the recent study of Thomas *et al.* (2016) investigating leaf and seeds "Ionome" in *B.napus*, it was demonstrated that the relationships between nutrient concentrations were tissue-specific. In a similar study on *Arabidopsis thaliana*, Buescher *et al.* (2010) and Baxter *et al.* (2012) showed that the relationships between mineral concentrations differed across root, leaf and seeds. In addition to the tissue-specificity, some of the pair-wise relationships were also developmental stage-specific, for example, a

significant correlation between N and Mn observed only at maturity within all root tissues and Stem B.

N concentration was strongly correlated to Ca, Mg, P and Zn concentration at the both growth stages. However, these relationships were tissue-specific as previously indicated. Broadley *et al.* (2004), in their study on 117 species of angiosperms at the vegetative growth under hydroponic conditions, concluded that shoot N concentration strongly correlated to P, Ca and Mg concentration. The ratio of N to other micronutrients was greater in seeds than other plant tissues across two growth stages. However, variation was existed among growth stages. For example, within seeds, N:P decreased from 4.2 to 3 and N:Ca decreased from 7.6 to 5.8, in contrast, N:K increased from 2.5 to 4.2 and N:Mg increased from 9.6 to 11.4; all comparisons at GS 6.2/6.3 Table 2.1 (page 72) and maturity Table 2.3 (page 81), respectively. Furthermore, within Stem B tissue, the ratio of N:P increased from 0.5 to 1.96 and N:Ca increased from 0.04 to 0.3, in contrast, the ratio of N:K decreased from 3.4 to 0.15, N:Mg decreased from 7.8 to 2.9 and N:Na decreased from 2.2 to 1.15; all comparisons at GS 6.2/6.3 and maturity, respectively. In the study of Broadley *et al.* (2004), averaged shoot ratio among 117 species between N and Mg, P, Ca, K and Na were 17, 7.8, 5.1, 1.2 and 47, respectively, whereas in *B. Oleracea* were 11.3, 9.3, 1.6, 1.5 and 197, respectively.

The seeds N:S ratio was also varied between the growth stages. A ratio of 7.3-fold observed at the GS 6.2/6.3, whereas of 5.8-fold observed at harvest. Moreover, seeds [N] and [S] were positively and strongly associated at the both growth stages. These results might be due to a confluence of two determining factors; the first is that proteins, consists about 17 – 24 %DW of *B.napus* L. seeds (Snowdon *et al.*, 2007;

Weightman *et al.*, 2010) and site for of N. Sulphur is also a key component of proteins through the two S-containing amino acids (Hawkesford *et al.*, 2012). The second is that *B.napus* L. seeds contain relatively a high glucosinolates content of 10 µmol/g (Khajali and Slominski, 2012), averaged 11.4 µmol/g in AHDB Winter OSR Recommended List 2017/2018 (AHDB, 2017) compared to other plant tissues, and 2-hydroxy-3-butenyl glucosinolate comprise about 80 % of the total glucosinolates within OSR seeds (Radojčić Redovniković *et al.*, 2008). Glucosinolates are S-rich compounds with S comprising up to 20 % of them (Falk *et al.*, 2007). Furthermore, N and S were surprisingly correlated strongly within all roots tissue and seeds (r >0.82) at GS 6.2/6.3 and (r >0.4) at maturity. A consistent ration N:S of approximately 2-fold was exhibited across roots tissues throughout both growth stages.

In comparison, the N:S ratio varied between the stem sections and between both growth stages. The highest ratio of 3.9-fold was observed within the Stem B at the GS 6.2/6.3 which then decreased to less than 1.2-fold at maturity. In contrast, a ratio of 1:1 was observed within Stem T at GS 6.2/6.3 and became 1:1.5 at maturity. Such relationship between N and S has previously been reported in *B.napus*. McGrath and Zhao (1996) demonstrated that N:S differed between plant tissues, in addition, the ratio N:S was continuously decreased (measured at the whole plant level) from the onset of flowering to the early pod development stage under field condition, where a ratio of 3-fold were observed at a similar growth stage (GS 6.2 and 6.3) to what the present study had at low N supply. Abdallah *et al.* (2010) reported a ratio of less than 4-fold in root and 5-fold in leaf at the rosette stage of cultivar Capitol under controlled conditions.

These finding could assist plant breeders to develop varieties with improved N Utilisation Efficiency. This could be aided by developing a new genetic mapping population, for instance, Ningyou 7 X Temple that could result in a significant segregation of genes underline N remobilisation and use efficiency, thus reproducing new highly N efficient genotypes with high seed yield at limited N sources. OREGIN has been developing new five DH mapping populations using five parental lines (the male lines) all crossed onto the cultivar Temple (the female) which selected for its good agronomic traits such as N use efficiency, good autumn vigour and high seed oil content.

Chapter 3 Variation in Mineral Element Concentrations of *Brassica napus* L.

3.1 Introduction

As it has been described in Chapter 1, plants require 14 essential mineral elements acquired from the soil solution in different forms to maintain their growth and development (Marschner, 2012a). The role of these mineral elements in plant growth and development is of critical importance. For example, the key function of P during the metabolic cycles, in the cell, is the storage of energy through molecules such as adenosine triphosphate (ATP). Furthermore, P plays a structural function as an essential constituent of the nucleic acids deoxyribonucleic acid (DNA) and ribonucleic acid (RNA), and also in membrane phospholipids (Raghothama and Karthikeyan, 2005). S is also an essential component of proteins through the two S-containing side-chain amino acids methionine (Met, M) and cysteine (Cys, C) which, in turn, are involved in synthesising S-containing compounds, for instance, enzymes, coenzymes and glucosinolates. Moreover, S is a structural component of these compounds and is responsible for disulphide bridge formation (Hawkesford *et al.*, 2012). Plants require sufficient, but not excessive, quantities of mineral elements in order to reach the optimum productivity; hence low availability of these minerals or the decrease in their acquisition for whatever reason will have a direct negative effect on plant growth and development. The effect of mineral deficiency varies from element to another, as well as due to the severity of the shortage and the interaction between elements. For example, Mg is known to be involved in the process of protein synthesis because of its key role in assembling of the ribosome subunits (Cammarano *et al.*, 1972). Hence Mg deficiency, or the presence of high concentration of K in the cell, results in dissociating of the ribosome subunits and thus cessation of protein synthesis (Sperrazza and Spremulli, 1983).

The availability of mineral elements in the soil is a complicated subject that involves interactions of many factors related to the physical and chemical properties of the soil and interaction between soil and plant roots as well as interaction between minerals (Comerford, 2005; Marschner, 2012a). Therefore, mineral element availability in the soil solution substantially limits plant growth and development (White and Brown, 2010). P is one of the most unavailable macronutrients in the soil solution and often limits crop productivity (Hammond *et al.*, 2009). Unavailable Zn makes up the majority of the total Zn content in the soil; hence Zn deficiency is the most commonly occurring micronutrient deficiency found in plants, especially in soils with a high pH (Broadley *et al.*, 2007). Increasing soil pH has also been reported to reduce soil Mn availability and thus inducing Mn deficiency in OSR plants, with severe Mn deficiency symptoms observed in pH 7.5 soils (Brennan and Bolland, 2015). Zn has been found to have a positive effect on the accumulation of several mineral elements. For example, the increase in *B. oleracea* L. shoot Zn accumulation (from 8 to 32 µg/plant) at high Zn supply was reported to increase the shoot content of some mineral elements such as K, Mg, Ca, S, Mn, Cu and Fe (Broadley *et al.*, 2010)

Mineral element content differs at the tissue level within the plant as well as under different growth conditions. In the study of Thomas *et al.* (2016), seeds had greater concentration of P, S, B, Cu and Zn than leaf, while leaf had greater concentration of the other six elements among a panel of 387 genotypes. In comparison, in the study by Baxter *et al.* (2012), leaves of *A. thaliana* grown hydroponically were higher than seeds in most of the mineral elements concentration except in case of S, Cu and Zn among a panel of 96 genotypes. In the same study, it was reported that the concentration of Ca, Mg, and B was higher in leaves than roots, while the other eight

elements were higher in root than leaves. Furthermore, The environmental effect of glasshouse vs. field conditions on shoot P (Hammond *et al.*, 2009) and K content (White *et al.*, 2010) has been reported for *B. oleracea* L.

In the study of Bus *et al.* (2014), investigating the shoot mineral composition of 11 mineral elements across a large diversity collection of 509 *B. napus* genotypes grown under controlled conditions for 30 days, mineral nutrients concentration varied from *ca.* 1.6-fold for Mg to 6-fold for P. In comparison, among a diversity collection of 387 genotypes of *B. napus* grown under non controlled conditions in a polytunnel (Thomas *et al.*, 2016), the rosette leaf mineral elements concentration varied from 1.8-fold for Fe to 6-fold for Mn. In the same study of Thomas *et al.* (2016), the genotypic variation in seed minerals composition varied from 1.7- to 14-fold for P and Na, respectively. Limited variation between the Tapidor DH and Ningyou 7 parents of the TNDH mapping population was observed in seven minerals concentration in the shoot at seedling stage (Liu *et al.*, 2009a). However, across 162 segregating lines, the variation ranged from 1.5-fold (1.8 – 2.8 %) for Ca to 10.4-fold (90 – 940 µg/g) for Fe under limiting B environment. In his study on the genetic variation in P accumulation and use efficiency among 14 genotypes of *B. napus* L. grown under controlled conditions, Akhtar *et al.* (2008) found no significant variation in the shoot P concentration, in contrast to *ca.* 2.5-fold of variation in root P concentration. However, genotypic differences in seed, stem and root P and K concentrations among three genotypes (Rose *et al.*, 2007), shoot K concentration among 84 genotypes (Damon *et al.*, 2007) have been reported. Significant variation in shoot P concentration of approximately 5-fold and 2.8-fold was reported among 355 accessions of *B. oleracea* grown under glasshouse conditions at low and high P supply, respectively

(Hammond *et al.*, 2009). Furthermore, shoot varied 2.3-fold for [Mg], 2-fold for [Ca] (Broadley *et al.*, 2008), and *ca.* 2.3-fold for [K] (White *et al.*, 2010). Substantial variation in shoot Zn (6.7-fold), Fe (5.8-fold), and Mn (2.5-fold) were observed across 111 accessions of *B. rapa* L. during vegetative growth (Wu *et al.*, 2007). The genetic analysis of plant mineral nutrients composition was demonstrated to be under pleiotropic effect in *B. napus* (Liu *et al.*, 2009a; Ding *et al.*, 2010). Many strong pair-wise correlations between mineral nutrients have been observed previously in *B. napus*; in shoot (Liu *et al.*, 2009a; Bus *et al.*, 2014), seeds (Ding *et al.*, 2010; Thomas *et al.*, 2016) and leaves (Thomas *et al.*, 2016).

Genotypes that obtain and utilise mineral elements efficiently in addition to a large scale of variation across various genotypes is important for plant breeders to select for these traits of interest, thereby increasing the availability of the mineral elements of interest simultaneously with a reduction in the amount of fertiliser application (White *et al.*, 2015).

3.2 The aim of this chapter

The aim of this chapter is to quantify and determine the relationships in the natural genetic variation of a set of eleven mineral elements in roots, stems and seeds at growth stage 6.2/6.3 and at harvest in a diverse panel of *B. napus* L. genotypes grown in a field in the absence of supplemental fertiliser.

3.3 Materials and methods

3.3.1 OREGIN field experiment

This field experiment was conducted at Rothamsted Research during the 2010/2011 growing season as part of the Defra OREGIN project (Hopkins *et al.*, 2010-2011). The 1.8 m x 1.5 m plots were drilled at 60 seeds/m^2 in September 2010 and grown at low N availability without addition of fertilisers as described in section 2.3.1 (page 56). Plants were sampled at two growth stages; GS 6.2/6.3 and at harvest.

3.3.2 Plant sampling at GS 6.2/6.3

Three plants for each of 14 genotypes were collected on 02/06/2011. Each plant was divided into seven tissue sections; the bottom of the stem (Stem B), the middle of the stem (Stem M), the top of the stem (Stem T), lateral roots (L.root), the top of taproot (T.root T), the bottom of taproot (T.root B) and seeds as described in Section 2.3.2 (page 57)

3.3.3 Plant sampling at harvest

Five plants for each of 30 genotypes were collected on 14/07/2011 and divided into seven tissue sections (Stem B, Stem M, Stem T, L.root, T.root T, T.root B and seeds) as described in Section 2.3.3 (page 59)

3.3.4 Sample preparation and mineral content determination

3.3.4.1 Kjeldahl digestion

All plant samples were oven-dried at 60 °C until a constant dry weight was achieved and then milled to 2 mm by machine mill. They were further oven dried prior to

digestion to ensure complete dehydration. For determination of P, K, Mg, Mn, Ca and Na, plant samples were digested in sulphuric acid following the Kjeldahl method as described in Section 2.3.5 (page 61) where the Kjeldahl digestion was initially used to determine the total Kjeldahl Nitrogen. The remaining digested samples were then analysed on inductively coupled plasma optical emission spectrometry (Horiba Jobin-Yvon, Ultima 2 ICP-OES, France) connected to an auto sampling system to determine the concentration of the six elements. The system is controlled by the Analyst V5.4 software. The ICP-OES relies on nebulising a fine mist of the liquid sample into the hot argon plasma which in turn excite the element atoms at an excessively high temperature (*ca*. 7000 °C). The released spectrum is then measured at each element specified wavelength nm: 178.229 for P, 766.490 for K, 279.553 for Mg, 257.610 for Mn, 317.933 for Ca and 589.592 for Na and the sample content of an element determined from its emission intensity (Skoog *et al.*, 1998).

A multi-elements standard was prepared by dilution of a stock multi-elements standard that contains 40, 50.5, 20, 5, 100 and 5 mg/L of P, K, Mg, Mn, Ca and Na, respectively. Calibration checks were applied after every tenth sample during the experimental runs. The multi-elements standard was prepared from monopotassium phosphate (KH_2PO_4), calcium carbonate ($CaCO_3$), sodium chloride (NaCl), 1000 ppm Fisher Mg and 1000 ppm Fisher Mn calibration standards. The accuracy of the newly prepared standard was always checked by running on the ICP-OES against a known standard (Qmx Laboratories Ltd, UK). 50 samples were analysed in each run and a total of 1344 samples were analysed. The macronutrients data were then converted to percentage of dry weight (%DW) using the following formula:

$$macronutrient\ \% = \frac{\text{macronutrient (mg L}^{-1}) * \text{final diluted volume (ml)}}{\text{dired weight of digested tissue (g)} * 10^4}$$

The micronutrients data (mg/L) were multiplied by the final diluted volume (ml) and divided by the dried weight of digested sample (g), and the data expressed as µg/g dry weight (µg/g DW). The elements limit of detection (LOD) were expressed as the mean concentration of the blank samples plus three times the standard deviation of the blank concentrations (Shrivastava and Gupta, 2011) based on the 0.1 g initial dried weight. As a result, LODs are; 56.8, 118.7, 0.962, 93.4 and $5.35 * 10^{-4}$ %DW for P, K, Mg, Ca and Na, respectively, and 0.571 µg/g DW for Mn.

For determination of B, Cu, Fe, Zn and S concentrations, plant samples were subjected to microwave-assisted nitric acid digestion (Wu *et al.*, 1997; Miller, 1998) despite the fact that these elements, except S, could also be determined from the Kjeldahl digestion. However, the concentration of these elements in the digest was not above their LODs. Detailed explanation of the analysis method and LODs is in the next section.

3.3.4.2 Microwave-assisted nitric acid digestion

Tissue samples (~0.35 g) were placed into digestion tubes (MARSXpress closed digestion vessels) to which 2 ml 70 % analytical grade nitric acid was added. Operational blank as well as in-house reference material from pooled dried canopy leaves of field-grown *B. napus* cultivar Temple were included in each digestion run. Prior to loading the digestion tubes into the microwave digestion system (MARS 5, CEM Corporation, USA) with a capacity of 40 vessels, tubes were mixed for ~10 sec

using Fisons WhirliMixer. The digestion vessels in the microwaves were subjected to the following programmed heating cycles for 34 min; (I) the vessels content temperature was elevated to 100 °C in three min and then held for two min, (II) temperature was elevated to 120 °C in one min and held for one min, (III) temperature was elevated to 160 °C in three min and then held for two min. (IV) finally, temperature was elevated to 180 °C in two min and held for 20 min. The tubes were allowed to cool to 60 °C or less and 23 mL R.O. water added to the tube for a total volume of 25 ml and mixed well using WhirliMixer. This solution was transferred to a scintillation vial and analysed on the ICP-OES (Horiba Jobin-Yvon, Ultima 2 ICP-OES, France) to determine concentrations of B, Cu, Fe, Zn and S against a nitric acid digest standard. The released spectrum was then measured at each element specified wavelength nm; 249.773 for B, 324.754 for Cu, 259.940 for Fe, 213.856 for Zn and 180.676 for S. A multi-elements standard were prepared as dilutions of the stock multi-elements standard containing 100 mg/L S and 5 mg/L B, Cu, Fe and Zn. Calibration checks was applied after every tenth sample during the experimental runs. The multi-element standard was prepared from potassium sulphate and 1000 ppm Fisher B, Cu, Fe and Zn calibration standards. The prepared standard was always checked by running on the ICP-OES against a known standard (Qmx Laboratories Ltd, UK).

The micronutrients data were then converted to µg/g DW, and the macronutrients converted to %DW as previously mentioned. LODs were calculated based on the 0.35 g initial dried weight and were; 2.217, 0.301, 3.365 and 0.525, and $19.12*10^{-4}$ %DW. the averaged concentration of B, for example, in the bottom of the stem at harvest is 13.4 µg/g DW using nitric acid digestion which is more than 6-fold greater than its LOD. In comparison, the averaged concentration in the Kjeldahl digest is 7-fold less

according the initial DW (0.1 g) and the final dilution volume (50 ml). Therefore, the averaged concentration of B in the bottom of the stem is 1.91 µg/g DW which is less than its LOD of 2.217 µg/g DW. Since two methods of digestion has been used, K was also determined in stem and roots tissue sections at harvest following the microwave-assisted nitric acid digestion for the purpose of comparison between the two methods.

3.3.5 Data analysis

The final concentration of P, K, Mg, Ca, Na and S was determined as a percentage of dry weight (%DW). The final concentration of Mn, B, Cu, Fe and Zn was determined as µg per g of dry weight (µg/g DW). Data were analysed as described in Section 2.3.6 (page 63) where analysis of variance (ANOVA) was applied to study the effect of the crop type, variety and tissue section, and the interaction between them on the concentration of each macronutrient and micronutrient at growth stages GS 6.2/6.3 and harvest. The proportion of total and partial variance in each mineral nutrient accounted for each treatment affect was reported as omega squared (ω^2) and partial omega squared (ω^2_p). The TukeyHSD analysis at 1 % significant level was used as a Post Hoc test when overall significant differences were observed. Pearson correlation analysis was performed on all 2926 possible combinations of the 77 traits (11 mineral elements and seven tissue sections) using variety means. Two samples t-test was conducted to study the effect of two different digestion methods, Kjeldahl and microwave-assisted digestion, on K concentration (K-H_2SO_4 and K-HNO_3), t statistic (t), P value and standard error of difference (SED) were reported. All statistical analysis were performed using the R environment for statistical computing and graphics (version 3.3.2, 2016).

3.4 Results

Stem, root and seed tissue samples were taken from plants grown in the absence of supplemental fertiliser from fourteen *B. napus* genotypes at GS 6.2/6.3 (n = 3) and from thirty genotypes at harvestable maturity (n = 5) and subjected to minerals analysis to quantify six macronutrients (P, K, Mg, Ca, S and Na) and five micronutrients (B, Cu, Fe, Mn and Zn). The variation in the two groups of nutrients across two growth stages in addition to the relationship between all quantified nutrients was analysed.

3.4.1 Variation in macronutrient concentrations at GS 6.2/6.3

Analysis of variance (ANOVA) between two treatments [tissue x genotype] was performed across all macronutrients. ANOVA revealed significant differences ($P < 0.00005$) between tissue type and variety in addition to the interaction between the two treatment factors. A large proportion of the partial variance in macronutrient concentrations were attributed to tissue type and ranged from 69 % in Na to 97 % in Ca, whereas genotype attribution ranged from about 11 % in Ca to 64 % in S, in contrast to about 0.4 and 14 %, respectively, of the total variance (Appendix 2, Table 1). Figure 3.1 shows that, as an average among all genotypes, the pattern of mineral accumulation is considerably different across the seven plant tissues. For example, the top of the plant represented by the seeds and the top of the stem (Stem T) display a tendency to accumulate high concentration of S (0.36 and 0.34 %DW, respectively) in contract with other tissues, whereas seeds and Stem T possessed the lowest Na concentration (0.0038 and 0.0334 %DW, respectively). The bottom of the stem (Stem B) displayed the highest concentration of P and Ca; [P] varied between 2- and 7-fold

in seeds and tap root, respectively. Interestingly, [Ca] varied between 15- and >52-fold in Stem T and taproots, respectively. In comparison, [K] was at the lowest level in the Stem B (0.17 %DW) and varied between 4.7-fold in taproots and 10-fold in the middle of the stem (Stem M). The average concentration of six macronutrients varied by more than two orders of magnitude in Stem B from 0.08 %DW (Mg) to 15 %DW (Ca), and in seeds from 0.004 %DW (Na) to 1 %DW (K) (Figure 3.1 and Appendix 3, Table 1 to 6). Numerous significant differences between tissue types were found ($P < 0.0001$) among the macronutrients. However, it was observed that difference between the two section of taproots (T.root B and T.root T) was not significant ($P > 0.05$) among all macronutrients.

There is moderate variation in the concentration of six macronutrients among the 14 *B. napus* genotypes across all analysed tissues of stem, roots and seeds Figure 3.1. Lateral roots (L.root) macronutrient concentrations varied from 2.1-fold (K) to 5.6-fold (S), both taproot sections (T.root B and T.root T) varied from >1.5-fold (Ca) to >4-fold (S). Stem B element concentrations varied from 1.9-fold (Ca) to 5.6-fold (Na), moreover, in Stem M elements varied between 1.4-fold for Ca and 4.4-fold for Na. The variation in the Stem T ranged between 2.1- and 3.2-fold for S and Na, respectively (Figure 3.1 and Appendix 3, Table 1 to 6).

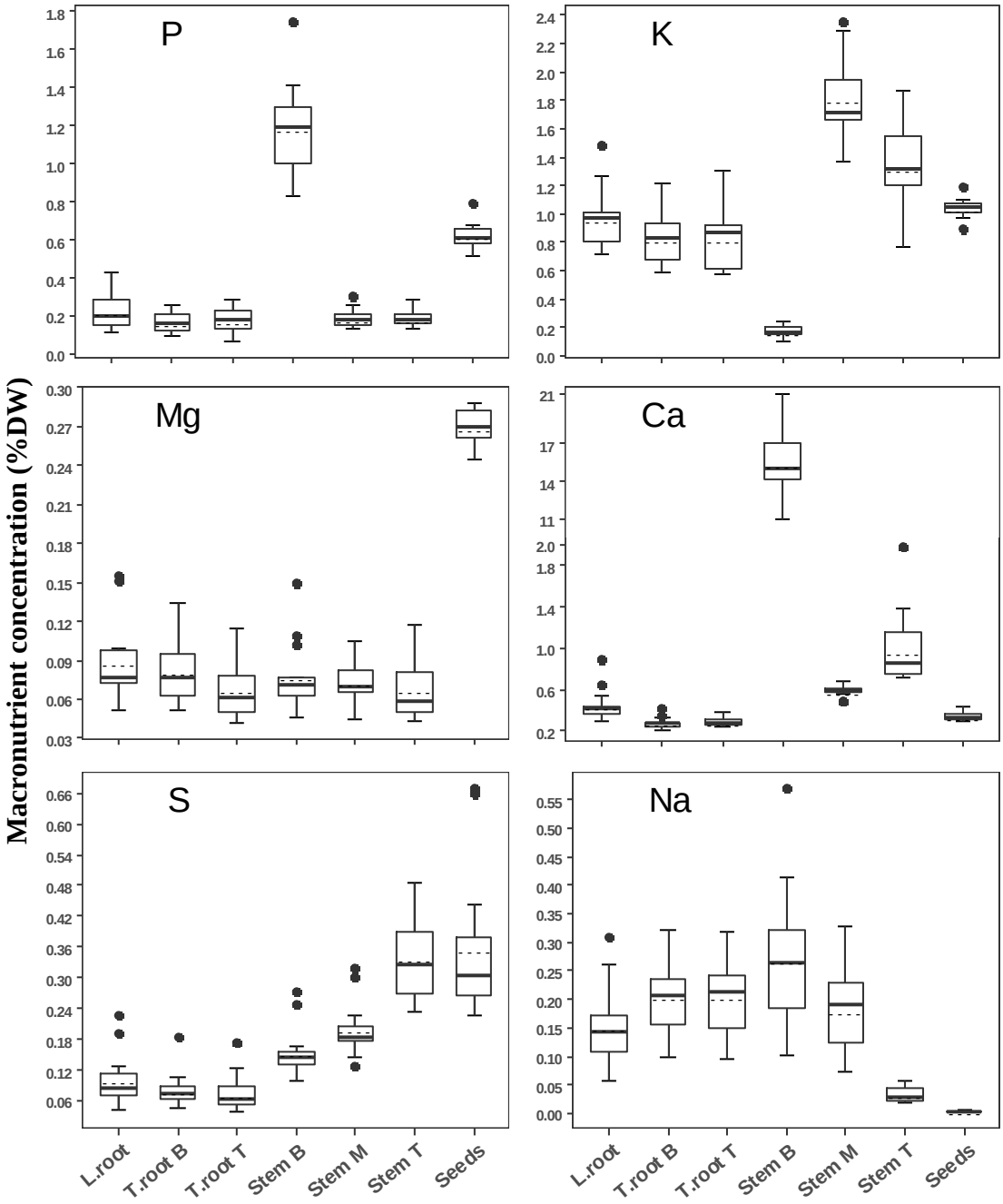

Figure 3.1 Variation in macronutrient concentrations across different tissues among 14 genotypes of *Brassica napus* at GS 6.2/6.3.

Six macronutrient concentrations (% dried weight, DW); P, K, Mg, Ca, Na (Kjeldahl-digest) and S (HNO_3-digest) were determined by ICP-OES. Data are the variety means (n=3). The lower and upper boundaries of the box represent the 25 and 75 percentiles, respectively. The solid and dashed lines within the box represent the median and mean, respectively. Whiskers closest and farthest to zero represent the smallest and largest non-outliers in the data set, respectively. Circles represent outliers.

3.4.2 Variation in micronutrient concentrations at GS 6.2/6.3

Significant differences were found between tissue type and genotype ($p > 0.00001$) in concentration of five micronutrients as well as significant interaction between tissue and genotype according to the analysis of variance. The largest proportion of the total variance attributed to tissue type ranged between 34 % for Cu and 88 % for Mn, whereas genotype attribution ranges between 1.8 % for Fe and 18 % for B in contrast to 14 and 52 %, respectively, of the partial variance. ANOVA tables according to the model [tissue x genotype] in addition to value of ω^2 and ω^2_p were shown (Appendix 2, Table 2).

Similar to macronutrients, and as an average among all genotypes, these five micronutrients varied by more than two orders of magnitude form 0.545 µg/g DW for Mn (Stem B) to 140 µg/g DW for Fe (L.root). Moreover, the accumulating pattern of these micronutrients differ remarkably between the seven plant tissue types Figure 3.2. For example, seeds tend to display the highest concentration of Mn and Zn (26.5 and 40.3 µg/g DW, respectively), while the two taproot sections possess a higher proportion of B and Fe than the stem and seeds. It was observed that [Mn] in the bottom of the stem (0.54 µg/g DW, Stem B) was significantly ($P < 0.00001$) less than Stem M, Stem T and seeds, and enormously varied more than 13-, 19- and 48-fold, respectively. There was also more than 6.5-fold of variation in [Fe] between L.root and Stem B, and in [Zn] between seeds and Stem B Figure 3.2 below and (Appendix 4, Table 1 to 5).

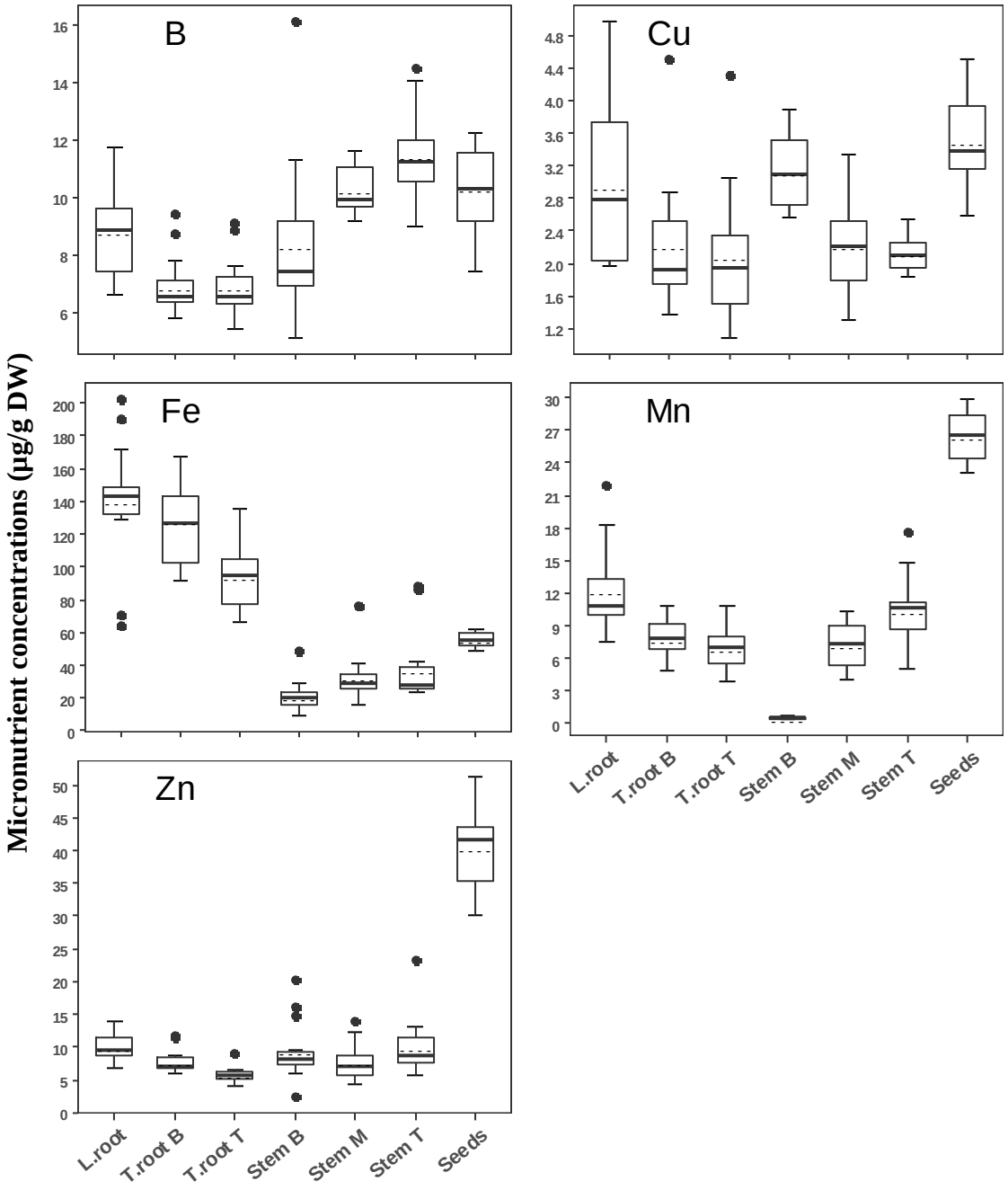

Figure 3.2 Variation in micronutrient concentrations across different tissues among 14 genotypes of *Brassica napus* at GS 6.2/6.3.

Five micronutrient concentrations (µg/g dried weight, DW); B, Cu, Fe, Zn (HNO_3-digest) and Mn (Kjeldahl-digest) were determined by ICP-OES. Data are the variety means (n=3). The lower and upper boundaries of the box represent the 25 and 75 percentiles, respectively. The solid and dashed lines within the box represent the median and mean, respectively. Whiskers closest and farthest to zero represent the smallest and largest non-outliers in the data set, respectively. Circles represent outliers.

Most of the differences between tissue types were significant (P <0.0001). However, similar to macronutrients, the difference between the two sections of the taproots was not significant (P >0.05) among all micronutrients except Fe. Furthermore, differences in [Zn] between stem and taproots were also not significant (P >0.05). Genotypic variation was reported in the concentration of these five micronutrients among the 14 genotypes across seven tissue types; L.root [micronutrients] varied between 1.8-fold for B and 3.2-fold for Fe, taproots varied between >1.6-fold for B and >3.3-fold for Cu. The variation ranged from 1.5-fold for Cu to 8.6-fold for Zn in Stem B, form 1.3-fold for B to 4.9-fold for Fe in Stem M, from 1.4-fold for Cu to 4.1-fold for Zn in Stem T and from 1.3-fold for Fe to 1.7-fold for Cu in seeds (Figure 3.2 and Appendix 4, Table 1 to 5).

3.4.3 The relationship between all mineral nutrients at GS 6.2/6.3

To establish the relationship between all mineral elements within one tissue as well as between tissues, Pearson correlation analysis was conducted on all possible 2926 pair-wise combinations of the 77 traits (11 mineral elements and seven tissue types) using variety means. Out of all combinations, 276 significant (P <0.05, df =12) and positive (r >0.53) pair-wise correlations were observed, of which 65 and 211 were within and between tissues, respectively Figure 3.3 below. The strongest correlation within tissues found (r =0.87, P =$5.5*10^{-5}$) between Cu and S in the bottom of the taproot (T.root B), whereas between tissues (r =0.98, P =$4.3*10^{-10}$) was in P between the two tissue types of taproot; T.root B and T.root T. Three strong positive pair-wise of associations found within all root tissues and top of the stem (Stem T); S/Ca (0.73< r <0.84, but this relationship was moderate and not significant in T.root B; r =0.45, P >0.05), Mg/P (0.63< r <0.71) and S/Mg (0.68< r <0.75).

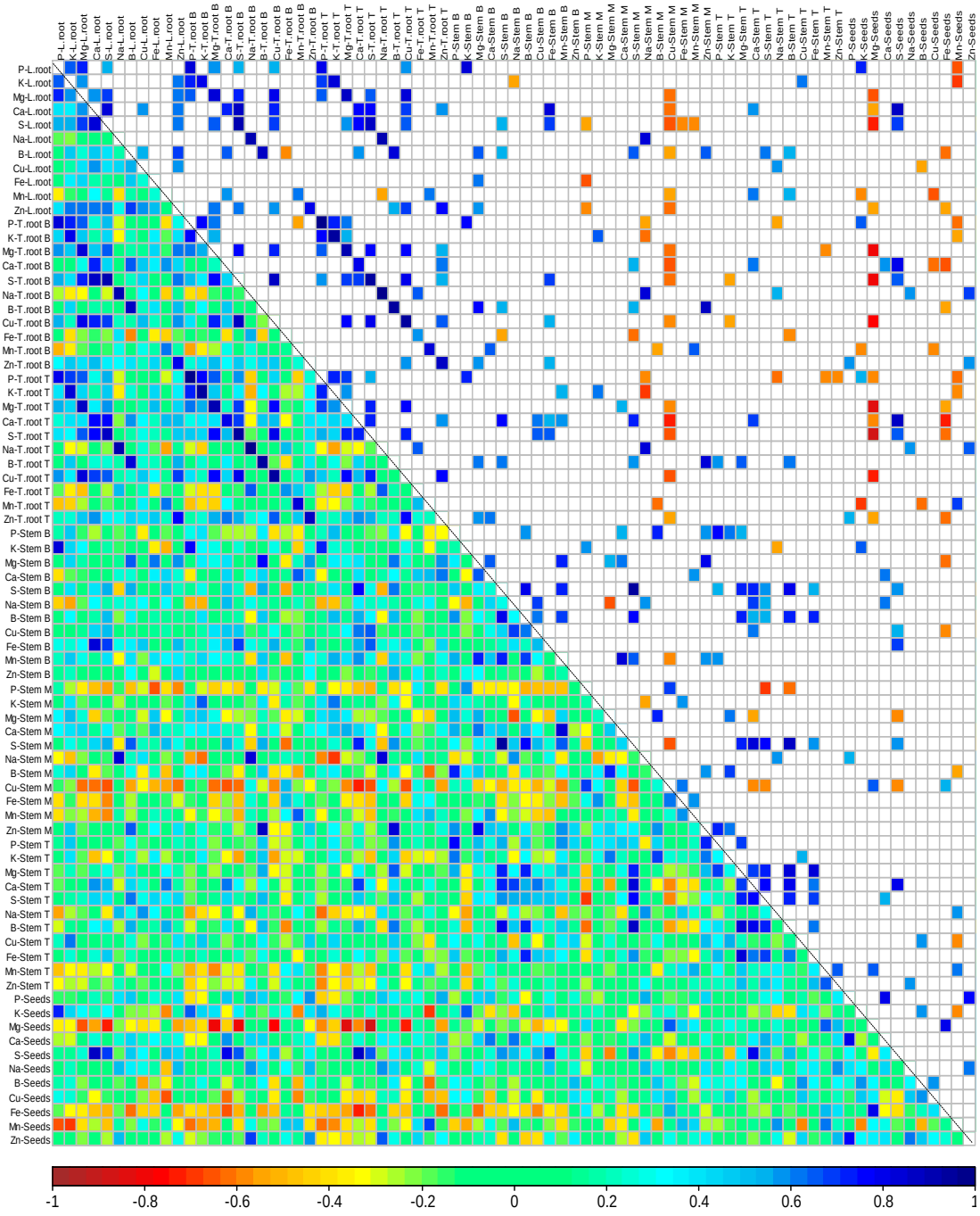

Figure 3.3 Pair-wise correlation analysis of all 77 traits in 14 genotypes of B.napus using genotype mean at GS 6.2/6.3.

77 traits of 11 mineral elements and seven tissue types of roots (L.root, T.root B and T.root T), stem (Stem B, M and T) and seeds. The lower triangle represents all 2926 possible pairs-wise correlations. The upper triangle represents only significant (P >0.05) correlations. Correlation coefficients panel are scaled from -1 (dark brown) to +1 (dark blue).

There were also three positive relationships only within root tissues, which ranged from strong association in K/P ($0.67 < r < 0.77$) to moderate association in Mg/K ($0.56 < r < 0.59$) and S/P ($0.51 < r < 0.54$, but this was not significant in T.root B; $P > 0.05$). Furthermore, Positive correlation ($0.54 < r < 0.62$) in Cu/B observed within L.root, Stem B and seeds. There were strong positive correlations ($0.73 < r < 0.87$) in Cu/S within taproot tissues, whereas it was strong negative correlation ($r = -0.65$, $P < 0.05$) in Stem M. In addition, Ca and Mg were significantly associated only within three tissues; L.root, Stem B and Stem T ($r = 0.58$, 0.65 and 0.70, respectively). Cu and Mg were strongly correlated ($0.73 < r < 0.77$) within both taproot tissues. Zn positively correlated ($0.57 < r < 0.76$) with Ca and Cu within both L.root and T.root T, and with B only in L.root. The strongest positive correlations in Stem B were between B/S, Mn/Mg, Mn/S and Mn/B ($0.69 < r < 0.81$), and in Stem M were between B/Mg and Cu/P ($r = 0.73$ and 0.69, respectively); all $P < 0.01$. Fe and Mg were very strongly associated within both Stem T ($r = 0.84$) and seeds ($r = 0.79$), moreover, very strong correlations were reported in Stem T concentrations of B and Mg ($r = 0.83$) and B and Ca ($r = 0.81$); all $P < 0.0005$, and in seeds concentrations of Ca and P ($r = 0.79$) and Zn and P ($r = 0.76$); all $P < 0.005$.

The strongest positive relationships between tissues were in concentrations of P, Na, K, Cu, B and S between both taproot tissues ($r > 0.94$, $P < 3.6*10^{-7}$), in [S] between Stem M and Stem B ($r = 94$), in [Na] and [S] between T.root B and L.root ($r = 0.93$ and 92, respectively), in [Na] between T.root T and L.root ($r = 91$), in [Mg] between T.root T and T.root B ($r = 0.89$), between S in seeds and Ca in L.root ($r = 0.88$) and between B in Stem T and S in Stem M ($r = 0.87$); all $P < 0.00005$.

92 significant (P <0.05, df =12) and negative (r <-0.53) pair-wise correlations were mostly observed in the above ground tissues, of which 4 and 88 were within and between tissues, respectively Figure 3.3 (page 109). The only four negative relationships were within Stem M Cu/S and Na/K (r =-0.65 and -0.54, respectively), seeds Mn/K (r =-0.59) and T.root B Mn/P (r =-0.54). On the other hand, the strongest negative relationships between tissues were observed between seeds [Mg] and the concentration of S, Mg and Cu in taproot tissues (-0.86< r <-0.72), between [Ca] in T.root T and seeds [Fe] (r =-0.72), between [Ca] in T.root T and Stem M [Cu] (r =-0.71) and between [Na] in Stem M and [K] in T.root T (r =-0.69); all P <0.006.

3.4.4 Variation in macronutrient concentration at harvest

Analysis of variance was conducted across all macronutrients according to the model [(croptype/genotype) x tissue]. Significant differences (P >$2.7*10^{-15}$) between three treatments in addition to the interaction between them. Tissue type accounted for the largest proportion and ranged from 23 % (Na) to 87 % (P) of the total variance in macronutrient concentrations, whereas crop type explained only between 0.2 % (P) and 7 % (Ca) of the total variance. The second largest proportion of the total variance attributed to the interaction between crop type, genotypes and tissue, ranged from 4.4 % (P) to 25 % (S). ANOVA tables and proportions of the total and partial variance accounted for all factors is given in Appendix 5, Table 2. Macronutrient concentrations differed greatly across seven tissues of root, stem and seeds as an averaged among all crop types and genotypes, for example, seeds possessed the highest concentrations of P, S and Mg (0.81, 0.45 and 0.22 %DW, respectively) in contrast they possessed the lowest concentrations of K, Ca and Na (0.56, 0.43 and 0.0038 %DW, respectively) (Figure 3.4, and Appendix 6, Tables 1 to 6).

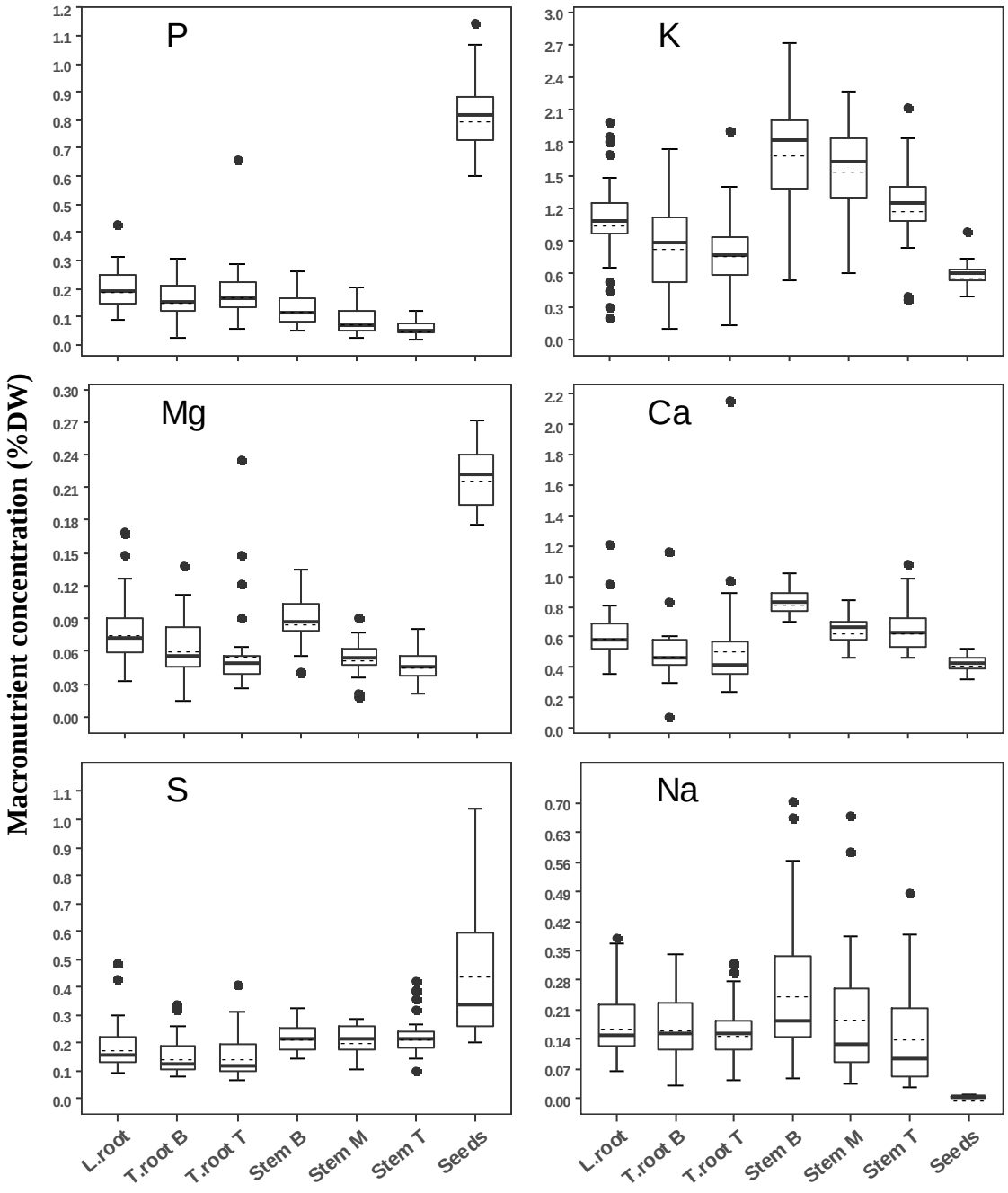

Figure 3.4 Variation in macronutrient concentrations across different tissues among 30 genotypes of *Brassica napus* at harvest.

Six macronutrient concentrations (% dried weight, DW); P, K, Mg, Ca, Na (Kjeldahl-digest) and S (HNO_3-digest) were determined by ICP-OES. Data are the variety means (n=5). The lower and upper boundaries of the box represent the 25 and 75 percentiles, respectively. The solid and dashed lines within the box represent the median and mean, respectively. Whiskers closest and farthest to zero represent the smallest and largest non-outliers in the data set, respectively. Circles represent outliers.

In comparison, Stem T displayed the lowest concentrations of P (0.06 %DW) and Mg (0.05 %DW), taproot displayed the lowest concentration of S (0.15 %DW), and Stem B possessed the greatest concentration of K, Ca and Na (1.71, 0.84 and 0.25 %DW, respectively). Interestingly, Na concentration was lower in seeds and varied between 38.5- and 65.6-fold in Stem M Stem B, respectively. Differences between tissue types were significant (TukeyHSD, $P < 0.001$) among all macronutrients except between; T.root B and T.root T across all macronutrients, all root tissues for Na and all stem tissues for S where differences were not significant (TukeyHSD, $P > 0.05$). The averaged concentration of six macronutrients varied by more than two orders of magnitude within seeds from 0.0038 %DW (Na) to 0.81 %DW (P), and only by one order of magnitude within stem tissues between Mg (<0.088 %DW) and K (>1.2 %DW).

Genotypic variation across six macronutrient concentrations among 30 genotypes across seven tissue types was observed, L.root macronutrient concentrations varied from 3.4-fold for Ca to 10.7-fold for K, taproot tissues; T.root B and T.root T varied from 4.3- and 6.2-fold for S to 15.9- and 17.9-fold for K, respectively, three stem tissue types; Stem B, Stem M and Stem T varied from 1.5-, 1.8- and 2.3-fold for Ca, to 15.2-, 18.6- and 20-fold for Na, respectively, and seeds varied from 1.5-fold for Mg to 5.2-fold for S (Figure 3.4 and Appendix 6, Tables 1 to 6). Swede (averaged among six genotypes) possessed greater mean of lateral and taproot six macronutrient concentrations than other crop types; Spring (five genotypes) and Winter OSR (19 genotypes). Swede had also greater mean of seeds macronutrient (P, K, Mg, S) concentrations than other crop types. Spring OSR possessed lower mean of L.root macronutrient concentrations (P, K, Mg, Na) and taproot (K, Mg, Na). Winter OSR

displayed greater mean of Stem B six macronutrient concentrations except for Na which was greater in Spring OSR than other crop types. Winter OSR had greater mean of Stem M macronutrients (P, K, Mg) in contrast Spring OSR had greater mean concentrations of S and Na than other crop types (Appendix 6, Tables 1 to 6).

3.4.5 Variation in micronutrient concentration at harvest

Significant differences (ANOVA, $P > 2.3*10^{-11}$) between genotype, genotypes, tissue and the interaction between them in concentration of five micronutrients. However, the differences between crop type in concentration of Mn and Zn was not significant ($P > 0.05$). Tissue attributed to a large proportion of the total variance in micronutrient concentrations, and ranged between 19 % and 74 % for B and Zn, respectively, whereas, crop type attribution has not exceeded 5 % (Cu). Genotype accounted for 3 - 44 % of the total variance in the concentration of Fe and B, respectively. ANOVA tables and proportions of the total and partial variance accounted for all treatment factors are shown in Appendix 5, Table 2. The accumulation pattern of these five micronutrients was different across all tissue types as an averaged among all crop types and genotypes. The greatest concentration of Mn and Zn (37 and 34.4 µg/g DW, respectively) was observed within seeds, Fe and Cu (252 and 3.56 µg/g DW, respectively) observed within L.root, and B (13 µg/g DW) observed within Stem B. In comparison, the lowest concentration of Cu, Zn and Mn (1.7, 7.1 and 9.2 µg/g DW, respectively) within Stem T, Fe (18.4 µg/g DW) within Stem M and B (~ 10 µg/g DW) within taproots. Interestingly, Fe concentration varied about 13.7-fold between L.root and Stem M (Figure 3.5 and Appendix 7, Tables 1 to 5).

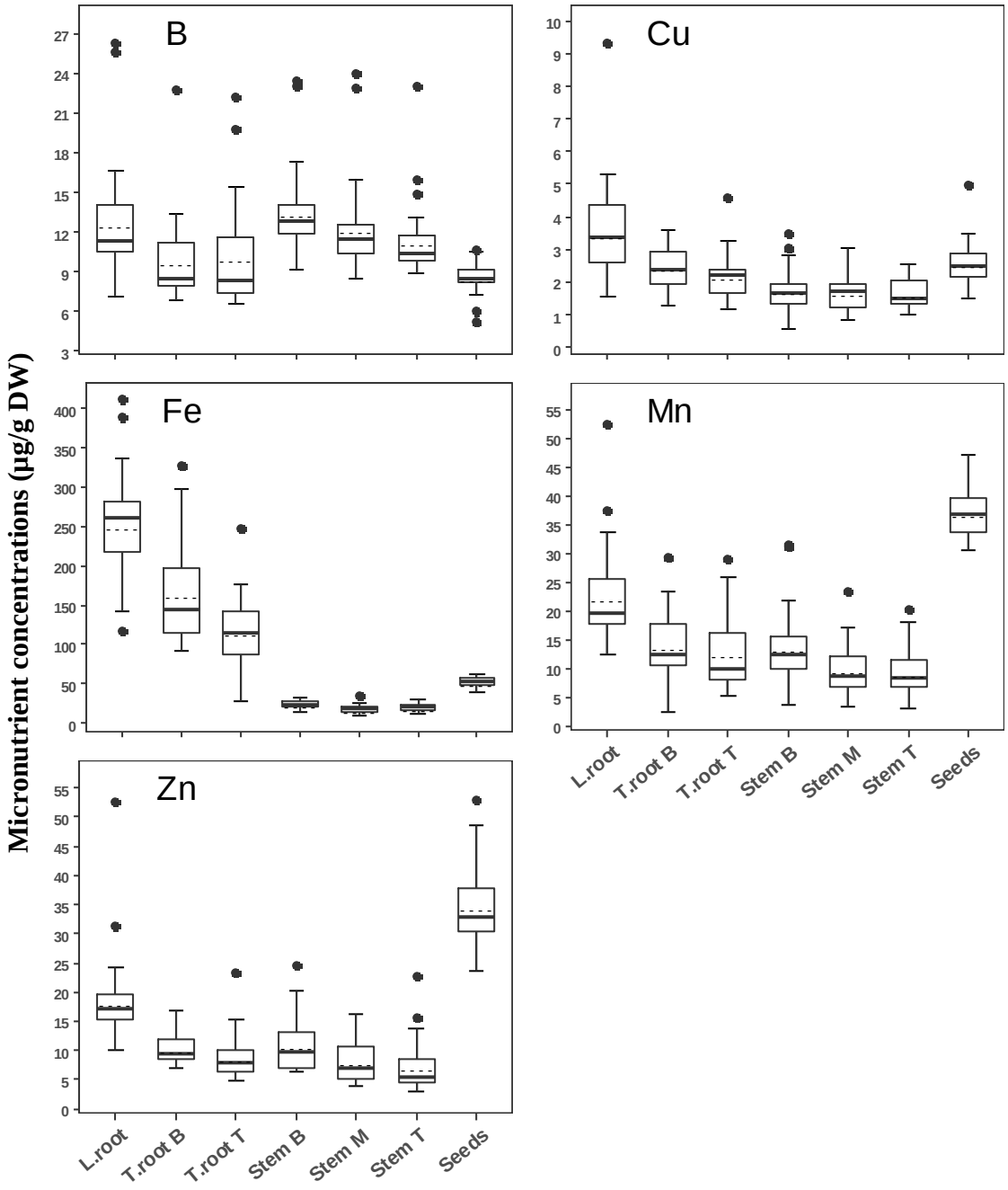

Figure 3.5 Variation in micronutrient concentrations across different tissues among 30 genotypes of *Brassica napus* at harvest.

Five micronutrient concentrations (µg/g dried weight, DW); B, Cu, Fe, Zn (HNO_3-digest) and Mn (Kjeldahl-digest) were determined by ICP-OES. Data are the variety means (n=5). The lower and upper boundaries of the box represent the 25 and 75 percentiles, respectively. The solid and dashed lines within the box represent the median and mean, respectively. Whiskers closest and farthest to zero represent the smallest and largest non-outliers in the data set, respectively. Circles represent outliers.

Differences in micronutrient (Cu, Fe, Zn) concentrations were significant (TukeyHSD, P <0.003) between T.root B and T.root T, but differences in [B] and [Mn] were not significant (, P >0.05). Furthermore, there were no significant differences (TukeyHSD, P >0.05) in [Cu] and [Fe] between three stem tissue sections, and also in [Mn] and [Zn] between Stem M and Stem T; all P >0.05, TukeyHSD.

Genotypic variation across five micronutrient concentrations among 30 genotypes across seven tissue types was observed, L.root varied between 3.6-fold for [Fe] and 6.1-fold for [Cu], T.root B varied between 2.4-fold for [Zn] and 11.5-fold for [Mn], T.root T varied between 3.4-fold for [B] and 9.2-fold for [Fe], Stem B varied between 2.2-fold for [Fe] and 8.8-fold for [Mn], Stem M varied between 2.8-fold for [B] and 7.1-fold for [Mn], Stem T varied between 2.5-fold for [Cu] and 8-fold for [Zn] and seeds varied between 1.5-fold for [Mn] and 3.3-fold for [Cu] (Figure 3.5 above and Appendix 7, Tables 1 to 5). Swede crop type (averaged among six genotypes) possessed the highest mean of lateral and taproots five micronutrient concentrations. In comparison, Winter OSR (averaged among 19 genotypes) possessed the lowest mean of lateral root micronutrients (Cu, Fe, Mn, Zn) as well as the lowest mean of taproot micronutrients (Cu, Fe, Mn) concentrations, whereas Spring OSR (averaged among five genotypes) possessed the lowest mean of B and Zn concentrations within taproot and B concentration within L.root. Swede possessed the lowest mean of stem and seeds tissues macronutrient (B, Fe, Mn, and Zn) concentrations, whereas Spring OSR had the lowest mean of Cu concentration within three stem tissue types.

3.4.6 The relationship between all mineral nutrients at harvest

Pearson correlation analysis was performed on all possible 2926 pair-wise combinations of the 77 traits (11 mineral nutrients and seven tissue types) using genotype means in order to elaborate the relationship between mineral elements within and between tissues. Out of all combinations, 490 significant ($P < 0.05$, df =28) and positive ($r > 0.36$) pair-wise correlations were reported, of which 122 and 368 were within and between tissues, respectively Figure 3.6 below. The strongest correlation within tissues ($r = 0.91$, $P = 2.5*10^{-12}$) observed between Ca and P in the top of the taproot (T.root T), whereas between tissues ($r = 0.97$, $P = 5.4*10^{-18}$) found between B concentration in the bottom and middle of the stem. Many other pair-wise positive relationships were reported within multiple tissues. For example, Ca/Mg within all tissues, ranged very strong ($r = 0.9$, $P = 1.9*10^{-11}$, T.root T) to moderate correlation ($r = 0.42$, $P = 0.02$, seeds), Mg/P within roots ($0.61 < r < 0.85$), seeds ($r = 0.82$) and Stem B ($r = 0.45$), Ca/P within taproot ($0.57 < r < 0.91$), seeds ($r = 0.52$) and Stem B ($r = 0.37$), S/Ca within roots ($0.48 < r < 0.83$) and Stem T ($r = 0.51$), Zn/Mn within roots ($0.57 < r < 0.79$), Stem B ($r = 0.52$) and Stem T ($r = 0.47$), S/Mg within roots ($0.53 < r < 0.75$) and Stem B ($r = 0.48$), S/P within roots ($0.37 < r < 0.74$) and seeds ($r = 0.53$), Mn/Fe within roots ($0.58 < r < 0.7$) and Stem M ($r = 0.45$), Mg/K within L.root, T.root B, Stem B and seeds ($r = 0.71$, 0.65, 0.42 and 0.52, respectively), K/P within L.root, Stem B and seeds ($r = 0.54$, 0.55 and 0.67, respectively), S/K within L.root ($r = 0.43$), stem ($r = \sim 0.45$) and seeds ($r = 0.52$), Zn/Fe within L.root, T.root B, stem and seeds ($0.4 < r < 0.54$) and B/Mg within roots and Stem M ($0.38 < r < 0.64$), Mn/S within L.root and T.root T ($r = 0.6$ and 0.66, respectively).

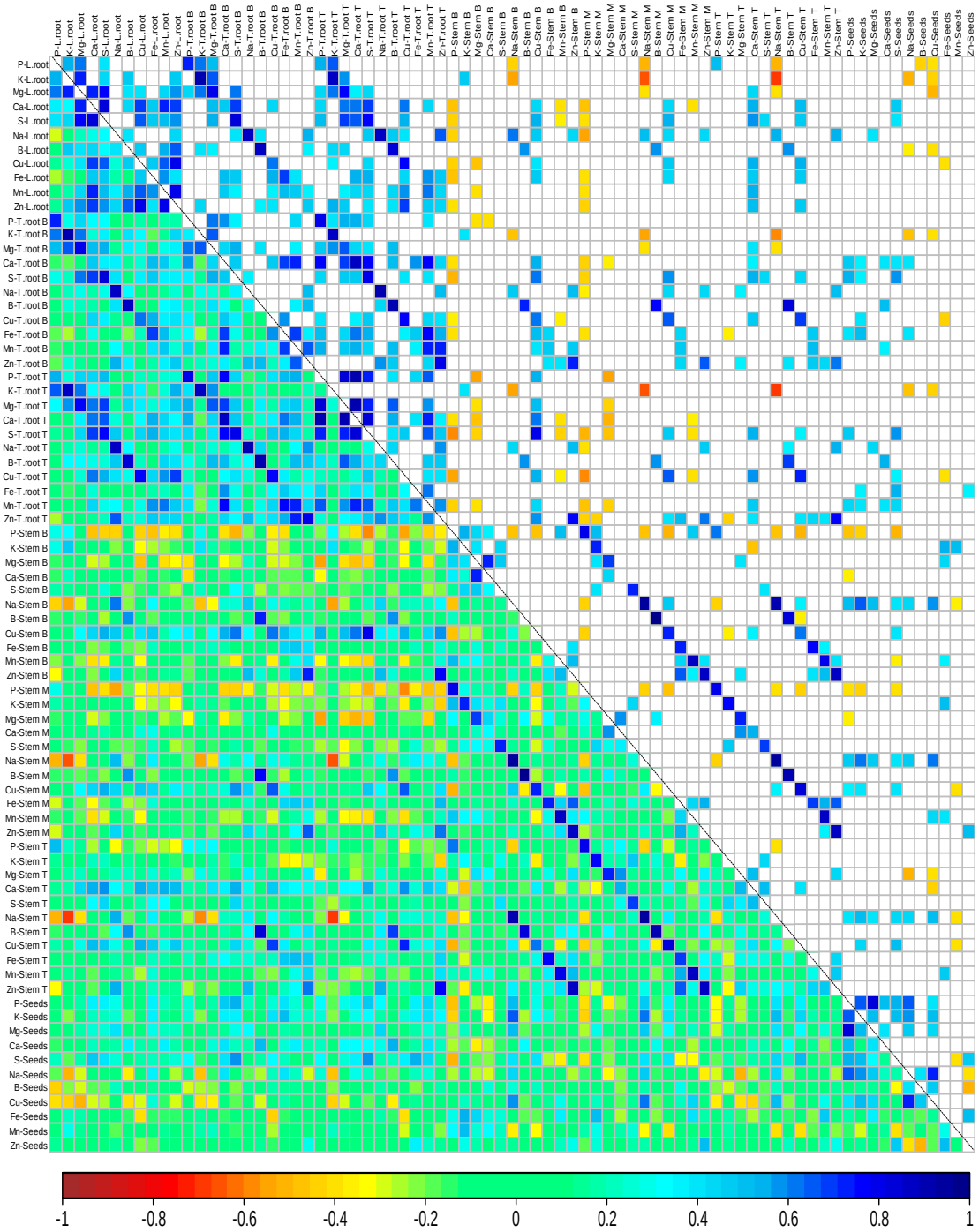

Figure 3.6 Pair-wise correlation analysis of all 77 traits in 30 genotypes of *B.napus* using genotype mean at harvest.

77 traits of 11 mineral elements and seven tissue types of roots (L.root, T.root B and T.root T), stem (Stem B, M and T) and seeds. The lower triangle represents all 2926 possible pairs-wise correlations. The upper triangle represents only significant (P >0.05) correlations. Correlation coefficients panel are scaled from -1 (dark brown) to +1 (dark blue).

Furthermore, there were two combinations of pair-wise relationships within L.root, T.root T and seeds; Zn/S (0.47< r <0.6) and B/Na (0.41< r <0.45). In addition, there were five pair-wise combinations within root tissues; Mn/Ca (0.71< r <0.73), Fe/Ca (0.41< r <0.68), Zn/B (0.48< r <0.67), Zn/Na (0.45< r <0.59) and Mn/B (0.37< r <0.53). The strongest positive relationships between tissues were in concentrations of B, Na, Mn and Zn between stem tissue types (0.78< r <0.97), in concentration of Na, B, K, Ca, S, Zn and P between taproot tissues (0.78< r <0.91), in concentration of K, Na, B, S and Mg between L.root and T.root B, and between L.root and T.root T (0.77< r <0.89), in B concentration between Stem T and T.root B (r =0.82), in B concentration between Stem M and T.root B (r =0.75), in Zn concentration between Stem T and T.root T (r =0.77), in Zn and B concentration between Stem B and T.root B (r =~0.73), and between [Cu] within Stem B and [S] within T.root T (r =0.78); all P >$4.4*10^{-6}$ Figure 3.6 above.

124 significant (P <0.05, df =28) and negative (r <-0.36) pair-wise correlations were also reported, of which 8 and 116 were within (only within above ground tissues) and between tissues, respectively Figure 3.6. The eight negative correlation combinations were Na/P (-0.4> r >-0.46) within all stem tissues, Cu/P within Stem M (r =-0.49) and Stem B (r =-0.47), and Zn/B, Zn/Na and Cu/S (r =-0.5, 0.4 and -0.39, respectively) within seeds. In comparison, the strongest negative correlations between tissues observed between [Na] in Stem T and [K] within all root tissue types (-0.7< r <-0.58), between [Na] in Stem M and [K] within all root tissue types (-0.55< r <-0.66), between [P] in Stem B and [S] in T.root T (r =-0.57), between [P] in Stem M and [Cu] in T.root T (r =-0.57) and between [Na] in Stem B and [K] in T.root T and L.root (r =-0.55); all P <0.003.

3.4.7 Comparison between both stages GS 6.2/6.3 and harvest

11 mineral elements were independently analysed during the growth stages GS 6.2/6.3 and harvest. Genotypic variation within tissues and between tissues were studied as well as the relationship between these nutrients. 14 genotypes of *B. napus* L. were shared between the two different stages. Therefore, combining the two stages together to elucidate differences in mineral nutrient concentrations in every tissue was of interest. Variation in macro and micronutrient concentrations were observed among two stages within seven tissue types. Significant differences (ANOVA, $P < 0.0001$) in all mineral concentrations within tissues between the two stages were observed. The effect of stage on macronutrient concentrations within tissue ranged from 2.3 % for Mg to 52 % for Ca of the total variance, whereas on micronutrient concentrations ranged between 3 % for Zn and 9 % for Cu and B. Tissue also, as previously reported, accounted for a large proportion of the total variance and ranged between macronutrients from 28 % for K to 81 % for Mg, and between micronutrients from 15 % for B to 79 % for Zn. ANOVA tables according to the model [stage x tissue x genotype] in addition to total and partial variance were shown in Appendix 8, Table 1.

Different patterns of mineral concentrations observed between tissues as an average among 14 genotypes in addition to genotypic differences within tissues across two stages. Stem tissue types possessed significantly lower concentration of P at harvest than the seed development stage GS 6.2/6.3, ranged between 6.9-fold (0.17 – 1.18 %DW, Stem B) and 1.7-fold (0.11 – 0.19 %DW, Stem M). Seeds possessed higher P concentration at harvest (1.2-fold, 0.62 – 0.75 %DW), however varietal differences were reported, for example, there was no difference in P concentration between both

growth stages among varieties FD502, Grizzly and Tapidor DH (Figure 3.7 and Appendix 3 and 6, Table 1).

The bottom of the stem had significantly greater K concentration (10-fold, 0.18 – 1.8 %DW), whereas seeds displayed significantly lower K concentration (1.8-fold, 0.57 – 1.04 %DW) at harvest than GS 6.2/6.3. Moreover, varietal differences in K concentration were revealed. For instance, Sun and Yudal had significantly greater (~2-fold) and lower (3.8- to 6-fold), respectively, concentration of K within all root tissues at harvest (Figure 3.8 and Appendix 3 and 6, Table 2). In comparison, Stem B possessed significantly greater concentration of Ca (18-fold, 0.85 – 15.3 %DW), whereas seeds exhibited lower concentration (1.3-fold, 0.34 – 0.43 %DW) at GS 6.2/6.3 than harvest. Furthermore, there were genotypic variation within tissues. For example, Darmor and FD502 displayed no differences in Ca concentration between both stages, however they significantly varied 2.5-fold (0.53 – 1.35 %DW at harvest and GS 6.2/6.3, respectively, Darmor) and 2-fold (0.68 - 1.38 %DW at harvest and GS 6.2/6.3, respectively, FD502) within Stem T (Figure 3.9 and Appendix 3 and 6, Table 4).

Significant differences in seed Mg concentration (1.3-fold) between two stages were found where seeds had greater concentration at GS 6.2/6.3 (Appendix 9, Figure 1). Roots and Stem B tissues displayed higher concentration of S at harvest than GS 6.2/6.3. Nonetheless, genotypic variation clearly existed (Appendix 9, Figure 2). There were also varietal differences in Na concentration within tissues, for example, Na concentration significantly differed between growth stages within the taproot of Sun (Appendix 9, Figure 3).

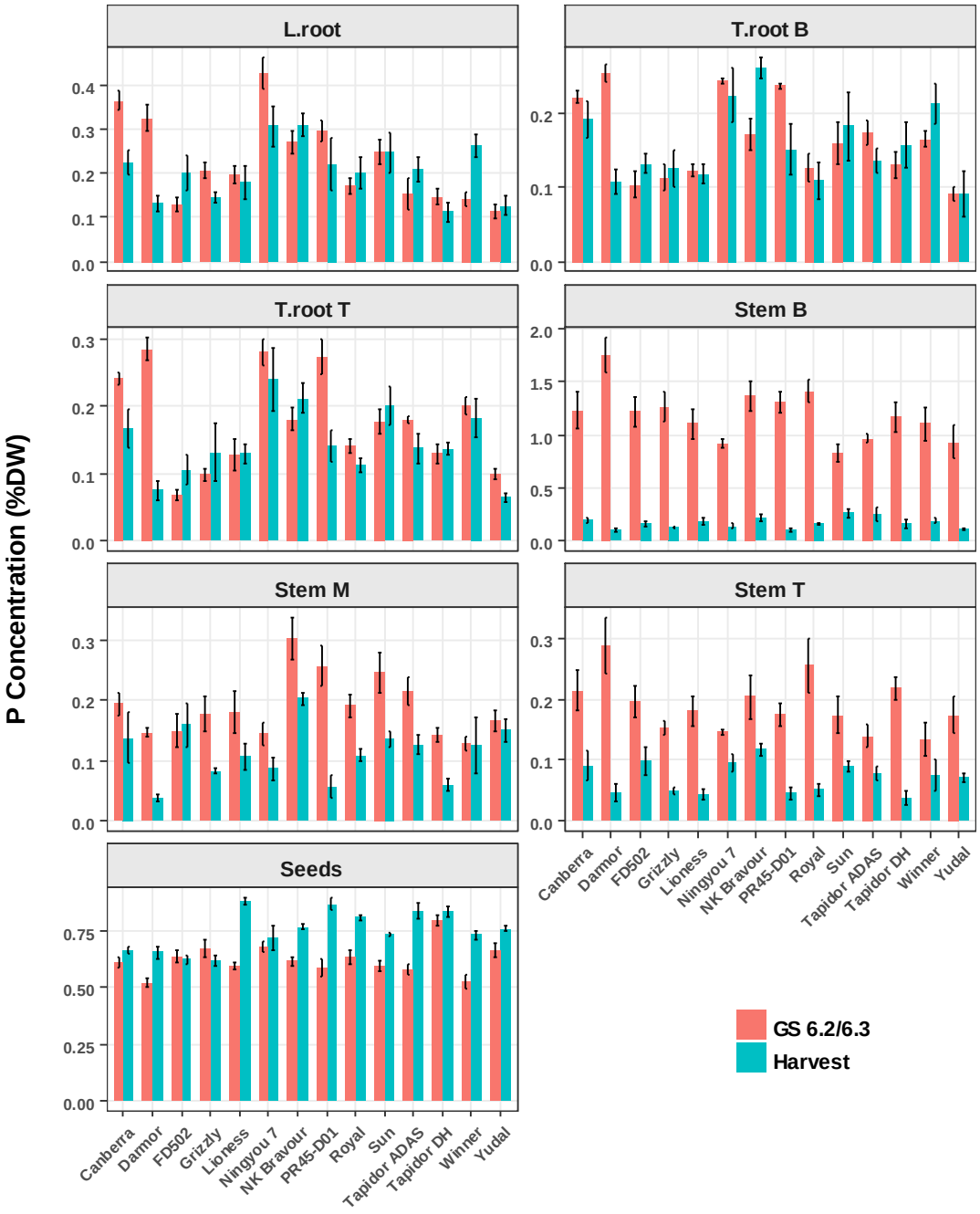

Figure 3.7 P concentration across seven tissues between two growth stages (GS 6.2/6.3 and harvest) among 14 *Brassica napus* genotypes.

Data are genotype mean ± SEM (n=3 and n=5 at GS 6.2/6.3 and harvest, respectively).

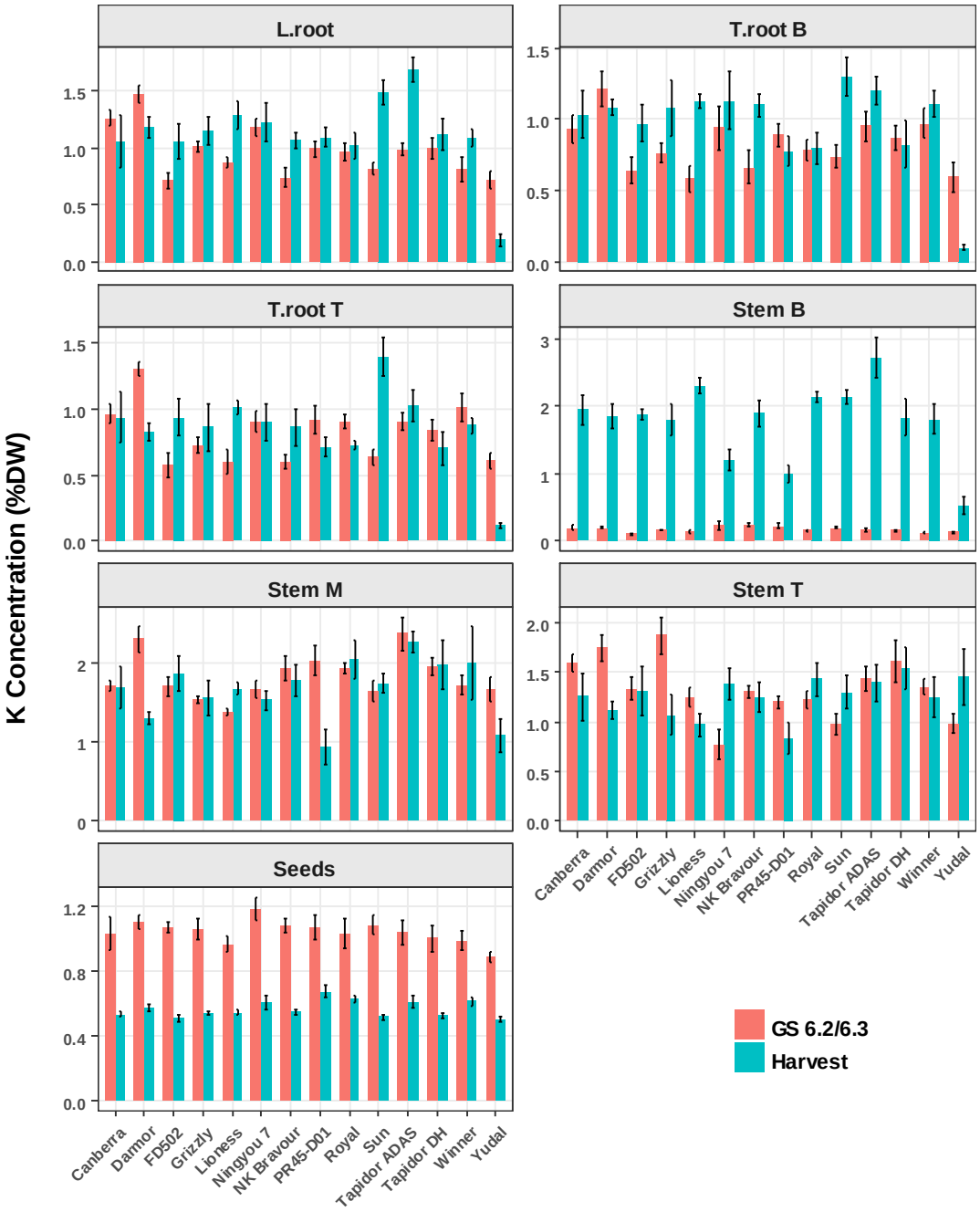

Figure 3.8 K concentration across seven tissues between two growth stages (GS 6.2/6.3 and harvest) among 14 *Brassica napus* genotypes.

Data are genotype mean ± SEM (n=3 and n=5 at GS 6.2/6.3 and harvest, respectively).

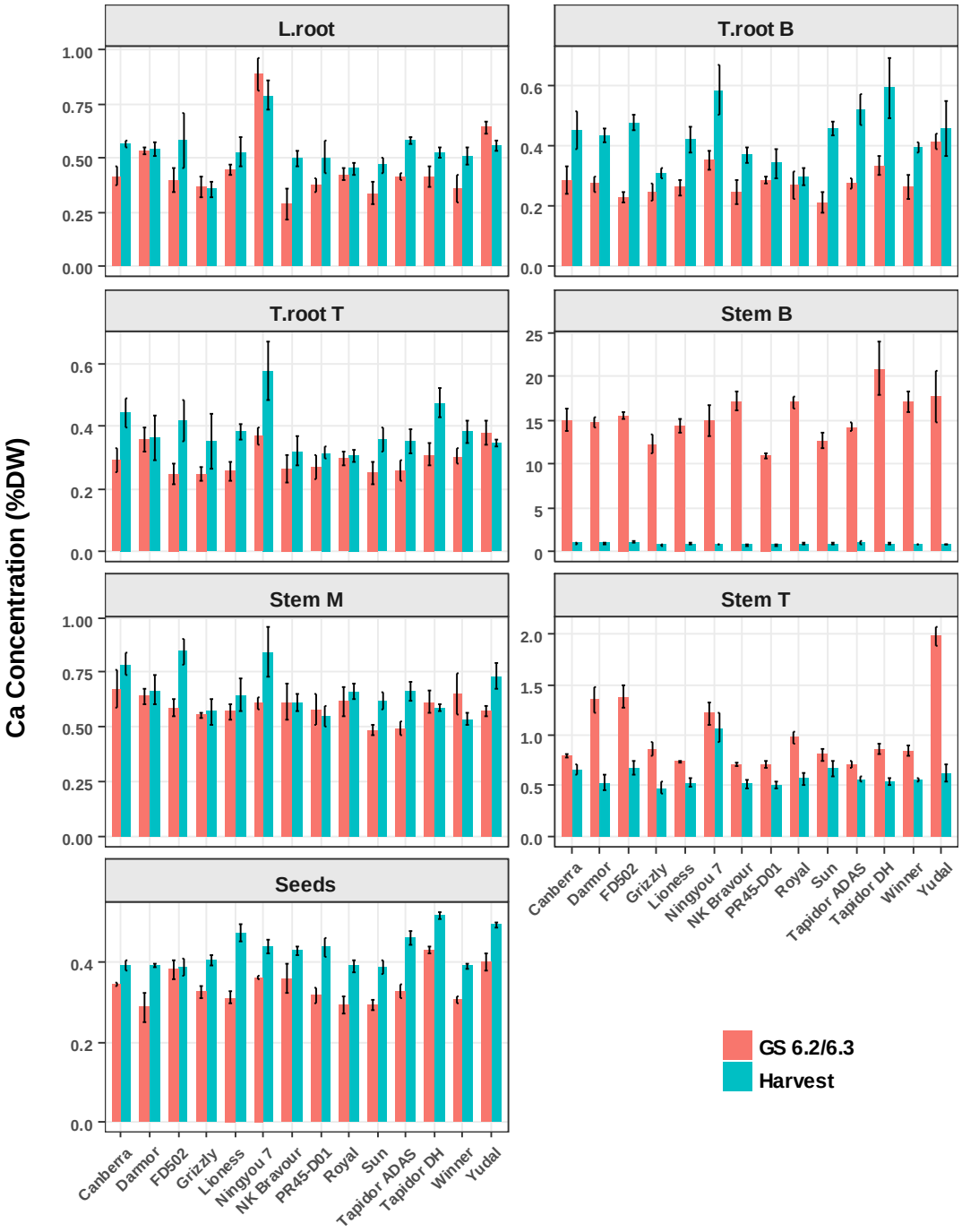

Figure 3.9 Ca concentration across seven tissues between two growth stages (GS 6.2/6.3 and harvest) among 14 *Brassica napus* genotypes.

Data are genotype mean ± SEM (n=3 and n=5 at GS 6.2/6.3 and harvest, respectively).

Three root tissue and two stem tissue types (Stem B and Stem M) had significantly greater concentration of B at harvest than GS 6.2/6.3, with a variation of ~1.5-fold (roots), 1.8-fold (Stem B) and 1.4-fold (Stem M) in contrast seeds B concentration decrease at harvest, with a difference of 1.2-fold. Interestingly, Tapidor DH possessed significantly higher B concentration (averaged 23.5 µg/g DW) within all root and stem tissues at harvest than other 13 varieties (averaged 11.8 µg/g DW), but nevertheless seeds possessed lower concentrating (8.2 µg/g DW) than genotype mean (8.8 µg/g DW). In comparison, NK Bravour had the lowest B concentration within root and stem tissues (averaged 9.1 µg/g DW). Nonetheless, seeds possessed similar concentration to seeds of cultivar Tapidor DH (Figure 3.10 below and Appendix 4 and 7, Table 1).

Concentration of Mn had increased within all tissue types except the top of the stem at harvest and significantly differed from GS 6.2/6.3 within Stem B (28-fold, ranged 0.38 – 0.70 µg/g DW at GS 6.2/6.3 and 8.52 – 31.52 µg/g DW at harvest) and seeds (1.4-fold, ranged 23.1 – 29.9 µg/g DW at GS 6.2/6.3 and 31 - 47.3 µg/g DW at harvest). Mn concentration was lower at harvest among all genotypes except Sun which had a greater concentration of Mn at harvest (20.3 µg/g DW) than GS 6.2/6.3 (10.8 µg/g DW) (Figure 3.11 and Appendix 4 and 7, Table 4). Concentration of Cu had decreased within stem and seeds at harvest and significantly differed from GS 6.2/6.3 within Stem B (2.2-fold) and seeds (1.4-fold). However, genotypic variation was observed across all tissues; for instance, there was no significant difference between two stages of Royal and Winner within seeds, and among varieties Canberra and Winner within Stem M (Appendix 9, Figure 4) and (Appendix 4 and 7, Table 2).

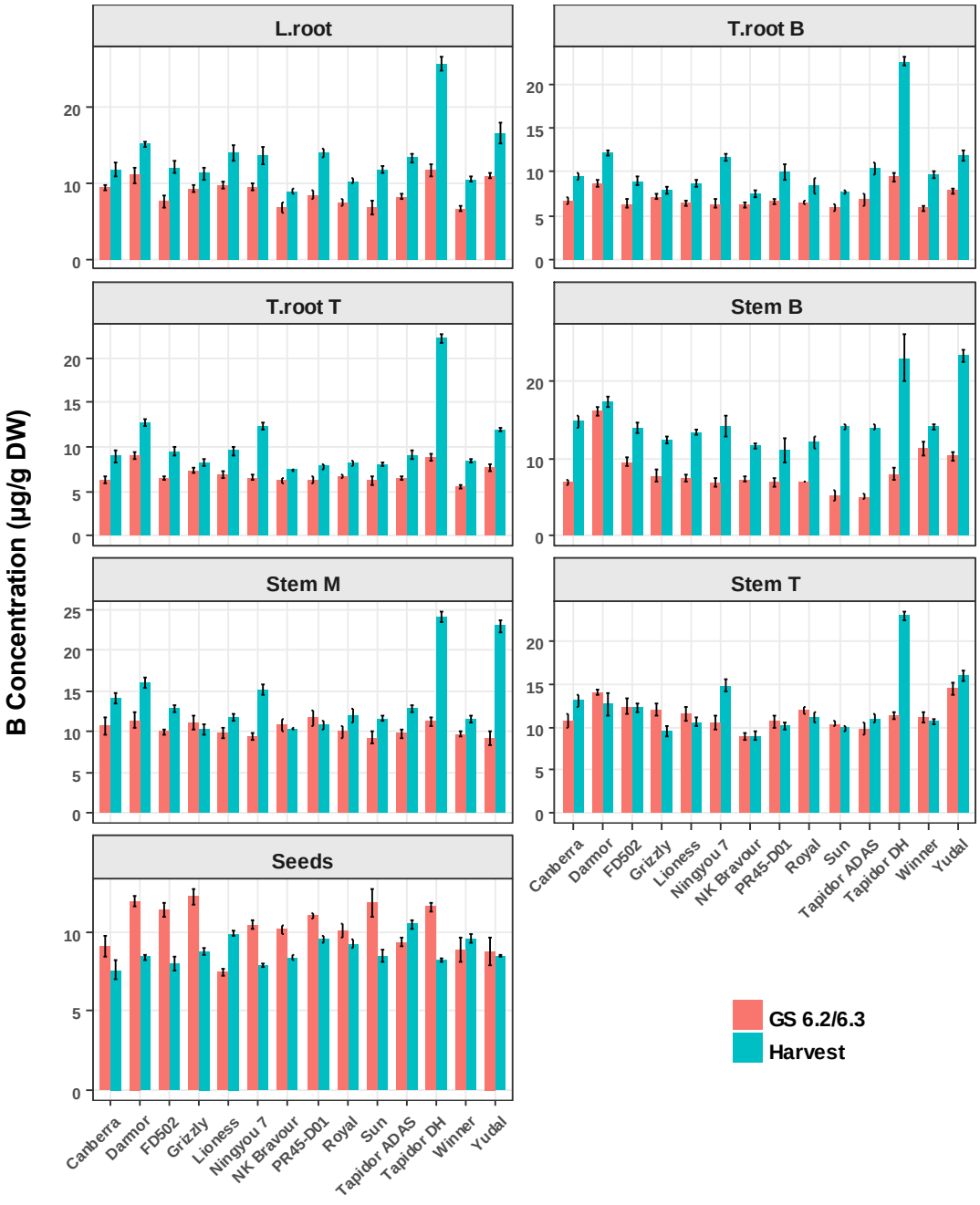

Figure 3.10 B concentration across seven tissues between two growth stages (GS 6.2/6.3 and harvest) among 14 *Brassica napus* genotypes.

Data are genotype mean ± SEM (n=3 and n=5 at GS 6.2/6.3 and harvest, respectively).

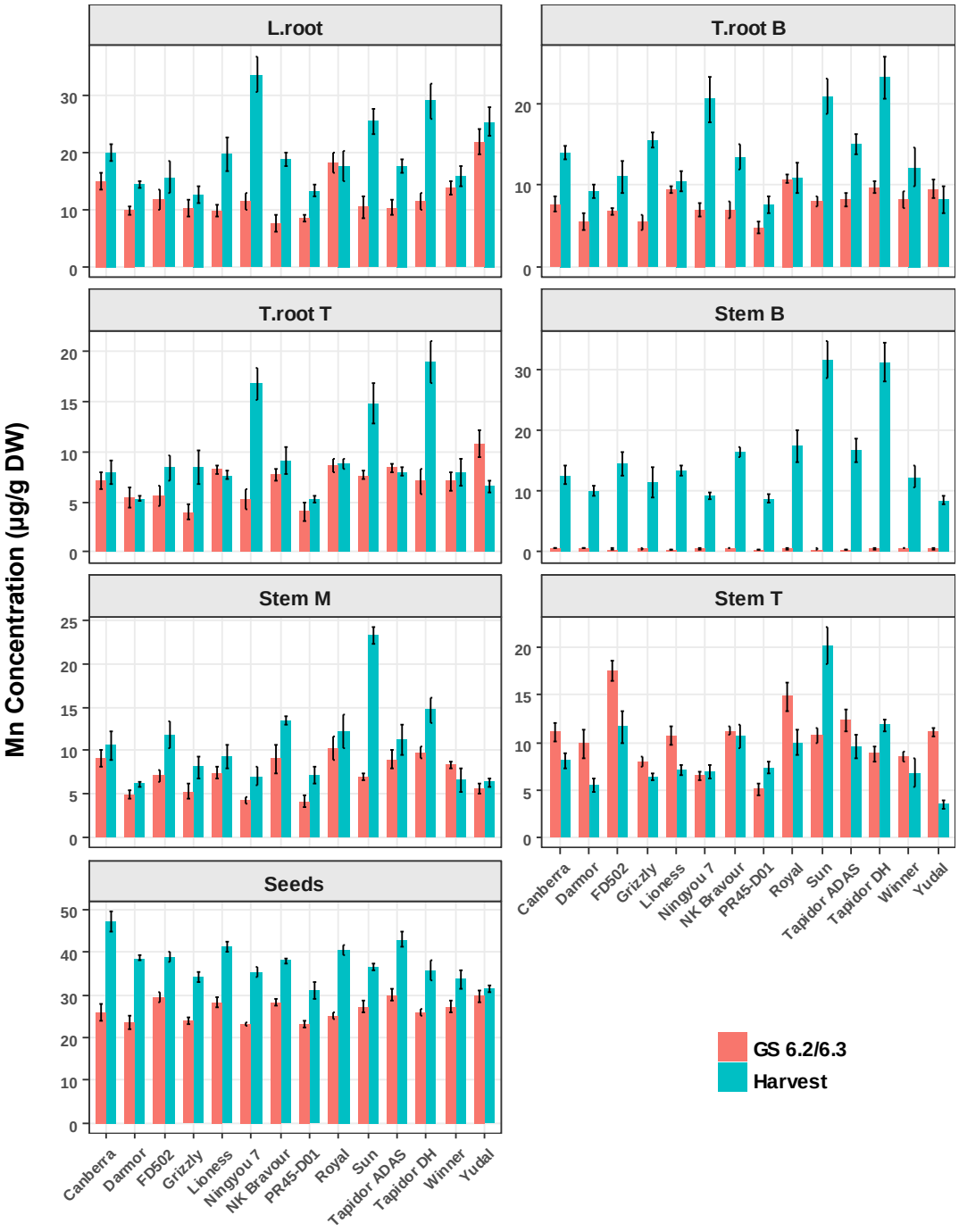

Figure 3.11 Mn concentration across seven tissues between two growth stages (GS 6.2/6.3 and harvest) among 14 *Brassica napus* genotypes.

Data are Data are genotype mean ± SEM (n=3 and n=5 at GS 6.2/6.3 and harvest, respectively).

Genotypic variation was also reported in Fe and Zn (Appendix 9, Figure 5 and 6, respectively). For example, Darmor and FD502 possessed significantly lower concentration of Fe at harvest (both 20.5 µg/g DW) than GS 6.2/6.3 (88.5 and 85.6 µg/g DW, respectively) within Stem T. In contrast there was not a significant difference between two stages among varieties such as Sun and Canberra (Appendix 4 and 7, Table 3). Furthermore, both Darmor and FD502 possessed lower concentration of Zn at harvest (3.8 and 5.3 µg/g DW, respectively) than GS 6.2/6.3 (8.7 and 23.3 µg/g DW, respectively) (Appendix 4 and 7, Table 5).

3.4.8 Comparison between Kjeldahl and HNO_3 digestion method

Two digestion methods; Kjeldahl and Microwave-assisted HNO_3 digestion had been used to determine 11 mineral nutrients. K was determined within stem and root tissue types at harvest following both digestion methods in order to compare between them. K concentration; K-Kjeldahl and K-HNO_3 (% of dried weight, DW) determined by ICP-OES as described previously in Section 3.3.4.1 and Section 3.3.4.2. Two samples t-test was conducted for K concentration in Kjeldahl and HNO_3. There was not a significant difference (t (916) =1.54, P =0.125, SED =0.0283) in K-Kjeldahl (1.1922 %DW) and K-HNO_3 (1.1967 %DW). Correlation analysis revealed a very strong association between the two methods (r =0.989, P <0.0001, df =915), where K-HNO_3 can be predicted according to the model $y = 0.969x + 0.041$. Genotype mean of K concentration and SEM within root and stem tissue types is shown in Figure 3.12.

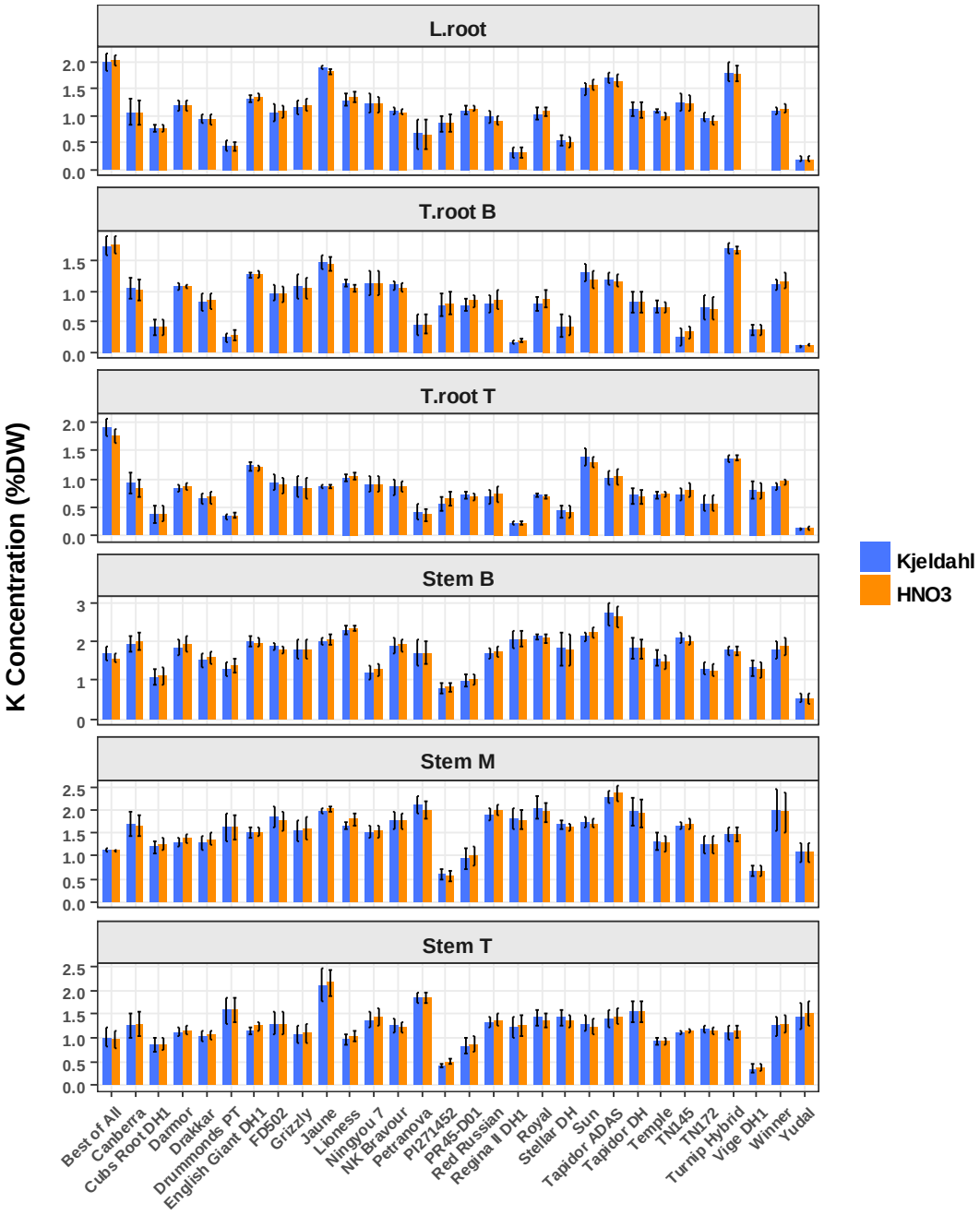

Figure 3.12 Comparison in K concentration (%DW) between two digestion methods.

K concentration determined within root and stem tissue among 30 Brassica napus genotypes at harvest following two digestion methods; Kjeldahl and microwave-assisted HNO_3. Data are genotype mean + SEM (n =5).

3.5 Discussion

Having determined six macronutrients (P, K, Mg, Ca, S and Na) and five micronutrients (B, Cu, Fe, Mn and Zn) concentration within seven plant tissue types of root, stem and seeds at two growth stages (GS 6.2/6.3, n =3 and harvest, n =5) from a number of field-grown *B. napus* L. genotypes (14, GS 6.2/6.3 and 30, harvest), mineral concentrations were found to vary significantly between the seven tissue types measured at both growth stages.

The concentration of 11 mineral nutrients varied by greater than five orders of magnitude from 0.54 ug/g for Mn (Figure 3.2 and Appendix 4, Table 4) to 153209 ug/g for Ca (Figure 3.1 and Appendix 3, Table 4) within Stem B at GS 6.2/6.3, whereas only two order of magnitude were observed between the same pair of elements at maturity. Within the other tissues, a maximum of three orders of magnitudes were observed at both stages. For example, between Cu and K within seeds at harvest. In comparison, four order of magnitudes were reported previously in *B.napus* among the same panel of mineral elements analysed in the present study between Cu and K, within leaves across a diversity collection of 387 genotypes grown under non controlled conditions in a polytunnel (Thomas *et al.*, 2016) and within 30-day old shoot across a large diversity collection of 509 genotypes grown under controlled conditions (Bus *et al.*, 2014). Moreover, three order of magnitude were reported within mature seeds (Thomas *et al.*, 2016). The composition of mineral nutrients varied within and between tissues as previously indicated and in accord with the finding of the present study. However, minerals compositions was found to vary between growth stages which is also in agreement with Rose *et al.* (2007) who

demonstrated that K and P concentrations varied within the same plant organs between different developmental growth stages of *B. napus* plants under controlled conditions.

In the present study, for example, K concentration decreased at GS 6.2/6.3 in the sequence; Stem M >Stem T >seeds >L.root >T.root B >T.root T >Stem B. Whereas K decreased at maturity in the sequence; Stem B >Stem M >Stem T > L.root > T.root B >T.root T > seeds. The considerable loss of K from OSR stems at harvest has been previously reported (Rose *et al.*, 2007). In the current study, Stem B possessed 1.7 %DW of K comparing to 0.8 %DW within taproot. This retention of K would be the equivalent of *ca.* 30 and 24 kg K/ha as calculated from the residues remaining within the 2.5 and 5 g DW of Stem B and taproot, respectively, per plant (See Chapter 2). If sufficient amount of K had already been transported to seeds at maturity (0.6 %DW) these substantial amounts of residual K found within the stem and root would explain the inefficiency of OSR in utilising K.

P concentration decreased at GS 6.2/6.3 in the sequences; Stem B >seeds >L.root >Stem T >Stem M> T.root T >T.root B, whereas at maturity decreased in the order; seeds >L.root >T.root T >T.root B >Stem B >Stem M >Stem T. Mature seeds P concentration averaged 0.81 %DW, in consistent with a reported concentration of 0.73 %DW averaged among three genotypes (Rose *et al.*, 2007) and 0.92 %DW (Thomas *et al.*, 2016). Moreover, ~0.2 %DW of P was retained in the root system at maturity which leads to a quantity of 6 kg P/ha remains within every 5 g DW of root per plant. This is approximately double that found in the stem averaged from the three sections. this is in agreement with (Rose *et al.*, 2007) whom reported a higher P loss with the roots than the stem and leaves. These results could highlight the inefficient mechanisms applied by plants to redistribute and utilise P, in particular, roots P.

However, substantial variations and significant genotypic differences were observed in roots.

The composition of mineral elements within the root system varied between lateral root and taproot where L.root possessed significantly greater mineral concentrations than taproot. There is no any previous study that investigated the composition of mineral elements within lateral root and taproot separately. Averaged across three root tissues, K was found in the greatest concentration followed in descending order by; Ca, P, Na, S, Mg, Fe, Mn, Zn, B and Cu, moreover, the concentration of P, Mg, Fe, Mn, Zn and Cu were found to be greater in root than stem. In comparison, Baxter *et al.* (2012) who investigated differences in mineral contents on 96 wild genotypes of *Arabidopsis thaliana* grown hydroponically for five weeks, reported that root had the greatest of K followed in the descending order by; S, P, Ca, Mg, Fe, Na, Zn, Mn, Cu and B. However, all mineral except Ca, Mg and B found to be in higher concentration in roots than leaves.

Macronutrient concentrations within mature seeds as an average across the 30 genotypes were 0.81 for P, 0.6 for K, 0.44 for S, 0.43 for Ca, 0.22 for Mg and 0.004 for Na; all %DW. In contrast, micronutrient concentrations of 52 for Fe, 37 for Mn, 34 for Zn, 8.5 for B and 2.5 for Cu; all µg/g DW, were reported. In comparison with the present study, Thomas *et al.* (2016) showed that seeds possessed macronutrient concentration of 0.92, 0.98, 0.80, 0.30, 0.43 and 0.0015 %DW for P, K, S, Ca, Mg and Na, respectively. In contrast, micronutrient concentrations of 42, 46, 54 and 3.2 µg/g DW for Mn, Zn, B and Cu, respectively, were found. In this study a large diversity collection of 389 genotypes were used in comparison with 30 genotypes used in the present study, which might account for the differences in the averaged mineral

concentrations. The lack of fertiliser application in the current study might explain the reason why seeds had low mineral concentrations.

However, in the study of Rose *et al.* (2007), seeds possessed 0.73 and 0.61 %DW of P and K, respectively, averaged among three Australian canola genotypes, in consistent with the present study. Thomas *et al.* (2016) found that Swede plants possessed significantly greater S concentration in their seeds than Winter and Spring OSR which is consistent with the present study. In fact, Swede possessed a higher concentration of all mineral elements when compared to other crop types within its lateral roots and taproot. It has not been possible to confirm these findings since there was no such study performed on any *B.napus* that investigated minerals composition within roots among different crop types. Furthermore, Swede had lower mean concentration of all micronutrients (B, Cu, Fe, Mn and Zn) and P in consistent with Bus *et al.* (2014) whom illustrated that shoot micronutrients and P concentration is lower among Swede plants than Winter and Spring OSR. However, in the same study, Swede croptype exhibited greater mean of shoot macronutrients (K, Mg, Ca, S and Na) which inconsistent with the present study which showed that Winter OSR possessed greater K, Mg and Ca concentrations and Spring OSR greater S and Na concentrations than other crop types. In the study of Thomas *et al.* (2016), the 11 mineral concentrations within leaf were lower among Swede than Winter and Spring OSR with a wide scale of variation within each crop type.

B is an essential micronutrient for plant normal growth and development. OSR plants have a high requirement of B and are very sensitive to B deficiency which in turn limits seed and oil production (Zhang *et al.*, 2014). Thus, developing B-efficient genotypes is of great importance. The cultivar Ningyou 7 was previously identified as

a B-efficient genotype whereas Tapidor DH identified as a B-inefficient genotype (Liu *et al.*, 2009a). In the present study, Tapidor DH was identified as an outlier as it possessed the greatest B concentration among all of the genotypes tested. This was found in all root and stem tissues, Tapidor averaged 23.5 µg/g DW, while Ningyou 7 had a low concentration, averaged 13.7 µg/g DW. In contrast, the two genotypes were approximately identical in seed B concentration (8 µg/g DW) (Figure 3.10 and Appendix 7, Table 1) which reflects the efficiency and inefficiency characteristics of Ningyou 7 and Tapidor DH, respectively. However, some genotypes such as NK Bravour had a lower B concentration (averaged 9.2 µg/g DW) within all root and stem tissues than Ningyou 7 but no significant difference in that found in the seeds [B]. This finding suggest that NK Bravour is a B-efficient genotype that could be genetically exploit in the future to improve B use efficiency and identify genes which regulate B uptake, accumulation and remobilisation. Interestingly, a significant difference between Tapidor DH and Tapidor ADAS was observed. Tapidor ADAS possessed a lower concentration of B within both root and stem tissues, averaged 10.8 µg/g DW, while seeds exhibited a greater concentration of 10.7 µg/g DW. This suggests that the genetic material derived from the same founder had diverged between both genotypes, something which has not been reported previously.

The present study identified many different mineral-efficient genotypes. For example, PI271452 possessed a low P concentration across root and stem tissues, which averaged 0.06 %DW (ranged 0.04 -0.09 %DW), with seeds that contained 0.9 %DW. In comparison, the cultivar NK Bravour had the greatest averaged concentration of 0.22 %DW within root and stem tissues and even lower than PI271452 in seeds P with 0.76 %DW. The cultivar Vige DH1 was found to possess the highest concentration of

P within its taproot which exceeded 0.48 %DW and in contrast a low concentration within the stem tissues that averaged 0.07 %DW, while seeds contained approximately a similar concentration to PI271452. Interestingly, the genotype PI271452 had the greatest Zn concentration within all root and stem tissues, averaged 20.64 µg/g DW. In comparison, the genotype NK Bravour had the lowest concentration, averaged 6.4 µg/g DW, with seeds possessed about 5 µg/g DW greater than PI271452. Likewise, these results might suggest that PI27145 is P-efficient but Zn-inefficient genotype and NK is P-inefficient and Zn-efficient genotype. These contrasting characteristic in mineral distribution within these genotypes could assist in identifying genes governing P and Zn accumulation and their redistribution in *B. napus*.

3.5.1 Mineral nutrients natural variation

As shown above natural variation in mineral nutrient concentrations was observed between all sampled tissues of root, stem and seeds at both plant growth stages, particularly at maturity. For example, among 30 genotypes at maturity, T.root T macronutrient concentrations varied 15.9-fold for K, 11.3-fold for P, 9.3-fold for Mg, 9-fold for Ca, 7.2-fold for Na and 6.2-fold for S (Figure 3.4 and Appendix 6, Tables 1 to 6), in contrast micronutrients varied for 9.2-fold for F, 5.5-fold for Mn, 4.8-fold for Zn, 3.9-fold for Cu and 3.4-fold for B (Figure 3.5 and Appendix 7, Table 1 to 5). As yet there is no any previous study that investigated the composition of mineral elements within root system in a similar or larger scale of diversity collection in *B .napus* or other *Brassica* species. In a different species such as *A. thaliana*, root macronutrients varied 10.2-fold for Na and less than 2.3-fold for Ca, K, Mg, P and S, while micronutrients varied 9.2-fold for Mn and 1.9- to 3.6-fold for Zn, Cu, B and Fe.

Furthermore, among three stem tissue types, Stem B macronutrient concentrations varied 5.5-, 5.1-, 3.3-, 2.3-, 1.5- and 15.2-fold for P, K, Mg, S, Ca and Na, respectively, in contrast micronutrients Mn, Cu, Zn, B and Fe varied 8.8-, 6.0-, 3.9-, 2.6- and 2.2-fold, respectively. In comparison, in the study of Bus *et al.* (2014) reported that macronutrient concentrations in 30-day old shoot of *B. napus* genotypes varied micronutrient concentrations varied *ca.* 2-fold for Ca and K, 6-fold for P, 1.6-fold for Mg, 2.3-fold for S and 2.7-fold for Na, whereas micronutrients varied *ca.* 5-fold for Mn, 2.5-fold for B and Cu, 3.5-fold for Fe and Zn. In a different study, there was 3-fold variation in shoot [K] after 37 days of vegetative growth in controlled conditions (Damon *et al.*, 2007).

In their study Liu *et al.* (2009a) investigated shoot mineral nutrient concentrations (seven minerals in comparison with the present study) among 162 segregating lines of the TNDH mapping population grown under low B supply, reported 2-fold of variation (0.42 – 0.85 %) in [P], 1.5-fold (1.8 – 2.8 %) in [Ca], 1.5-fold (0.32 – 0.47 %) in [Mg], 6-fold (1.8 – 11.2 µg/g) in [Cu], 2.2-fold (32 – 70 µg/g) in [Zn], 10.4-fold (90 – 940 µg/g) in [Fe], and 2.9-fold (3.6 – 10 µg/g) in [B]. Moreover, limited variation between the Tapidor DH and Ningyou 7 parents of the TNDH mapping population was observed in shoot mineral concentrations, for instance, [P] only ranged from 0.7 %DW in Tapidor DH to 0.65 %DW in Ningyou 7 while in the present study significant differences were reported between both genotypes. The rosette leaf macronutrient concentrations varied 2-fold (P), 2.1-fold (K), 2.5-fold (S), 2.6-fold (Mg), 3-fold (Ca) and 3.4-fold (Na), while the micronutrient concentrations varied 1.8-fold (Fe), 2.7-fold (Cu), 2.8-fold (Zn), 4.7-fold (B) and 6-fold (Mn) (Thomas *et al.*, 2016). In a different *Brassica* species, significant variation in shoot P concentration of

approximately 5-fold (ranged between 0.1 and 0.5 %DW) and 2.8-fold (ranged between 0.2 and 0.56 %DW) was reported among 355 accessions of *B. oleracea* grown under glasshouse conditions at low and high P supply, respectively (Hammond *et al.*, 2009), variation of 2.3-fold (ranged between 0.35 and 0.80 %DW) in Mg concentration, 2-fold in Ca concentration (ranged between 1.7 and 3.3 %DW) (Broadley *et al.*, 2008), *ca.* 2.3-fold of in K concentration (ranged between 2.8 and 6.6 %DW) (White *et al.*, 2010) and a wide scale variation observed in shoot Zn concentration (ranged from traces to 663, and to 223 µg/g DW under low and high P supply, respectively) (Broadley *et al.*, 2010).

Seeds macronutrient concentrations varied 1.9-fold for P, 2.5-fold for K, 1.5-fold for Mg, 1.6-fold for Ca and 5.2-fold for S, while micronutrients varied 2-fold for B, 3.3-fold for Cu, 1.6-fold for Fe, 1.5-fold for Mn and 2.2-fold for Zn. In comparison, among diversity collection of 398 genotypes of *B. napus*, there were genotypic variation in seeds macronutrient concentrations of 1.7-fold for P, 2-fold for K, 2.1-fold for Mg, 3.1-fold for Ca, 7.5-fold for S and 14-fold for Na, in contrast there were genotypic variation in seeds concentration of four micronutrients of 2.7-, 2.8- 3.4- and 5.8-fold for Zn, Cu, B and Mn, respectively (Thomas *et al.*, 2016). In a different study, K concentration varied 1.3-fold, ranged from 0.54 to 0.7 %DW (Rose *et al.*, 2007), in comparison with a range of 0.39 – 0.98 %DW in the present study. The findings of the present study in addition to the findings of previous studies suggest that mineral nutrients composition in *B. napus* is under genetic control. However, the plant organs are independently regulated.

3.5.2 Mineral nutrients relationship

In this chapter, 11 mineral nutrient concentrations have been quantified within every plant tissue types at two growth stages. The relationships among these mineral concentration were evaluated by analysis of Pearson correlation. Interestingly, most of the pair-wise relationships; 65/69 at GS 6.2/6.3 Figure 3.3 (page 109) and 122/130 at maturity Figure 3.6 (page 118), between mineral nutrients within all tissue types were positive. Likewise, Bus *et al.* (2014) reported positive pair-wise relationships between the same 11 mineral concentrations within 30-day old shoot of *B. napus,* and Thomas *et al.* (2016) reported positive relationships between 21 mineral concentration (including the 11 minerals determined in the present study) within rosette leaf. Therefore, it is believed that there are shared pathways involved in minerals uptake and accumulation of the correlated nutrients, or pleiotropic gene effects among those associated mineral nutrients. This was previously demonstrated in *B. napus* through QTLs colocalisation between Ca/Mg, B/P, and B/Cu (Liu *et al.*, 2009a), in *A. thaliana* between Ca/K and Mn/Zn (Vreugdenhil *et al.*, 2004) and in *B. oleracea* between Ca and Mg (Broadley *et al.*, 2008). On the other hand, the relationships between mineral nutrient concentrations in the present study were tissue-specific. For example, strong correlations were interestingly observed between S/Mg, S/Ca and Mg/P within only all root tissues and Stem T. In the recent study of Thomas *et al.* (2016) investigating leaf and seeds mineral nutrients composition in *B. napus*, it was observed that the pattern of relationships among nutrient concentrations varied between leaf and seeds. Likewise, In the study of Buescher *et al.* (2010) and Baxter *et al.* (2012) on *A. thaliana*, reported that the relationships between mineral concentrations were tissue-specific and varied among root, leaf and seeds. Some of the pair-wise correlations in

the present study varied according to the growth stage. For example, a significant positive association between Ca and Mn (r =0.7, P <0.00001) observed within all root tissues only at maturity, and between Zn and Mn (0.47< r <0.79, P <0.0093) observed within all root tissues and Stem B and Stem T at maturity. These result can suggest that the relationships among mineral nutrient concentrations were also plant age-specific.

There was no any association among mineral nutrient concentrations between rosette leaf and seeds of *B. napus* either between the same element or different pairs of elements (Thomas *et al.*, 2016). This is inconsistent with the present study where there were strong positive correlations (0.56< r <0.82, P <0.0013) between both taproot tissues and all of the three stem tissues in the mineral elements (B, Cu and Zn), between later root and each of the three stem tissues (0.41< r <0.61, P <0.05) in the mineral nutrients (B, Cu and Na), between seeds and all three root tissues (0.40< r <0.60, P <0.05) in S concentration and between seeds and all three stem tissues (0.44< r <0.49, P <0.016) in Na concentration. Likewise, in the study of Baxter *et al.* (2012), significant positive correlations were observed between the root and leaf grown hydroponically in minerals composition such as Mo, Zn and P (r =0.93, 0.51 and 0.28, respectively). Furthermore, very strong associations were observed between all root tissue types in the minerals (Na, S, P, Ca, Mg, K, B, Zn, Cu and Mn).

Several pair-wise relationships were previously reported in *B. napus* among the same 11 minerals determined in the present study; within 30-day old shoot (0.54< r >0.64) between Mn/B, Mn/Cu, Mn/Zn, Ca/Mg, Ca/Na, Zn/Cu and Zn/Fe (Bus *et al.*, 2014), and within rosette stage leaves (0.50< r >0.88) between Ca/Mg, Mg/Na, Ca/Na, Ca/Mn, Mn/Fe, Mn/B, S/Na, S/P and S/Mg (Thomas *et al.*, 2016). In the study of Liu

et al. (2009a), there were significant correlation between Ca/Mg, Ca/P and Cu/Fe, Zn/B, Cu/B in the shoot. The strong relationships between Zn/Fe and Mn/Zn were also reported within leaf of *B. rapa* L. (Wu *et al.*, 2007) All of these pair-wise relationships except Ca/Na were observed in the present study, in addition to many other strong positive associations were also observed at both growth stages, GS 6.2/6.3 Figure 3.3 (page 109) and maturity Figure 3.6 (page 118) despite the fact that these associations were tissue-specific as previously elucidated.

In the study of Thomas *et al.* (2016), the strongest positive relationships within seeds found between B and Na (r =0.40) and between S and Zn (r =0.47) in consistent with the correlation coefficient reported in the present study (r =0.41 and 0.47, respectively), however several stronger correlations were found, for example, between Mg/P, Cu/Na, K/P, Na/P, S/P, Ca/P (r = 0.82, 0.73, 0.69, 0.66, 0.53, 0.52, respectively, P <0.0034). This relationship between P and the cations Mg, K, Na and Ca might reflect the storage role of phytates, the mineral cation-salt of phytic acid ($C_6H_{18}O_{24}P_6$), to these cations since phytates are the principle storage form of P in plant tissues, particularly in seeds (Campbell *et al.*, 1991; Lott *et al.*, 2000). In OSR, phytates constitute the majority (75 -80 %) of the total seeds P concentration (Peng *et al.*, 2001), mainly in the form of Ca, Mg and K phytate salts (Yiu *et al.*, 1982; Ockenden *et al.*, 2004). Negative correlations (r >-0.46) were reported within seeds between, Zn/B, S/B and Ca/K (Thomas *et al.*, 2016). In the present study, negative relationship between Zn and B (r =0.50, P <0.0054) was also observed as well as between Zn/Na and Mn/S (r =0.40, P <0.031). Nonetheless, the associations between Zn/B and Zn/Na were significantly positive within all root tissues.

Such relationship between Ca and Mg has been reported previously in *B. napus* with a Ca:Mg ratio of > 6.5 observed in the shoot (Broadley *et al.*, 2004; Liu *et al.*, 2009a; Bus *et al.*, 2014), 1.3 in leaves (ranged from 1.0 to 1.7) and 0.7 in seeds (ranged from 0.38 to 1.5) (Thomas *et al.*, 2016). This relationship was also reported within different plant species, a ratio of 4.4 in root and 6 in leaf observed in *A. thaliana* (Baxter *et al.*, 2012) and ~4.1 (ranged from 3.2 to 5.6) observed in the shoot of *B. oleracea* (Broadley *et al.*, 2008). Likewise, the present study showed that the ratio of Ca to Mg is tissue-dependent as well as developmental stage-dependent. The ratios of Ca to Mg at the GS 6.2/6.3 and maturity, respectively were; 5.1 and 7.9 for L.root, 3.5 and 7.8 for T.root B, 4.3 and 9.1 for T.root T, 198.8 and 9.5 for Stem B, 8.1 and 11.9 for Stem M, 14.7 and 13.4 for Stem T, and 1.3 and 1.9 for seeds. Wide variation in the ratio of Ca:Mg was existed among genotypes, for example, variation ranged from 6.7 to 18.3 in Stem B and from 1.4 to 2.6 in seeds at maturity. It appears that these values of Ca:Mg ratio were, except Stem B, in a similar range as those reported previously within different plant organs in different species. The averaged value of this ratio within all root and stem tissue except Stem B was 6.9 at GS 6.2/6.3 and increased to 9.1 at maturity which was due to an averaged increase of 0.066 %DW in Ca concentration as well as a decrease of 0.011 in Mg concentration. However, the increase in the Ca to Mg ratio in mature seeds was due to an increase of 0.09 %DW and a decrease of 0.05 in Ca and Mg, respectively. At maturity mean Ca concentration in the root increased to about 1.6-fold of its concentration at GS6.2/6.3 which might reflect on the relative immobility of Ca through the phloem from old tissues where mature cells have tendency to sequestrate Ca in the vacuoles, the mechanism which regulated by Ca^{2+}/H^{+} antiporters encoded by *CAX* genes in *A. thaliana* and

autoinhibited Ca^{2+}-ATPases encoded by *ACA4* and *ACA11* (White and Broadley, 2003; Lee *et al.*, 2007; Maathuis, 2009). In addition to the antagonistic relationship between Mg and other cations such as NH_4^+, K, Ca and Na in the soil, there is also a competitive relationship between these cations and Mg for binding sites of several proteins within the plant which in turn limits Mg acquisition into root and translocation to different tissue in the plant (Merhaut, 2007). It was not possible to compare the value of Ca to Mg ratio, in particular, in the bottom of the stem which interestingly ranged from 138 to 282 among 14 genotypes at GS 6.2/ 6.3, with other studies due to the lack of previous published research that investigated minerals composition either within different sections of plant organs nor different developmental growth stages. This extremely high value was mainly due the great Ca concentration of 15.3 %DW which is significantly decreased from to only 0.84 %DW at maturity. In previous studies, shoot Ca concentration of ~2.6 %DW, ranged approximately from 2.0 to 3.8 %DW (Bus *et al.*, 2014), and 2.44 %DW (Broadley *et al.*, 2003) were reported in *B. napus*. It might be speculated that the bottom of the stem operated as a Ca buffering store during the vegetative growth until early stages of seeds development for later re-translocation to seeds when it was needed during late seed developmental stages and maturity since large proportion of Ca located in the seed coat.

Chapter 4 Changes in Protein Profile During the Life Cycle of *Brassica napus* L.

4.1 Introduction

As described in the main introduction plants assimilate essential nutrients into various compounds where, these nutrient elements are stored for later use (Staswick, 1994; Hell and Mendel, 2010; Marschner, 2012a). For example plants absorb N from the soil in mineral forms such as NO_3^- and NH_4^+ which are assimilated into amino acids in the vegetative tissue. These amino acids are required by cell through numerous metabolism pathways, especially for protein synthesis, for the optimum plant growth and development (Daniel-Vedele *et al.*, 2010; Hawkesford *et al.*, 2012).

It was reported by Ulas *et al.* (2013) that at the onset of flowering stores of N are equally distributed between OSR plant stem and leaves. In contrast, by the end of flowering approximately 40 % of the total shoot N has been shown to be located in pod walls (also known as valves) (Schjoerring *et al.*, 1995). N is required for photosynthesis in these valves which is the primary source of sugars used within seed development. The vegetative organs of OSR plants (stem, taproot and leaves) are crucial components in supplying N during these seed development stages. However, the maximum quantity of N recovered from the seeds has not been found to exceed 70 % of the total plant N (Gombert *et al.*, 2010; Zhang *et al.*, 2010). This has been presumed to be as a direct result of inefficient mechanisms responsible for the translocation of N to siliques during seed filling stages (Schjoerring *et al.*, 1995; Rossato *et al.*, 2001). This is believed to be a self-evident consequence of the high percentage of N losses due to leaf drop (>15 % of total plant N) (Rossato *et al.*, 2001) as well as the relatively high quantity of residual N (16 %) found at maturity within the stem (Ulas *et al.*, 2013) or within both stem and root (26 %) (Rossato *et al.*, 2001).

Protein is the primary store of N in the vegetative parts of the plants. Enzymes are involved in the degradation process through which N is released and redistributed mainly to the reproductive parts of the plant (Masclaux-Daubresse *et al.*, 2010). A putative 23 kDa VSP has been previously identified in the taproot of *B. napus* which is thought to play a role as a storage buffer for N loss from senescing leaves (Rossato *et al.*, 2001). Further evidence for the role of this protein is currently lacking. Several VSPs has been observed previously in various herbaceous (Staswick, 1994) and woody (Stepien *et al.*, 1994) plant species and has been described in chapter 1. These proteins are also thought to play numerous roles in the plants due to their multiple biological activities. The importance of such proteins as storage proteins can therefore sometimes be forgotten due to other attributed functions.

4.2 The aim of this chapter

This chapter aims to identify possible vegetative storage proteins (VSPs) and/or other key genes involved in N remobilisation within *B.napus* L. plants at different growth stages. This was investigated through analysis of soluble protein profiles of several tissues of the root, stem and pod walls using SDS-PAGE technique. Followed by protein identification on gel protein bands varied between the plant developmental stages. In addition, the impact on the expression of putative VSPs was investigated through altering the sink-source relationship.

4.3 Materials and methods

4.3.1 Plant culture

Seeds of two varieties of *B.napus* L. Tapidor DH (Winter) and Ningyou7 (semi-Spring) were collected from Warwick Genetic Resources Unit at Warwick Crop Centre at the University of Warwick. One seed was planted per rounded plastic pot (235 mm diameter x 220 mm height); each contained Levington M2 compost (Scotts Miracls-Gro Company, UK; containing 192 mg/L N, 98 mg/L P and 319 mg/L K) as growing medium and placed randomly in the glasshouse compartment (40 m^2) for their entire lifecycle at Warwick Crop Centre. The glasshouse was set to a temperature of 15 °C day and night, with automatic ventilation at 17 °C day and night, and supplementary lighting (400 W high pressure sodium luminaires) to provide a 16 hour light period. Light threshold was set to switch off above 300 W/m^2. The shade screen was set to close when external light level goes above 500 W/m^2.

Plants were irrigated as necessary with 4 ml/L liquid feed Vitafeed 214 (Vitax Limited, Coalville, Leicester, UK), an NPK [16-8-32] fertiliser with 0.09 % magnesium oxide and Mn, Fe, Cu, B and Molybdenum (Mo) to provide trace elements to meet plant growth requirements of mineral nutrients. Insecticide and fungicide were applied to control pests and diseases following the Horticulture Service standards and as necessary. After two months of growth in the glasshouse, Tapidor DH plants were transferred to a 5 °C vernalisation room with 8 hour light period (start at 08:00 and stop at 16:00 hours) for a period of 6 weeks to trigger flowering since it has very strong requirements of vernalisation (Qiu *et al.*, 2006), and then returned to the glasshouse.

4.3.2 Plant sampling

Plants were sampled at five different growth stages (GS) codded according to Sylvester-Bradley and Makepeace (1984);

I. Rosette stage GS 2.0; prior to stem elongation, samples collected at this developmental stage were labelled (VC).
II. The beginning of flowering GS 4.0; when one to five flowers were observed on the main inflorescence, samples collected from at this stage were labelled (C).
III. The end of flowering GS 4.9; when more than 90 % of all buds were opened, occurred approximately a month after the onset of flowering, samples collected from at this stage labelled (C1).
IV. Seed development stage GS 6.4; when plants had all potential pods and most seeds were green-brown mottled, occurred approximately two months after the onset of flowering, samples collected at this stage labelled (C2).
V. Maturity; when all siliques were yellow, samples collected at this stage labelled (C3).

Three plants were collected at each different developmental stage. Plants were then separated into different tissue types of root, stem and pod walls as appropriate for the developmental stage reached. Plant root were collected at all sampling stages, washed with deionized water (dH_2O) prior to sectioning and divided into the taproot (T.root) and lateral root (L.root). A section of 10 cm or what was available from the bottom of the stem (Stem B) was also collected at all sampling stages, while a section from the top of the stem (Stem T) below the first pod on the main inflorescence was sampled

from the onset of flowering until maturity stages. The inflorescence stems which holding the siliques (Stem S) in addition to the silique walls were only collected from the end of the flowering until maturity stages. All plant tissues were separated into two parts for soluble protein extraction and RNA extraction. The sampled tissues were immediately packed into 50 ml centrifuge tubes and kept in liquid nitrogen during sampling and sectioning time and later were stored at -80 °C prior to protein extraction for soluble protein profiling or RNA extraction for QRT-PCR.

4.3.3 Effect of sink-source status experiment

In addition to the control plants which were sampled at different growth stages as described above, a deflowering (DF) and depodding (DP) experiment was performed in the glasshouse under same conditions previously described on both Ningyou 7 and Tapidor DH which was imitated at the beginning of flowering in order to monitor changes in putative VSPs and other proteins during flowering and seed filling stages.

The group of plants assigned for deflowering were subjected to the removal of the top of the main inflorescence stem at end of bud development stage prior to flowering (GS 4.0). This was followed by day-to-day removal of newly formed buds before becoming followers until the end of experiments which is maturity comparing with non-deflowered and non-depodded plants (control plants). Three deflowered plants were sequentially harvested in parallel with the control plants at only the three occasions after flowering; GS 4.9, GS 6.4 and maturity as described above. The sampled tissues of root (T.root and L.root) and stem (Stem B and Stem T) collected form the deflowered plants at the stage GS 4.9 were labelled (DF1), while the samples collected at the stage GS 6.4 and maturity were labelled (DF2) and (DF3), respectively.

Similarly, the group of plans assigned for depodding were subjected to continuous pods removal. Formed pods were removed on day-to-day basis from being observed (less than 1 cm length) until the end of the experiment which is maturity stage comparing to control plants. Three depodded plants were sequentially harvested and sampled in parallel with the control plants at only the three GS after flowering; GS 4.9, GS 6.4 and maturity as described above. The sampled tissues of root (T.root and L.root) and stem (Stem B, Stem T and Stem S) collected form the depodded plants at the stage GS 4.9 were labelled (DP1), while the samples collected at the stage GS 6.4 and maturity were labelled (DP2) and (DP3), respectively. All plant tissues were separated into two parts for soluble protein extraction and RNA extraction. The sampled tissues were immediately placed into 50 ml centrifuge tubes and kept in liquid nitrogen during sampling and sectioning time, and later were stored at -80 °C until either soluble protein extraction for SDS-PAGE or RNA extraction for QRT-PCR.

4.3.4 Soluble protein extraction

Soluble proteins were extracted following the extraction method described by Rossato *et al.* (2001). Two grams of fresh plant tissue were ground by pestle and mortar with liquid nitrogen to a fine powder. The grounded tissues were mixed with 14 ml of 50 mM Tris buffer (pH 7.5) containing 10 μM leupeptin, 2 mM phenylymethylsulphonyl fluoride (PMSF), 1 mM Ethylenediaminetetraacetic acid (EDTA), and 0.1 % β-mercaptoethanol (βME). The mixture was centrifuged at 5000 g for 10 min. In the case of root samples, 1 mg/ml of protamine sulphate were added to the supernatant. The remaining supernatant was then transferred to 2 ml Eppendorf tubes and stored at -80°C until needed.

The 2 ml tubes were centrifuged at 18000 g for 12 min. the remaining supernatant were received sodium deoxycholate (0.15 %) for 10 min. the mixture was then received trichloroacetic acid (TCA, 7.2 %) and left on ice for 10 min. The precipitated soluble proteins were centrifuged at 15000 g for 6 min. The obtained protein pellet were rinsed with acetone three times and re-suspended in Laemmli sample buffer (Laemmli, 1970) contained (62.5 mM Tris HCl pH 6.8, 2 % sodium dodecyl sulphate (SDS), 25 % glycerol, 0.03 % bromophenol blue and 5 % βME) , denatured for 8 min at 95°C and centrifuged at 10000 g for 1 min. The protein content was determined by using Bio-Rad RC DC protein assay kit based on the Lowry method (Lowry *et al.*, 1951) following the procedure provided with the kit and bovine serum albumin (BSA) was used as the standard protein.

4.3.5 Protein analysis by SDS-PAGE

Polyacrylamide gel electrophoresis (PAGE) is broadly used for separating proteins. Laemmli (1970) developed the most commonly used method that uses a discontinuous denaturing system buffer containing SDS. The denatured and negatively charged proteins migrate and separate according to their size in an electrical field.

For SDS-PAGE analysis, 4 % acrylamide stacking gel and 12 or 15 % acrylamide resolving gel were used. The Tris/glycine/SDS electrophoresis buffer was used, containing (0.25 M Tris, 1.92 M glycine and 1 % SDS). 45 µl of the soluble protein was loaded into each well of the gel (long gel) and protein size standards were loaded into the outside-wells. The gels were run for 3-4 hours at constant 200 volt. Gels then were stained in Coomassie blue R-250 (0.1 %) staining solution contained (50 % methanol, 10 % glacial acetic acid and 40 % water) for 5 hours and then de-stained

with de-stained solution (50 % methanol, 10 % glacial acetic acid and 40 % water) until the gel background was clear (Baines, 2001; Walker, 2009).

4.3.6 In-gel band protein identification

Three procedures needed to be able to identify proteins on any gel slices. Firstly, peptides need to be extracted from the gel. Secondly, the extracted peptides subject to mass spectrometry analysis. Lastly, the acquired MS-based spectra subject to proteomic database search.

4.3.6.1 In-gel digestion and peptide extraction

Protein bands of interest were separated from an SDS-PAGE gel by using a razor blade. The Coomassie stained gel pieces were processed and tryptically digested (Granvogl *et al.*, 2007). Using the following 3-day protocol, gel pieces were subjected to sequential washing for 20 min at 50 °C with shaking in 50 mM ammonium bicarbonate (ABC) until the gel pieces became de-stained, and then dehydrated for 5 min at 55 °C in absolute ethanol. Gel pieces were incubated with 50 mM ABC containing 10 mM dithiothreitol (DTT) at 56 °C for 40 min to reduce disulphide bonds. Cysteine resides were then alkylated in 50 mM ABC containing 55 mM iodoacetamide at room temperature in the dark. Gel pieces were washed twice with 50 % ethanol in 50 mM ABC, and then dehydrated in absolute ethanol for 5 min at room temperature. Afterwards, trypsin protease (2.5 ng/µl) was added to gel pieces and incubated at 37 °C overnight in a water bath. Trypsin cleaves proteins into smaller peptides on the C-terminal side Lysine (K) or Arginine (R) residues except when they are immediately followed by a Proline (P) residue (Martínez-Maqueda *et al.*, 2013). This mixture was next subjected to sequential additions of 25 % acetonitrile containing 5 % formic acid

(three times) to terminate the digestion and then sonicated in a water-bath for 10 min. The supernatant which includes the extracted peptides was then transferred to a new Eppendorf tube and dried at 40 °C overnight in a speed vacuum concentrator (miVac Duo concentrator, Genevac). The dried samples were re-suspended in 2.5 % acetonitrile containing 0.05 % trifluoroacetic acid (TFA) and sonicated for 30 min. Afterwards, samples were centrifuged at 17000 g for 5 min and the supernatant transferred to a 1 ml glass vial. The extracted peptides were then analysed by means of nanoLC-ESI-MS/MS.

4.3.6.2 Tandem mass spectrometry analysis

The obtained tryptic peptides were analysed by means nanoflow liquid chromatography using a nanoAcquity UPLC system (Waters Corporation, Milford, MA, USA) prior to mass spectrometry analysis using. Two columns were utilised, a trapping column with the following physical characteristics, Symmetry C18, 180 µm internal diameter, 20 mm length, 5 µm particle size and 100 Å pore size (Waters Corporation, USA) and an analytical capillary column had the following physical properties, high strength silica (HSS) T3, 75 µm internal diameter, 150 mm length, 1.8 µm particle size and 100 Å pore size (Waters Corporation, USA). The mobile phases, mobile phase A was consist of 0.1 % aqueous formic acid and mobile phase B was consist of 0.1 % formic acid in acetonitrile. A linear gradient of 5 – 40 % mobile phase B over 15 min was utilized with a total run time of 20 min. The eluted peptides were then ionised by means of electrospray ionisation with capillary voltage of 3.0 kV, sample cone voltage of 35 V and a source temperature of 80 ℃, and analysed by quadrupole time-of-flight tandem mass spectrometry on Q-TOF Ultima Global MS (Waters Corporation, Milford, MA, USA) in the Proteomics Service in the School of

Life Sciences at the University of Warwick. A survey scan of peptide precursors from 300 to 1950 m/z were performed using positive ion mode and accurate mass on TOF MS, followed by MS/MS data-dependent acquisition using collision energy of 30 eV. Monoisotopic precursors ions with charge state 1 to 6 were selected during 0.7 s cycle time. The system was entirely controlled by MassLynx v4.0 software (Waters Corporation, Milford, MA, USA).

4.3.6.3 Database search and protein identification

The data obtained from the MS/MS data-dependent acquisition were than processed by MSConvert in ProteoWizard Toolkit v3.0.5759 and converted to pkl files. The pkl files were searched with Mascot engine (Matrix Science, v2.4.1) against *B. oleracea*, *B. rapa* and *B. napus* proteomes predicted from the published genome sequences (Wang *et al.*, 2011b; Chalhoub *et al.*, 2014; Parkin *et al.*, 2014). Peptides were generated from a tryptic digestion with up to two missed cleavages as variable modifications. Precursor mass tolerance was set to 20 ppm and product ions were searched at 0.8 Da tolerances. The proteome software Scaffold v4.3.2 (Searle, 2010) used to validate tandem MS based peptide and protein identifications. Peptides identification threshold was set to 95 % probability assigned by the Scaffold local false discovery rate algorithm. Proteins identification threshold was set to 95 % probability assigned by the Protein Prophet algorithm (Nesvizhskii *et al.*, 2003), and sustained a minimum of two unique peptides of those identified.

4.3.7 The entire proteomic profile at tissue level

4.3.7.1 Protein and Peptide extraction

The soluble proteins extracted from plant tissues were subjected to tryptic digestion for the purpose of analysing the whole proteomic profile of the tissue of interest. Following a modified method of filter-aided sample preparation (FASP) (Wisniewski *et al.*, 2009), the obtained Protein pellet (described previously in section 4.3.4 were resuspended in 120 µl of SDT-lysis buffer (100 mM Tris-HCl pH 7.6, 4 % SDS and 100 mM DTT) and heated at 100 °C for 10 min. The mixture was then centrifuged at 17000 g for 5 min.

The extract was transferred to a 10-kDa filter column (Amicon Ultra-0.5 ml, Millipore). 400 µl of 100 mM Tris-HCl buffer containing 8 M urea (UA) was added to the mixture and centrifuged at 14000 g for 40 min at room temperature, this step was repeated twice and the flow-through was discarded. After incubating the mixture (with mixing at 600 rpm for 1 min and for 5 min without mixing) in 50 mM iodoacetamide (IAA) in UA solution, the filter unit was centrifuged at 14000 g for 30 min. Sequential additions (three times) of 100 mM tris-HCl pH 8 containing 8 M urea to the filter unit and centrifuged for 40 min each time. Prior to incubating the mixture with trypsin (1/100 trypsin to protein) at 37 °C overnight, it was washed three times with 400 µl of ABC with a centrifuge for 40 min every time. Afterward, the filter unit was transferred to a new collection tube and centrifuged for 40 min. An addition of 50 µl of 0.5 M sodium chloride was applied to the filter unit and centrifuged for 20 min. TFA was then added to the mixture to a final concentration of 0.5 % and transferred to a glass vial. The extracted peptide mixture was next desalted using ZipTip tips

(Millipore) following the manufacture protocol then analysed by means of nanoLC-ESI-MS/MS by the Proteomics Service in the School of Life Sciences, University of Warwick.

4.3.7.2 Tandem MS analysis and protein identification

The extracted peptides were first separated using reversed phase chromatography. Two column were used and installed on the Ultimate 3000 RSLCnano system (Thermo Scientific). First, an Acclaim PepMap µ-precolumn with the following physical properties, 300 µm internal diameter, 5 mm length, 5 µm particle size and 100 Å pore size (Thermo Scientific). Second, an Acclaim PepMap RSLC C18 with the following physical characteristics, 75 µm internal diameter x 25 cm length, 2 µm particle size and 100 Å pore size (Thermo Scientific). Mobile phase buffer A was composed of 0.1 % formic acid in water and mobile phase buffer B composed of 0.1 % formic acid in acetonitrile. Samples were loaded onto the µ-precolumn equilibrated in 2 % aqueous acetonitrile containing 0.1 % trifluoroacetic acid for 8 min at a flow rate of 10 µL/min. Peptides were then eluted onto the analytical column at a flow rate of 300 nL/min where the mobile phase B concentration increased from 3 % B to 35 % over 40 min then to 90 % B over 5 min. This was followed by a 15 min re-equilibration at 3 % B.

The eluted peptides were then subjected to ESI and converted to gaseous ions, and analysed by Q-OT-qIT mass spectrometry on Orbitrap Fusion (Thermo Scientific) in the Proteomics Service in the School of Life Sciences at the University of Warwick. A survey scan of peptide precursors were recorded at a resolution of 120000 full width at half maximum (FWHM) at 200 m/z with an automatic gain control (AGC) target of 4×10^5. Spectra were acquired using a scan range from 350 to 1500 m/z. Tandem MS analysis was performed with the precursor isolation window width was set to 1.6

m/z, the normalized collision energy was set to 35 in the higher-energy collisional dissociation cell for fragmentation, and rapid scan MS analysis in the ion trap. Monoisotopic precursor selection was turned on. Precursors with charge state 2 to 7 were selected and sampled for MS2 where the AGC target was set to 10^4 and the maximum injection time was set to 200 ms. The dynamic exclusion duration was set to 45 s and with a mass tolerance of 10 ppm around the selected precursor and its isotopes. The instrument was run in top speed mode with 2 s cycles. The system was entirely controlled by the Thermo Scientific Xcalibur v3.0 software.

The resulting MS/MS spectra were interrogated using the proteomic database of the three proteomes of *B. oleracea*, *B. rapa* and *B. napus* using Mascot Server version 2.4.1 (Matrix Science). Peptides were generated from a tryptic digestion with up to two missed cleavages, carbamidomethylation of cysteines as fixed modifications, and oxidation of methionines as variable modifications. Precursor mass tolerance was set to 5 ppm and product ions were searched at 0.8 Da tolerances. The resulting data was then accessed using Proteome Software Scaffold v2.4.1 (Searle, 2010) as described above in section 4.3.6.3.

4.4 Results

4.4.1 Soluble protein profiles

To assess the variability in protein content during the growth and development of oilseed rape, two contrasting lines, Tapidor DH and Ningyou 7 (the female and male parents, respectively, of the reference TNDH mapping population), were grown in a glasshouse and changes in the soluble protein in different plant tissues at different development stages were detected by SDS-PAGE.

Proteins of approximately 21 and 22 kDa were detected in the taproot and lateral roots at the beginning of flowering in the control plants of Ningyou 7 (Figure 4.1 gel lane C). These proteins were fully hydrolysed during seed development stages in the control plants (gel lanes C2 and C3). However, the removal of flowers and siliques did not increase the accumulation of these proteins in both the taproot and lateral roots (gel lanes DF1, 2, 3 and DP1, 2, 3).

The accumulation of the ~21 kDa protein was substantially greater in lateral roots than in taproots. Nonetheless, a 17 kDa appeared to be the most dominant protein, particularly in lateral roots (Figure 4.1). The accumulation pattern of this protein did not show any significant change in the deflowered and depodded plants. To identify these proteins the gel bands were excised and subjected to protein identification following the previously described methodology. A full list of the identified proteins is summarised in the Table 1.1

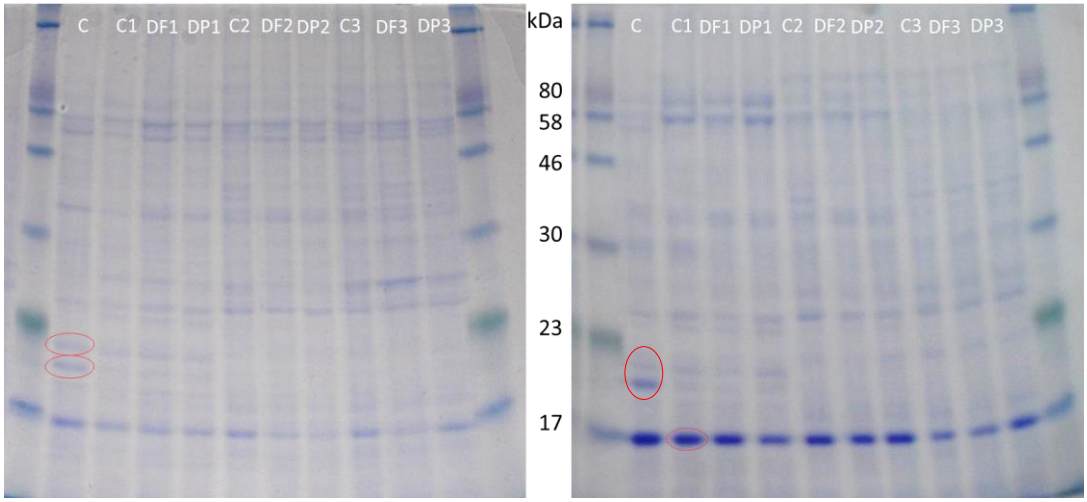

Figure 4.1 Change in SDS-PAGE profile of soluble proteins in roots of Ningyou 7 variety.

Soluble proteins extracted from taproots (left) and lateral roots (right) of Ningyou 7 genotype grown in glasshouse. Each well was loaded with a the same amount of soluble proteins (45 µg) and the position of molecular weight markers is indicated in between the two gel images. Columns C, C1, C2 and C3 indicate the control at the beginning of flowering, the end of flowering GS 4.9, the seed development stage GS 6.4 and maturity, respectively, as described in section 4.3.2. DF1, DF2 and DF3 indicate the deflowering plants at GS 4.9, GS 6.4 and maturity, respectively, in parallel with the developmental stages of the control plants. DP1, DP2 and DP3 indicate the depodding plants at GS 4.9, GS 6.4 and maturity, respectively, in comparison with the control plants as described in section 4.3.3. A red ring indicates the bands that were excised for sequencing.

A protein of 23 kDa was detected in plant tissues, taproot and lateral roots, of Tapidor DH during vegetative growth (Figure 4.2 gel lane CV) and the beginning of flowering (gel lane C). This protein was completely hydrolysed and disappeared after a month of flowering (gel lane C1) and during seed filling stages (gel lanes C2 and C3) of the control plants which initially suggested the possibility of it being involved in Nitrogen remobilisation.

Furthermore, the 23 kDa protein reappeared in taproots and later in the deflowered plants after a month of flowering (gel lane DF1) and after three months of flowering (gel lane DF3) compared to control plants, whereas it was not visualised after two

months of flowering (gel lane DF2). Interestingly, the continuous removal of siliques did not increase or even retain the accumulation of the 23 kDa protein in the depodded plants in taproot and later roots (gel lanes DP1, 2 and 3). Moreover, The 23 kDa protein expression was accompanied with another protein that was smaller in the molecular weight and not as strongly stained as the 23 kDa protein Figure 4.2.

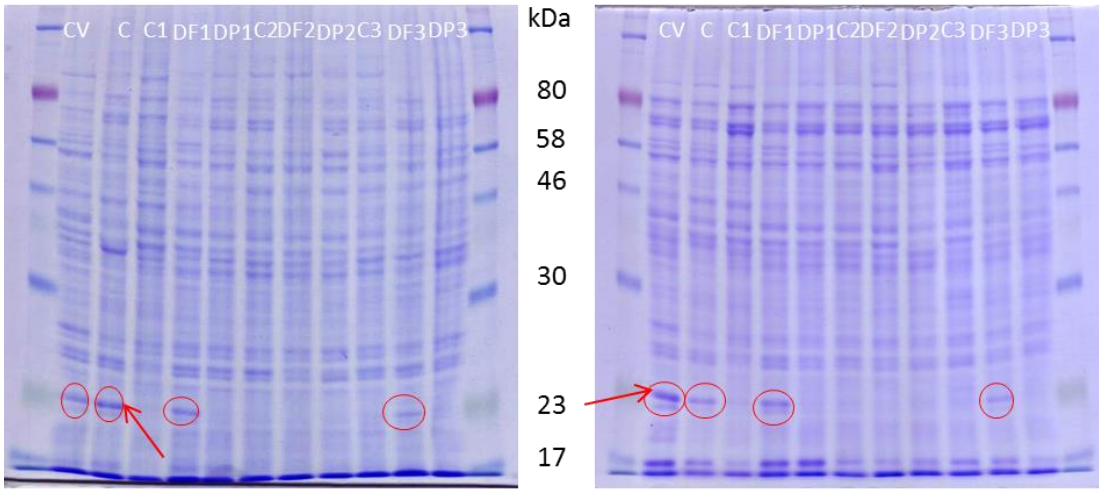

Figure 4.2 Changes in SDS-PAGE profile of soluble proteins in roots of Tapidor DH variety.

Soluble proteins extracted from taproots (left) and lateral roots (right) of Tapidor DH genotype grown in glasshouse. Each well was loaded with the same amount of soluble proteins (45 µg) and the size of the protein size standards loaded in the outside lanes is given. Lane CV indicates the control plant at the rosette growth stage. The rest of the lanes are as described in Figure 4.1 and section 4.3.2 and 4.3.3 Red rings indicate the band has been sequenced and the red arrow indicates the 23 and 22 kDa proteins.

The 23 kDa or the other smaller proteins were not detected in the bottom of the stem of Ningyou 7, whereas the 23 kDa protein was detected in Tapidor DH at the vegetative growth stage (the gel lane CV) and the beginning of flowering (Figure 4.3 gel lane C). Continuous removal of either flowers or siliques did not increase the accumulation of these proteins in the bottom of the stem in either genotype.

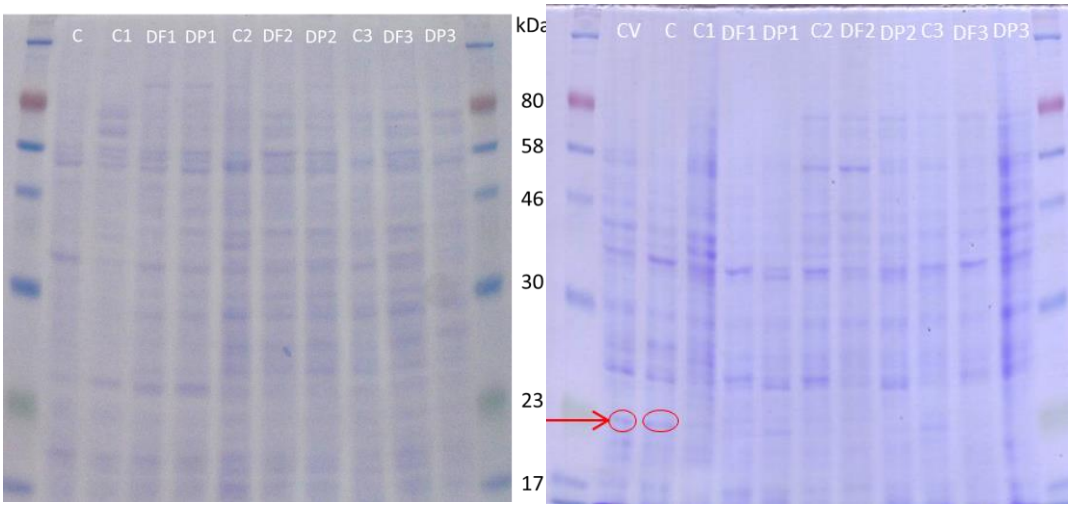

Figure 4.3 Changes in SDS-PAGE profile of soluble proteins in bottom of the stem of Ningyou 7 and Tapidor DH varieties.

Soluble proteins extracted from bottom of the stem of Ningyou 7 (left) and Tapidor DH (right) genotype grown in glasshouse. Each well was loaded with a constant amount of soluble proteins (45 μg) and the position of molecular weight markers is indicated on each side. The gel lane CV indicates the control plant at the rosette growth stage. The rest of the lanes are as described in Figure 4.1 and section 4.3.2 and 4.3.3. Red rings indicate the band has been sequenced and the red narrow indicates the 23 kDa protein.

Figure 4.4 shows interesting changes in the accumulation pattern of some proteins at the top of the stem adjacent to the siliques (Stem S) and in the silique walls. A protein of approximately 25 kDa was detected after a month of flowering (gel lane C1), but completely disappeared after two months of flowering (gel lanes C2 and C3). However, a protein bigger than 30 kDa was detected in each time point in both tissues (gel lane C1, 2, 3), but its levels increased after two and three months of flowering in the stem adjacent to the siliques (gel lane C2 and C3 Stem S) but not in pod walls.

Interestingly, several proteins between 23 and 30 kDa show an increased accumulation in silique walls after three months of flowering when senescence occurred (Figure 4.4 gel lane C3 Siliques wall). These proteins were detected in both genotypes.

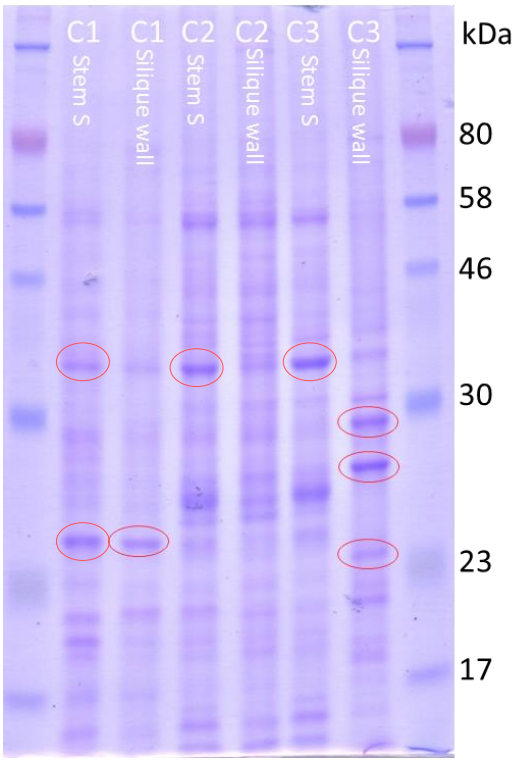

Figure 4.4 changes in SDS-PAGE profile of soluble proteins extracted from silique walls and the stem adjacent to siliques (stem S) of Tapidor DH.

Each well was loaded with a constant amount of soluble proteins (45 µg) and the position of molecular weight markers is indicated on each side. Lanes C1, C2 and C3 indicate the control plants at three growth stages; the end of flowering GS 4.9, the seed development stage GS 6.4 and maturity, respectively. Stem S is the inflorescence stem which carries siliques as described in section 4.3.2. Red rings indicate the bands excised for sequencing.

4.4.2 Protein identification of gel bands

All protein bands of interested (indicated by a red ring across all figures) were excised from the gel, subjected to trypsin digestion as described in section 4.3.6 and analysed by means of nanoLC-ESI-MS/MS using the NanoAcquity/Ultima Global instrumentation (Waters). The highly accurate molecular weights of the tryptic digest fragments were used to screen a database of the molecular weights of an *in silico*

trypsin digestion of the proteins predicted from the published *B. napus*, *B. oleracea* and *B. rapa* genome sequences (refs). Table 4.1 lists the top matching candidate proteins for each of the bands analysed. This is based on the number of individual peptides that match a predicted peptide for a protein and the percentage of the overall protein these correspond to. The best matches identified for the 21, 22, 23 kDa gel protein bands in the taproot, lateral roots and the bottom of the stem, were trypsin inhibitors proteins, while the band for the 35 kDa protein from the stem adjacent to siliques was beta 1,3-glucanase, whereas the seed storage proteins dominated in pod walls.

Table 4.1 Summary of the identified proteins from gel bands.

The identified proteins for each tissue and gel band were ordered descending according to the number of exclusive unique peptides were identified. Accession names commence with Bo and Bra indicate that the proteins identified on *B. oleracea* and *B. rapa* genomes, respectively.

Tissue and band size	Protein name	Accession	Molecular weight (Da)	Unique peptide count	Coverage (%)
T.root C (23 kDa)	Trypsin inhibitor	Bo6rg116580.1	23,255.9	3	27.1
	S-phase kinase-associated protein 1 (SKP1)	Bo6rg085070.1,Bra003735	17,791.2	2	16.9
	Glutathione peroxidase	Bo2g108730.1,Bra033140	25,363.0	2	10.5
	Trypsin inhibitor	Bo6rg116640.1	17,409.6	2	8.3
T.root C (22 kDa)	Glutathione peroxidase	Bo2g108730.1,Bra033140	25,363.0	5	24.0
	Water-soluble chlorophyll protein	Bo02800s010.1	21,440.3	3	19.3
	Trypsin and protease inhibitor	Bra016002	23,546.1	2	15.0
	Wound-induced protein	Bo3g058580.1,Bra001123	23,083.5	2	13.6
	Peroxiredoxin, putative	Bo5g144820.1,Bra020782	21,378.0	2	11.0
	peptidyl-prolyl cis-trans isomerase	Bra010728	18,310.7	2	9.9

Tissue and band size	Protein name	Accession	Molecular weight (Da)	Unique peptide count	Coverage (%)
L.root CV (23 kDa)	Protein of unknown function (DUF640)	Bo3g036160.1,Bra000269	19,880.8	3	27.7
	Trypsin inhibitor	Bo6rg116580.1	23,255.9	3	27.1
	copper chaperone	Bra003234,Bra007230	13,650.8	2	22.0
	Trypsin and protease inhibitor	Bra016002	23,546.1	2	15.0
	Unknown molecular function	Bra010932,Bra030054	19,688.6	2	11.5
	Chitinase	Bo5g133420.1,Bra034754	37,262.0	2	6.2
L.root CV (22 kDa)	Water-soluble chlorophyll protein	Bo02800s010.1	21,440.3	4	34.5
	Peroxiredoxin, putative	Bo5g144820.1,Bra020782	21,378.0	5	31.5
	peptidyl-prolyl cis-trans isomerase	Bra010728	18,310.7	3	18.0
	Trypsin and protease inhibitor	Bra016002	23,546.1	2	15.0
	Peptidyl-prolyl cis-trans isomerase	Bo8g090480.1,Bra007214	19,654.2	2	14.2
	Wound-induced protein	Bo3g058580.1,Bra001123	23,083.5	2	13.6
	Glutathione peroxidase	Bo2g108730.1,Bra033140	25,363.0	2	10.9
L.root DF1 (23 kDa)	Protein of unknown function (DUF640)	Bo3g036160.1,Bra000269	19,880.8	3	21.5
	Trypsin inhibitor	Bo6rg116580.1	23,255.9	2	15.9
	Water-soluble chlorophyll protein	Bo02800s010.1	21,440.3	2	15.2
	Trypsin and protease inhibitor	Bra016002	23,546.1	2	14.5
	Glutathione peroxidase	Bo2g108730.1,Bra033140	25,363.0	2	10.9
	Trypsin inhibitor	Bo6rg116640.1	17,409.6	2	8.3
	allene oxide cyclase	Bo8g065370.1	27,407.7	2	10.8
L.root DF1 (22 kDa)	Water-soluble chlorophyll protein	Bo02800s010.1	21,440.3	4	34.5
	Peroxiredoxin, putative	Bo5g144820.1,Bra020782	21,378.0	5	31.5
	Glutathione peroxidase	Bo2g108730.1,Bra033140	25,363.0	3	16.2
Stem B (23 kDa)	Trypsin and protease inhibitor	Bra016002	23,546.1	3	31.3

Tissue and band size	Protein name	Accession	Molecular weight (Da)	Unique peptide count	Coverage (%)
	60S ribosomal protein L18A	Bo3g027750.1,Bo4g039790.1,Bo4g182640.1,Bra005421	21,306.9	4	27.5
	Trypsin inhibitor	Bo6rg116640.1	17,409.6	2	16.6
	Trypsin inhibitor	Bo6rg116580.1	23,255.9	2	26.2
	Trypsin inhibitor	Bo6rg116620.1	21,207.1	2	11.9
	Protein of unknown function (DUF640)	Bo3g036160.1,Bra000269	19,880.8	2	15.8
	Peptidyl-prolyl cis-trans isomerase	Bo7g119650.1,Bra033574	18,383.8	3	25.6
N T.root C (22 kDa)	Water-soluble chlorophyll protein	Bo02800s010	21,426.0	5	25.9
	Peptidyl-prolyl cis trans isomerase	Bo3g149530	18,358.0	4	22.7
	Trypsin inhibitor	Bo6rg116620.1	21,207.1	2	15.5
	Peptidyl-prolyl cis trans isomerase	Bo4g060010	21,714.0	2	7.5
	Trypsin inhibitor	Bo6rg116580.1	23,255.9	2	10.8
	Peptidyl-prolyl cis trans isomerase	Bo8g097590	27,437.0	3	10.7
L.root CV (17 kDa)	Polyketide cyclase/dehydrase and lipid transport superfamily protein	Bo7g078440.1	17,491.7	8	43.0
	PACid_22696349	Bra024879	17,465.3	3	37.1
	Polyketide cyclase/dehydrase and lipid transport superfamily protein	Bo9g070120.1	17,389.5	2	23.8
	Nucleoside diphosphate kinase	Bo2g109120.1,Bra033163	25,576.1	3	12.8
Stem S C1 (25 kDa)	Superoxide dismutase	Bo1g039700	23,832.0	4	14.6
	Beta-1,3-glucanase	Bo6g054040	37,842.0	4	16.4
	Peroxiredoxin	Bo3g064370	28,745.0	3	13.4
	Flavoprotein wrbA	Bo2g041750	21,760.0	3	17.2
Stem S C1 (35 kDa)	Beta-1,3-glucanase	Bo6g054040	37,842.0	15	50.4
	Beta-1,3-glucanase	Bo4g111320	41,049.0	11	29.6
	Malate dehydrogenase	Bo3g183840	39,631.0	5	16.6

Tissue and band size	Protein name	Accession	Molecular weight (Da)	Unique peptide count	Coverage (%)
	Enoyl-ACP reductase	Bo7g026690	40,773.0	3	9.4
	Beta-1,3-glucanase	Bo4g111370	11,902.0	3	38.9
	Beta-1,3-glucanase	Bo8g091600	33,892.0	2	10.8
pod walls C1 (25 kda)	Beta-1,3-glucanase	Bo6g054040	37,842.0	3	10.3
	Superoxide dismutase	Bo1g039700	23,832.0	3	7.1
	Beta-1,3-glucanase	Bo4g111370	11,902.0	2	24.1
pod walls C3 ~(24 kda)	11S seed storage globulin A	Bo1g017390.1, Bra011036	54,379.0	10	28.4
	11S seed storage globulin A	Bo5g004180.1	51,426.8	5	12.7
	11S seed storage globulin B	Bo8g054380.1	28,757.0	4	23.1
	Kunitz trypsin inhibitor	Bo6g038930.1	39,444.0	2	8.3
pod walls C3 ~(27 kda)	11S seed storage globulin A	Bo5g004180.1	51,394.0	8	22.8
	11S seed storage globulin A	Bo5g004180.1	51,426.8	8	18.9
	11S seed storage globulin A	Bo1g017390.1,Bra011036	54,412.2	6	14.5
	Kunitz trypsin inhibitor	Bo6rg087900.1	39,469.2	4	12.9
	Chitinase putative	Bo1g021980.1	41,225.0	3	9.7
	11S seed storage globulin B	Bo7g067090.1	53,751.6	2	7.0
pod walls C3 ~(29 kda)	11S seed storage globulin A	Bo5g004180.1	51,426.8	8	29.9
	11S seed storage globulin A	Bo1g017390.1,Bra011036	54,412.2	8	20.0
	11S seed storage globulin B	Bo7g067090	53,719.0	4	10.8
	2S seed storage protein 1	Bra010363	54,700.0	4	19.1
	Kunitz trypsin inhibitor	Bo6rg087900.1	39,469.2	4	13.8
	cellulase/ hydrolase, hydrolyzing O-glycosyl compounds	Bra003273	37,666.7	2	8.9

4.4.3 Protein identification of the entire proteomic profile

In addition to protein identification form gel bands, the whole soluble proteomic profile in the bottom of the stem was analysed from both Ningyou 7 and Tapidor DH. Peptides were extracted from the protein mixture using FASP methodology as described above. The identified peptides and proteins were visualised and analysed using Scaffold as previously described. Figure 4.5 shows an overview of protein identified using Scaffold.

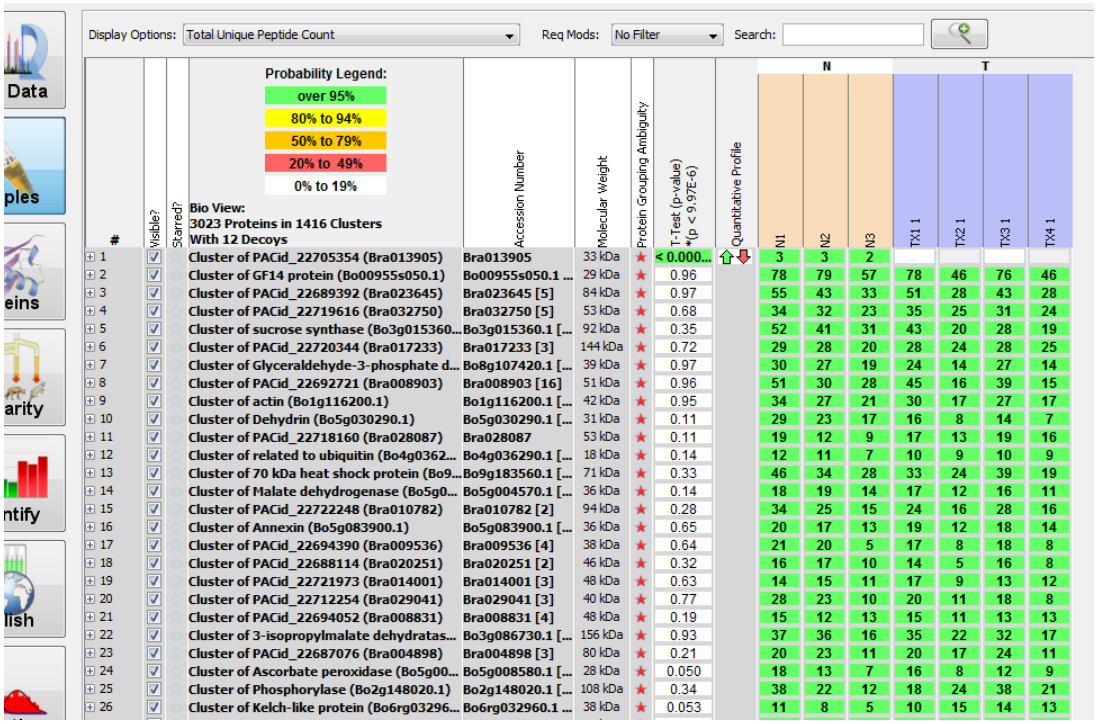

Figure 4.5 Overview of protein identification using Scaffold.

From left to right, column show the protein names or cluster of the identified proteins with a coloured threshold legends (green is above 95 %). Followed by accession number, molecular weight, T-test probability, quantification profile and the samples identified (Ningyou 7 in brown and Tapidor DH in purple). This picture was generated using scaffold v4.5.

Under the described thresholds, more than 1650 proteins were identified in Ningyou 7 and more than 1600 in Tapidor DH (Figure 4.6). 1261 of these proteins are shared between Ningyou 7 and Tapidor DH; 399 proteins were only identified in Tapidor DH, and 347 proteins were identified only in Ningyou 7.

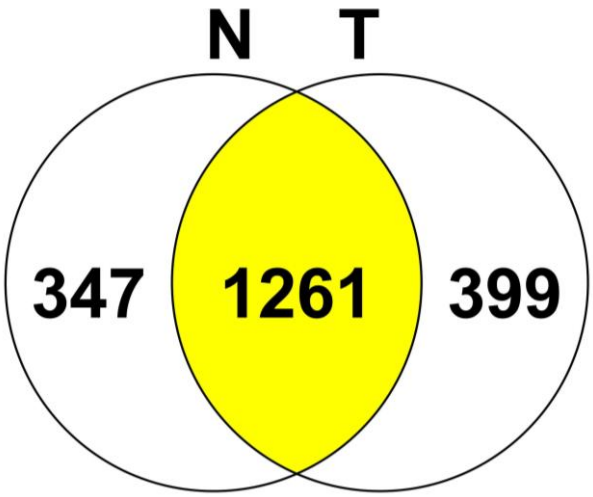

Figure 4.6 Number of identified proteins in Ningyou 7 (N) and Tapidor DH (T).

The number of shared proteins between the both genotypes are in yellow. To the left of the shared portion (N) is the number proteins identified only in cultivar Ningyou 7, and to the right (T) is the number proteins identified only in cultivar Tapidor DH.

This represents a significant difference (T-test, P <0.01, Scaffold v4.5) between Ningyou 7 and Tapidor DH related to presence of some proteins was observed. Figure 4.7 shows the quantitative differences between the both genotypes in terms of the total number of identified spectra for each protein.

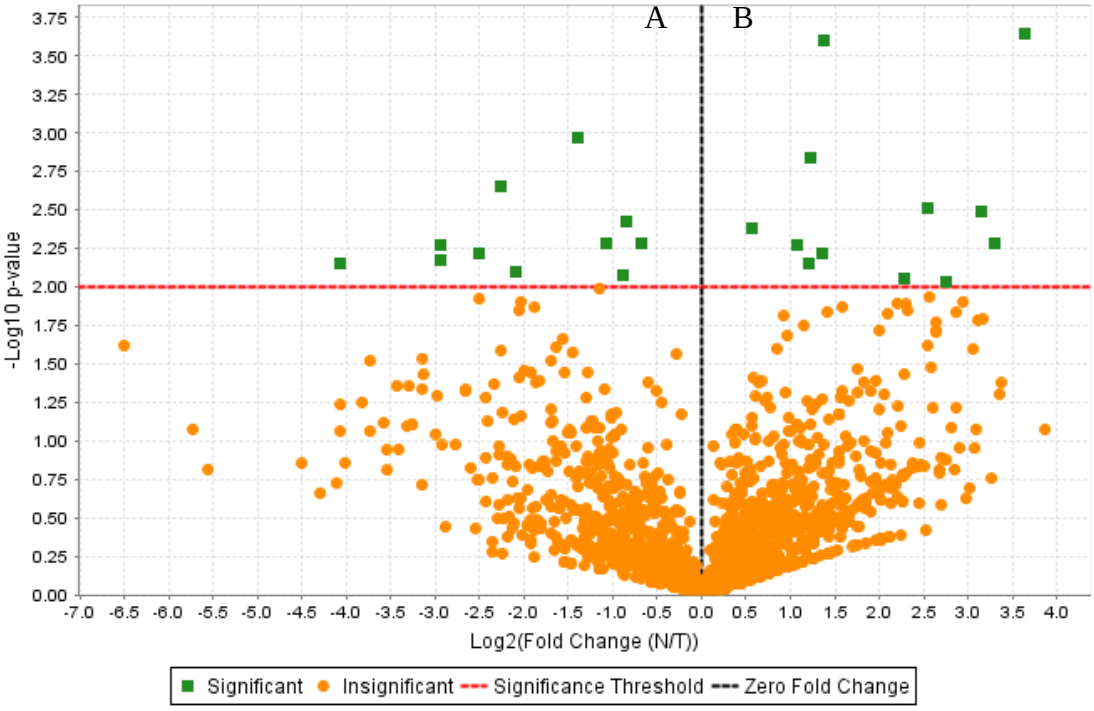

Figure 4.7 Quantitative difference between the genotypes Ningyou 7 and Tapidor DH.

Volcano plot (T-test, P <0.01) shows quantitative differences between Ningyou 7 (N) and Tapidor DH (T). Horizontal axis represents the log2 of the fold change in the total numbers of spectra that were identified. Green squares indicate proteins that show a significant difference in abundance. The top left square (A) indicate more abundant proteins in T compared with N, and vice versa in the top left right square (B).

Two examples of these differences between Ningyou 7 and Tapidor DH in the abundance of indole-3-acetonitrile nitrilase (NIT2) and myosin-like protein are shown in Figure 4.8. The myosin-like protein was expressed in 3-fold higher in Ningyou 7 than Tapidor DH. In contrast, the NIT2 was not expressed in Ningyou 7, but significant expression was occurred in Tapidor DH in the bottom of the stem at the beginning of flowering.

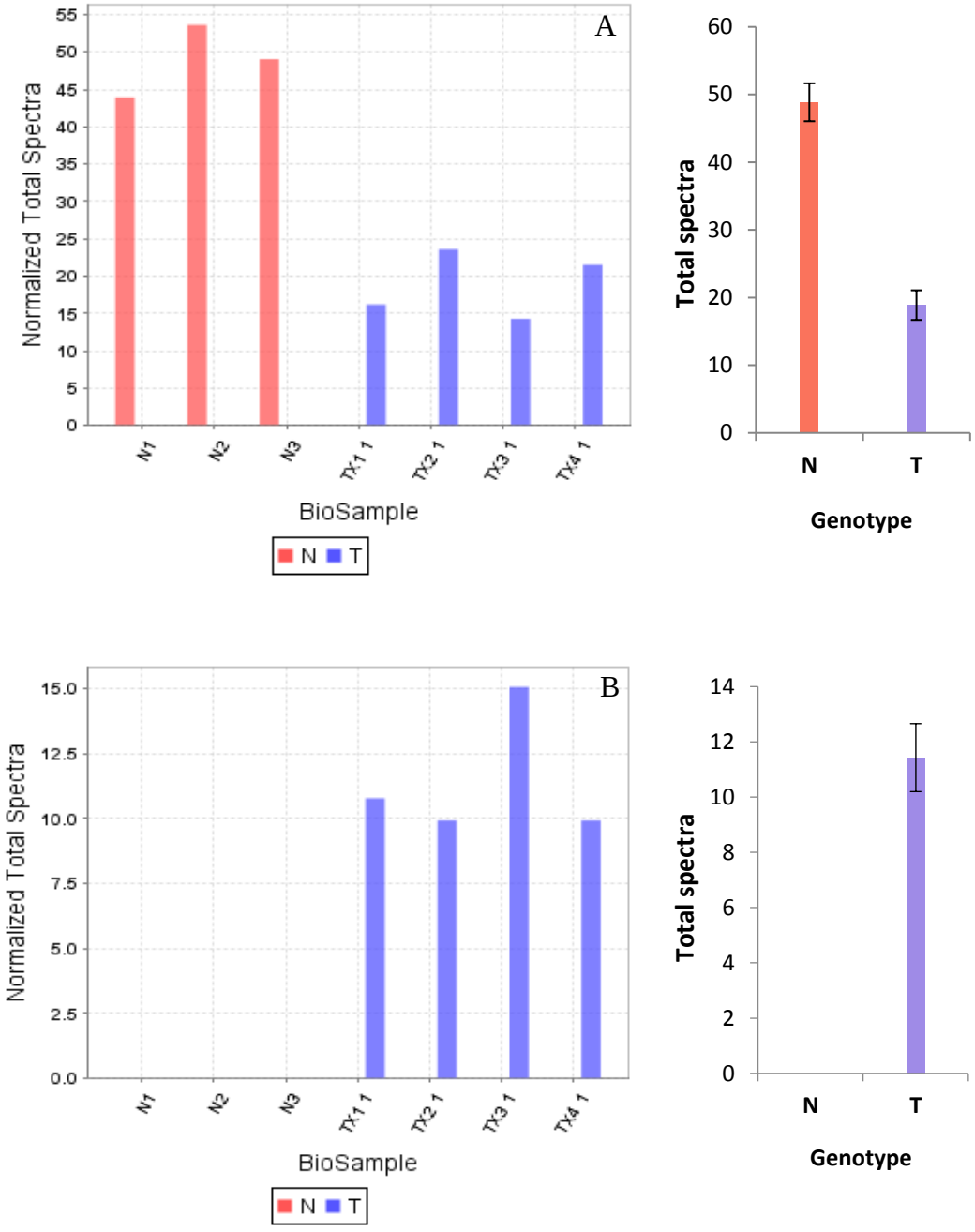

Figure 4.8 Differences in the expression of two identified proteins between Ningyou 7 and Tapidor DH.

The expression of myosin-like protein (A), and the expression of NIT2 (B) between Ningyou 7 (N) and Tapidor DH (T). The left figure of each of them represents biological replications and the figure to the right represents the mean value of the total spectra. Error bars represents standard error (n = 3 and 4). Pink represents Ningyou 7 and purple represents Tapidor DH.

4.5 Discussion

The results show that there was a considerable difference in the proteins found at different stages of development in both the roots and stems of both Tapidor and Ningyou 7. The most important point was with regards to the 23 kDa protein identified previously by Rossato *et al.* (2001) as a crucial vegetative storage protein. A 23 kDa protein was identified in the Tapidor DH plants that accumulated at both the rosette and flowering stages as shown in Figure 4.2 (page 159), this contrasted with the results from the Ningyou 7 plants in which the corresponding band was absent, however two other proteins of a slightly lower molecular mass were detected (21 and 22 kDa) Figure 4.1 (page 158).

This shows that there is an apparent difference in the proteins produced and potentially stored between these two mapping population parental lines suggesting that this could be genetically mapped if these proteins can be accurately quantified in the TNDH population derived from these lines. This would make this a trait amenable for QTL analysis. Such an approach will be described in chapter 4.

The hypothesis that the 23 kDa protein might play an important role in N storage for use in seed formation was supported by the deflowering and depodding experiments. In this case following approximately a month of flowering, the 23 kDa band disappeared (control plants) and then reappeared in the deflowered plants by the end of flowering. There were also key differences observed between taproots and lateral roots which contradict the findings of Rossato *et al.* (2001); Rossato *et al.* (2002a); Rossato *et al.* (2002b); Noquet *et al.* (2004) who detected this protein only in the taproots in a different oilseed rape variety (Capitol).

This highlights the importance of looking at all possible tissues to determine the site of accumulation and fate of storage proteins in particular. The other finding was that at the bottom of the stem there are also clear differences between the parent lines. In Tapidor DH, the amount of the 23 kDa putative storage protein was lower than that found in the roots and also the amount of this protein in this part of the plant did not vary in amount when measured at different plant growth stages unlike the pattern detected in the roots. This finding also contrasts with the aforementioned studies sine this protein was not detected in the stem.

The study of Schjoerring *et al.* (1995) investigating N remobilisation within OSR under field conditions, showed that silique walls possessed the maximum content of N on the 25th day prior to harvest which correspond to the stage GS 6.4 when the silique walls samples for the second time in the present study. When the siliques were studied at this stage, the SDS-PAGE gel of the soluble protein profile in Figure 4.4 (lane C2 silique walls) illustrated a relative abundance in protein quantity. Moreover, it was found that at maturity which occurred after about three months of flowering there was a large accumulation of three proteins. When these proteins were separated from the gel and analysed using the tandem mass spectrometry, they were all found to be putative seed storage proteins. These proteins were present in the siliques walls even at harvest when seed development was completed and the siliques dry. These proteins were found in both parents and suggest that this is a source of Nitrogen loss which it might be possible to address. This might be supported by the finding of Wagstaff *et al.* (2009) who reported the significant up-regulated seed storage proteins in the senescing pod walls of Arabidopsis and the finding of Koeslin-Findeklee and Horst (2016) who illustrated that silique walls contained a great proportion (~26 %)

of the total shoot N at maturity. Furthermore, The increasing accumulation of the ~35 kDa protein in the inflorescence stems adjacent to the siliques during seed development GS 6.4 and senescence in the both genotypes could also reported as a source of N loss and the possibility for further work to be considered. This protein could possess glucanase activity as was identified by MS/MS.

Mass spectrophotometric analysis of various bands which showed clear differences between the parent lines or in different life stages allowed us to identify a number of proteins which might shed light on the proteins involved in nitrogen storage. Interestingly none of the proteins correspond to that suggested by the French group. One of the main dominant proteins identified as a putative 23 kDa VSP is a trypsin inhibitor which is in agreement with the study of Tian *et al.* (2007) and Liu *et al.* (2009b) who reported the trypsin inhibition activity of the *LcVSP1* (22 kDa) in *L. chinensis* and the 23 kDa VSP in *S. mukorassi*, respectively. It was illustrated that N remobilisation associated with OSR leaf senescence is accompanied with disappearance of trypsin inhibition activity (Etienne *et al.*, 2007). Furthermore, one of the main dominant proteins identified in the 22 kDa protein band (a concomitant band to the 23 kDa Protein band in Tapidor DH) is water-soluble chlorophyll protein Table 4.1 (page 162). It was reported that this protein involved in N remobilisation in OSR young leaves under N starvation conditions and possessed protease inhibition activity by which leaf senescence is delayed (Desclos *et al.*, 2008; Avice and Etienne, 2014). Moreover, Avice *et al.* (2003) demonstrated that the 32 kDa VSP observed in taproot of *M. sativa* possessed class III chitinase activity and could plays a role in plant protection against pathogenesis. In the present study, one of the proteins identified as a putative 23 kDa VSP within lateral root is chitinase.

Continuous removal of pods resulted in a significant increase in the shoot length comparing to the control plants, in agreement with Noquet *et al.* (2004) whom reported that flowers and pods removal contributed to the shoot growth. Furthermore, continuous removal of flowers, during the seed development stages compared with the control plants, has increased the formation of new shoots and delayed the senescence in contrast to the control plants. Since N uptake decreases after the onset of flowering (Jensen *et al.*, 1997; Gabrielle *et al.*, 1998; Rossato *et al.*, 2001; Malagoli *et al.*, 2004; Zhang *et al.*, 2010; Ulas *et al.*, 2013) or after the early stages of the seed development (Malagoli *et al.*, 2005a; Gombert *et al.*, 2010), and the N storage reserves are the major source to support the increasing requirements of N for the growing shoots (depodded plants) or the formation of new shoots (deflowered plants), it might explain to some extent the lack of the increasing accumulation of the putative VSPs during seed filling stages in the depodded plants and after two months of flowering in the deflowered plants.

By studying the whole proteomic profile more than 1600 proteins were identified, at the beginning of flowering, in the bottom of the stem for each genotype. These proteins represent a fraction (1.66 %) of the total putative proteins coded by the *B. napus* genome (Chalhoub *et al.*, 2014). The abundance of these proteins varied significantly within each genotype which might reflect the importance of these proteins for the cell.

Genotypic variation in the abundance of these proteins was also observed, as at least 347 proteins were detected in only one genotype. 1261 proteins were presented in both genotypes, of which 11 and 12 proteins were overexpressed in Tapidor DH and Ningyou 7, respectively (Figure 4.7). Proteins were expressed that represented members of the housekeeping protein groups used in the protein and gene expression

studies. The most constant and abundant proteins from five families are; Bo8g065470.1, Bra016729 encoded glyceraldehyde-3-phsphate dehydrogenase, Bo9g169510.1, Bra008903 encoded tubulin beta chain, Bo2g133940.1, Bra014334 encoded 60S ribosomal protein L7, Bo6rg049540.1 encoded actin-2 and Bo3g039510.1 which encoded ubiquitin. Hence, these proteins accessions would be good choices as reference proteins in further study. Nonetheless, the expression patterns of these proteins interestingly varied among each family member. For example, the Bo5g016460.1 which encoded glyceraldehyde-3-phosphate dehydrogenase was not identified in Ningyou 7 in contrast to the Bo8g065470.1 protein. This results might raise concerns about using multiple copies of these housekeeping protein for normalisation of gene and protein expression data. The results clearly show the strength of studying protein expression but there are difficulties in this approach which still need to be overcome to make this a more commonly used approach.

Chapter 5 Quantitative Traits Underlying Nitrogen Use Efficiency in *Brassica napus* L.

5.1 Introduction

The principle of chromosomal segregation during the reproductive phase allows the identification of Quantitative Trait Loci (QTL) or genes that control traits of interest (Tanksley, 1993). This is mediated by a segregating population and suitable statistical algorithms that reveal the association between the genetic markers and the phenotypic data (Kearsey and Farquhar, 1998; Collard and Mackill, 2008). These mapping populations could also be tested under different environments by which the interaction between the genetic and environmental factor can be estimated (Vreugdenhil *et al.*, 2005). The major challenge facing breeders after QTLs have been detected is the identification of the gene and the nucleotide polymorphisms by which the variation in the phenotypic trait is defined or closely associated markers to track introgressions (Collard *et al.*, 2005; Vreugdenhil *et al.*, 2005). Identification of QTLs in a mapping population is affected by many determining factors such as the genetic properties of the genomic regions that control traits, the mapping population size and the experimental design by which phenotypic data are generated (Asíns, 2002; Collard *et al.*, 2005; Vreugdenhil *et al.*, 2005).

QTLs have been mapped for a number of agronomic traits in *B.napus* L. These include QTLs associated with flowering time (Long *et al.*, 2007; Wang *et al.*, 2011a; Javed *et al.*, 2016), seeds content of glucosinolates (Howell *et al.*, 2003; Feng *et al.*, 2012), seeds content of oil (Qiu *et al.*, 2006; Jiang *et al.*, 2014), yield and yield related traits (Quijada *et al.*, 2006; Radoev *et al.*, 2008; Shi *et al.*, 2009; Bouchet *et al.*, 2014), abiotic stress, resistance to diseases (Butruille *et al.*, 1999; Zhao and Meng, 2003; Zhang *et al.*, 2016a), seed (Ding *et al.*, 2010) and shoot (Liu *et al.*, 2009a) minerals concentration, N use efficiency (Miro, 2010), B use efficiency (Zhao *et al.*, 2012), P

use efficiency (Ding *et al.*, 2012) and root morphology and architecture under P stress (Yang *et al.*, 2010; Shi *et al.*, 2013a).

As it was described in Chapter 1, OSR is characterised with poor N Use Efficiency. Hence, improvement in N use efficiency is a major priority for plant breeders. This could be possible through the potential optimisation of traits associated with N remobilisation efficiency (Bouchet *et al.*, 2014). Nevertheless, QTL mapping for proteins associated with N remobilisation such as putative VSPs are very rare, essentially due to the difficulty in the identification of such proteins and then establishing the appropriate methodology required for an accurate quantitative analysis. N is significantly associated with plant biomass, architecture and yield related traits. Svečnjak and Rengel (2006a) reported that in oilseed rape the average shoot content of N was 2.7 % of the dry weight. Thus, more work is required to elucidate the genetic mechanism by which plants control these traits

5.2 The objectives of this chapter

This chapter aims to identify QTL associated with the expression of a putative 23 kDa VSPs in the TNDH oilseed rape mapping population, as well as other proteins previously identified by MS/MS (chapter 3), through establishing and optimising the methodology to quantify proteins of interest in a complex protein mixture by means of nanoLC-ESI-MS/MS. In addition, it aims to identify QTL for other developmental traits that contribute to N use efficiency, including flowering time, architectural and yield related traits, under N replete conditions.

5.3 Material and methods

5.3.1 The mapping population and the linkage map

The segregating mapping population used in this study was a doubled haploid population derived from the F1 cross between the two contrasting *B. napus* lines Tapidor DH and Ningyou 7 (the female and male parents, respectively, of the reference TNDH mapping population) by microspore culture. A genetic map for the 202 lines of this population has been produced by (Qiu *et al.*, 2006) comprising 692 markers arranged in 19 linkage groups in accord with the *B. napus* 19 chromosomes, named as A01 to A10 (from *B. rapa* A genome) and C1 to C9 (form *B. oleracea* C genome). These linkage groups varied in length from 62.33 to 148.8 cM for chromosomes C1 and C3, respectively. Markers cover a total length of 2031.1 cM with an average distance of 3.02 cM between adjacent markers. The smallest and largest interval between two adjacent markers was 0.01 and 31.68 cM on chromosomes A4 and C4, respectively.

5.3.2 Plant material and experimental design

120 lines of the TNDH mapping population in addition to the parental lines were selected on the basis of being suitable for cultivation in the UK and being the most genetically informative (Defra Oilseed Rape Genetic Improvement Network project) and grown under controlled environment in a 40 m^2 glasshouse compartment for 35 days (from sowing seeds until 4 – 5 leaves were established). Seeds were provided by Graham Teakle from Warwick Genetic Resources Unit at Warwick Crop Centre at the University of Warwick. Six seeds from each line including parental lines were initially sown (29/01/2014) per rounded plastic pot (5 L, 230 mm diameter $_X$ 200 mm height)

filled with Levington M2 compost (Scotts Miracls-Gro Company, UK; containing 192 mg/L N, 98 mg/L P and 319 mg/L K) as growing medium and placed in the glasshouse at Warwick Crop Centre for 35 days. Upon germination the pots were thinned to two plants per pot. The glasshouse was set to a temperature of 15 °C day and night, with automatic ventilation at 17 °C day and night, and supplementary lighting (400 W high pressure sodium luminaires) to provide a 16 hour light period. Light threshold setting was set to switch off above 30 Klx. Plants were irrigated as and when necessary with 4 ml/L liquid feed Vitafeed 214 (Vitax Limited, Coalville, Leicester, UK), an N-P-K [16-8-32] fertiliser with 0.09 % magnesium oxide and Mn, Fe, Cu, B and Mo as trace elements to meet plant growth requirements of mineral nutrients. Insects and diseases were controlled Insecticide and fungicide were applied to control pests and diseases following the Horticulture Service standards and as necessary. To reduce the environmental effect, the population was grown in randomised block design containing four blocks of 122 pots and each pot contained two plants Figure 5.1.

This population is a cross between Tapidor DH with a strong vernalisation requirements and Ningyou 7 with a low vernalisation (Qiu *et al.*, 2006; Long *et al.*, 2007), so for the purpose of providing natural vernalisation, the plants were transferred (04/03/2014) to a semi open polytunnel, in the same randomised design until they were harvested. Plants were grown under natural light and watered as and when required, with the same liquid feed previously used in the glasshouse. Insects and diseases were all controlled in the same manner according to Horticulture Service standard as and when was necessary.

Figure 5.1 TNDH mapping population grown in the glasshouse.

122 lines, two plants per pot, a total of 488 pots were arranged in a randomised block design. Four blocks, each of which contains 244 plants in a 122 pots. The photograph of the plants in the glasshouse was taken 24 days after sowing.

5.3.3 Phenotypic traits

A number of phenotypic traits associated with N remobilisation, primarily, the expression patterns of proteins identified as putative 23 kDa VSP, other proteins showing significant expression variation in the parental lines, and putative proteins thought to be involved in nitrate transport as well as housekeeping proteins. In total, the expression pattern of 32 proteins were identified as the subject of this study and their details are summarised in Table 5.1. These proteins were studied in the bottom of the stem (10 cm from the soil surface).

Table 5.1 List of proteins subjected to quantification study

32 proteins were divided into five groups; 12 proteins identified to represent a putative 23 kDa VSP, five housekeeping proteins, six proteins were only expressed in Tapidor DH, five proteins were only expressed in Ningyou 7 and four putative nitrate transporter proteins.

Group	Protein name	Protein accession
putative VSPs	Trypsin inhibitor	Bo6rg116580.1
	Trypsin inhibitor	Bra016002
	Trypsin inhibitor	Bo6rg116620.1
	Trypsin inhibitor	Bo6rg116640.1
	Protein of unknown function (DUF640)	Bo3g036160.1, Bra000269
	Wound-induced protein	Bo3g058580.1, Bra001123
	Glutathione peroxidase	Bo2g108730.1, Bra033140
	Peroxiredoxin, putative	Bo5g144820.1, Bra020782
	Water-soluble chlorophyll protein	Bo02800s010.1
	Peptidyl-prolyl cis-trans isomerase	Bo8g090480.1
	Peptidyl-prolyl cis-trans isomerase	Bra007214
	Translationally controlled tumor protein	Bo3g068470.1
housekeeping proteins	Glyceraldehyde-3-phosphate dehydrogenase	Bo8g065470.1, Bra016729
	Tubulin beta chain	Bo9g169510.1, Bra008903
	60S ribosomal protein L7	Bo2g133940.1, Bra014334
	Actin-2	Bo6rg049540.1
	Ubiquitin	Bo3g039510.1
Proteins were expressed only in Tapidor DH	Indole-3-acetonitrile nitrilase	Bra035006
	Pathogenesis-related thaumatin superfamily protein	Bo5g027350.1
	Glycosyl hydrolase family protein	Bo3g134130.1

Group	Protein name	Protein accession
	Glucan endo-1,3-beta-glucosidase, putative	Bo1g007240.1
	Peptidyl-prolyl cis-trans isomerase, putative	Bo5g155110.1
	Glyceraldehyde-3-phosphate dehydrogenase	Bo5g016460.1
Proteins were expressed only in Ningyou 7	Catalytic/ methylthioadenosine nucleosidase	Bra010725
	Phosphorylase	Bo3g134100.1
	Alpha-glucan phosphorylase 2	Bra018180
	HXXXD-type acyl-transferase family protein	Bo1g056990.1
	Conserved hypothetical protein	Bo3g061790.1
Nitrate transporter family	High affinity nitrate transporter	Bo8g065100.1
	High affinity nitrate transporter	Bo5g008780.1
	high affinity nitrate transporter 2.6	Bo9g147020.1
	high affinity nitrate transporter 2.7	Bo2g012010.1

Furthermore, other agronomic traits associate with architectural characteristics of plants such as flowering time, biological mass, number of lateral main stems arising from the base of the plant (tillers), number of the main branches and plant height, as well as yield related traits such as number of pods and seed number per pod were studied Table 5.2. These traits were considered to be indirectly associated with N use efficiency. In addition to these traits, the mineral elements content of the bottom of the stem was also determined.

Flowering date was recorded on the whole set of lines (eight plants each) when the first flower was observed on the main inflorescence. Flowering time was then estimated as the number of days from germination date to flowering date.

Four plants from each line (one plant from each block) were harvested when 5 – 10 flowers were observed on the main inflorescence. The bottom 10 cm of the stem was separated and divided into three sections, two sections for protein analysis and RNA extraction were stored at -80 °C, and one section for mineral analysis was oven dried at 60 °C. The other four plants from each line (the remaining plant from each block) were harvested after 45 days from the flowering date. The bottom 10 cm of the stem was separated and divided into three sections as previously described. The rest of the stems with branches were first weight (fresh weight) and oven dried at 60 °C until constant weight and re-weighed (dried weight). In addition, 10 phenotypic traits were recorded and are summarised in Table 5.2.

Table 5.2 List of the phenotypic traits measured.

These traits were recorded on four plants of each line (one plant each block) after 45 days of flowering date.

Phenotypic trait	Abbreviation	Measurement description
Flowering time	FT	Number of days from germination until the first flower was observed on the main inflorescence (MF) (days).
Stem height to the first branch	SHB	Stem height from the surface to the first branch (cm).
Stem height to the first pod	SHP	Stem height form the surface to the first pod on MF (cm).
Main inflorescence height	MFH	The length from the first pod to the top (cm).
Plant height	PH	The total plant height from the surface to the top of MF (cm).
Number of branches	NB	Number of the main branches
Number of pods on the MF	NPMF	Number of pods on the MF.
Number of pods on the branches	NPB	Number of pods on all braches.
Total number of pods	TNP	Total number of pods on the whole plant.
Number of seed per pod	NSP	The average of seeds number in up to 30 pods on MF from bottom to top.
Fresh weight	FW	Fresh weight of the stem and branches (g).
Dried weight	DW	Dried weight of the stem and braches after being oven dried at 60 °C.
Lateral main stem	LS	Lines with one main stem (same as Ningyou 7); lines with more than one main stem (same as Tapidor DH).

5.3.4 Protein quantitative workflow

One of the main disadvantages of the proteomic quantification using a triple quadrupole is that the instrument must be programmed what to record in advance (Picotti and Aebersold, 2012; Kinter and Kinter, 2013c). This is achieved through establishing a correct method that includes the m/z of every single product able to be detected by MS/MS, as well as the collision energy by which the selected precursor would be fragmented in the second quadruple Q2. These products are referred to as "transition" and the method is referred to as Selected Reaction Monitoring, SRM (Lange *et al.*, 2008; Gallien *et al.*, 2011; Picotti and Aebersold, 2012; Kinter and Kinter, 2013b). An essential step before designing the method is to build a spectral library by running the sample initially on tandem mass spectrometry. For this study, the spectral library used was generated as previously described in Chapter 4.

The SRM method was designed using the open-source Skyline software (MacLean *et al.*, 2010). Three to five unique peptides were selected for each protein of interest, usually with the highest relative intensity, one doubled charge precursor for each peptide. For each precursor, three to five fragments (transitions) with the y ion according the peptide fragmentation (optimum range between y7 and y12) were selected. Aiming to obtain a high signal to noise ratio by increasing the time spent on each transition to be acquired (is referred to as dwell time), would limit the number of the transitions that can be measured during the same run (Lange *et al.*, 2008; Picotti and Aebersold, 2012; Liebler and Zimmerman, 2013). Nonetheless, once the SRM experiment has been validated and retention time of the transitions is known and valid,

through multiple runs of the samples with different transitions methods and a detection window of an hour, it is possible to set a scheduled acquisition. During this the spectra for the specific products are monitored (Picotti and Aebersold, 2012; Kinter and Kinter, 2013a). 10 min was used in this study. For the 32 selected proteins, 123 peptides, 123 precursors and 408 transitions were designed based on the collision energy for each precursor. Moreover, a list of 122 decoy peptides including 400 transitions were also created for the purpose of improving the accuracy and the confidence that the selected peak is related to the targeted peptides (MacLean *et al.*, 2010; Reiter *et al.*, 2011; Rost *et al.*, 2014). Afterwards, the methods can be extracted to an excel file and applied to the triple quadruple. Figure 5.2 shows the output of designing transition in skyline and the extracted transition to excel.

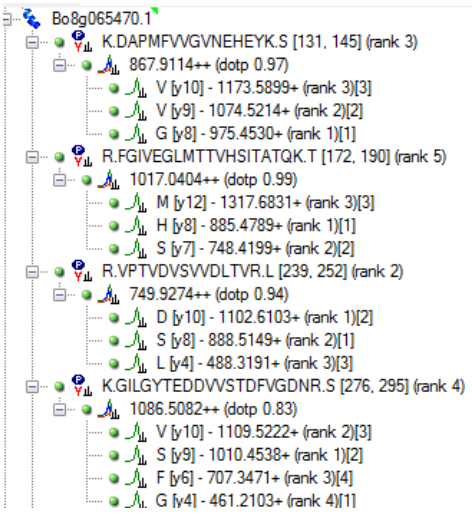

Compound	Start Time (min)	End Time (min)	Polarity	Precursor (m/z)	Product (m/z)	Collision Energy (V)
VGFVPEEENLNIK(+2)	15.56	25.56	Positive	744.3907	1085.55	25.2
VGFVPEEENLNIK(+2)	15.56	25.56	Positive	744.3907	988.495	25.2
VGFVPEEENLNIK(+2)	15.56	25.56	Positive	744.3907	859.452	25.2
SLFIAAGPKPEAGGEDS	14.85	24.85	Positive	944.9736	1229.58	31.3
SLFIAAGPKPEAGGEDS	14.85	24.85	Positive	944.9736	1004.43	31.3
SLFIAAGPKPEAGGEDS	14.85	24.85	Positive	944.9736	593.253	31.3
GLVIGSTPPFGYPFEVVF	30.91	40.91	Positive	1077.088	964.55	35.2
GLVIGSTPPFGYPFEVVF	30.91	40.91	Positive	1077.088	867.497	35.2
GLVIGSTPPFGYPFEVVF	30.91	40.91	Positive	1077.088	720.429	35.2
GLVIGSTPPFGYPFEVVF	30.91	40.91	Positive	1077.088	591.386	35.2
GPEGGGLTLTPR(+2)	17.64	27.64	Positive	577.8118	1000.54	20.2
GPEGGGLTLTPR(+2)	17.64	27.64	Positive	577.8118	871.5	20.2
GPEGGGLTLTPR(+2)	17.64	27.64	Positive	577.8118	814.478	20.2
GPEGGGLTLTPR(+2)	17.64	27.64	Positive	577.8118	700.435	20.2

Figure 5.2 Overview of the SRM method output.

Overview of designing transitions method in Skyline (left), four peptides and precursors were selected for the Bo8g065470.1 protein, the first precursor (m/z 867.9114) has three transitions (y8 to y10). The extracted methods to excel (right) shows the peptide, the start and end time of detection, precursor and transition m/z, and the collision energy required to fragment each peptide.

Proteins were extracted from the bottom of the stem, and then peptides were extracted using the FASP methodology as described previously in Section 4.3.7.1. The extracted peptide mixture was then separated by reversed phase chromatography using Ultimate 3000 RSLCnano (Thermo Scientific) as described previously in Section 4.3.7.2, however, peptides were eluted onto the analytical column at a flow rate of 300 nL/min where the mobile phase B concentration increased from 4 % B to 50 % over 33 min then to 90 % B over 5 min. This was followed by a 20 min re-equilibration at 4 % B. The eluted peptides were next subjected to ESI and converted to gaseous ions, and analysed on QQQ-MS (TSQ Quantiva mass spectrometer, Thermo Scientific) using the SRM method. Cycle time was set to 1.2 sec and the resolution in Q1 and Q3 was set to 0.7 FWHM. The spray voltage was set to 1800 V and ion transfer tube temperature was set to 325 °C. The collision gas pressure for CID was set to 2 mTorr.

An aliquot of 5 µl was used in each injection. Three technical replicates (three injections) were used for each sample (biological replicate). Each two lines (four biological replicates each) were run together as one patch. The order in which the biological and technical replicates were analysed was randomised to reduce the experimental bias.

The generated output was then visualised in Skyline (Figure 5.3), and quantitative analysis performed by Skyline and also in the MSstats R package for proteomic-based statistical quantitative analysis (Surinova *et al.*, 2013; Broudy *et al.*, 2014).

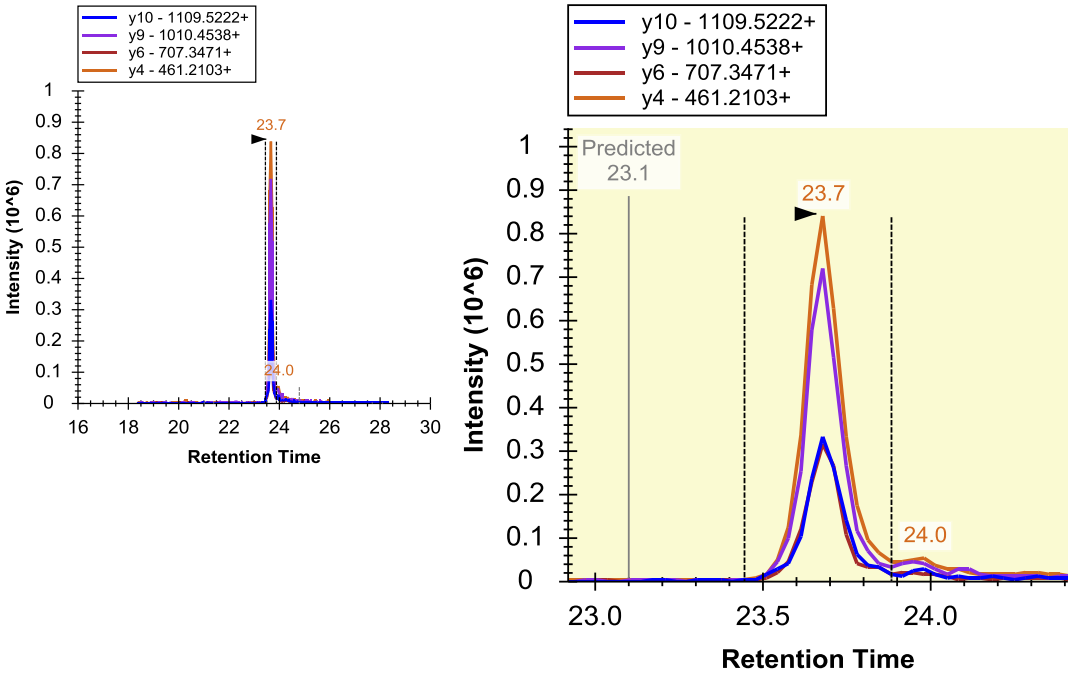

Figure 5.3 Skyline interface for a peptide precursor.

The measured data on the QQQ were loaded to Skyline. The picture represents one precursor (1086.5082 m/z) of the Bo8g065470 protein Figure 5.2 which includes four transitions (y4, 6, 9 and 10) shown in different colours. Transitions were detected in the 23.7 when the intensity was recorded. In theory, it was this precursor that was predicted to be detected in the 23.1 min.

5.3.5 Data analysis

5.3.5.1 Phenotypic data

One-way Analysis of Variance (ANOVA) of the randomised blocks was applied to allocate the amount of variation between population lines and blocks. The mean value, standard deviation (SD, n =4) and coefficient variance (% CV) across the 11 phenotypic traits were determined. The normality of the distribution of the phenotypic traits was verified using the Shapiro-Wilks normality test (W) (Shapiro and Wilk, 1965). A frequency distribution was also generated for each phenotypic trait. Pearson

correlation analysis was applied to determine the Correlation Coefficient (*r*) between traits. All statistical analyses were performed using GenStat (17th edition, VSN international, UK).

5.3.5.2 QTL detection

QTL mapping was performed using MapQTL software v.6. Initially the genome-wide (GW) LOD threshold for detecting significant QTL was estimated using 1000-permutation test (*P* =0.05). The non-parametric Kruskal-Wallis test was then applied to identify markers exhibiting linkage to the traits. The interval mapping (IM) method (Jansen and Stam, 1994; Jansen, 2008) was then performed to determine the QTL likelihood profile for each position on the genome. Further power for detecting additional QTL was obtained using Multiple-QTL mapping (MQM) analysis, where nearby markers of the identified QTL from the IM or Kruskal-Wallace analysis, were used as cofactors (Jansen, 2008; Van Ooijen and Kyazma, 2009). 1 and 2 LOD confidence intervals where then constructed from LOD differences on either side of the most likely QTL position. The contribution of female parent (Tapidor DH) to the identified QTL was presented as a positive additive, whereas the contribution of the male parent (Ningyou 7) was presented as a negative additive. The percentage of the variation in the phenotypic traits arising from the identified QTL was also determined. MapChart v 2.3 (Voorrips, 2002) was used for plotting the linkage maps with the identified QTLs.

5.4 Results

5.4.1 Phenotypic variation among traits

13 phenotypic traits (listed in Table 5.2, page 184) were evaluated after 45 days from the flowering date on 120 lines of the TNDH population as well as the parental lines grown in a glasshouse and polytunnel. A normal distribution was observed for all phenotypic traits among the TNDH population lines (W >0.96, Table 5.3), and illustrated in histograms for all traits in Figures 5.4 and 5.5. Substantial variation was observed between the parental lines and the TNDH population lines for flowering time (FT). The low vernalisation requirement parent (Ningyou 7) flowered 86 days after germination, whereas the strong vernalisation requirement parent (Tapidor DH) was significantly delayed in flowering and flowered more than a month later. Flowering time was normally distributed among the population lines and ranged from 63 to 126 days (Table 5.3).

The stem height to the first branch (SHB) also differed between Ningyou 7 (53 cm) and Tapidor DH (80 cm). A considerable transgressive variation between the TNDH population lines was also observed and ranged from 35 to 106 cm (Table 5.3). There was only a range of 9 cm variation between the parents lines related to the stem height to the first pod (SHP), whereas the variation between the population lines ranged from 61 to 122 cm. The parental lines exhibited a substantial difference in the length of the main inflorescence (MFH); Ningyou 7 possessed the longest (75 cm) and Tapidor DH the shortest (40 cm). Interestingly, Tapidor DH possessed the greater number of pods (72) on the main inflorescence (NPMF), whereas Ningyou 7 possessed the lowest number of pods (28). Approximately 3-fold (MFH) and 2-fold (NPMF) variation was

observed in the DH progeny (Table 5.3). Positive and significant correlations were observed between flowering time and SHB and SHP (r =0.47 and 0.44, respectively, P >0.00001), whereas, the MFH was negatively and significantly associated with FT (r =-0.51, P >0.000).

Plant height (PH) varied between 133 and 159 cm in Tapidor DH and Ningyou 7, respectively, in addition a 2-fold variation was observed between population lines. An average of 5 and 6 branches were observed on Tapidor DH and Ningyou 7, respectively, whereas the number of branches (NB) ranged from 2 to 10 across the population lines (Table 5.3).

Table 5.3 Phenotypic traits estimates of the parental lines and the TNDH population.

Table shows values of mean, standard deviation (SD), minimum, maximum, coefficient variance (CV) and Shapiro-Willks test (W) of the parent line and the TNDH population.

Traits	Parental lines				TNDH population					
	Ningyou 7	SD	Tapidor DH	SD	Mean	Min	Max	SD	CV%	W
FT	86	3.2	117	2.6	104	63	126	11.2	10.8	0.96
SHB	53	16.9	80	11.0	66	35	106	12.7	19.2	0.99
SHP	84	9.0	93	9.4	90	61	122	10.9	12.2	0.99
MFH	75	12.7	40	4.1	60	34	100	16.3	27.2	0.97
PH	159	20.6	133	12.5	150	102	194	19.9	13.3	0.99
NB	6	1.0	5	1.5	6	2	10	1.6	27.9	0.98
NPMF	28	3.8	72	21.2	36	17	70	12.3	33.9	0.96
NPB	86	19.2	35	8.9	61	13	159	28.0	45.6	0.96
TNP	113	21.9	107	22.4	98	25	201	34.3	35.2	0.98
NSP	12	1.8	17	1.1	15	6	22	3.4	23.2	0.99
FW	41.0	6.4	44.4	11.3	41.9	15.5	84.2	13.1	31.1	0.97
DW	9.7	1.7	10.4	2.2	9.6	4.4	15.9	2.6	26.7	0.98

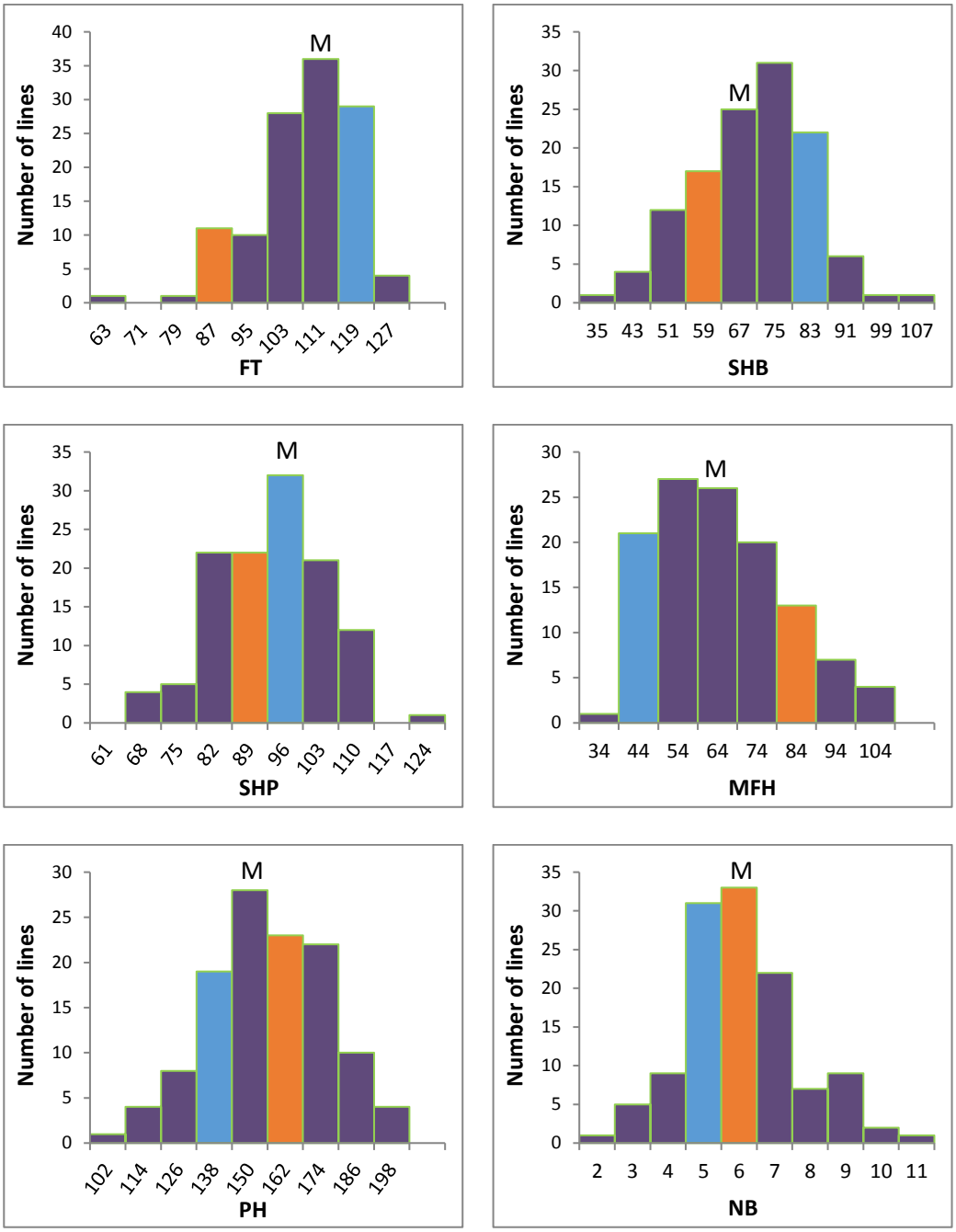

Figure 5.4 Frequency distribution of six phenotypic traits in the TNDH mapping population.

Traits abbreviation are as described previously in Table 5.2 (page 184). M indicates where the mean value of the TNDH population lines occurred. The bars coloured in orange and blue indicate where Ningyou 7 and Tapidor DH occurred, respectively.

In contrast to the NPMF, Ningyou 7 possessed the greatest number of pods on branches (NPB) with 86 pods, whereas Tapidor DH possessed the lowest number with only 35 pods and thus the total number of pods (TNP) were very similar. Nevertheless, considerable variation was exhibited between the TNDH population lines in NPB which ranged from 13 to 159, and in TNP ranged from 25 to 201 (Table 5.3).

The parental lines varied in the number of seeds per pod (NSP), Tapidor DH possessed the highest number with 17 seeds and Ningyou 7 possessed the lowest with 12 seeds. More than 3-fold variation was observed in the DH progeny, with lines ranging from 6 to 22 seeds per pod (Table 5.3, page 191). The difference between the parental lines in the fresh weight (FW) was less than 4 g and the dry weight was observed to be approximately similar. However, the TNDH population varied significantly in FW (15.5 – 84.2 g), and in DW (4.4 – 15.9 g) (Table 5.3) (page 191).

It was observed that 22 lines of the TNDH segregating population possessed more than a single main stem (tiller) which was the case for Tapidor DH, whereas the rest of the lines were like Ningyou 7 and possessed a single main stem.

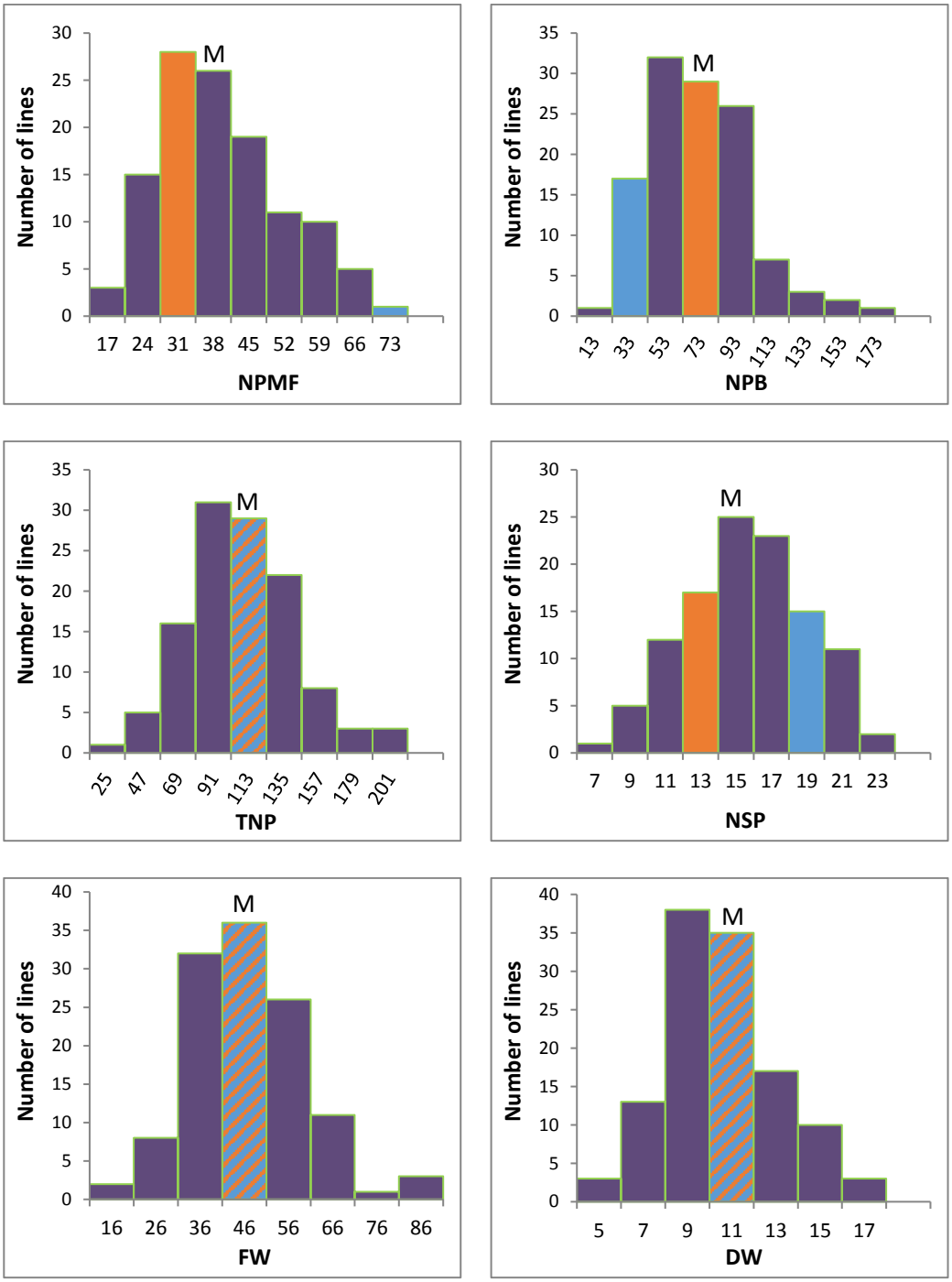

Figure 5.5 Frequency distribution of six phenotypic traits in the TNDH segregating population.

Traits abbreviation used are as described previously in Table 5.2 (page 184). M indicates where the mean value of the TNDH population lines occurred. The bars coloured in orange and blue indicate where Ningyou 7 and Tapidor DH occurred, respectively. The double-coloured striped bar indicates where both parents occurred.

5.4.2 Analysis of QTLs mapping phenotypic traits

The 120 TNDH mapping population lines and their parents (Tapidor DH and Ningyou 7) were grown in the glasshouse house for a month and transferred to a polytunnel afterwards for the purpose of allowing sufficient vernalisation naturally. 13 phenotypic traits, listed in Table 5.2 (page 184), were evaluated after 45 days of the date of first flower opening and subjected to QTL analysis to determine their genetic control.

MQM analysis revealed a total of 21 QTL regions (Table 5.4) distributed across 12 linkage groups (LGs). Six QTLs associated with flowering time (FT) explaining between 9.2 and 33.6 of the phenotypic variation were identified. These QTLs distributed on five LG of the A genome (Figure 5.6 and Figure 5.8) and one LG of the C genome (Figure 5.9), and their additive effect was dominantly influenced by the winter-type parental line, Tapidor DH. Three QTLs associated with number of seed per pod (NSP) were detected, explained 10.2 – 14.2 % of the phenotypic variation, distributed on two LG of the A genome (Figure 5.6 and Figure 5.7) and one on the C genome (Figure 5.8). The additive effect for two genomic regions were influenced by the semi winter-type parental line, Ningyou 7, and the third influenced by Tapidor DH. In addition, three QTLs were affecting number of pods on the main inflorescence (NPMF) distributed on three A genome LGs; A02, A03 (Figure 5.6) and A09 (Figure 5.8), accounted for 15.8, 13.4 and 16.2 % of the phenotypic variation. Two QTLs associated with stem height to the first branch (SHB) were identified on LG A03 (Figure 5.6) and A05 (Figure 5.7). The parent Tapidor DH contributes the alleles for the increasing NPMF and SHB.

Table 5.4 QTLs detected for nine phenotypic traits in 120 lines of the TNDH population.

Trait abbreviations as described in Table 5.2 (page 184). Table shows linkage group, position, maker name, LOD score, LOD threshold, the explained variance, additive effect and the confidence interval for each identified QTL. LOD threshold was determined at 1000 permutation test for each trait. One and two LOD confidence intervals are shown for each detected QTL position (cM). Positive additive effect associated with Tapidor DH, whereas negative additive effect associated with Ningyou 7.

Trait	Linkage Group	Position (cM)	Locus	LOD	GW LOD threshold	Increasing allele	Variance %	Additive effect	Minus 2 LOD position (cM)	Minus 1 LOD position (cM)	Plus 1 LOD position (cM)	Plus 2 LOD position (cM)
FT	A01	85.04	pW190a	3.61	3.3	Tapidor DH	9.6	3.5444	70.55	70.55	87.72	87.72
FT	A02	91.55	CNU389	5.02	3.3	Tapidor DH	13.8	5.6810	81.55	81.55	95.3	95.3
FT	A03	73.81	IGF3165c	5.97	3.3	Tapidor DH	13.6	4.1604	66.07	66.07	75.31	82.15
FT	A09	137.27	IGF1134a	3.87	3.3	Tapidor DH	9.2	3.5578	126.37	130.12	139.63	139.63
FT	A10	44.21	sN8474	13.22	3.3	Tapidor DH	33.6	6.7896	39.05	39.05	53.76	53.76
FT	C7	45.11	IGF5702e	6.89	3.3	Tapidor DH	15.5	4.5671	37.32	37.32	54.68	54.68
SHB	A03	73.81	IGF3165c	5.87	3.3	Tapidor DH	17.8	5.4725	61.52	64	82.15	82.15
SHB	A05	31.556	BRMS-061	3.54	3.3	Tapidor DH	10.5	4.1410	13.487	28.534	36.965	38.201
SHP	C3	7.74	HBr085	3.47	3.2	Ningyou 7	11.7	-4.5424	0	0	22.25	22.25
SHP	A06	111.47	JICB0541	3.58	3.2	Ningyou 7	11.4	-3.9167	95.04	95.04	131.17	132.47

Trait	Linkage Group	Position (cM)	Locus	LOD	GW LOD threshold	Increasing allele	Variance %	Additive effect	Minus 2 LOD position (cM)	Minus 1 LOD position (cM)	Plus 1 LOD position (cM)	Plus 2 LOD position (cM)
MFH	A10	39.05	sN8502	4.71	3.3	Ningyou 7	15.3	-6.7368	25.41	35.28	44.21	62.91
MFH	C9	71.39	HR-C017-C9	4.19	3.3	Ningyou 7	11.8	-5.6269	61.1	68.92	79.42	79.42
NB	A02	52.49	HR-Sp1-210	3.46	3.2	Tapidor DH	11.5	0.5413	81.55	81.55	95.3	95.3
NPMF	A03	82.15	CNU215	4.29	3.3	Tapidor DH	13.4	4.5859	66.07	77.11	85.17	91.09
NPMF	A09	69.02	IGF1207c	4.73	3.3	Tapidor DH	16.2	5.0497	53.28	56.81	81.42	86.87
NPMF	A02	65.76	pW144	5.28	3.3	Tapidor DH	15.8	5.0490	54.45	64.08	70.06	74.35
NSP	C1	29.09	HR-S3-230	3.21	3.2	Ningyou 7	10.2	-1.1142	7.79	7.79	31.19	51.87
NSP	A04	56.11	HR-Tp4-300	4.37	3.2	Tapidor DH	14.2	1.3130	37.22	53.24	63.28	65.91
NSP	A03	15.43	IGF5154c	3.96	3.2	Ningyou 7	12.8	-1.3324	4.71	15.43	20.16	20.16
FW	C7	64.08	BRMS-185	3.58	3.2	Ningyou 7	11.2	-4.5503	60.91	60.91	69.59	88.66
DW	A06	90.89	HBr029	3.42	3.2	Ningyou 7	11.7	-0.9556	82.05	82.05	90.089	111.47

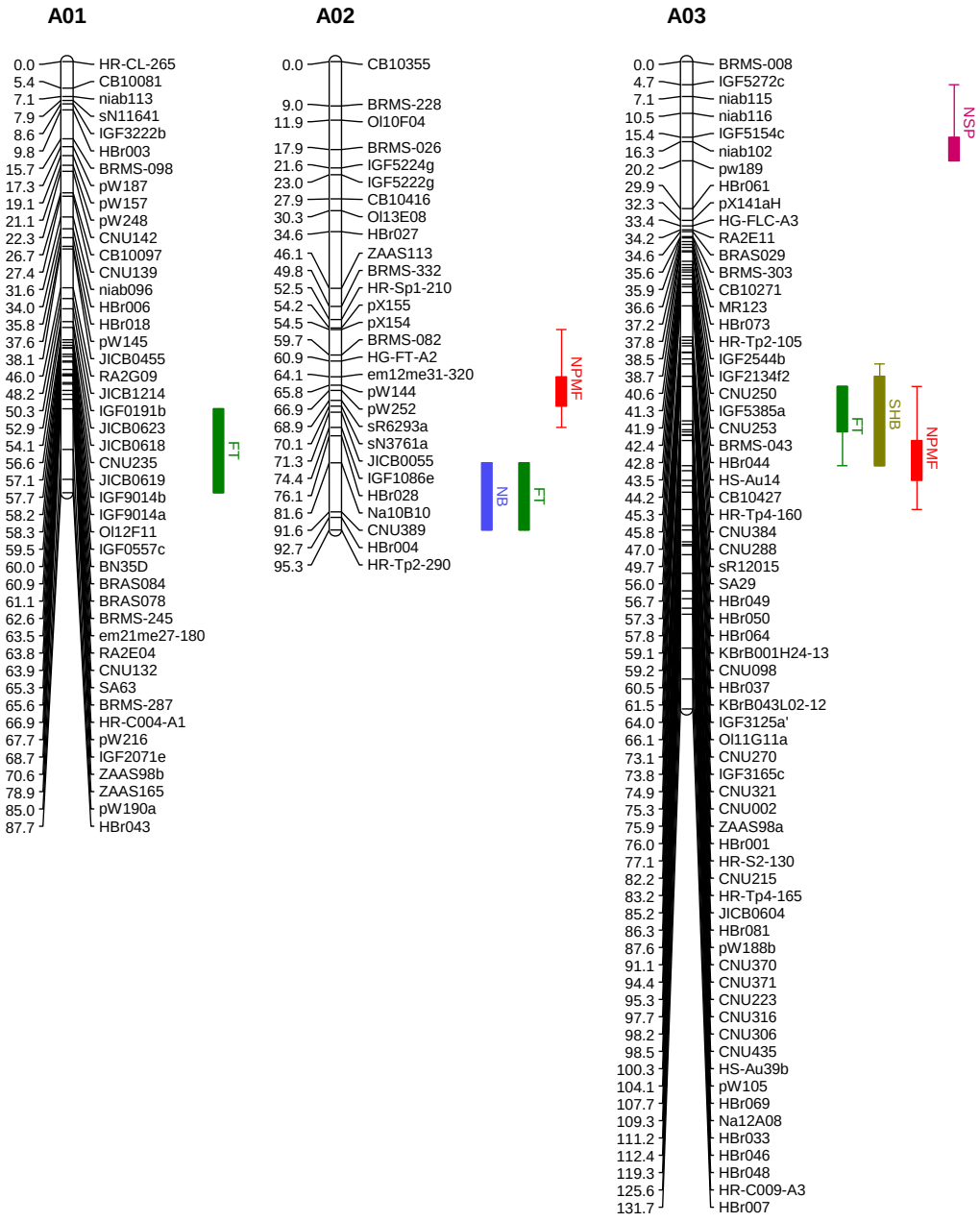

Figure 5.6 The linkage map for three linkage groups (A01, 02 and 03) depicts the detected QTLs.

The linkage groups are shown as vertical bars with markers names are indicated to the right and the positions (cM) of markers are shown on the left. QTL are represented by coloured bars (1-LOD confidence interval) and whiskers (2-LOD confidence interval) to the right of the linkage group. There is no whisker when the same marker defining the confidence interval satisfies both the 1- and 2-LOD positions. The QTLs associated with traits FT (flowering time), NB (branches number), NPMF (pods number on main inflorescence), SHB (stem height to the first branch) and NSP (seeds number per pod).

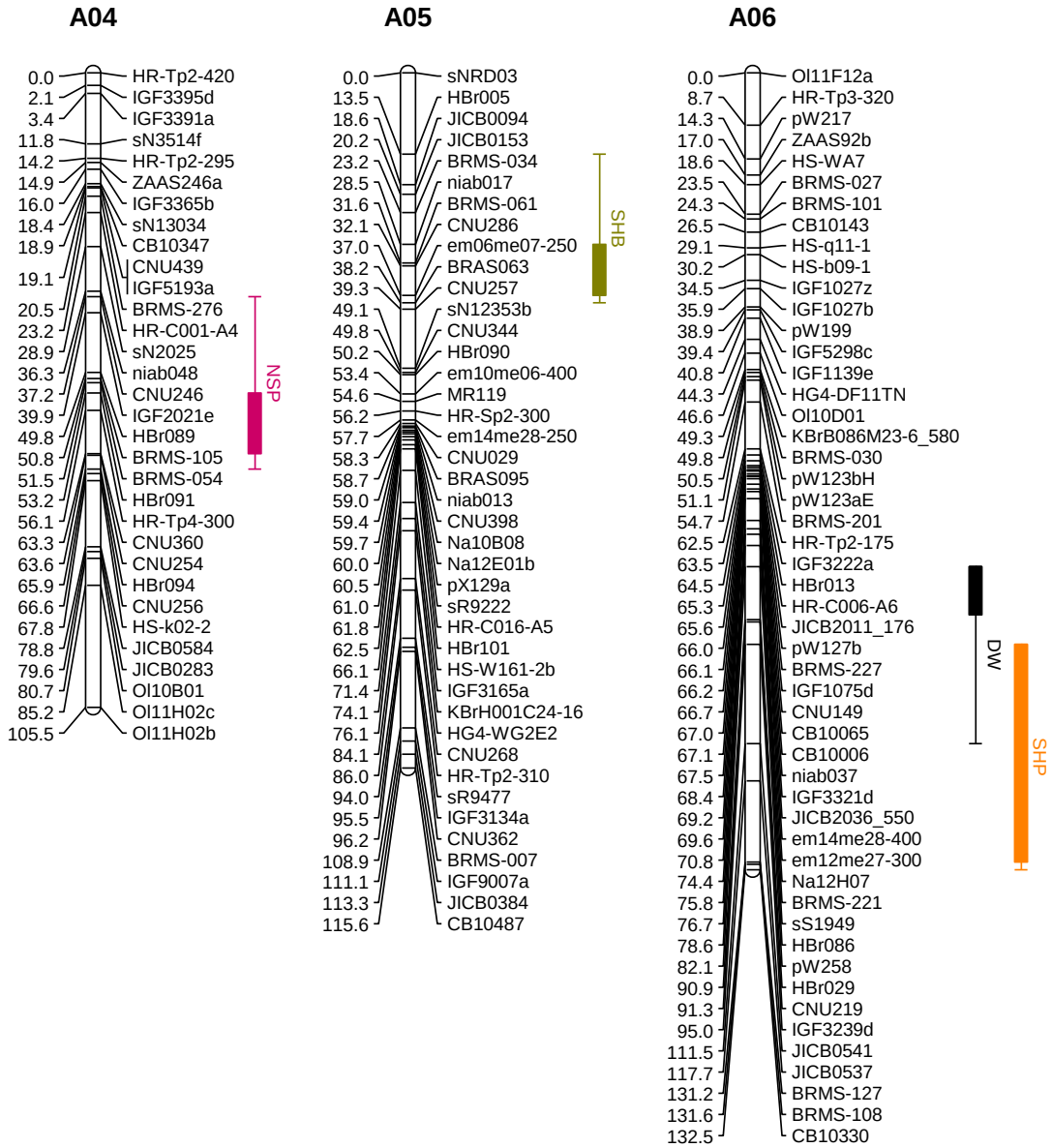

Figure 5.7 The linkage map for three linkage groups (A04, 05 and 06) depicts the detected QTLs.

LG description as for Figure 5.6. The QTLs associated with traits NSP, SHB, SHP (stem height to the first pod) and DW (dried weight).

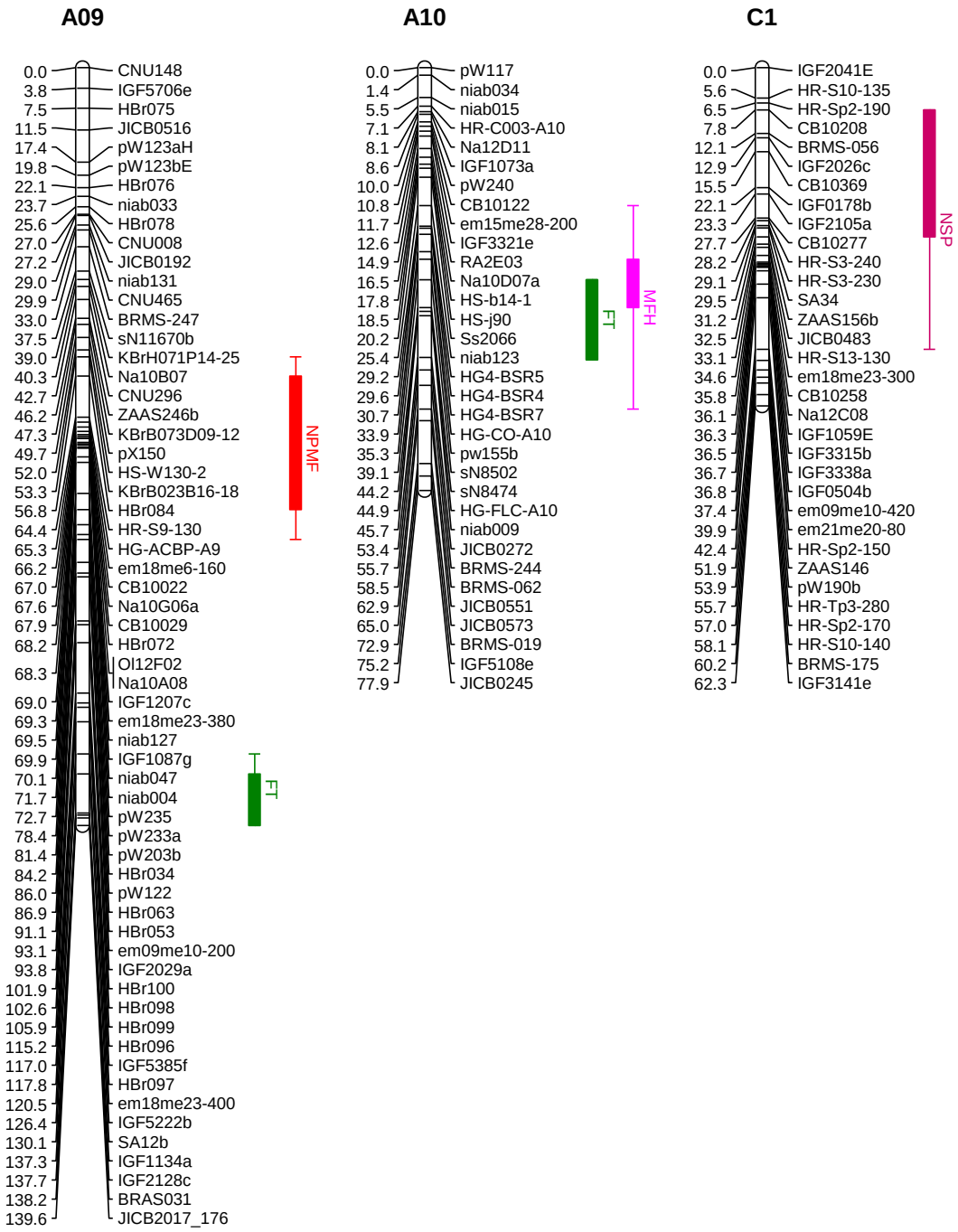

Figure 5.8 The linkage map for three linkage groups (A09, 10 and C1) depicts the identified QTLs.

LG description as for Figure 5.6. The QTLs associated with traits FT, NPMF, NSP and MFH (the length of main inflorescence).

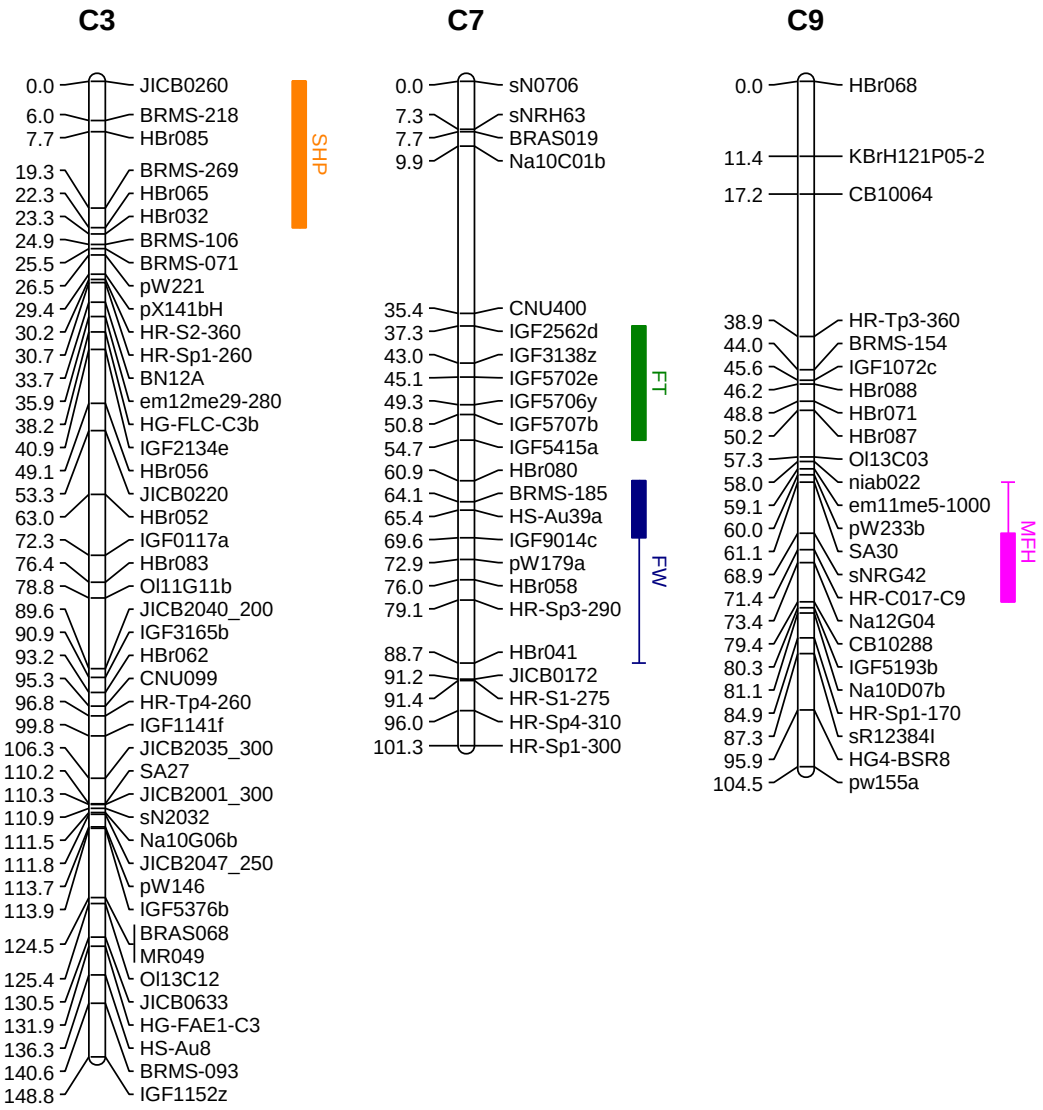

Figure 5.9 The linkage map for three linkage groups (C3, 7 and 9) depicts the identified QTLs.

LG description as for Figure 5.6. The QTLs associated with traits SHP, FT, MFH and FW (fresh weight).

In contrast to SHB, stem height to the first pod (SHP) was associated with two different QTLs on different LGs A06 (Figure 5.7) and C3 (Figure 5.9) with their additive genetic effect, interestingly, was influenced by Ningyou 7. Two QTL were detected affecting the length of the main inflorescence (MFH) on different LG A10

(Figure 5.8) and C9 (Figure 5.9), explained 15.3 and 11.8 % of the trait variation, respectively. A single QTL was found to be associated with each of the number of branches (NB) on LG A02 (Figure 5.6), fresh weight (FW) on LG C7 (Figure 5.9) and dry weight (DW) on LG A06 (Figure 5.7), accounted for 11.2 – 11.7 % of the phenotypic variation. Nevertheless, four phenotypic traits were not associated with any QTL regions are, pods number on branches (NPB), total pods number (TNP), plant height (PH) and lateral main stem (LS).

5.4.3 Quantitative analysis of proteins of interest

The 32 previously proteins identified, divided into four groups Table 5.1 (page 181), were subjected to the targeted proteomic quantitative analysis using Selected Reaction Monitoring (SRM) experiment as described previously in Section 5.3.4 (page 185), mediated by Skyline software and an external tool, MSstats. This quantitative analysis was performed on ten segregating TNDH lines and the two parents. In a comparison between the parental lines, the 32 proteins were expressed differently. Using the un-normalised data 12 proteins were found to be up-regulated in Tapidor DH compared to Ningyou 7 while the rest showed no difference between them (Figure 5.10). However, after normalisation to the housekeeping protein Glyceraldehyde-3-phospate dehydrogenase (GAPDH, Bo8g065470), 26 proteins were found to be up-regulated in Tapidor DH compared to Ningyou 7 (Figure 5.11). Of these nine were previously identified as putative VSPs such as trypsin inhibitor, Water-soluble chlorophyll protein and protein of unknown function. Three out of four high-affinity nitrate transporters family were also up-regulated; Bo8g065100.1, Bo59008780.1 and Bo2g012010.1 (Figure 5.11).

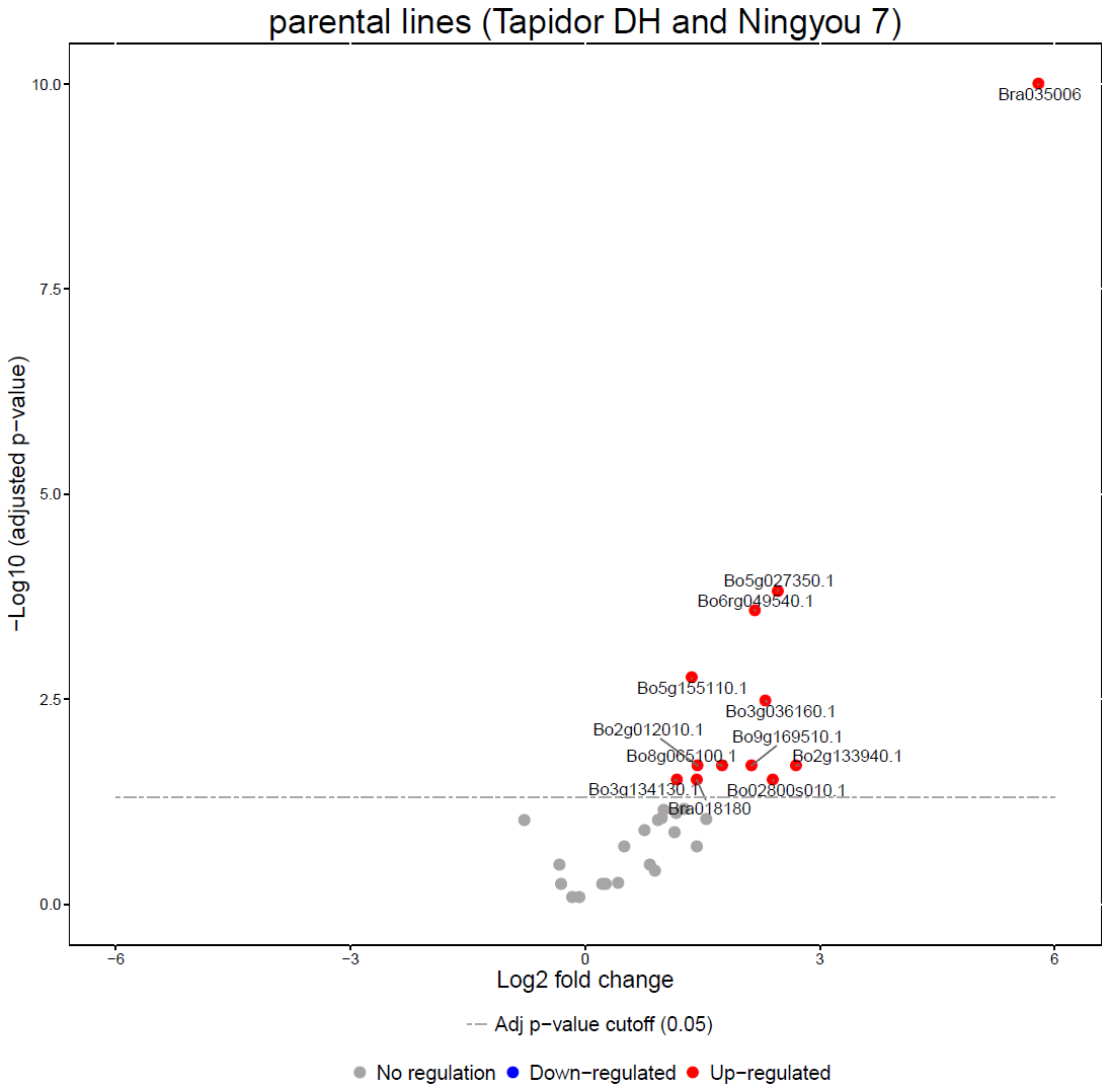

Figure 5.10 Protein expression pattern without normalisation.

The relative expression levels of 32 proteins (listed in Table 5.1 page 181) were compared between Tapidor DH and Ningyou 7. 12 were up-regulated in Tapidor DH without normalisation to any of the housekeeping proteins. The Figure was generated using MSstats group comparison function. The horizontal axis represents the log2 of the fold change in the intensity of proteins. The vertical axis represents the -log10 of adjusted P value. Dashed line indicates threshold of adjusted P value (0.05). Red circles indicate up-regulated expression of proteins.

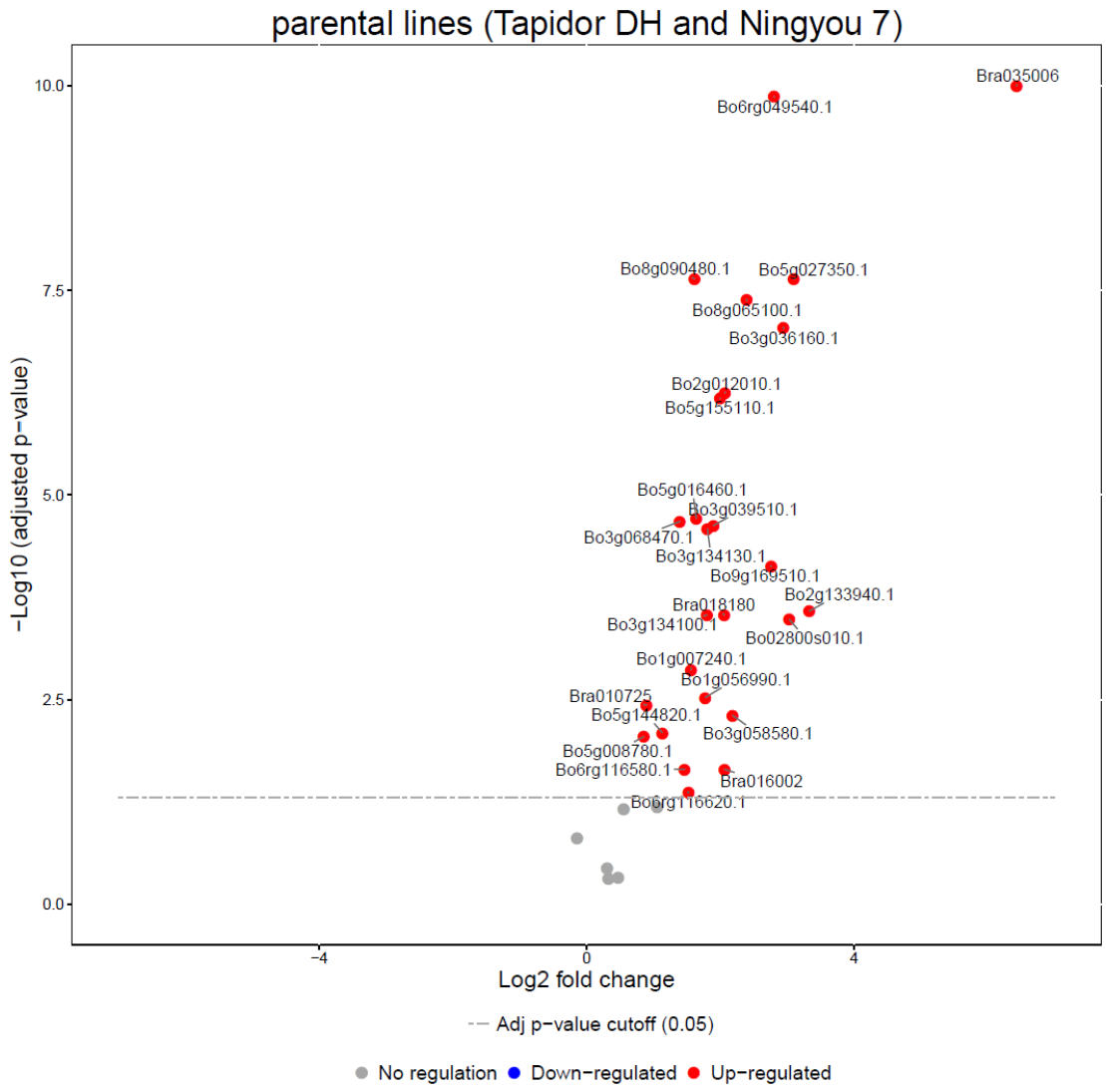

Figure 5.11 Protein expression pattern with normalisation to GAPDH.

26 proteins were up-regulated in Tapidor DH in comparison to Ningyou 7. Of these nine were previously identified as putative VSPs (22 and 23 kDa in Tapidor DH) such as Bo02800s010.1 (water soluble chlorophyll protein), and Bo6rg116580.1 and Bra016002 (trypsin inhibitors). Three HANTs, Bo8g065100.1, Bo59008780.1 and Bo2g012010.1. The full list of proteins and accessions number in (Table 5.1 page 181).

The ten lines selected to optimise the quantitative method (SRM experiment) a range of variation in comparison to the parental lines when the expression normalised to housekeeping proteins such as GAPDH. For example, the protein of unknown function

DUF640 (Bo3g036160.1) which previously found to be a putative VSP, showed differential expression between the parental lines as well as between the 10 analysed lines of the segregating population Figure 5.12.

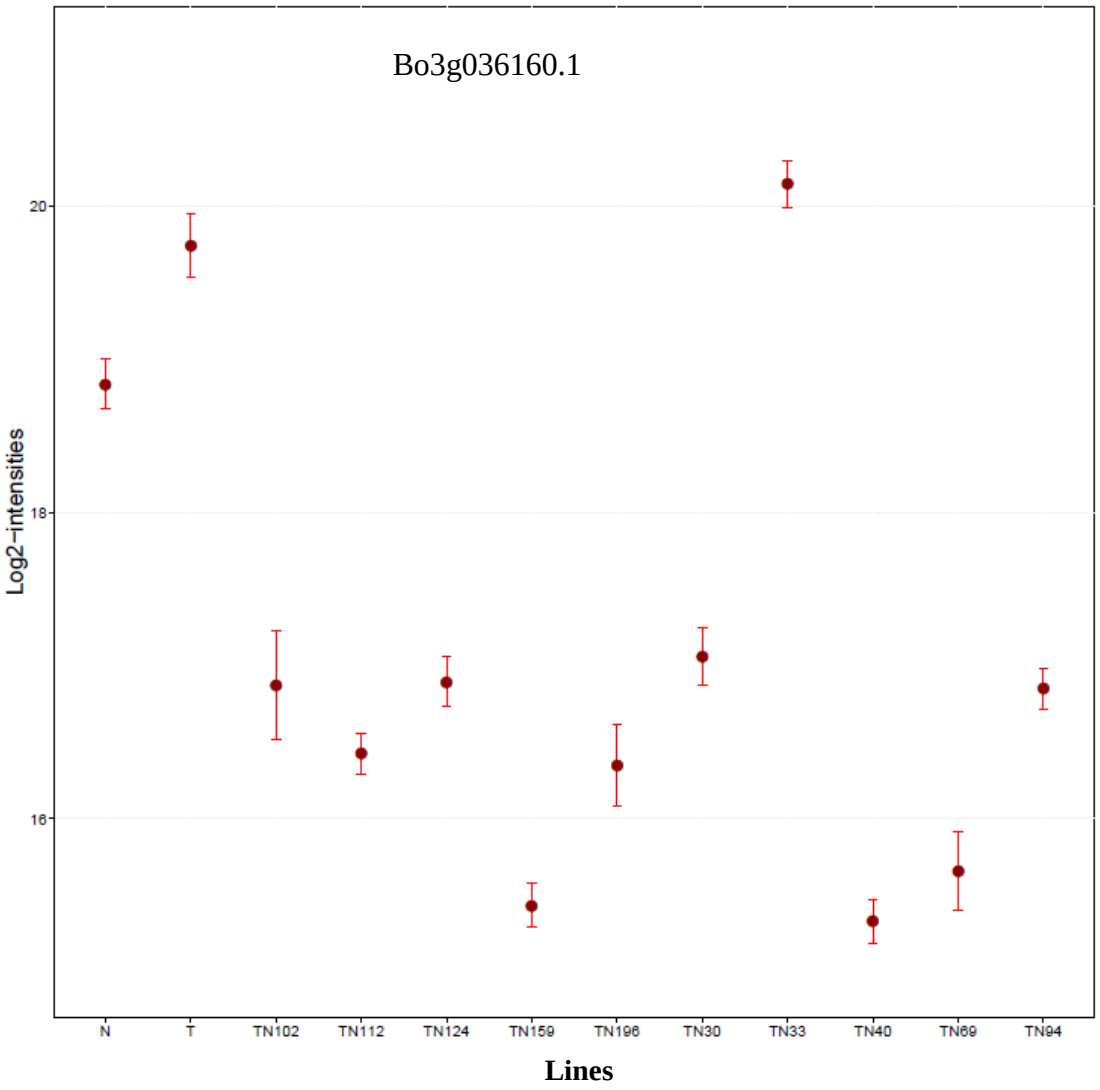

Figure 5.12 The expression pattern of the unknown function protein in ten lines of the TNDH population with the parental lines.

Variation in the expression of the unknown function protein between ten lines of the TNDH mapping population with the parental lines (Ningyou 7, N and Tapidor DH, T). The vertical axis represents the log2 of the protein intensity. Data represent the mean value of each line with error bars representing confidence interval at 95 % significant level.

Another interesting example is the expression pattern of indole-3-acetonitrile nitrilase NIT2 (Bra035006) Figure 5.13, which was previously identified in Tapidor DH and not in Ningyou 7. The quantitative analysis shows a substantial difference between the two parents and also between the ten TNDH lines.

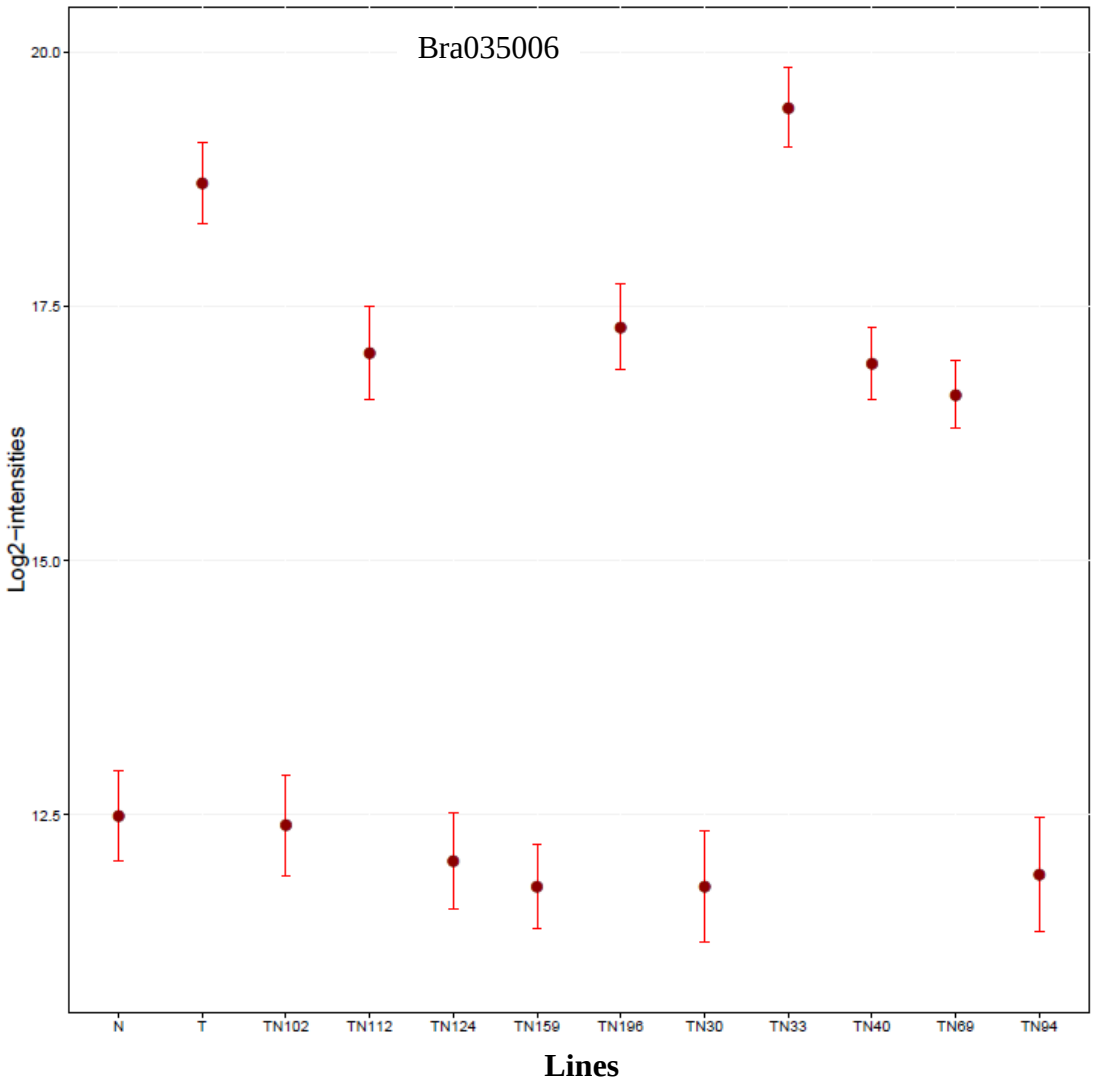

Figure 5.13 The expression pattern of NIT2 in ten lines of the TNDH population with its parental lines.

The expression was normalised against GAPDH. Figures show significant variation between the parents and the ten lines. Data are the mean value of the log2 of the intensity with error bars representing 95 % confidence interval.

5.5 Discussion

The aim of the study was to identify genetic loci associated with N remobilisation and architectural and yield related traits. 32 proteins listed in Table 5.1, were selected for further quantification analysis based on in-gel protein identification and differences between whole proteomic profiles of the parental line of the TNDH population in Stem B (chapter 4). Of these 32, 12 proteins had similarity to a putative 23 kDa VSP, 11 proteins showed contrasting expression in the whole proteomic profile of the parental genotypes, four appeared to be putative members of the nitrate transporter family, and five represented well-known housekeeping proteins that showed consistent expression within the proteomic profile of both genotypes. However, due to the time-consuming quantitative analysis of the proteomic-based experiment directly related to optimising a reliable quantitative method, in addition, unpredictable issues experiencing instrumental instability of obtaining quality data, the proteomic quantitative analysis has only been completed for ten lines of the TNDH population randomly selected and the two parental lines

Variation in the expression pattern of most of these proteins was reported among the 12 studied genotypes. The unknown function protein Bo3g036160.1, for example, is one of the putative proteins for VSP that was upregulated in Tapidor DH in comparison with Ningyou 7 when normalised to GAPDH (Bo8g065470.1, Bra016729), a key enzyme in glycolysis pathway (Sirover, 2011) and one of the most widely used reference proteins used in comparisons of protein and gene expression data (Barber *et al.*, 2005). Bo3g036160.1showed a pattern that was consistent with a presence or absence phenotype, in the parents in Ningyou 7 it is absent, while it was

expressed, in Tapidor DH, and in the offspring the same pattern is observed as shown in Figure 5.12.

In comparison, the NIT2 protein (Bra035006) which had only been found to be expressed in Tapidor DH,(section 4.3.3) was found in five lines that also showed a similar expressed pattern with just one line exceed the expression of Tapidor DH.

This is a novel approach using proteomics to map proteins as quantitative traits in a segregating population, is referred to as pQTL and was first used in the study by Wu *et al.* (2013) to identify genomic regions associated with protein expression level within lymphoblastic cell lines in human. The strength of the technique is the identification of genes that underlying newly detected QTL which is considered a major challenge after QTL detection. Using LC-MS/MS technique to measure an array of proteins abundance and the difference in their expression within segregation population which then can be correlated with the genomic variation through the methods of QTL analysis. The primary challenge underlying pQTL is establishing reliable quantification method to determine proteins abundance level. Targeted proteomic such as selected monitored reaction, SRM, is a promising technique which could be used to help optimise this approach.

Regarding to the architectural and yield rated traits, a total of 21 QTL were identified associated with nine morphological traits. This relatively high number of detected QTL contributes to our understanding of the multiple genetic effects controlling such traits. Flowering time (FT) is a key physiological trait known to be highly associated with plant growth, and yield related traits (Diepenbrock, 2000). One of the main strategies to increase yield is to bring FT forward, thus expanding the seed

determination period during which seed number is defined (Berry and Spink, 2006). A major gene controlling differences in FT in *B. rapa* was identified to be loci of *Flowering Locus C* (*FLC)* (Long *et al.*, 2007). This gene was first shown to be a key regulator of the vernalisation pathway in Arabidopsis (Sheldon *et al.*, 2000). A gene controlling flowering time in *B. oleracea* was also identified as *BoFLC2* (Okazaki *et al.*, 2006). Six QTL were detected in this study associated with FT. The major FT QTL was identified on the LG A10 which was localised to the HG-FLC-A10 marker. This is known to be a well-known FL gene regulating response to vernalisation was previously mapped to be a major locus affecting FT in *B. napus* using the TNDH population grown under field conditions and several environments (Long *et al.*, 2007). Interestingly, this QTL was found to overlap with a QTL identified to be associated with the length of the main inflorescence (MFH) which be explained by the later the FT occurs the shorter the main inflorescence. This was supported by the negative correlation (r =-0.51, p >0.000) that was found between these two phenotypic traits. In total, two QTL were identified for the MFH in agreement with three QTL previously identified (Yi *et al.*, 2006) and eight identified by Chen *et al.* (2007).

One identified QTL affecting the number of branches (NB) on LG A02, is in agreement with Yi *et al.* (2006) who identified two QTL to be related with NB and also with Chen *et al.* (2007) whom reported six QTL to be associated with NB on different LG. Interestingly, this QTL co-localised with the FT-related QTL which might be explained by the fact that delayed flowering promotes a greater canopy accumulated more nutrients could be used to grow more branches. However, no correlation was found between the two phenotypic traits. Three QTL were identified in this study associated with number of pods on the main inflorescence (NPMF) and

seeds number per pod (NSP). One for each of them were localised on the same LG A03 and the other two were localised on different LG. In comparison, QTLs related to NSP were previously identified on chromosome A03 (Ding *et al.*, 2012; Shi *et al.*, 2013b) and C1 (Radoev *et al.*, 2008; Shi *et al.*, 2013b) consistent with the present study. A novel QTL for NSP located on chromosome A04 were mapped in the present study. A number of loci associated with number of pods were previously mapped on chromosome A03 in several studies (Shi *et al.*, 2009; Ding *et al.*, 2012; Shi *et al.*, 2015) and on chromosome A09 (Radoev *et al.*, 2008; Shi *et al.*, 2013b) in agreement with the present study. Recently, Shi *et al.* (2015) detected two novel QTLs associated with number of pods and NSP co-localised on chromosome A06. Further fine mapped to a 180 kb genomic region contained 33 annotated genes. It was concluded that the co-localisation between these two QTL was not due to pleiotropic effect, but to tight linkage.

In this study, four phenotypic traits were not affected by QTLs reigns are, PH, NPB, TNP and LS. The reason could be directly related the size of the population used in this study, 120 lines, grown under this specific environment which influence the power of the statistical analysis and thus it could significantly affect the power of QTL detection as reported by a number of reports (Jansen and Stam, 1994; Kearsey and Farquhar, 1998; Asíns, 2002; Collard *et al.*, 2005; Vreugdenhil *et al.*, 2005; Druka *et al.*, 2010). 22 lines of the TNDH populations were observed to possess more than one main stem which is the case with the parental line, Tapidor DH, whereas the rest possessed one main stem as it is the case with Ningyou 7. It was found, under this small size of population, that this trait might follow Mendelian inheritance (X^2 =2.98, P >0.05).

It is known that plant height is one of the most determining traits associated with plant architecture. However, it is also an important traits associated with yield (Wang *et al.*, 2015). No QTL regions were detected associated with plant height (PH) and total number of pods (TNP). Nevertheless, a number of previous studies detected QTLs associated with these traits such as Yi *et al.* (2006) whom reported three QTLs associated with PH and one associated with TNP suing DH population (Zhongyou 821 X Bao 604) grown under field condition, Chen *et al.* (2007) who detected five QTL regions associated with PH using 258 lines of a DH population grown in the field, Wang *et al.* (2015) reported 20 QTL associated with PH at harvest and different QTL were detected at different growth stages using 348 lines of a DH population, named KNDH, grown under field condition.

The novel approach discussed above and the preliminary results that were obtained shows how a combination of protein detection with genomic knowledge could be used to map traits which have so far been largely ignored due to their complexity.

Chapter 6 General Discussion and Future Work

6.1 General discussion

The aim of this thesis was to elucidate the pathways underlying both mineral nutrient accumulation and remobilisation during different growth stages/conditions in *B. napus*. It is believe that this will increase the capacity to breed for improved nutrient use efficiency and hence improve the economics of its production. Understanding the breadth of the natural variation in minerals use among various *B. napus* genotypes under limiting minerals environment is thus an important objective. This was achieved by quantifying mineral nutrient composition including seven macronutrients (N, P, K, Mg, Ca, S and Na) and five micronutrients (B, Cu, Fe, Mn and Zn) within seven plant tissue types from three different plant organs; root, stem and seeds. Mineral concentrations were determined at two growth stages (GS 6.2/6.3 and maturity) from a diverse set of *B. napus*; 14 at GS 6.2/6.3 and 30 at maturity, field-grown under limited nutrients availability without fertiliser application (Hopkins *et al.*, 2010-2011).

In Chapters 2 and 3, the composition of minerals was shown to vary between the plant organs of the root, stem and seeds in *B. napus*, this is in agreement with Thomas *et al.* (2016) whom reported differences between leaf and seeds, as did Baxter *et al.* (2012) whom reported differences between root and leaf in *A. thaliana*. Additionally, the present study has illustrated the importance of analysing all tissues of the plant given the significance differences found between mineral accumulations between a number of tissues from the same organ of the plant. For instance, lateral roots appeared to act as a significant reservoir of accumulated minerals in the root system, while the taproot did not show the same levels of accumulation. In addition, the bottom of the stem differed significantly from other sections of the stem. As shown in chapter two and three significant differences in N, P, K, Ca and Mn concentrations within Stem B were

observed at GS 6.2/6.3. The Ca and P concentrations in Stem B were found to be 15- and 6-fold greater than Stem T, respectively. In contrast, Mn and K concentrations in Stem B were found to be 19- and 7.6-fold lower than Stem T, respectively. These results can suggest that mineral accumulation and translocation in the plant are subject to complex regulation mechanisms and differ between tissue types according to its importance. Furthermore, the accumulation pattern of mineral nutrients differed between growth stages. For example, root N concentration increased from GS 6.2/6.3 to maturity, while it was decreased in the stem. A reduction of 18-fold in [Ca] and 9-fold in [P] at maturity compared to GS 6.2/63 was observed in Stem B. In contrast, Mn and K concentrations increased significantly at harvest to *ca.* 25- and 10-fold, respectively, compared to GS 6.2/6.3.

A significant amount of mineral elements were found to remain in both the stem and root tissues at harvest of all plants. However this differed between the lines examined, which in turn, highlights the inefficient mechanisms utilised by *B. napus* plants to redistribute and move mineral nutrients such as N (Gombert *et al.*, 2010), P, K (Rose *et al.*, 2007) and S (McGrath and Zhao, 1996). These mineral nutrients are those most in demand during OSR plant growth and development and need to be added as mineral-based fertilisers according to Fertiliser Manual RB209 (Defra, 2010). The cost of this represents 60 % of the total variable costs associated with OSR production (Weightman *et al.*, 2010). Reducing the amount of minerals remaining in the plant tissues after harvest could therefore increase mineral use efficiency. For example, reducing N concentration from 0.438 %DW in Ningyou 7 to 0.046 %DW in genotype Best of All reduced the amount of residual N in Stem B from 8.76 to 0.92 kg N/ha.

Likewise, reducing K concentration 2.7 %DW in Tapidor DH to 0.53 %DW in cultivar Yudal will reduce the residual K in Stem B from 47 to 9 kg K/ha.

A large range of variation in all mineral elements concentration was observed (Chapter 2 and 3), across all the lines and the seven analysed tissues at both growth stages. At maturity, for example, L.root varied from ca. 3.2-fold for N to 10.7-fold for K, T.root B varied from ca. 2.8-fold for Cu to 18-fold for K, T.root B varied ca. 3.4-fold for B to 16-fold for K, Stem B varied from approximately 1.5-fold for Ca to 15-fold for Na, Stem M from 1.8-fold for Ca to 18.6-fold for Na, Stem T from 2.3-fold for Ca to 20-fold for Na, and seeds varied from 1.54-fold for Mg and Mn to 5.2-fold for S. Genotypic variation in mineral composition has been reported previously in *B. napus* within the leaf and seeds (Thomas *et al.*, 2016) and shoot (Bus *et al.*, 2014), in *B. oleracea* (C genome) within shoot (Broadley *et al.*, 2008; White *et al.*, 2010), in *B. rapa* (A genome) within shoot (Wu *et al.*, 2007; Wu *et al.*, 2008). The genotypic differences could be used by genome-wide association analysis to identify genomic regions that could be later exploited to breed crops with either low or high content of a mineral element dependent on its utilisation. Such findings are of great importance, in particular, if we are to continue to reduce the inputs required for optimal plant growth and to enhance sustainability of crop production. Such work could be enhanced through developing further genetic mapping populations, for instance, Ningyou 7 x Temple or Winner x NK Bravour, that could result in further segregation of genes that underline N and P remobilisation and use efficiency, respectively, thus allowing us to identify the genes involved which would lead to identification of the best allelic combinations required in order for the development of new highly N and P efficient genotypes with high seed yields grown on limited N and other minerals environment.

In Chapters 2 and 3, the relationships between mineral elements concentration were evaluated within and between tissues. Numerus pair-wise associations were found within tissue, many of them were previously reported in *B. napus* (Liu *et al.*, 2009a; Ding *et al.*, 2010; Bus *et al.*, 2014; Thomas *et al.*, 2016) and other plant species such as *B. oleracea* (Broadley *et al.*, 2008) and *A. thaliana* (Baxter *et al.*, 2012), in addition novel relationships were also detected. Furthermore, various relationships were observed between plant organs with the strongest correlation found in B, Cu and Zn concentration between all root and stem tissues. However, these relationship between minerals were found to be tissue-specific, for example, S/Ca, S/Mg and Mg/P were strongly associated only within roots and Stem T. Ca and Mg were correlated strongly in the stem but not in the seed at maturity. Moreover, these relationships were growth stage-specific, for instance, Ca and Mn correlated significantly within roots only at maturity. These findings suggest that minerals accumulation and translocation are regulated either completely or at least partly by independent mechanisms, or are under pleiotropic effects as were previously demonstrated (Liu *et al.*, 2009a; Buescher *et al.*, 2010).

Many previous studies showed that improvement in N use efficiency has been a major target for plant breeders for the last two decades (Bouchet *et al.*, 2016). Different strategies have been suggested by the findings shown here that suggest improving N remobilisation within OSR plants should be a major goal. A significant source of N is that stored within proteins. In Chapter 4, putative vegetative storage proteins, VSPs, were identified and we have suggested that these could be associated with N remobilisation. Using LC-MS/MS techniques for protein identification, it was found that trypsin inhibitor was one of the main dominant proteins identified as a putative

23 kDa VSP. Previous studies showed that the *L. chinensis* 22 kDa *LcVSP1* (Tian *et al.*, 2007) and the *S. mukorassi* 23 kDa VSP (Liu *et al.*, 2009b), possessed trypsin inhibitor activity. Furthermore, water-soluble chlorophyll protein was also identified as a putative 22 kDa VSP. This was found previously to be involved in N remobilisation within young leaves in B. napus under N deficiency and to possess protease inhibition activity (Desclos *et al.*, 2008; Avice and Etienne, 2014). Several other proteins were shown to be accumulated significantly in the top part of the plants, particularly in the senescing siliques walls and the stem adjacent to them. These proteins were identified bioinformatically as putative seed storage proteins in the pod walls and beta-1, 3-glucanase in the stem. Interestingly, it was previously showed that seed storage proteins were overexpressed in the senescing pod walls of *A. thaliana* (Wagstaff *et al.*, 2009). It was also recently shown by Koeslin-Findeklee and Horst (2016) that pod walls had 26 % of the total shoot N at maturity. Since sufficient amount of N were remobilised to the seed during development, the increased accumulation of these proteins would clearly elucidate the inefficiency of OSR in utilising N, which has been supported by numerous previous reports such as Rossato *et al.* (2001) and Schjoerring *et al.* (1995).

In Chapter 5, the number of QTLs that have been identified associated with architectural and yield related morphological traits showed an appropriate strategy was deployed. However the problems with the proteomics highlights the difficulties that still exist of measuring proteins in a quantifiable manor (Liebler and Zimmerman, 2013). Developing screening strategy through which quantitative analysis could be performed on a proteomic based experiment would doubtlessly be an important strategy to identify protein QTL (pQTL) regions associate with N remobilisation and

utilisation in plants (Wu *et al.*, 2013). The results show that an appropriate method has been developed but time constraints prevented the whole mapping population from being analysed. This was frustrating and yet highlights the problems that can be encountered. Further work suggested below indicates the steps which might yet lead to the development of enhanced breeding material which will enable more sustainable production of oilseed rape in the future. Such developments will lead to significant benefits both economically and socially worldwide as this should lead to increased crop yields while requiring lower crop inputs.

6.2 Future work

It was not possible to partition the amount of variation observed in the present study between the genetic and environmental variation since the plant materials collected for this study were from one replicate. Therefore, further plant materials (the whole plant) were collected at harvest in July 2014 from 12 *B. napus* L. genotypes grown under low N application (without N fertiliser) form the 2013/2014 OREGIN field trial. Four plants from each variety was collected from two blocks (a total of 48 plants from each block). Plants were separated into numerous sections; roots, stem, siliques walls and seeds, and grounded to fine powder. By further analysing these OSR plant materials, further understanding of the breadth of the genetic variation underlines mineral use under different environments will be obtained. Different approaches could be applied to analyse the component of variance in theses unbalanced data such as restricted/residual maximum likelihood, REML (Harville, 1977), which produces unbiased estimate of the variance components.

Moreover, further studies need to be carried out to explore regulation pathways underlying the accumulation of VSPs, and to address the increased accumulation of seed storage proteins during senescence. For example, investigations into the effect of different variables such as air temperature, soil minerals availability - particularly N, water deficiency and factors that influence N source sink relationship, on the accumulation of these proteins need to be carried out. In addition further characterisation of the VSPs by means of immunoelectophoresis and to study the activity of proteinase inhibitor of the purified VSPs *in vitro* is required. In addition to both phenotyping and proteomic developments it is envisaged that a further direction would be through further use of modern molecular techniques. For example the use of Quantitative Real Time PCR, QRT-PCR (Livak and Schmittgen, 2001) could be used to look at the change in gene expression encoding the proteins which were identified as putative storage proteins.

Several QTLs related to architecture and yield related traits were mapped in the present study, the identification of the genes underlying these detected QTLs will provide a better understanding of pathways regulate such traits in *B. napus*. This will be the first step towards fine mapping analysis to identify candidate genes (Kearsey and Farquhar, 1998). Further, markers associated with these identified genomic regions can be useful for Marker Assisted Selection, MAS programs (Collard and Mackill, 2008). This can be linked to comparative genomic approaches utilising the synteny between *B. napus* and *A. thaliana*. This aids in gene discovery in order to develop genotypes with the desired agronomical traits. In addition, Backcross strategies can be applied to refine the size of the mapped QTL interval through which the identification of such candidate genes will be accelerated.

Performing proteomic based experiment would doubtlessly be an important strategy to identify pQTLs associate with N utilisation in plants. Therefore, it is important to continue analysing the remaining TNDH mapping population and quantify the amount of putative VSPs to be able to map and thus identify potential QTLs associated with N remobilisation. The identified pQTLs would be very useful approach to directly identify markers associated with these QTLs, and thus can be utilised in MAS breeding programs for further analysis to develop genotypes with the desired traits. Using different approaches to refine the interval underlying these QTLs would be of great importance for candidate genes identification. Providing the necessary funding, this would also allow determining minerals concentration in the bottom of the stem at two growth stages; at flowering and after 45 days after flowering, by which QTLs associated with minerals accumulation would be identified.

It would also be useful to carry out full transcriptomics experiments using Next Generation Sequencing, NGS (McKenna *et al.*, 2010) approaches which have been developed recently to elucidate differences in the metabolic pathways involved in the transportation of minerals within the plants. This could be done through studying closely related TNDH lines which indicate significant differences in their N transport as measured in the results shown. Further scientific breakthroughs in the methodologies used to measure metabolomics, proteomics and genomics will undoubtedly allow such studies to be completed in far more depth than I have been able to. The requirement for accurate phenotyping is however always going to be a key tool in plant breeding approaches.

References

Abdallah, M., Dubousset, L., Meuriot, F., Etienne, P., Avice, J.-C., and Ourry, A. (2010). Effect of mineral sulphur availability on nitrogen and sulphur uptake and remobilization during the vegetative growth of *Brassica napus* L. *Journal of Experimental Botany* **61,** 2635-2646.

Addona, T. A., Abbatiello, S. E., Schilling, B., Skates, S. J., Mani, D. R., Bunk, D. M., Spiegelman, C. H., Zimmerman, L. J., Ham, A.-J. L., Keshishian, H., Hall, S. C., Allen, S., Blackman, R. K., Borchers, C. H., Buck, C., Cardasis, H. L., Cusack, M. P., Dodder, N. G., Gibson, B. W., Held, J. M., *et al.* (2009). Multi-site assessment of the precision and reproducibility of multiple reaction monitoring–based measurements of proteins in plasma. *Nature Biotechnology* **27,** 633-641.

Aebersold, R., and Mann, M. (2003). Mass spectrometry-based proteomics. *Nature* **422,** 198-207.

AHDB. (2017). Agriculture and Horticulture Development Board (AHDB) Recommended Lists for cereals and oilseeds (2017/2018). ([https://cereals.ahdb.org.uk/media/800462/ahdb-recommended-list-web.pdf] Accessed 18 June 2017.

Akhtar, M. S., Oki, Y., and Adachi, T. (2008). Genetic Variability in Phosphorus Acquisition and Utilization Efficiency from Sparingly Soluble P-Sources by Brassica Cultivars under P-Stress Environment. *Journal of Agronomy and Crop Science* **194,** 380-392.

Anderson, N. G., and Anderson, N. L. (1996). Twenty years of two-dimensional electrophoresis: Past, present and future. *Electrophoresis* **17,** 443-453.

ArifUzZaman, M., Mamidi, S., McClean, P., and Rahman, M. (2016). QTL mapping for root vigor and days to flowering in *Brassica napus* L. *Canadian Journal of Plant Science* **97,** 99-109.

Armengaud, P., Sulpice, R., Miller, A. J., Stitt, M., Amtmann, A., and Gibon, Y. (2009). Multilevel analysis of primary metabolism provides new insights into the role of potassium nutrition for glycolysis and nitrogen assimilation in arabidopsis roots1[W][OA]. *Plant Physiology* **150,** 772-785.

Arora, S. K., and Luchra, Y. P. (1970). Metabolism of Sulphur Containing Amino Acids in Phaseolus Aureus Linn. *Zeitschrift für Pflanzenernährung und Bodenkunde* **126,** 151-158.

Asíns, M. J. (2002). Present and future of quantitative trait locus analysis in plant breeding. *Plant Breeding* **121,** 281-291.

Avice, J.-C., and Etienne, P. (2014). Leaf senescence and nitrogen remobilization efficiency in oilseed rape (*Brassica napus* L.). *Journal of Experimental Botany* **65,** 3813-3824.

Avice, J. C., Dily, F. L., Goulas, E., Noquet, C., Meuriot, F., Volenec, J. J., Cunningham, S. M., Sors, T. G., Dhont, C., Castonguay, Y., Nadeau, P., Bélanger, G., Chalifour, F. P., and Ourry, A. (2003). Vegetative storage proteins in overwintering storage organs of forage legumes: roles and regulation. *Canadian Journal of Botany* **81,** 1198-1212.

Baines, D. (2001). Analysis of purity. In *Protein purification techniques : a practical approach*, 2nd ed., S. Roe, ed (New York, US: Oxford University Press), pp. 27-49.

Balint, T., and Rengel, Z. (2008). Nitrogen efficiency of canola genotypes varies between vegetative stage and grain maturity. *Euphytica* **164,** 421-432.

Banerjee, S., and Mazumdar, S. (2012). Electrospray Ionization Mass Spectrometry: A Technique to Access the Information beyond the Molecular Weight of the Analyte. *International Journal of Analytical Chemistry* **2012,** 40.

Barber, R. D., Harmer, D. W., Coleman, R. A., and Clark, B. J. (2005). GAPDH as a housekeeping gene: analysis of GAPDH mRNA expression in a panel of 72 human tissues. *Physiological Genomics* **21,** 389-395.

Barker, A. V., and Pilbeam, D. J. (2007). *Handbook of Plant Nutrition*. (Boca Raton, FL: CRC Press/Taylor & Francis).

Baxter, I., Hermans, C., Lahner, B., Yakubova, E., Tikhonova, M., Verbruggen, N., Chao, D.-Y., and Salt, D. E. (2012). Biodiversity of mineral nutrient and trace element accumulation in Arabidopsis thaliana. *PLoS One* **7,** e35121.

Berger, S., Bell, E., Sadka, A., and Mullet, J. E. (1995). Arabidopsis thaliana Atvsp is homologous to soybean VspA and VspB, genes encoding vegetative storage protein acid phosphatases, and is regulated similarly by methyl jasmonate, wounding, sugars, light and phosphate. *Plant Molecular Biology* **27,** 933-942.

Berry, P., Teakle, G., Foulkes, J., White, P., and Spink, J. (2010a). Breeding for improved nitrogen use efficiency in oilseed rape. (International Society for Horticultural Science (ISHS), Leuven, Belgium), pp. 97-102

Berry, P., Cook, S., Ellis, S., Gladders, P., and Roques, S. (2014). Oilseed rape guide. (ADAS: HGCA) Accessed 14 April 2017.

Berry, P., White, C., Carvalho, P., Foulkes, J., Teakle, G., Jennaway, R., Bowman, J., Nightingale, M., Padbury, N., White, P., Seymour, J., Grundy, A., McVittie, J., Saunders, B., Waterhouse, S., and Roques, S. (2011). Breeding oilseed rape with a low requirement for fertiliser N.

Berry, P. M., and Spink, J. H. (2006). A physiological analysis of oilseed rape yields: Past and future. *The Journal of Agricultural Science* **144,** 381-392.

Berry, P. M., Spink, J., Foulkes, M. J., and White, P. J. (2010b). The physiological basis of genotypic differences in nitrogen use efficiency in oilseed rape (*Brassica napus* L.). *Field Crops Research* **119,** 365-373.

Blakesley, R. W., and Boezi, J. A. (1977). A new staining technique for proteins in polyacrylamide gels using Coomassie Brilliant Blue G250. *Analytical Biochemistry* **82,** 580-582.

Boja, E. S., and Rodriguez, H. (2011). The Path to Clinical Proteomics Research: Integration of Proteomics, Genomics, Clinical Laboratory and Regulatory Science. *The Korean Journal of Laboratory Medicine* **31,** 61-71.

Bouchet, A.-S., Laperche, A., Bissuel-Belaygue, C., Snowdon, R., Nesi, N., and Stahl, A. (2016). Nitrogen use efficiency in rapeseed. A review. *Agronomy for Sustainable Development* **36,** 38.

Bouchet, A.-S., Nesi, N., Bissuel, C., Bregeon, M., Lariepe, A., Navier, H., Ribière, N., Orsel, M., Grezes-Besset, B., Renard, M., and Laperche, A. (2014). Genetic control of yield and yield components in winter oilseed rape (*Brassica napus* L.) grown under nitrogen limitation. *Euphytica* **199,** 183-205.

Bradstreet, R. B. (1965). *The Kjeldahl method for organic nitrogen*. (London, UK: Academic Press).

Brennan, R. F., and Bolland, M. D. A. (2015). Manganese Deficiency in Canola Induced by Liming to Ameliorate Soil Acidity. *Journal of Plant Nutrition* **38,** 886-903.

Broadley, M. R., White, P. J., Hammond, J. P., Zelko, I., and Lux, A. (2007). Zinc in plants. *New Phytologist* **173,** 677-702.

Broadley, M. R., Bowen, H. C., Cotterill, H. L., Hammond, J. P., Meacham, M. C., Mead, A., and White, P. J. (2003). Variation in the shoot calcium content of angiosperms. *Journal of Experimental Botany* **54,** 1431-1446.

Broadley, M. R., Bowen, H. C., Cotterill, H. L., Hammond, J. P., Meacham, M. C., Mead, A., and White, P. J. (2004). Phylogenetic variation in the shoot mineral concentration of angiosperms. *Journal of Experimental Botany* **55,** 321-336.

Broadley, M. R., Lochlainn, S., Hammond, J. P., Bowen, H., Cakmak, I., Eker, S., Erdem, H., King, G. J., and White, P. J. (2010). Shoot zinc (Zn) concentration varies widely within Brassica oleracea L. and is affected by soil Zn and phosphorus (P) levels. *Journal of Horticultural Science and Biotechnology* **85,** 375-380.

Broadley, M. R., Hammond, J. P., King, G. J., Astley, D., Bowen, H. C., Meacham, M. C., Mead, A., Pink, D. A., Teakle, G. R., Hayden, R. M., Spracklen, W. P., and White, P. J. (2008). Shoot calcium and magnesium concentrations differ between subtaxa, are highly heritable, and associate with potentially pleiotropic loci in Brassica oleracea. *Plant Physiology* **146,** 1707-1720.

Broudy, D., Killeen, T., Choi, M., Shulman, N., Mani, D. R., Abbatiello, S. E., Mani, D., Ahmad, R., Sahu, A. K., Schilling, B., Tamura, K., Boss, Y., Sharma, V., Gibson, B. W., Carr, S. A., Vitek, O., MacCoss, M. J., and MacLean, B. (2014). A framework for installable external tools in Skyline. *Bioinformatics*.

Bruins, A. P. (1998). Mechanistic aspects of electrospray ionization. *Journal of Chromatography A* **794,** 345-357.

Buescher, E., Achberger, T., Amusan, I., Giannini, A., Ochsenfeld, C., Rus, A., Lahner, B., Hoekenga, O., Yakubova, E., and Harper, J. F. (2010). Natural genetic variation in selected populations of Arabidopsis thaliana is associated with ionomic differences. *PLoS One* **5,** e11081.

Bunting, E. S. (1984). Oilseed rape in perspective. In *Oilseed rape,* D.H. Sherisbrick and R.W. Daniels, eds (Great Britain: Collins Professional), pp. 3-15.

Bus, A., Körber, N., Parkin, I. A. P., Samans, B., Snowdon, R. J., Li, J., and Stich, B. (2014). Species- and genome-wide dissection of the shoot ionome in *Brassica napus* and its relationship to seedling development. *Frontiers in plant science* **5,** 485.

Butruille, D. V., Guries, R. P., and Osborn, T. C. (1999). Linkage Analysis of Molecular Markers and Quantitative Trait Loci in Populations of Inbred Backcross Lines of *Brassica napus* L. *Genetics* **153,** 949-964.

Butterbach-Bahl, K., Baggs, E. M., Dannenmann, M., Kiese, R., and Zechmeister-Boltenstern, S. (2013). Nitrous oxide emissions from soils: how well do we understand the processes and their controls? *Philosophical Transactions of the Royal Society of London B: Biological Sciences* **368**.

Cakmak, I., Hengeler, C., and Marschner, H. (1994). Partitioning of shoot and root dry matter and carbohydrates in bean plants suffering from phosphorus, potassium and magnesium deficiency. *Journal of experimental botany* **45,** 1245-1250.

Cammarano, P., Felsani, A., Gentile, M., Gualerzi, C., Romeo, A., and Wolf, G. (1972). Formation of active hybrid 80-S particles from subunits of pea seedlings and mammalian liver ribosomes. *Biochimica et Biophysica Acta (BBA)-Nucleic Acids and Protein Synthesis* **281,** 625-642.

Campbell, M., Dunn, R., Ditterline, R., Pickett, S., and Raboy, V. (1991). Phytic acid represents 10 to 15% of total phosphorus in alfalfa root and crown. *Journal of Plant Nutrition* **14,** 925-937.

Cantor, C. R. (2000). Mass Spectrometry After the Human Genome Project. In *Mass Spectrometry in Biology & Medicine*, A.L. Burlingame, S.A. Carr, and M.A. Baldwin, eds (Totowa, NJ: Humana Press), pp. 515-529.

Cao, Z., Tian, F., Wang, N., Jiang, C., Lin, B., Xia, W., Shi, J., Long, Y., Zhang, C., and Meng, J. (2010). Analysis of QTLs for erucic acid and oil content in seeds on A8 chromosome and the linkage drag between the alleles for the two traits in Brassica napus. *Journal of Genetics and Genomics* **37,** 231-240.

Chace, D. H. (2003). Measuring Mass: From Positive Rays to Proteins. *Clinical Chemistry* **49,** 342-343.

Chace, D. H., Kalas, T. A., and Naylor, E. W. (2002). The Application of Tandem Mass Spectrometry to Neonatal Screening for Inherited Disorders of Intermediart Metabolism. . *Annual Review of Genomics and Human Genetics* **3,** 17-45.

Chalhoub, B., Denoeud, F., Liu, S., Parkin, I. A. P., Tang, H., Wang, X., Chiquet, J., Belcram, H., Tong, C., Samans, B., Corréa, M., Da Silva, C., Just, J., Falentin, C., Koh, C. S., Le Clainche, I., Bernard, M., Bento, P., Noel, B., Labadie, K., *et al.* (2014). Early allopolyploid evolution in the post-Neolithic *Brassica napus* oilseed genome. *Science* **345,** 950-953.

Chamorro, A. M., Tamagno, L. N., Bezus, R., and Sarandón, S. J. (2002). Nitrogen accumulation, partition, and nitrogen-use efficiency in canola under different nitrogen availabilities. *Communications in Soil Science and Plant Analysis* **33,** 493-504.

Chen, J.-Y., Guo, L., Ma, H., Chen, Y.-Y., Zhang, H.-W., Ying, J.-Z., and Zhuang, J.-Y. (2014). Fine mapping of qHd1, a minor heading date QTL with pleiotropism for yield traits in rice (*Oryza sativa* L.). *Theoretical and Applied Genetics* **127,** 2515-2524.

Chen, W., Zhang, Y., Liu, X., Chen, B., Tu, J., and Tingdong, F. (2007). Detection of QTL for six yield-related traits in oilseed rape (*Brassica napus*) using DH and immortalized F2 populations. *Theoretical and Applied Genetics* **115,** 849-858.

Chin, J. H., Gamuyao, R., Dalid, C., Bustamam, M., Prasetiyono, J., Moeljopawiro, S., Wissuwa, M., and Heuer, S. (2011). Developing Rice with High Yield under Phosphorus Deficiency: Pup1 Sequence to Application. *Plant Physiology* **156,** 1202-1216.

Clauser, K. R., Baker, P., and Burlingame, A. L. (1999). Role of accurate mass measurement (±10 ppm) in protein identification strategies employing MS or MS/MS and database searching. *Analytical Chemistry* **71,** 2871-2882.

Cobo, F. (2013). Application of MALDI-TOF Mass Spectrometry in Clinical Virology: A Review. *The Open Virology Journal* **7,** 84-90.

Coleman, G. D., Chen, T. H. H., Ernst, S. G., and Fuchigami, L. (1991). Photoperiod Control of Poplar Bark Storage Protein Accumulation. *Plant Physiology* **96,** 686-692.

Collard, B. C. Y., and Mackill, D. J. (2008). Marker-assisted selection: an approach for precision plant breeding in the twenty-first century. *Philosophical Transactions of the Royal Society B: Biological Sciences* **363,** 557-572.

Collard, B. C. Y., Jahufer, M. Z. Z., Brouwer, J. B., and Pang, E. C. K. (2005). An introduction to markers, quantitative trait loci (QTL) mapping and marker-assisted selection for crop improvement: The basic concepts. *Euphytica* **142,** 169-196.

Comerford, N. B. (2005). Soil Factors Affecting Nutrient Bioavailability. In *Nutrient Acquisition by Plants: An Ecological Perspective*, H. BassiriRad, ed (Berlin, Heidelberg: Springer Berlin Heidelberg), pp. 1-14.

Courbot, M., Willems, G., Motte, P., Arvidsson, S., Roosens, N., Saumitou-Laprade, P., and Verbruggen, N. (2007). A Major Quantitative Trait Locus for Cadmium Tolerance in Arabidopsis halleri Colocalizes with HMA4, a Gene Encoding a Heavy Metal ATPase. *Plant Physiology* **144,** 1052-1065.

Cox, A., Skipper, J., Chen, Y., Henderson, R., Darrow, T., Shabanowitz, J., Engelhard, V., Hunt, D., and Slingluff, C. (1994). Identification of a peptide recognized by five melanoma-specific human cytotoxic T cell lines. *Science* **264,** 716-719.

Cox, J., and Mann, M. (2011). Quantitative, High-Resolution Proteomics for Data-Driven Systems Biology. *Annual Review of Biochemistry* **80,** 273-299.

Crompton, T. R. (2001). *Determination of Metals in Natural and Treated Water*. (Taylor & Francis).

Cyr, D. R., and Bewley, J. D. (1990). Seasonal variation in nitrogen storage reserves in the roots of leafy spurge (Euphorbia esula) and responses to decapitation and defoliation. *Physiologia Plantarum* **78,** 361-366.

Damon, P. M., Osborne, L. D., and Rengel, Z. (2007). Canola genotypes differ in potassium efficiency during vegetative growth. *Euphytica* **156,** 387-397.

Daniel-Vedele, F., Krapp, A., and Kaiser, W. M. (2010). Cellular Biology of Nitrogen Metabolism and Signaling. In *Cell Biology of Metals and Nutrients*,

R. Hell and R.-R. Mendel, eds (Berlin, Heidelberg: Springer Berlin Heidelberg), pp. 145-172.

Defra. (2010). Fertiliser Manual (RB209). *London, UK: Department for Environment, Food and Rural Affairs*.

Defra, and EA. (2016). Department for Environment, Food and Rural Affairs (defra) and Environmental Agency (EA), Using nitrogen fertilisers in nitrate vulnerable zones. ([https://www.gov.uk/guidance/using-nitrogen-fertilisers-in-nitrate-vulnerable-zones] Accessed 20 March 2016.

Dejoux, J.-F., Recous, S., Meynard, J.-M., Trinsoutrot, I., and Leterme, P. (2000). The fate of nitrogen from winter-frozen rapeseed leaves: mineralization, fluxes to the environment and uptake by rapeseed crop in spring. *Plant and Soil* **218,** 257-272.

Delourme, R., Falentin, C., Huteau, V., Clouet, V., Horvais, R., Gandon, B., Specel, S., Hanneton, L., Dheu, J. E., Deschamps, M., Margale, E., Vincourt, P., and Renard, M. (2006). Genetic control of oil content in oilseed rape (*Brassica napus* L.). *Theoretical and Applied Genetics* **113,** 1331-1345.

Desclos, M., Dubousset, L., Etienne, P., Le Caherec, F., Satoh, H., Bonnefoy, J., Ourry, A., and Avice, J.-C. (2008). A Proteomic Profiling Approach to Reveal a Novel Role of *Brassica napus* Drought 22 kD/Water-Soluble Chlorophyll-Binding Protein in Young Leaves during Nitrogen Remobilization Induced by Stressful Conditions. *Plant Physiology* **147,** 1830-1844.

DeWald, D. B., Mason, H. S., and Mullet, J. E. (1992). The soybean vegetative storage proteins VSP alpha and VSP beta are acid phosphatases active on polyphosphates. *Journal of Biological Chemistry* **267,** 15958-15964.

Diepenbrock, W. (2000). Yield analysis of winter oilseed rape (*Brassica napus* L.): a review. *Field Crops Research* **67,** 35-49.

Ding, G., Yang, M., Hu, Y., Liao, Y., Shi, L., Xu, F., and Meng, J. (2010). Quantitative trait loci affecting seed mineral concentrations in *Brassica napus* grown with contrasting phosphorus supplies. *Annals of Botany* **105,** 1221-1234.

Ding, G., Zhao, Z., Liao, Y., Hu, Y., Shi, L., Long, Y., and Xu, F. (2012). Quantitative trait loci for seed yield and yield-related traits, and their responses to reduced phosphorus supply in Brassica napus. *Annals of Botany* **109,** 747-759.

Domon, B., and Aebersold, R. (2006). Mass Spectrometry and Protein Analysis. *Science* **312,** 212-217.

Downey, R. K., and Rimmer, S. R. (1993). Agronomic Improvement in Oilseed Brassicas. In *Advances in agronomy*, L.S. Donald, ed (Academic Press), pp. 1-66.

Dreccer, M. F., Schapendonk, A. H. C. M., Slafer, G. A., and Rabbinge, R. (2000). Comparative response of wheat and oilseed rape to nitrogen supply: absorption and utilisation efficiency of radiation and nitrogen during the reproductive stages determining yield. *Plant and Soil* **220,** 189-205.

Druka, A., Potokina, E., Luo, Z., Jiang, N., Chen, X., Kearsey, M., and Waugh, R. (2010). Expression quantitative trait loci analysis in plants. *Plant Biotechnology Journal* **8,** 10-27.

EEA. (2016). European Environment Agency (EEA), Sulphur dioxide (SO2) emissions. ([http://www.eea.europa.eu/data-and-maps/indicators/eea-32-sulphur-dioxide-so2-emissions-1/assessment-3/#sulphur-dioxide-so2-emissions] Accessed 17 March 2016.

Eichert, T., and Fernández, V. (2012). Chapter 4 - Uptake and Release of Elements by Leaves and Other Aerial Plant Parts A2 - Marschner, Petra. In *Marschner's Mineral Nutrition of Higher Plants (Third Edition)*, (San Diego: Academic Press), pp. 71-84.

Emonet, S., Shah, H. N., Cherkaoui, A., and Schrenzel, J. (2010). Application and use of various mass spectrometry methods in clinical microbiology. *Clinical Microbiology and Infection* **16,** 1604-1613.

Epstein, E., and Bloom, A. J. (2005). *Mineral Nutrition of Plants: Principles and Perspectives*. 2nd ed. (Sunderland, Massachusetts: Sinauer Associates).

Etienne, P., Desclos, M., Le Gou, L., Gombert, J., Bonnefoy, J., Maurel, K., Le Dily, F., Ourry, A., and Avice, J.-C. (2007). N-protein mobilisation associated with the leaf senescence process in oilseed rape is concomitant with the disappearance of trypsin inhibitor activity. *Functional Plant Biology* **34,** 895-906.

Falk, K. L., Tokuhisa, J. G., and Gershenzon, J. (2007). The Effect of Sulfur Nutrition on Plant Glucosinolate Content: Physiology and Molecular Mechanisms. *Plant Biology* **9,** 573-581.

Feng, J., Long, Y., Shi, L., Shi, J., Barker, G., and Meng, J. (2012). Characterization of metabolite quantitative trait loci and metabolic networks that control glucosinolate concentration in the seeds and leaves of *Brassica napus*. *New Phytologist* **193,** 96-108.

Fenn, J. B., Mann, M., Meng, C. K., Wong, S. F., and Whitehouse, C. M. (1989). Electrospray ionization for mass spectrometry of large biomolecules. *Science* **246,** 64-71.

Finehout, E. J., and Lee, K. H. (2004). An introduction to mass spectrometry applications in biological research. *Biochemistry and Molecular Biology Education* **32,** 93-100.

Forster, B. P., Heberle-Bors, E., Kasha, K. J., and Touraev, A. (2007). The resurgence of haploids in higher plants. *Trends in Plant Science* **12,** 368-375.

Fournier, P.-E., Drancourt, M., Colson, P., Rolain, J.-M., Scola, B. L., and Raoult, D. (2013). Modern clinical microbiology: new challenges and solutions. *Nature Reviews Microbiology* **11,** 574-585.

Fraile-Escanciano, A., Kamisugi, Y., Cuming, A. C., Rodríguez-Navarro, A., and Benito, B. (2010). The SOS1 transporter of Physcomitrella patens mediates sodium efflux in planta. *New Phytologist* **188,** 750-761.

Furihata, T., Suzuki, M., and Sakurai, H. (1992). Kinetic Characterization of Two Phosphate Uptake Systems with Different Affinities in Suspension-Cultured Catharanthus roseus Protoplasts. *Plant and Cell Physiology* **33,** 1151-1157.

Gabrielle, B., Denoroy, P., Gosse, G., Justes, E., and Andersen, M. N. (1998). A model of leaf area development and senescence for winter oilseed rape. *Field Crops Research* **57,** 209-222.

Gallien, S., Duriez, E., and Domon, B. (2011). Selected reaction monitoring applied to proteomics. *Journal of Mass Spectrometry* **46,** 298-312.

Gana, J. A., Kalengamaliro, N. E., Cunningham, S. M., and Volenec, J. J. (1998). Expression of β-Amylase from Alfalfa Taproots. *Plant Physiology* **118,** 1495-1506.

Garcia, I. R., and Gaskell, S. J. (2006). Peptide Analysis using LC-MS. In *Applications of LC-MS in Toxicology*, A. Polettini, ed (Italy: Pharamaceutical Press), pp. 243 - 245.

Gaspari, M., and Cuda, G. (2011). Nano LC–MS/MS: A Robust Setup for Proteomic Analysis. In *Nanoproteomics: Methods and Protocols*, A.S. Toms and J.R. Weil, eds (Totowa, NJ: Humana Press), pp. 115-126.

Girondé, A., Poret, M., Etienne, P., Trouverie, J., Bouchereau, A., Le Cahérec, F., Leport, L., Orsel, M., Niogret, M.-F., Deleu, C., and Avice, J.-C. (2015). A profiling approach of the natural variability of foliar N remobilization at the rosette stage gives clues to understand the limiting processes involved in the low N use efficiency of winter oilseed rape. *Journal of Experimental Botany* **66,** 2461-2473.

Glass, A. D., Britto, D. T., Kaiser, B. N., Kinghorn, J. R., Kronzucker, H. J., Kumar, A., Okamoto, M., Rawat, S., Siddiqi, M., and Unkles, S. E. (2002). The regulation of nitrate and ammonium transport systems in plants. *Journal of Experimental Botany* **53,** 855-864.

Gombert, J., Etienne, P., Ourry, A., and Le Dily, F. (2006). The expression patterns of SAG12/Cab genes reveal the spatial and temporal progression of leaf senescence in *Brassica napus* L. with sensitivity to the environment. *Journal of Experimental Botany* **57,** 1949-1956.

Gombert, J., Le Dily, F., Lothier, J., Etienne, P., Rossato, L., Allirand, J.-M., Jullien, A., Savin, A., and Ourry, A. (2010). Effect of nitrogen fertilization on nitrogen dynamics in oilseed rape using 15N-labeling field experiment. *Journal of Plant Nutrition and Soil Science* **173,** 875-884.

Granvogl, B., Plöscher, M., and Eichacker, L. A. (2007). Sample preparation by in-gel digestion for mass spectrometry-based proteomics. *Analytical and Bioanalytical Chemistry* **389,** 991-1002.

Gül, M. K. (2003). QTL Mapping and Analysis of QTL x Nitrogen Interactions for Some Yield Components in *Brassica napus* L. *Turkish Journal of Agriculture and Forestry* **27,** 71-76.

Gupta, P. K., Varshney, R. K., Sharma, P. C., and Ramesh, B. (1999). Molecular markers and their applications in wheat breeding. *Plant Breeding* **118,** 369-390.

Gygi, S. P., Rist, B., Griffin, T. J., Eng, J., and Aebersold, R. (2002). Proteome Analysis of Low-Abundance Proteins Using Multidimensional Chromatography and Isotope-Coded Affinity Tags. *Journal of Proteome Research* **1,** 47-54.

Hammond, J. P., Broadley, M. R., White, P. J., King, G. J., Bowen, H. C., Hayden, R., Meacham, M. C., Mead, A., Overs, T., Spracklen, W. P., and Greenwood, D. J. (2009). Shoot yield drives phosphorus use efficiency in Brassica oleracea and correlates with root architecture traits. *Journal of Experimental Botany* **60,** 1953-1968.

Han, X., Aslanian, A., and Yates, J. R. (2008). Mass Spectrometry for Proteomics. *Current Opinion in Chemical Biology* **12,** 483-490.

Harville, D. A. (1977). Maximum likelihood approaches to variance component estimation and to related problems. *Journal of the American Statistical Association* **72,** 320-338.

Hawkesford, M., Horst, W., Kichey, T., Lambers, H., Schjoerring, J., Møller, I. S., and White, P. (2012). Chapter 6 - Functions of Macronutrients. In *Marschner's Mineral Nutrition of Higher Plants*, 3rd ed., P. Marschner, ed (San Diego: Academic Press), pp. 135-189.

Hawkesford, M. J., and De Kok, L. J. (2006). Managing sulphur metabolism in plants. *Plant, Cell & Environment* **29,** 382-395.

Hawkesford, M. J., Kopriva, S., and De Kok, L. J. (2014). *Nutrient Use Efficiency in Plants: Concepts and Approaches*. (Cham: Springer International Publishing).

Hell, R., and Mendel, R.-R. (2010). *Cell Biology of Metals and Nutrients*. (Berlin, Heidelberg: Springer Berlin Heidelberg).

Hendershot, K. L., and Volenec, J. J. (1993). Taproot nitrogen accumulation and use in overwintering alfalfa (Medicago sativa L.). *Journal of Plant Physiology* **141,** 68-74.

Hillenkamp, F., Karas, M., Beavis, R. C., and Chait, B. T. (1991). Matrix-Assisted Laser Desorption/Ionization Mass Spectrometry of Biopolymers. *Analytical Chemistry* **63,** 1193A-1203A.

Hirel, B., Le Gouis, J., Ney, B., and Gallais, A. (2007). The challenge of improving nitrogen use efficiency in crop plants: towards a more central role for genetic variability and quantitative genetics within integrated approaches. *Journal of experimental botany* **58,** 2369-2387.

Hirose, T. (2011). Nitrogen use efficiency revisited. *Oecologia* **166,** 863-867.

Ho, C. S., Lam, C. W. K., Chan, M. H. M., Cheung, R. C. K., Law, L. K., Lit, L. C. W., Ng, K. F., Suen, M. W. M., and Tai, H. L. (2003). Electrospray Ionisation Mass Spectrometry: Principles and Clinical Applications. *The Clinical Biochemist Reviews* **24,** 3-12.

Hoffmann, E. d. (1996). Tandem mass spectrometry: A primer. *Journal of Mass Spectrometry* **31,** 129-137.

Hoffmann, E. d., and Stroobant, V. (2007a). Introduction. In *Mass Spectrometry: principles and Applications*, 3rd ed., (Chichester, England: John Wiley & Sons, Ltd), pp. 1 - 13.

Hoffmann, E. d., and Stroobant, V. (2007b). Ion Sources. In *Mass Spectrometry: principles and Applications*, 3rd ed., (Chichester, England: John Wiley & Sons, Ltd), pp. 15-83.

Holford, I. C. R. (1997). Soil phosphorus: its measurement, and its uptake by plants. *Soil Research* **35,** 227-240.

Hopkins, C. J., Welham, S. J., Teakle, G. R., Peplow, K.-S., Pink, D. A. C., Carion, P. W. C., King, G. J., and Barker, J. (2010-2011). Oilseed Rape Genetic Improvement Network Diversity Demonstration Trial - Year 2. (Rothamsted Research, Harpenden) [http://www.oregin.info/resources/trials.php] Accessed 14 January 2016.

Horneck, D. A., and Miller, R. O. (1998). Determination Of Total Nitrogen In Plant Tissue. In *Handbook of reference methods for plant analysis*, Y.P. Kalra, ed (Boca Raton: CRC Press), pp. 75-83.

Horst, W. J., Behrens, T., Heuberger, H., Kamh, M., Reidenbach, G., and Wiesler, F. (2003). Genotypic differences in nitrogen use-efficiency in crop plants. *Innovative soil–plant systems for sustainable agricultural production. OECD***,** 75-92.

Howell, P. M., Sharpe, A. G., and Lydiate, D. J. (2003). Homoeologous loci control the accumulation of seed glucosinolates in oilseed rape (*Brassica napus*). *Genome* **46,** 454-460.

Huang, N. C., Chiang, C. S., Crawford, N. M., and Tsay, Y. F. (1996). CHL1 encodes a component of the low-affinity nitrate uptake system in Arabidopsis and shows cell type-specific expression in roots. *The Plant Cell* **8,** 2183-2191.

Huang, N. C., Liu, K. H., Lo, H. J., and Tsay, Y. F. (1999). Cloning and Functional Characterization of an Arabidopsis Nitrate Transporter Gene That Encodes a Constitutive Component of Low-Affinity Uptake. *The Plant Cell* **11,** 1381-1392.

Huang, X.-Q., Huang, T., Hou, G.-Z., Li, L., Hou, Y., and Lu, Y.-H. (2016). Identification of QTLs for seed quality traits in rapeseed (*Brassica napus* L.) using recombinant inbred lines (RILs). *Euphytica* **210,** 1-16.

Hunt, D., Henderson, R., Shabanowitz, J., Sakaguchi, K., Michel, H., Sevilir, N., Cox, A., Appella, E., and Engelhard, V. (1992). Characterization of peptides bound to the class I MHC molecule HLA-A2.1 by mass spectrometry. *Science* **255,** 1261-1263.

Huynh, M.-L., Russell, P., and Walsh, B. (2009). Tryptic Digestion of In-Gel Proteins for Mass Spectrometry Analysis. In *Two-Dimensional Electrophoresis Protocols*, R. Tyther and D. Sheehan, eds (Totowa, NJ: Humana Press), pp. 507-513.

Jansen, R. C. (2008). Quantitative Trait Loci in Inbred Lines. In *Handbook of Statistical Genetics*, (John Wiley & Sons, Ltd), pp. 587-622.

Jansen, R. C., and Stam, P. (1994). High Resolution of Quantitative Traits into Multiple Loci via Interval Mapping. *Genetics* **136,** 1447-1455.

Javed, N., Geng, J., Tahir, M., McVetty, P. B. E., Li, G., and Duncan, R. W. (2016). Identification of QTL influencing seed oil content, fatty acid profile and days to flowering in *Brassica napus* L. *Euphytica* **207,** 191-211.

Jensen, L. S., Christensen, L., Mueller, T., and Nielsen, N. E. (1997). Turnover of residual 15N-labelled fertilizer N in soil following harvest of oilseed rape (*Brassica napus* L.). *Plant and Soil* **190,** 193-202.

Jiang, C., Shi, J., Li, R., Long, Y., Wang, H., Li, D., Zhao, J., and Meng, J. (2014). Quantitative trait loci that control the oil content variation of rapeseed (*Brassica napus* L.). *Theoretical and Applied Genetics* **127,** 957-968.

Johnson, R. S., Martin, S. A., Biemann, K., Stults, J. T., and Watson, J. T. (1987). Novel fragmentation process of peptides by collision-induced decomposition in a tandem mass spectrometer: differentiation of leucine and isoleucine. *Analytical Chemistry* **59,** 2621-2625.

Juraschek, R., Dülcks, T., and Karas, M. (1999). Nanoelectrospray—more than just a minimized-flow electrospray ionization source. *Journal of the American Society for Mass Spectrometry* **10,** 300-308.

Kamh, M., Wiesler, F., Ulas, A., and Horst, W. J. (2005). Root growth and N-uptake activity of oilseed rape (*Brassica napus* L.) cultivars differing in nitrogen efficiency. *Journal of Plant Nutrition and Soil Science* **168,** 130-137.

Kearsey, M. J., and Farquhar, A. G. L. (1998). QTL analysis in plants; where are we now? *Heredity* **80,** 137-142.

Kessel, B., Schierholt, A., and Becker, H. C. (2012). Nitrogen Use Efficiency in a Genetically Diverse Set of Winter Oilseed Rape (*Brassica napus* L.). *Crop Science* **52,** 2546-2554.

Khajali, F., and Slominski, B. A. (2012). Factors that affect the nutritive value of canola meal for poultry. *Poultry Science* **91,** 2564-2575.

Kinter, M., and Kinter, C. S. (2013a). Specificity of Detection Is the Key Attribute of Selected Reaction Monitoring. In *Application of Selected Reaction Monitoring to Highly Multiplexed Targeted Quantitative Proteomics: A Replacement for Western Blot Analysis*, (New York, NY: Springer New York), pp. 9-13.

Kinter, M., and Kinter, C. S. (2013b). Designing a Selected Reaction Monitoring Method. In *Application of Selected Reaction Monitoring to Highly Multiplexed Targeted Quantitative Proteomics: A Replacement for Western Blot Analysis*, (New York, NY: Springer New York), pp. 15-33.

Kinter, M., and Kinter, C. S. (2013c). *Application of Selected Reaction Monitoring to Highly Multiplexed Targeted Quantitative Proteomics*. (New York, NY: Springer New York).

Kirkby, E. (2012). Chapter 1 - Introduction, Definition and Classification of Nutrients. In *Marschner's Mineral Nutrition of Higher Plants*, 3rd ed., P. Marschner, ed (San Diego: Academic Press), pp. 3-5.

Klemm, P. (1984). Manual Edman Degradation of Proteins and Peptides. In *Proteins*, J.M. Walker, ed (Totowa, NJ: Humana Press), pp. 243-254.

Koeslin-Findeklee, F., and Horst, W. J. (2016). Contribution of Nitrogen Uptake and Retranslocation during Reproductive Growth to the Nitrogen Efficiency of Winter Oilseed-Rape Cultivars (*Brassica napus* L.) Differing in Leaf Senescence. *Agronomy* **6,** 1.

Kopriva, S. (2006). Regulation of Sulfate Assimilation in Arabidopsis and Beyond. *Annals of Botany* **97,** 479-495.

Labboun, S., Tercé-Laforgue, T., Roscher, A., Bedu, M., Restivo, F. M., Velanis, C. N., Skopelitis, D. S., Moshou, P. N., Roubelakis-Angelakis, K. A., Suzuki, A., and Hirel, B. (2009). Resolving the Role of Plant Glutamate Dehydrogenase. I. in vivo Real Time Nuclear Magnetic Resonance Spectroscopy Experiments. *Plant and Cell Physiology* **50,** 1761-1773.

Laemmli, U. K. (1970). Cleavage of structural proteins during the assembly of the head of bacteriophage T4. *Nature* **227,** 680-685.

Lambers, H., Brundrett, M. C., Raven, J. A., and Hopper, S. D. (2010). Plant mineral nutrition in ancient landscapes: high plant species diversity on infertile soils is linked to functional diversity for nutritional strategies. *Plant and Soil* **334,** 11-31.

Lange, V., Picotti, P., Domon, B., and Aebersold, R. (2008). Selected reaction monitoring for quantitative proteomics: a tutorial. *Molecular Systems Biology* **4,** 222-222.

Lebaudy, A., Véry, A.-A., and Sentenac, H. (2007). K+ channel activity in plants: Genes, regulations and functions. *FEBS Letters* **581,** 2357-2366.

Lee, B.-R., Jin, Y.-L., Park, S.-H., Zaman, R., Zhang, Q., Avice, J.-C., Ourry, A., and Kim, T.-H. (2015). Genotypic variation in N uptake and assimilation estimated by 15N tracing in water deficit-stressed *Brassica napus*. *Environmental and Experimental Botany* **109,** 73-79.

Lee, S. M., Kim, H. S., Han, H. J., Moon, B. C., Kim, C. Y., Harper, J. F., and Chung, W. S. (2007). Identification of a calmodulin-regulated autoinhibited Ca2+-ATPase (ACA11) that is localized to vacuole membranes in Arabidopsis. *FEBS Letters* **581,** 3943-3949.

Leustek, T., Martin, M. N., Bick, J.-A., and Davies, J. P. (2000). Pathways and Regulation of Sulfur Metabolism Revealed Through Molecular and Genetic Studies. *Annual Review of Plant Physiology and Plant Molecular Biology* **51,** 141-165.

Li, P., Chen, F., Cai, H., Liu, J., Pan, Q., Liu, Z., Gu, R., Mi, G., Zhang, F., and Yuan, L. (2015). A genetic relationship between nitrogen use efficiency and seedling root traits in maize as revealed by QTL analysis. *Journal of experimental botany* **66,** 3175-3188.

Liebler, D. C., and Zimmerman, L. J. (2013). Targeted Quantitation of Proteins by Mass Spectrometry. *Biochemistry* **52,** 3797-3806.

Lin, S.-H., Kuo, H.-F., Canivenc, G., Lin, C.-S., Lepetit, M., Hsu, P.-K., Tillard, P., Lin, H.-L., Wang, Y.-Y., Tsai, C.-B., Gojon, A., and Tsay, Y.-F. (2008).

Mutation of the Arabidopsis NRT1.5 Nitrate Transporter Causes Defective Root-to-Shoot Nitrate Transport. *The Plant Cell* **20,** 2514-2528.

Liu, J., Yang, J., Li, R., Shi, L., Zhang, C., Long, Y., Xu, F., and Meng, J. (2009a). Analysis of genetic factors that control shoot mineral concentrations in rapeseed (*Brassica napus*) in different boron environments. *Plant and Soil* **320,** 255-266.

Liu, S.-B., Wang, X.-C., Shi, M.-J., Chen, Y.-Y., Hu, Z.-H., and Tian, W.-M. (2009b). Vegetative Storage Protein with Trypsin Inhibitor Activity Occurs in Sapindus mukorassi, a Sapindaceae Deciduous Tree. *Journal of Integrative Plant Biology* **51,** 352-359.

Liu, Y., Ahn, J.-E., Datta, S., Salzman, R. A., Moon, J., Huyghues-Despointes, B., Pittendrigh, B., Murdock, L. L., Koiwa, H., and Zhu-Salzman, K. (2005). Arabidopsis Vegetative Storage Protein Is an Anti-Insect Acid Phosphatase. *Plant Physiology* **139,** 1545-1556.

Livak, K. J., and Schmittgen, T. D. (2001). Analysis of Relative Gene Expression Data Using Real-Time Quantitative PCR and the 2−ΔΔCT Method. *Methods* **25,** 402-408.

Liyanage, R., and Lay, J. O. (2006). An Introduction to MALDI-TOF MS. In *Identification of Microorganisms by Mass Spectrometry*, (John Wiley & Sons, Inc.), pp. 39-60.

Long, Y., Shi, J., Qiu, D., Li, R., Zhang, C., Wang, J., Hou, J., Zhao, J., Shi, L., Park, B.-S., Choi, S. R., Lim, Y. P., and Meng, J. (2007). Flowering Time Quantitative Trait Loci Analysis of Oilseed Brassica in Multiple Environments and Genomewide Alignment with Arabidopsis. *Genetics* **177,** 2433-2444.

Lott, J. N. A., Ockenden, I., Raboy, V., and Batten, G. D. (2000). Phytic acid and phosphorus in crop seeds and fruits: a global estimate. *Seed Science Research* **10,** 11-33.

Loudet, O., Chaillou, S., Krapp, A., and Daniel-Vedele, F. (2003a). Quantitative trait loci analysis of water and anion contents in interaction with nitrogen availability in Arabidopsis thaliana. *Genetics* **163,** 711-722.

Loudet, O., Chaillou, S., Merigout, P., Talbotec, J., and Daniel-Vedele, F. (2003b). Quantitative Trait Loci Analysis of Nitrogen Use Efficiency in Arabidopsis. *Plant Physiology* **131,** 345-358.

Lowry, O. H., Rosebrough, N. J., Farr, A. L., and Randall, R. J. (1951). Protein Measurment with The Folin Phenol Reagent. *Journal of Biological Chemistry* **193,** 265-275.

Lynch, J. P. (2015). Root phenes that reduce the metabolic costs of soil exploration: opportunities for 21st century agriculture. *Plant, Cell & Environment* **38,** 1775-1784.

Maathuis, F. J. M. (2009). Physiological functions of mineral macronutrients. *Current Opinion in Plant Biology* **12,** 250-258.

Macdonald, A. J., Poulton, P. R., Powlson, D. S., and Jenkinson, D. S. (1997). Effects of season, soil type and cropping on recoveries, residues and losses of 15N-labelled fertilizer applied to arable crops in spring. *The Journal of Agricultural Science* **129,** 125-154.

MacLean, B., Tomazela, D. M., Shulman, N., Chambers, M., Finney, G. L., Frewen, B., Kern, R., Tabb, D. L., Liebler, D. C., and MacCoss, M. J. (2010). Skyline: an open source document editor for creating and analyzing targeted proteomics experiments. *Bioinformatics* **26,** 966-968.

Mahmuti, M., West, J. S., Watts, J., Gladders, P., and Fitt, B. D. L. (2009). Controlling crop disease contributes to both food security and climate change mitigation. *International Journal of Agricultural Sustainability* **7,** 189-202.

Malagoli, P., Laine, P., Rossato, L., and Ourry, A. (2005a). Dynamics of nitrogen uptake and mobilization in field-grown winter oilseed rape (*Brassica napus*) from stem extension to harvest I. Global N flows between vegetative and reproductive tissues in relation to leaf fall and their residual N. *Annals of Botany* **95,** 853-861.

Malagoli, P., Laine, P., Rossato, L., and Ourry, A. (2005b). Dynamics of nitrogen uptake and mobilization in field-grown winter oilseed rape (*Brassica napus*) from stem extension to harvest. II. An 15N-labelling-based simulation model of N partitioning between vegetative and reproductive tissues. *Annals of Botany* **95,** 1187-1198.

Malagoli, P., Lainé, P., Le Deunff, E., Rossato, L., Ney, B., and Ourry, A. (2004). Modeling Nitrogen Uptake in Oilseed Rape cv Capitol during a Growth Cycle Using Influx Kinetics of Root Nitrate Transport Systems and Field Experimental Data. *Plant Physiology* **134,** 388-400.

Mann, M., Hendrickson, R. C., and Pandey, A. (2001). Analysis of proteins and proteomes by mass spectrometry. *Annual Review of Biochemistry* **70,** 437-473.

Mano, N., and Goto, J. (2003). Biomedical and Biological Mass Spectrometry. *Analytical Sciences* **19,** 3-14.

Marschner, P. (2012a). *Marschner's Mineral Nutrition of Higher Plants*. 3rd ed. (San Diego: Academic Press).

Marschner, P. (2012b). *Marschner's mineral nutrition of higher plants*. 3rd ed. (San Diego: Academic press).

Martínez-Maqueda, D., Hernández-Ledesma, B., Amigo, L., Miralles, B., and Gómez-Ruiz, J. Á. (2013). Extraction/Fractionation Techniques for Proteins and Peptides and Protein Digestion. In *Proteomics in Foods: Principles and*

Applications, F. Toldrá and L.L.M. Nollet, eds (Boston, MA: Springer US), pp. 21-50.

Marx, V. (2013). Targeted proteomics. *Nature Methods* **10,** 19-22.

Masclaux-Daubresse, C., Daniel-Vedele, F., Dechorgnat, J., Chardon, F., Gaufichon, L., and Suzuki, A. (2010). Nitrogen uptake, assimilation and remobilization in plants: challenges for sustainable and productive agriculture. *Annals of Botany* **105,** 1141-1157.

McCully, M. E., Miller, C., Sprague, S. J., Huang, C. X., and Kirkegaard, J. A. (2008). Distribution of glucosinolates and sulphur-rich cells in roots of field-grown canola (*Brassica napus*). *New Phytologist* **180,** 193-205.

McGrath, S. P., and Zhao, F. J. (1996). Sulphur uptake, yield responses and the interactions between nitrogen and sulphur in winter oilseed rape (*Brassica napus*). *The Journal of Agricultural Science* **126,** 53-62.

McKenna, A., Hanna, M., Banks, E., Sivachenko, A., Cibulskis, K., Kernytsky, A., Garimella, K., Altshuler, D., Gabriel, S., Daly, M., and DePristo, M. A. (2010). The Genome Analysis Toolkit: A MapReduce framework for analyzing next-generation DNA sequencing data. *Genome Research* **20,** 1297-1303.

McMaster, M. C. (2006). Advantages and Disadvantages of HPLC. In *HPLC*, (John Wiley & Sons, Inc.), pp. 1-13.

Merhaut, D. J. (2007). Chapter 6 - Magnesium. In *Handbook of Plant Nutrition*, A.V. Barker and D.J. Pilbeam, eds (Boca Raton, FL: CRC Press/Taylor & Francis.

Meuriot, F., Avice, J.-C., Decau, M.-L., Simon, J.-C., Lainé, P., Volenec, J. J., and Ourry, A. (2003). Accumulation of N reserves and vegetative storage protein (VSP) in taproots of non-nodulated alfalfa (Medicago sativa L.) are affected by mineral N availability. *Plant Science* **165,** 709-718.

Miller, A. J., and Cramer, M. D. (2004). Root Nitrogen Acquisition and Assimilation. *Plant and Soil* **274,** 1-36.

Miller, A. J., and Cramer, M. D. (2005). Root nitrogen acquisition and assimilation. In *Root Physiology: from Gene to Function*, H. Lambers and T.D. Colmer, eds (Dordrecht: Springer Netherlands), pp. 1-36.

Miller, R. O. (1998). Microwave digestion of plant tissue in a closed vessel. In *Handbook and reference methods for plant analysis*, Y.P. Kalra, ed (Boca Raton: CRC Press), pp. 69-74.

Mimura, T. (2001). Physiological control of phosphate uptake and phosphate homeostasis in plant cells. *Functional Plant Biology* **28,** 655-660.

Miro, B. (2010). *Identification of traits for nitrogen use efficiency in oilseed rape (Brassica napus L.).* (PhD Thesis), Newcastle University, Newcastle, UK. [https://theses.ncl.ac.uk/dspace/handle/10443/1067] Accessed 10 March 2016.

Miwa, K., and Fujiwara, T. (2010). Role of Boron in Plant Growth and its Transport Mechanisms. In *Cell Biology of Metals and Nutrients*, R. Hell and R.-R. Mendel, eds (Berlin, Heidelberg: Springer Berlin Heidelberg), pp. 1-15.

Mohan, M., Nair, S., Bhagwat, A., Krishna, T. G., Yano, M., Bhatia, C. R., and Sasaki, T. (1997). Genome mapping, molecular markers and marker-assisted selection in crop plants. *Molecular Breeding* **3,** 87-103.

Munson, M. S. B., and Field, F. H. (1966). Chemical Ionization Mass Spectrometry. I. General Introduction. *Journal of the American Chemical Society* **88,** 2621-2630.

Näsholm, T., Kielland, K., and Ganeteg, U. (2009). Uptake of organic nitrogen by plants. *New Phytologist* **182,** 31-48.

Nesvizhskii, A. I., Keller, A., Kolker, E., and Aebersold, R. (2003). A statistical model for identifying proteins by tandem mass spectrometry. *Analytical Chemistry* **75,** 4646-4658.

Nikiforova, V. J., Gakière, B., Kempa, S., Adamik, M., Willmitzer, L., Hesse, H., and Hoefgen, R. (2004). Towards dissecting nutrient metabolism in plants: a systems biology case study on sulphur metabolism. *Journal of experimental botany* **55,** 1861-1870.

Noquet, C., Avice, J.-C., Rossato, L., Beauclair, P., Henry, M.-P., and Ourry, A. (2004). Effects of altered source–sink relationships on N allocation and vegetative storage protein accumulation in *Brassica napus* L. *Plant Science* **166,** 1007-1018.

Nussaume, L., Kanno, S., Javot, H., Marin, E., Pochon, N., Ayadi, A., Nakanishi, T. M., and Thibaud, M.-C. (2011). Phosphate Import in Plants: Focus on the PHT1 Transporters. *Frontiers in Plant Science* **2,** 83.

Nyikako, J., Schierholt, A., Kessel, B., and Becker, H. C. (2014). Genetic variation in nitrogen uptake and utilization efficiency in a segregating DH population of winter oilseed rape. *Euphytica* **199,** 3-11.

Ockenden, I., Dorsch, J. A., Reid, M. M., Lin, L., Grant, L. K., Raboy, V., and Lott, J. N. (2004). Characterization of the storage of phosphorus, inositol phosphate and cations in grain tissues of four barley (Hordeum vulgare L.) low phytic acid genotypes. *Plant Science* **167,** 1131-1142.

Ogunlela, V. B., Kullmann, A., and Geisler, G. (1989). Leaf Growth and Chlorophyll Content of Oilseed Rape (*Brassica napus* L.) as Influenced by Nitrogen Supply. *Journal of Agronomy and Crop Science* **163,** 73-89.

Okazaki, K., Sakamoto, K., Kikuchi, R., Saito, A., Togashi, E., Kuginuki, Y., Matsumoto, S., and Hirai, M. (2006). Mapping and characterization of FLC homologs and QTL analysis of flowering time in *Brassica oleracea*. *Theoretical and Applied Genetics* **114,** 595-608.

Olejnik, S., and Algina, J. (2000). Measures of Effect Size for Comparative Studies: Applications, Interpretations, and Limitations. *Contemporary Educational Psychology* **25,** 241-286.

Parkin, I. A., Koh, C., Tang, H., Robinson, S. J., Kagale, S., Clarke, W. E., Town, C. D., Nixon, J., Krishnakumar, V., Bidwell, S. L., Denoeud, F., Belcram, H., Links, M. G., Just, J., Clarke, C., Bender, T., Huebert, T., Mason, A. S., Pires, J. C., Barker, G., *et al.* (2014). Transcriptome and methylome profiling reveals relics of genome dominance in the mesopolyploid Brassica oleracea. *Genome Biology* **15,** 1-18.

Peng, J., Slominsiki, B. A., Guenter, W., Campbell, L. D., and Xiong, Y. Z. (2001). The anti-nutritional factors in Chinese double-low rapeseed meal. *J Chinese Cereals and Oil Association* **16,** 6-10.

Perkins, D. N., Pappin, D. J. C., Creasy, D. M., and Cottrell, J. S. (1999). robability-based protein identification by searching sequence databases using mass spectrometry data. *Electrophoresis* **20,** 3551-3567.

Picotti, P., and Aebersold, R. (2012). Selected reaction monitoring-based proteomics: workflows, potential, pitfalls and future directions. *Nature Methods* **9,** 555-566.

Pitt, J. J. (2009). Principles and Applications of Liquid Chromatography-Mass Spectrometry in Clinical Biochemistry. *The Clinical Biochemist Reviews* **30,** 19-34.

Portolés, T., Pitarch, E., López, F. J., Hernández, F., and Niessen, W. M. A. (2011). Use of soft and hard ionization techniques for elucidation of unknown compounds by gas chromatography/time-of-flight mass spectrometry. *Rapid Communications in Mass Spectrometry* **25,** 1589-1599.

Qiu, D., Morgan, C., Shi, J., Long, Y., Liu, J., Li, R., Zhuang, X., Wang, Y., Tan, X., Dietrich, E., Weihmann, T., Everett, C., Vanstraelen, S., Beckett, P., Fraser, F., Trick, M., Barnes, S., Wilmer, J., Schmidt, R., Li, J., *et al.* (2006). A comparative linkage map of oilseed rape and its use for QTL analysis of seed oil and erucic acid content. *Theoretical and Applied Genetics* **114,** 67-80.

Quijada, P. A., Udall, J. A., Lambert, B., and Osborn, T. C. (2006). Quantitative trait analysis of seed yield and other complex traits in hybrid spring rapeseed (*Brassica napus* L.): 1. Identification of genomic regions from winter germplasm. *Theoretical and Applied Genetics* **113,** 549-561.

Radoev, M., Becker, H. C., and Ecke, W. (2008). Genetic Analysis of Heterosis for Yield and Yield Components in Rapeseed (*Brassica napus* L.) by Quantitative Trait Locus Mapping. *Genetics* **179,** 1547-1558.

Radojčić Redovniković, I., Glivetić, T., Delonga, K., and Vorkapić-Furač, J. (2008). Glucosinolates and their potential role in plant. *Periodicum biologorum* **110,** 297-309.

Raghothama, K. G., and Karthikeyan, A. S. (2005). Phosphate Acquisition. *Plant and Soil* **274,** 37-49.

Rathke, G. W., Christen, O., and Diepenbrock, W. (2005). Effects of nitrogen source and rate on productivity and quality of winter oilseed rape (Brassica napus L.) grown in different crop rotations. *Field Crops Research* **94,** 103-113.

Reiter, L., Rinner, O., Picotti, P., Huttenhain, R., Beck, M., Brusniak, M.-Y., Hengartner, M. O., and Aebersold, R. (2011). mProphet: automated data processing and statistical validation for large-scale SRM experiments. *Nature Methods* **8,** 430-435.

Richardson, A. E., and Simpson, R. J. (2011). Soil Microorganisms Mediating Phosphorus Availability Update on Microbial Phosphorus. *Plant Physiology* **156,** 989-996.

Roepstorff, P., and Fohlman, J. (1984). Letter to the editors. *Biological Mass Spectrometry* **11,** 601-601.

Rose, T. J., Rengel, Z., Ma, Q., and Bowden, J. W. (2007). Differential accumulation patterns of phosphorus and potassium by canola cultivars compared to wheat. *Journal of Plant Nutrition and Soil Science* **170,** 404-411.

Rossato, L., Laine, P., and Ourry, A. (2001). Nitrogen storage and remobilization in Brassica napus L. during the growth cycle: nitrogen fluxes within the plant and changes in soluble protein patterns. *Journal of Experimental Botany* **52,** 1655-1663.

Rossato, L., Le Dantec, C., Laine, P., and Ourry, A. (2002a). Nitrogen storage and remobilization in Brassica napus L. during the growth cycle: identification, characterization and immunolocalization of a putative taproot storage glycoprotein. *Journal of Experimental Botany* **53,** 265-275.

Rossato, L., MacDuff, J. H., Laine, P., Le Deunff, E., and Ourry, A. (2002b). Nitrogen storage and remobilization in Brassica napus L. during the growth cycle: effects of methyl jasmonate on nitrate uptake, senescence, growth, and VSP accumulation. *Journal of Experimental Botany* **53,** 1131-1141.

Rost, H. L., Rosenberger, G., Navarro, P., Gillet, L., Miladinovic, S. M., Schubert, O. T., Wolski, W., Collins, B. C., Malmstrom, J., Malmstrom, L., and Aebersold, R. (2014). OpenSWATH enables automated, targeted analysis of data-independent acquisition MS data. *Nature Biotechnology* **32,** 219-223.

Saito, K. (2004). Sulfur Assimilatory Metabolism. The Long and Smelling Road. *Plant Physiology* **136,** 2443-2450.

Salvi, S., and Tuberosa, R. (2005). To clone or not to clone plant QTLs: present and future challenges. *Trends in Plant Science* **10,** 297-304.

Sánchez-Calderón, L., Chacon-López, A., Pérez-Torres, C.-A., and Herrera-Estrella, L. (2010). Phosphorus: Plant Strategies to Cope with its Scarcity. In *Cell Biology of Metals and Nutrients*, R. Hell and R.-R. Mendel, eds (Berlin, Heidelberg: Springer Berlin Heidelberg), pp. 173-198.

Schjoerring, J. K., Bock, J. G. H., Gammelvind, L., Jensen, C. R., and Mogensen, V. O. (1995). Nitrogen incorporation and remobilization in different shoot components of field-grown winter oilseed rape (*Brassica napus* L.) as affected by rate of nitrogen application and irrigation. *Plant and Soil* **177,** 255-264.

Schulte auf'm Erley, G., Behrens, T., Ulas, A., Wiesler, F., and Horst, W. J. (2011). Agronomic traits contributing to nitrogen efficiency of winter oilseed rape cultivars. *Field Crops Research* **124,** 114-123.

Schulte auf'm Erley, G., Wijaya, K. A., Ulas, A., Becker, H., Wiesler, F., and Horst, W. J. (2007). Leaf senescence and N uptake parameters as selection traits for nitrogen efficiency of oilseed rape cultivars. *Physiologia Plantarum* **130,** 519-531.

Searle, B. C. (2010). Scaffold: a bioinformatic tool for validating MS/MS-based proteomic studies. *Proteomics* **10,** 1265-1269.

Semagn, K., Bjørnstad, å., and Ndjiondjop, M. N. (2006). An overview of molecular marker methods for plants. *African Journal of Biotechnology* **5,** 2540-2568.

Shapiro, S. S., and Wilk, M. B. (1965). An Analysis of Variance Test for Normality (Complete Samples). *Biometrika* **52,** 591-611.

Sheldon, C. C., Rouse, D. T., Finnegan, E. J., Peacock, W. J., and Dennis, E. S. (2000). The molecular basis of vernalization: The central role of FLOWERING LOCUS C (FLC). *Proceedings of the National Academy of Sciences of the United States of America* **97,** 3753-3758.

Shi, J., Li, R., Qiu, D., Jiang, C., Long, Y., Morgan, C., Bancroft, I., Zhao, J., and Meng, J. (2009). Unraveling the Complex Trait of Crop Yield With Quantitative Trait Loci Mapping in *Brassica napus*. *Genetics* **182,** 851-861.

Shi, J., Zhan, J., Yang, Y., Ye, J., Huang, S., Li, R., Wang, X., Liu, G., and Wang, H. (2015). Linkage and regional association analysis reveal two new tightly-linked major-QTLs for pod number and seed number per pod in rapeseed (*Brassica napus* L.). *Scientific Reports* **5,** 14481.

Shi, L., Shi, T., Broadley, M. R., White, P. J., Long, Y., Meng, J., Xu, F., and Hammond, J. P. (2013a). High-throughput root phenotyping screens identify genetic loci associated with root architectural traits in Brassica napus under contrasting phosphate availabilities. *Annals of Botany* **112,** 381-389.

Shi, T., Li, R., Zhao, Z., Ding, G., Long, Y., Meng, J., Xu, F., and Shi, L. (2013b). QTL for Yield Traits and Their Association with Functional Genes in Response to Phosphorus Deficiency in *Brassica napus*. *PLoS One* **8,** e54559.

Shrivastava, A., and Gupta, V. (2011). Methods for the determination of limit of detection and limit of quantitation of the analytical methods. *Chronicles of Young Scientists* **2,** 21-25.

Shukla, A. K., and Futrell, J. H. (2000). Tandem mass spectrometry: dissociation of ions by collisional activation. *Journal of Mass Spectrometry* **35,** 1069 - 1090.

Sieling, K., and Kage, H. (2010). Efficient N management using winter oilseed rape. A review. *Agronomy for Sustainable Development* **30,** 271-279.

Simpson, R. J. (1986). Translocation and metabolism of nitrogen: whole plant aspects. In *Fundamental, ecological and agricultural aspects of nitrogen metabolism in higher plants*, H. Lambers, J.J. Neeteson, and I. Stulen, eds (Dordrecht: Springer Netherlands), pp. 71-96.

Sirover, M. A. (2011). On the functional diversity of glyceraldehyde-3-phosphate dehydrogenase: Biochemical mechanisms and regulatory control. *Biochimica et Biophysica Acta (BBA) - General Subjects* **1810,** 741-751.

Skoog, D. A., Holler, F. J., and Nieman, T. A. (1998). *Principles of instrumental analysis*. 5th ed. (Orlando, Florida: Harcourt Brace).

Smith, B. E. (2002). Nitrogenase reveals its inner secrets. *Science* **297,** 1654.

Snowdon, R., Lühs, W., and Friedt, W. (2007). Oilseed Rape. In *Oilseeds*, C. Kole, ed (Berlin, Heidelberg: Springer Berlin Heidelberg), pp. 55-114.

Sperrazza, J. M., and Spremulli, L. L. (1983). Quantitation of cation binding to wheat germ ribosomes: Influences on submit association equilibria and ribosome activity. *Nucleic Acids Research* **11,** 2665-2679.

Staswick, P. E. (1990). Novel Regulation of Vegetative Storage Protein Genes. *The Plant Cell* **2,** 1-6.

Staswick, P. E. (1994). Storage Proteins of Vegetative Plant Tissues. *Annual Review of Plant Physiology and Plant Molecular Biology* **45,** 303-322.

Steen, H., and Mann, M. (2004). The abc's (and xyz's) of peptide sequencing. *Nature Review Molecular Cell Biology* **5,** 699-711.

Stepien, V., Sauter, J. J., and Martin, F. (1994). Vegetative storage proteins in woody plants. *Plant Physiology and Biochemistry* **32,** 185-192.

Suelter, C. H. (1970). Enzymes Activated by Monovalent Cations. *Science* **168,** 789-795.

Surinova, S., Hüttenhain, R., Chang, C.-Y., Espona, L., Vitek, O., and Aebersold, R. (2013). Automated selected reaction monitoring data analysis workflow for large-scale targeted proteomic studies. *Nature Protocols* **8,** 1602-1619.

Svečnjak, Z., and Rengel, Z. (2006a). Canola cultivars differ in nitrogen utilization efficiency at vegetative stage. *Field Crops Research* **97,** 221-226.

Svečnjak, Z., and Rengel, Z. (2006b). Nitrogen Utilization Efficiency in Canola Cultivars at Grain Harvest. *Plant and Soil* **283,** 299-307.

Syka, J. E. P., Coon, J. J., Schroeder, M. J., Shabanowitz, J., and Hunt, D. F. (2004). Peptide and protein sequence analysis by electron transfer dissociation mass spectrometry. *Proceedings of the National Academy of Sciences of the United States of America* **101,** 9528-9533.

Sylvester-Bradley, R., and Makepeace, R. J. (1984). A code for stages of development in oilseed rape (*Brassica napus* L.). *Aspects of Applied Biology* **6,** 399-419.

Sylvester-Bradley, R., and Kindred, D. R. (2009). Analysing nitrogen responses of cereals to prioritize routes to the improvement of nitrogen use efficiency. *Journal of Experimental Botany* **60,** 1939-1951.

Tanksley, S. D. (1993). Mapping Polygenes. *Annual Review of Genetics* **27,** 205-233.

Tegeder, M., and Rentsch, D. (2010). Uptake and partitioning of amino acids and peptides. *Molecular Plant* **3,** 997-1011.

Thiede, B., Höhenwarter, W., Krah, A., Mattow, J., Schmid, M., Schmidt, F., and Jungblut, P. R. (2005). Peptide mass fingerprinting. *Methods* **35,** 237-247.

Thomas, C. L., Alcock, T. D., Graham, N. S., Hayden, R., Matterson, S., Wilson, L., Young, S. D., Dupuy, L. X., White, P. J., Hammond, J. P., Danku, J. M. C., Salt, D. E., Sweeney, A., Bancroft, I., and Broadley, M. R. (2016). Root morphology and seed and leaf ionomic traits in a *Brassica napus* L. diversity panel show wide phenotypic variation and are characteristic of crop habit. *BMC Plant Biology* **16,** 214.

Tian, W.-M., Peng, S.-Q., Wang, X.-C., Shi, M.-J., Chen, Y.-Y., and Hu, Z.-H. (2007). Vegetative storage protein in Litchi chinensis, a subtropical evergreen fruit tree, possesses trypsin inhibitor activity. *Annals of Botany* **100,** 1199-1208.

Tilsner, J., Kassner, N., Struck, C., and Lohaus, G. (2005). Amino acid contents and transport in oilseed rape (Brassica napus L.) under different nitrogen conditions. *Planta* **221,** 328-338.

Tsay, Y.-F., Chiu, C.-C., Tsai, C.-B., Ho, C.-H., and Hsu, P.-K. (2007). Nitrate transporters and peptide transporters. *FEBS Letters* **581,** 2290-2300.

Twining, S., and Clarke, J. (2009). Future of UK winter oilseed rape production. (Crop Protection Association Agricultural Industries Confederation: ADAS) [http://www.voluntaryinitiative.org.uk/_attachments/resources/1152_s4.pdf] Accessed 22 September 2015.

Ulas, A., Behrens, T., Wiesler, F., Horst, W. J., and Schulte auf'm Erley, G. (2013). Does genotypic variation in nitrogen remobilisation efficiency contribute to nitrogen efficiency of winter oilseed-rape cultivars (*Brassica napus* L.)? *Plant and Soil* **371,** 463-471.

Van Ooijen, J. W., and Kyazma, B. V. (2009). MapQTL 6.0: Software for the calculation of QTL positions on genetic maps (user manual). (Wageningen, the Netherland, from Plant Research International) Accessed 5 Febrauary 2016.

Vauclare, P., Kopriva, S., Fell, D., Suter, M., Sticher, L., Von Ballmoos, P., Krähenbühl, U., Den Camp, R. O., and Brunold, C. (2002). Flux control of sulphate assimilation in Arabidopsis thaliana: adenosine 5′-phosphosulphate reductase is more susceptible than ATP sulphurylase to negative control by thiols. *The Plant Journal* **31,** 729-740.

Voorrips, R. E. (2002). MapChart: Software for the Graphical Presentation of Linkage Maps and QTLs. *Journal of Heredity* **93,** 77-78.

Vreugdenhil, D., Aarts, M. G., and Koornneef, M. (2005). Exploring natural genetic variation to improve plant nutrient content. In *Plant Nutritional Genomics*, M.R. Broadley and P.J. White, eds, pp. 201-219.

Vreugdenhil, D., Aarts, M. G. M., Koornneef, M., Nelissen, H., and Ernst, W. H. O. (2004). Natural variation and QTL analysis for cationic mineral content in seeds of Arabidopsis thaliana. *Plant, Cell & Environment* **27,** 828-839.

Wagstaff, C., Yang, T. J. W., Stead, A. D., Buchanan-Wollaston, V., and Roberts, J. A. (2009). A molecular and structural characterization of senescing Arabidopsis siliques and comparison of transcriptional profiles with senescing petals and leaves. *The Plant Journal* **57,** 690-705.

Walker, D. J., Leigh, R. A., and Miller, A. J. (1996). Potassium homeostasis in vacuolate plant cells. *Proceedings of the National Academy of Sciences of the United States of America* **93,** 10510-10514.

Walker, J. M. (2009). SDS Polyacrylamide Gel Electrophoresis of Proteins. In *The Protein Protocols Handbook*, J.M. Walker, ed (Totowa, NJ: Humana Press), pp. 177-185.

Wang, N., Qian, W., Suppanz, I., Wei, L., Mao, B., Long, Y., Meng, J., Müller, A. E., and Jung, C. (2011a). Flowering time variation in oilseed rape (Brassica napus L.) is associated with allelic variation in the FRIGIDA homologue BnaA.FRI.a. *Journal of Experimental Botany*.

Wang, X., Wang, H., Long, Y., Liu, L., Zhao, Y., Tian, J., Zhao, W., Li, B., Chen, L., Chao, H., and Li, M. (2015). Dynamic and comparative QTL analysis for plant height in different developmental stages of Brassica napus L. *Theoretical and Applied Genetics* **128,** 1175-1192.

Wang, X., Wang, H., Wang, J., Sun, R., Wu, J., Liu, S., Bai, Y., Mun, J.-H., Bancroft, I., Cheng, F., Huang, S., Li, X., Hua, W., Wang, J., Wang, X., Freeling, M., Pires, J. C., Paterson, A. H., Chalhoub, B., Wang, B., *et al.* (2011b). The genome of the mesopolyploid crop species Brassica rapa. *Nature Genetics* **43,** 1035-1039.

Waters, B. M., and Grusak, M. A. (2008). Quantitative trait locus mapping for seed mineral concentrations in two *Arabidopsis thaliana* recombinant inbred populations. *New Phytologist* **179,** 1033-1047.

Webhofer, C., and Schrader, M. (2011). Chapter 7 Bioinformatic Tools for the LC-MS/MS Analysis of Proteins and Peptides. In *Protein and Peptide Analysis by LC-MS: Experimental Strategies*, (The Royal Society of Chemistry), pp. 87-103.

Weightman, R., Gladders, P., and Berry, P. (2010). Chapter 7 Oilseed Rape. In *Energy Crops*, N.G. Halford and A. Karp, eds (Cambridge: The Royal Society of Chemistry), pp. 116-147.

Westermeier, R., Naven, T., and Höpker, H.-R. (2008a). Mass Spectrometry. In *Proteomics in Practice*, 2nd ed., (Wiley-VCH Verlag GmbH & Co. KGaA), pp. 215-272.

Westermeier, R., Naven, T., and Höpker, H.-R. (2008b). Liquid Chromatography Techniques. In *Proteomics in Practice*, 2nd ed., (Wiley-VCH Verlag GmbH & Co. KGaA), pp. 151-213.

White, P., George, T., Dupuy, L., Karley, A., Valentine, T., Wiesel, L., and Wishart, J. (2013). Root traits for infertile soils. *Frontiers in Plant Science* **4**.

White, P. J. (2012a). Chapter 3 - Long-distance Transport in the Xylem and Phloem A2 - Marschner, Petra. In *Marschner's Mineral Nutrition of Higher Plants (Third Edition)*, (San Diego: Academic Press), pp. 49-70.

White, P. J. (2012b). Chapter 2 - Ion Uptake Mechanisms of Individual Cells and Roots: Short-distance Transport A2 - Marschner, Petra. In *Marschner's Mineral Nutrition of Higher Plants (Third Edition)*, (San Diego: Academic Press), pp. 7-47.

White, P. J., and Broadley, M. R. (2003). Calcium in Plants. *Annals of Botany* **92,** 487-511.

White, P. J., and Brown, P. H. (2010). Plant nutrition for sustainable development and global health. *Annals of Botany* **105,** 1073-1080.

White, P. J., Bowen, H. C., Farley, E., Shaw, E. K., Thompson, J. A., Wright, G., and Broadley, M. R. (2015). Phylogenetic effects on shoot magnesium concentration. *Crop and Pasture Science* **66,** 1241-1248.

White, P. J., Hammond, J. P., King, G. J., Bowen, H. C., Hayden, R. M., Meacham, M. C., Spracklen, W. P., and Broadley, M. R. (2010). Genetic analysis of potassium use efficiency in Brassica oleracea. *Annals of Botany* **105,** 1199-1210.

Wilkins, M. R., Sanchez, J.-C., Gooley, A. A., Appel, R. D., Humphery-Smith, I., Hochstrasser, D. F., and Williams, K. L. (1996). Progress with Proteome Projects: Why all Proteins Expressed by a Genome Should be Identified and How To Do It. *Biotechnology and Genetic Engineering Reviews* **13,** 19-50.

Willems, G., Dräger, D. B., Courbot, M., Godé, C., Verbruggen, N., and Saumitou-Laprade, P. (2007). The Genetic Basis of Zinc Tolerance in the Metallophyte *Arabidopsis halleri* ssp. *halleri* (Brassicaceae): An Analysis of Quantitative Trait Loci. *Genetics* **176,** 659-674.

Willems, G., Frérot, H., Gennen, J., Salis, P., Saumitou-Laprade, P., and Verbruggen, N. (2010). Quantitative trait loci analysis of mineral element concentrations in an *Arabidopsis halleri* × *Arabidopsis lyrata petraea* F2 progeny grown on cadmium-contaminated soil. *New Phytologist* **187,** 368-379.

Wink, M. (2006). Tandem Mass Spectrometers. In *An Introduction to Molecular Biotechnology : Molecular Fundamental Methods and Applications in Modern Biotechnology*, M. Wink, ed (Germany: Wiley-Verlag), pp. 155 - 156.

Wisniewski, J. R., Zougman, A., Nagaraj, N., and Mann, M. (2009). Universal sample preparation method for proteome analysis. *Nature Methods* **6,** 359-362.

Wissuwa, M., Wegner, J., Ae, N., and Yano, M. (2002). Substitution mapping of Pup1: a major QTL increasing phosphorus uptake of rice from a phosphorus-deficient soil. *Theoretical and Applied Genetics* **105,** 890-897.

Wittenbach, V. A. (1983). Purification and characterization of a soybean leaf storage glycoprotein. *Plant Physiology* **73,** 125-129.

Wolters, D. A., Washburn, M. P., and Yates, J. R. (2001). An Automated Multidimensional Protein Identification Technology for Shotgun Proteomics. *Analytical Chemistry* **73,** 5683-5690.

Woods, J., Williams, A., Hughes, J. K., Black, M., and Murphy, R. (2010). Energy and the food system. *Philosophical Transactions of the Royal Society of London B: Biological Sciences* **365,** 2991-3006.

Wu, J., Schat, H., Sun, R., Koornneef, M., Wang, X., and Aarts, M. G. M. (2007). Characterization of natural variation for zinc, iron and manganese accumulation and zinc exposure response in *Brassica rapa* L. *Plant and Soil* **291,** 167-180.

Wu, J., Yuan, Y.-X., Zhang, X.-W., Zhao, J., Song, X., Li, Y., Li, X., Sun, R., Koornneef, M., Aarts, M. G. M., and Wang, X.-W. (2008). Mapping QTLs for mineral accumulation and shoot dry biomass under different Zn nutritional conditions in Chinese cabbage (*Brassica rapa* L. ssp. *pekinensis*). *Plant and Soil* **310,** 25-40.

Wu, L., Candille, S. I., Choi, Y., Xie, D., Li-Pook-Than, J., Tang, H., and Snyder, M. (2013). Variation and Genetic Control of Protein Abundance in Humans. *Nature* **499,** 79-82.

Wu, S., Feng, X., and Wittmeier, A. (1997). Microwave Digestion of Plant and Grain Reference Materials in Nitric Acid or a Mixture of Nitric Acid or a Mixture of Nitric Acid and Hydrogen Peroxide for the Determination of Multi-elements by Inductively Coupled Plasma Mass Spectrometry. *Journal of Analytical Atomic Spectrometry* **12,** 797-806.

Xu, F., Sun, X., Chen, Y., Huang, Y., Tong, C., and Bao, J. (2015). Rapid Identification of Major QTLs Associated with Rice Grain Weight and Their Utilization. *PLoS One* **10,** e0122206.

Xu, G., Fan, X., and Miller, A. J. (2012). Plant Nitrogen Assimilation and Use Efficiency. *Annual Review of Plant Biology* **63,** 153-182.

Yang, M., Ding, G., Shi, L., Feng, J., Xu, F., and Meng, J. (2010). Quantitative trait loci for root morphology in response to low phosphorus stress in *Brassica napus*. *Theoretical and Applied Genetics* **121,** 181-193.

Yates, J. R. (2004). Mass Spectral Analysis in Proteomics. *Annual Review of Biophysics and Biomolecular Structure* **33,** 297-316.

Yi, B., Chen, W., Ma, C., Fu, T., and Tu, J. (2006). Mapping of quantitative trait loci for yield and yield components in Brassica napus L. *Zuo wu xue bao* **32,** 676-682.

Yiu, S. H., Poon, H., Fulcher, R. G., and Altosaar, I. (1982). The Microscopic Structure and Chemistry of Rapeseed and its Products. *Food Structure* **1,** 135-143.

Young, V. (1989). Instrumental Methods of Analysis, Seventh Edition (Dean, John A.; Merritt, Lynne L., Jr.; Settle, Frank A., Jr.; Willard, Hobart H.). *Journal of Chemical Education* **66,** A46.

Zhang, D., Zhao, H., Shi, L., and Xu, F. (2014). Physiological and genetic responses to boron deficiency in Brassica napus: A review. *Soil Science and Plant Nutrition* **60,** 304-313.

Zhang, H., Feng, J., Hwang, S. F., Strelkov, S. E., Falak, I., Huang, X., and Sun, R. (2016a). Mapping of clubroot (Plasmodiophora brassicae) resistance in canola (Brassica napus). *Plant Pathology* **65,** 435-440.

Zhang, W., and Chait, B. T. (2000). ProFound: An expert system for protein identification using mass spectrometric peptide mapping information. *Analytical Chemistry* **72,** 2482-2489.

Zhang, Y., Fonslow, B. R., Shan, B., Baek, M.-C., and Yates, J. R. (2013). Protein Analysis by Shotgun/Bottom-up Proteomics. *Chemical Reviews* **113,** 2343-2394.

Zhang, Y., Thomas, C. L., Xiang, J., Long, Y., Wang, X., Zou, J., Luo, Z., Ding, G., Cai, H., Graham, N. S., Hammond, J. P., King, G. J., White, P. J., Xu, F., Broadley, M. R., Shi, L., and Meng, J. (2016b). QTL meta-analysis of root traits in *Brassica napus* under contrasting phosphorus supply in two growth systems. *Scientific Reports* **6,** 33113.

Zhang, Z.-H., Song, H.-X., Liu, Q., Rong, X.-M., Peng, J.-W., Xie, G.-X., Zhang, Y.-P., and Guan, C.-Y. (2010). Nitrogen Redistribution Characteristics of Oilseed Rape (Brassica napus L.). Varieties with Different Nitrogen-Use Efficiencies during Later Growth Period. *Communications in Soil Science and Plant Analysis* **41,** 1693-1706.

Zhao, J., and Meng, J. (2003). Genetic analysis of loci associated with partial resistance to Sclerotinia sclerotiorum in rapeseed (*Brassica napus* L.). *Theoretical and Applied Genetics* **106,** 759-764.

Zhao, Z., Wu, L., Nian, F., Ding, G., Shi, T., Zhang, D., Shi, L., Xu, F., and Meng, J. (2012). Dissecting Quantitative Trait Loci for Boron Efficiency across Multiple Environments in *Brassica napus*. *PLoS One* **7,** e45215.

Zhou, Q.-H., Fu, D.-H., Mason, A. S., Zeng, Y.-J., Zhao, C.-X., and Huang, Y.-J. (2014). In silico integration of quantitative trait loci for seed yield and yield-related traits in *Brassica napus*. *Molecular Breeding* **33,** 881-894.

Zubarev, R. (2006). Protein primary structure using orthogonal fragmentation techniques in Fourier transform mass spectrometry. *Expert Review of Proteomics* **3,** 251-261.

Zubarev, R. A., Kelleher, N. L., and McLafferty, F. W. (1998). Electron Capture Dissociation of Multiply Charged Protein Cations. A Nonergodic Process. *Journal of the American Chemical Society* **120,** 3265-3266.

Appendices

Appendix 1 N concentration at two growth stages GS 6.2/6.3 and Harvest

Table 1, averaged N concentration (%DW) in seven tissue types among 14 genotypes of *B.napus* at the growth stage GS 6.2/6.3.

Variety	L.root	T.root B	T.root T	Stem B	Stem M	Stem T	Seeds
Canberra	0.201	0.107	0.126	0.438	0.156	0.399	2.401
Darmor	0.258	0.142	0.140	0.527	0.189	0.514	2.550
FD502	0.142	0.081	0.086	0.679	0.135	0.408	2.410
Grizzly	0.125	0.111	0.101	0.457	0.143	0.333	2.530
Lioness	0.167	0.136	0.115	0.597	0.134	0.343	2.304
NK Bravour	0.107	0.086	0.097	0.523	0.178	0.336	2.324
Ningyou 7	0.468	0.295	0.332	0.813	0.124	0.246	3.378
PR45-D01	0.193	0.130	0.140	0.651	0.116	0.265	2.478
Royal	0.138	0.086	0.070	0.663	0.119	0.370	2.508
Sun	0.148	0.087	0.097	0.369	0.114	0.322	2.779
Tapidor ADAS	0.136	0.129	0.127	0.718	0.155	0.363	2.600
Tapidor DH	0.184	0.139	0.178	0.903	0.236	0.265	2.903
Winner	0.221	0.149	0.178	0.550	0.120	0.326	2.143
Yudal	0.258	0.136	0.156	0.565	0.166	0.271	2.989
mean	0.196	0.129	0.139	0.604	0.149	0.340	2.593

Appendix 1

Table 2, averaged N concentration (%DW) in seven tissue types among three crop types and 30 genotypes of *B.napus* at the harvest.

Croptype	Variety	T.root B	T.root T	L.root	Stem B	Stem M	Stem T	Seeds
Spring OSR	**Cubs Root DH1**	0.407	0.484	0.557	0.353	0.221	0.243	2.752
Spring OSR	**Drakkar**	0.319	0.356	0.351	0.277	0.244	0.212	2.160
Spring OSR	**Regina II DH1**	0.291	0.347	0.317	0.231	0.146	0.150	3.772
Spring OSR	**Stellar DH**	0.259	0.274	0.308	0.167	0.082	0.077	2.275
Spring OSR	**Yudal**	0.292	0.248	0.403	0.386	0.398	0.157	2.613
Spring OSR	**mean**	**0.314**	**0.342**	**0.387**	**0.283**	**0.218**	**0.168**	**2.714**
Swede	**Best of All**	0.231	0.286	0.561	0.046	0.069	0.028	2.042
Swede	**Drummonds PT**	0.214	0.368	0.301	0.072	0.039	0.047	2.983
Swede	**Jaune**	0.311	0.360	0.462	0.131	0.097	0.102	2.490
Swede	**Petranova**	0.287	0.289	0.383	0.221	0.129	0.097	2.270
Swede	**Turnip Hybrid**	0.337	0.381	0.437	0.136	0.120	0.123	2.711
Swede	**Vige DH1**	0.454	0.831	NA	0.184	0.130	0.123	2.675
Swede	**mean**	**0.306**	**0.419**	**0.429**	**0.132**	**0.097**	**0.087**	**2.529**
Winter OSR	**Canberra**	0.332	0.378	0.407	0.393	0.267	0.235	2.386
Winter OSR	**Darmor**	0.244	0.169	0.282	0.269	0.154	0.159	2.456
Winter OSR	**English Giant DH1**	0.150	0.174	0.231	0.126	0.109	0.093	3.847
Winter OSR	**FD502**	0.316	0.261	0.361	0.344	0.321	0.253	2.593
Winter OSR	**Grizzly**	0.251	0.254	0.304	0.341	0.252	0.232	2.346
Winter OSR	**Lioness**	0.260	0.224	0.312	0.317	0.197	0.183	2.003
Winter OSR	**NK Bravour**	0.264	0.236	0.296	0.269	0.168	0.159	2.318
Winter OSR	**Ningyou 7**	0.503	0.487	0.672	0.438	0.259	0.213	3.060
Winter OSR	**PI271452**	0.243	0.178	0.283	0.208	0.138	0.075	1.810
Winter OSR	**PR45-D01**	0.286	0.221	0.385	0.217	0.170	0.171	2.663
Winter OSR	**Red Russian**	0.349	0.388	0.496	0.233	0.166	0.156	2.958
Winter OSR	**Royal**	0.199	0.231	0.305	0.322	0.275	0.240	1.948
Winter OSR	**Sun**	0.339	0.370	0.371	0.414	0.256	0.220	2.041
Winter OSR	**TN145**	0.187	0.173	0.280	0.172	0.127	0.088	2.616
Winter OSR	**TN172**	0.200	0.225	0.268	0.203	0.107	0.090	2.746
Winter OSR	**Tapidor ADAS**	0.346	0.310	0.404	0.422	0.252	0.257	1.862
Winter OSR	**Tapidor DH**	0.375	0.411	0.378	0.369	0.194	0.197	2.947
Winter OSR	**Temple**	0.118	0.185	0.212	0.117	0.075	0.085	1.679
Winter OSR	**Winner**	0.250	0.263	0.301	0.231	0.151	0.172	1.762
Winter OSR	**mean**	**0.274**	**0.270**	**0.345**	**0.284**	**0.191**	**0.173**	**2.423**
Overall mean		**0.287**	**0.312**	**0.367**	**0.254**	**0.177**	**0.155**	**2.493**

Appendix 2 Analysis of variance of all mineral nutrients at GS 6.2/6.3

Table 1, ANOVA tables for six macronutrients; P, K, Ca, Mg, S and Na with proportion of partial and total variance reported as ω^2_p and ω^2, respectively. The colon represents interaction between factors.

			P				
Source of variation	**df**	**SS**	**MS**	**F value**	**P value**	**ω²p**	**ω²**
Tissue	6	37.245	6.2075	733.41	2.4E-131	0.9373	0.8813
Variety	13	0.7809	0.0601	7.0969	3.0E-11	0.2123	0.0159
Tissue:Variety	78	2.5112	0.0322	3.8037	2.5E-14	0.4266	0.0439
Residuals	196	1.6589	0.0085				
Total	293	42.196					
			K				
Tissue	6	63.998	10.666	428.81	8.4E-110	0.8972	0.7918
Variety	13	5.2464	0.4036	16.225	8.6E-25	0.4023	0.0610
Tissue:Variety	78	6.4977	0.0833	3.3491	5.3E-12	0.3839	0.0565
Residuals	196	4.8753	0.0249				
Total	293	80.617					
			Ca				
Tissue	6	7931.2	1321.9	1467.1	6.4E-160	0.9677	0.9471
Variety	13	43.995	3.3843	3.7562	2.3E-05	0.1086	0.0039
Tissue:Variety	78	215.44	2.7620	3.0655	1.6E-10	0.3540	0.0173
Residuals	196	176.59	0.9010				
Total	293	8367.2					
			Mg				
Tissue	6	1.3626	0.2271	1175.7	9.9E-151	0.9600	0.8775
Variety	13	0.0407	0.0031	16.194	9.4E-25	0.4019	0.0246
Tissue:Variety	78	0.1103	0.0014	7.3214	9.8E-30	0.6265	0.0614
Residuals	196	0.0379	0.0002				
Total	293	1.5515					
			S				
Tissue	6	3.4947	0.5824	424.91	1.9E-109	0.8964	0.6655
Variety	13	0.7232	0.0556	40.584	1.7E-48	0.6364	0.1346
Tissue:Variety	78	0.7513	0.0096	7.0265	1.3E-28	0.6152	0.1230
Residuals	196	0.2687	0.0014				
Total	293	5.2378					
			Na				
Tissue	6	2.3678	0.3946	112.03	1.4E-60	0.6938	0.5261
Variety	13	0.6660	0.0512	14.542	1.4E-22	0.3745	0.1390
Tissue:Variety	78	0.7327	0.0094	2.6668	2.1E-08	0.3066	0.1027
Residuals	196	0.6904	0.0035				
Total	293	4.4570					

Appendix 2

Table 2, ANOVA tables for five micronutrients; B, Cu, Fe, Mn and Zn with proportion of partial and total variance reported as ω^2_p and ω^2, respectively. The colon represents interaction between treatment factors.

Source of variation	df	SS	MS	F value	P value	ω²p	ω²
B							
Tissue	6	776.90	129.48	138.19	1.2E-67	0.7368	0.4628
Variety	13	311.13	23.933	25.542	2.0E-35	0.5204	0.1794
Tissue:Variety	78	393.80	5.0487	5.3882	7.6E-22	0.5379	0.1925
Residuals	196	183.65	0.9370				
Total	293	1665.5					
Cu							
Tissue	6	83.109	13.852	106.60	5.6E-59	0.6830	0.3431
Variety	13	21.256	1.6351	12.583	7.8E-20	0.3387	0.0815
Tissue:Variety	78	110.02	1.4106	10.855	2.2E-41	0.7233	0.4162
Residuals	196	25.469	0.1299				
Total	293	239.86					
Fe							
Tissue	6	572619	95436	352.92	3.6E-102	0.8778	0.7585
Variety	13	16818	1293.7	4.7838	3.3E-07	0.1433	0.0177
Tissue:Variety	78	110093	1411.4	5.2194	4.3E-21	0.5282	0.1182
Residuals	196	53003	270.42				
Total	293	752532					
Mn							
Tissue	6	16320	2720.0	969.10	9.4E-143	0.9518	0.8800
Variety	13	731.43	56.264	20.047	1.8E-29	0.4572	0.0375
Tissue:Variety	78	921.96	11.820	4.2114	2.3E-16	0.4600	0.0379
Residuals	196	550.11	2.8067				
Total	293	18523					
Zn							
Tissue	6	37023	6170.5	583.16	4.6E-122	0.9373	0.8647
Variety	13	1304.5	100.34	9.4832	3.7E-15	0.2123	0.0273
Tissue:Variety	78	2329.7	29.868	2.8228	3.1E-09	0.4266	0.0352
Residuals	196	2073.9	10.581				
Total	293	42731.2					

Appendix 3 Macronutrient concentrations at the growth stages GS 6.2/6.3

Table 1, averaged **P** concentration (%DW) in seven tissue types among 14 genotypes of *B.napus* at GS 6.2/6.3.

Variety	L.root	T.root B	T.root T	Stem B	Stem M	Stem T	Seeds
Canberra	0.363	0.221	0.241	1.231	0.194	0.215	0.609
Darmor	0.325	0.253	0.284	1.750	0.147	0.289	0.519
FD502	0.130	0.103	0.068	1.219	0.150	0.196	0.635
Grizzly	0.206	0.113	0.098	1.263	0.177	0.154	0.670
Lioness	0.197	0.122	0.128	1.102	0.180	0.182	0.592
NK Bravour	0.270	0.171	0.181	1.365	0.303	0.204	0.613
Ningyou 7	0.425	0.243	0.280	0.919	0.145	0.147	0.678
PR45-D01	0.295	0.236	0.273	1.312	0.257	0.175	0.582
Royal	0.171	0.127	0.141	1.413	0.192	0.256	0.630
Sun	0.248	0.159	0.177	0.831	0.247	0.175	0.592
Tapidor ADAS	0.152	0.174	0.181	0.969	0.215	0.140	0.577
Tapidor DH	0.146	0.130	0.130	1.173	0.143	0.219	0.795
Winner	0.141	0.165	0.201	1.103	0.129	0.134	0.523
Yudal	0.112	0.091	0.100	0.932	0.167	0.174	0.663
mean	**0.227**	**0.165**	**0.177**	**1.184**	**0.189**	**0.190**	**0.620**

Table 2, averaged **K** concentration (%DW) in seven tissue types among 14 genotypes of *B.napus* at GS 6.2/6.3.

Variety	L.root	T.root B	T.root T	Stem B	Stem M	Stem T	Seeds
Canberra	1.262	0.931	0.963	0.202	1.703	1.592	1.031
Darmor	1.480	1.211	1.301	0.204	2.292	1.747	1.103
FD502	0.711	0.637	0.575	0.103	1.698	1.335	1.066
Grizzly	1.014	0.762	0.721	0.162	1.531	1.870	1.059
Lioness	0.868	0.582	0.603	0.147	1.374	1.243	0.965
NK Bravour	0.741	0.664	0.596	0.243	1.918	1.301	1.082
Ningyou 7	1.180	0.937	0.908	0.232	1.659	0.767	1.184
PR45-D01	0.990	0.887	0.916	0.221	2.021	1.201	1.071
Royal	0.963	0.782	0.904	0.156	1.922	1.218	1.033
Sun	0.813	0.734	0.636	0.202	1.638	0.979	1.085
Tapidor ADAS	0.987	0.947	0.906	0.167	2.360	1.427	1.035
Tapidor DH	1.000	0.872	0.841	0.157	1.945	1.609	1.003
Winner	0.805	0.969	1.009	0.124	1.715	1.350	0.986
Yudal	0.718	0.593	0.610	0.127	1.662	0.976	0.888
mean	**0.966**	**0.822**	**0.821**	**0.175**	**1.817**	**1.330**	**1.042**

Appendix 3

Table 3, averaged **Mg** concentration (%DW) in seven tissue types among 14 genotypes of *B.napus* at GS 6.2/6.3.

Variety	L.root	T.root B	T.root T	Stem B	Stem M	Stem T	Seeds
Canberra	0.151	0.103	0.106	0.109	0.104	0.059	0.270
Darmor	0.099	0.089	0.075	0.102	0.085	0.118	0.260
FD502	0.072	0.071	0.042	0.055	0.066	0.105	0.289
Grizzly	0.067	0.063	0.042	0.062	0.074	0.070	0.286
Lioness	0.094	0.073	0.071	0.070	0.071	0.058	0.257
NK Bravour	0.052	0.052	0.044	0.074	0.070	0.054	0.283
Ningyou 7	0.155	0.134	0.111	0.068	0.055	0.053	0.244
PR45-D01	0.089	0.093	0.079	0.065	0.090	0.045	0.263
Royal	0.061	0.051	0.052	0.073	0.069	0.083	0.284
Sun	0.078	0.082	0.056	0.047	0.067	0.048	0.277
Tapidor ADAS	0.077	0.064	0.053	0.052	0.065	0.044	0.281
Tapidor DH	0.075	0.095	0.067	0.150	0.090	0.072	0.264
Winner	0.099	0.109	0.114	0.076	0.076	0.049	0.249
Yudal	0.073	0.058	0.050	0.077	0.044	0.090	0.268
mean	**0.089**	**0.081**	**0.069**	**0.077**	**0.073**	**0.068**	**0.270**

Table 4, averaged **Ca** concentration (%DW) in seven tissue types among 14 genotypes of *B.napus* at GS 6.2/6.3.

Variety	L.root	T.root B	T.root T	Stem B	Stem M	Stem T	Seeds
Canberra	0.417	0.284	0.292	15.000	0.673	0.798	0.345
Darmor	0.536	0.274	0.359	14.801	0.640	1.351	0.287
FD502	0.400	0.231	0.248	15.536	0.588	1.383	0.383
Grizzly	0.369	0.247	0.247	12.255	0.553	0.863	0.326
Lioness	0.450	0.262	0.257	14.301	0.569	0.741	0.312
NK Bravour	0.287	0.247	0.266	17.115	0.615	0.718	0.360
Ningyou 7	0.890	0.354	0.368	14.923	0.610	1.219	0.361
PR45-D01	0.377	0.285	0.271	10.953	0.581	0.713	0.319
Royal	0.427	0.270	0.298	17.029	0.617	0.982	0.293
Sun	0.338	0.213	0.251	12.674	0.489	0.807	0.293
Tapidor ADAS	0.416	0.275	0.259	14.196	0.494	0.717	0.328
Tapidor DH	0.417	0.334	0.310	20.875	0.612	0.870	0.433
Winner	0.358	0.264	0.305	17.118	0.648	0.852	0.305
Yudal	0.643	0.414	0.380	17.717	0.574	1.981	0.402
mean	**0.452**	**0.282**	**0.294**	**15.321**	**0.590**	**1.000**	**0.339**

Appendix 3

Table 5, averaged **S** concentration (%DW) in seven tissue types among 14 genotypes of *B.napus* at GS 6.2/6.3.

Variety	L.root	T.root B	T.root T	Stem B	Stem M	Stem T	Seeds
Canberra	0.096	0.075	0.059	0.167	0.225	0.390	0.251
Darmor	0.190	0.106	0.100	0.273	0.302	0.425	0.442
FD502	0.084	0.061	0.049	0.131	0.209	0.484	0.305
Grizzly	0.064	0.045	0.042	0.150	0.183	0.349	0.316
Lioness	0.110	0.086	0.071	0.130	0.187	0.306	0.228
NK Bravour	0.041	0.046	0.038	0.141	0.156	0.247	0.249
Ningyou 7	0.226	0.183	0.172	0.146	0.189	0.369	0.660
PR45-D01	0.088	0.075	0.077	0.131	0.178	0.246	0.270
Royal	0.084	0.066	0.062	0.160	0.178	0.263	0.382
Sun	0.082	0.080	0.057	0.110	0.146	0.232	0.302
Tapidor ADAS	0.047	0.061	0.050	0.100	0.128	0.282	0.264
Tapidor DH	0.068	0.064	0.064	0.141	0.193	0.384	0.364
Winner	0.113	0.098	0.125	0.150	0.181	0.294	0.273
Yudal	0.126	0.088	0.090	0.247	0.319	0.459	0.671
mean	**0.101**	**0.081**	**0.075**	**0.155**	**0.198**	**0.338**	**0.355**

Table 6, averaged **Na** concentration (%DW) in seven tissue types among 14 genotypes of *B.napus* at GS 6.2/6.3.

Variety	L.root	T.root B	T.root T	Stem B	Stem M	Stem T	Seeds
Canberra	0.057	0.098	0.095	0.102	0.074	0.032	0.0038
Darmor	0.098	0.132	0.134	0.220	0.078	0.018	0.0044
FD502	0.156	0.235	0.222	0.413	0.233	0.049	0.0048
Grizzly	0.151	0.218	0.220	0.225	0.249	0.038	0.0040
Lioness	0.308	0.307	0.318	0.332	0.328	0.055	0.0040
NK Bravour	0.176	0.274	0.295	0.309	0.216	0.022	0.0041
Ningyou 7	0.189	0.235	0.246	0.306	0.214	0.024	0.0043
PR45-D01	0.106	0.154	0.172	0.161	0.120	0.022	0.0027
Royal	0.113	0.166	0.149	0.124	0.075	0.024	0.0026
Sun	0.118	0.193	0.212	0.189	0.169	0.021	0.0035
Tapidor ADAS	0.161	0.236	0.212	0.184	0.153	0.057	0.0040
Tapidor DH	0.259	0.323	0.312	0.311	0.277	0.044	0.0050
Winner	0.133	0.156	0.148	0.324	0.139	0.020	0.0031
Yudal	0.085	0.155	0.140	0.570	0.212	0.040	0.0029
mean	**0.151**	**0.206**	**0.205**	**0.269**	**0.181**	**0.033**	**0.0038**

Appendix 4 Micronutrient concentrations at the growth stages GS 6.2/6.3

Table 1, averaged **B** concentration (µg/g DW) in seven tissue types among 14 genotypes of *B.napus* at GS 6.2/6.3.

Variety	L.root	T.root B	T.root T	Stem B	Stem M	Stem T	Seeds
Canberra	9.45	6.64	6.29	6.96	10.61	10.77	9.08
Darmor	11.00	8.76	9.10	16.14	11.37	14.03	11.92
FD502	7.58	6.35	6.50	9.54	9.96	12.44	11.38
Grizzly	9.23	7.16	7.35	7.81	11.14	11.98	12.22
Lioness	9.65	6.44	6.91	7.50	9.89	11.47	7.41
NK Bravour	6.77	6.22	6.22	7.37	10.83	8.98	10.13
Ningyou 7	9.48	6.37	6.57	6.93	9.42	10.54	10.42
PR45-D01	8.47	6.60	6.26	6.94	11.64	10.65	11.04
Royal	7.39	6.49	6.68	7.01	9.93	11.92	10.10
Sun	6.84	5.86	6.23	5.20	9.25	10.43	11.85
Tapidor ADAS	8.22	6.84	6.54	5.13	9.78	9.82	9.36
Tapidor DH	11.76	9.40	8.84	7.99	11.21	11.35	11.57
Winner	6.61	5.82	5.45	11.30	9.64	11.09	8.88
Yudal	10.97	7.81	7.63	10.31	9.19	14.49	8.77
mean	**8.82**	**6.91**	**6.90**	**8.30**	**10.28**	**11.43**	**10.30**

Table 2, averaged **Cu** concentration (µg/g DW) in seven tissue types among 14 genotypes of *B.napus* at GS 6.2/6.3.

Variety	L.root	T.root B	T.root T	Stem B	Stem M	Stem T	Seeds
Canberra	3.02	2.76	3.05	2.61	1.64	2.14	3.45
Darmor	3.17	1.80	1.79	3.47	1.98	2.43	4.30
FD502	2.52	1.55	1.09	3.53	2.27	1.94	3.75
Grizzly	1.98	1.36	1.18	2.72	2.80	2.54	4.50
Lioness	4.98	2.86	2.70	2.71	2.17	1.97	3.59
NK Bravour	2.01	1.87	1.47	3.02	3.33	1.93	3.98
Ningyou 7	4.14	4.51	4.30	3.58	1.51	2.20	3.15
PR45-D01	2.10	1.90	1.59	3.26	2.47	1.87	3.27
Royal	2.00	1.72	1.92	2.56	2.54	2.27	2.81
Sun	2.23	1.95	2.05	2.68	2.35	2.23	4.19
Tapidor ADAS	4.23	1.68	1.36	2.76	3.16	2.07	3.30
Tapidor DH	3.11	2.01	2.32	3.15	1.80	2.30	3.20
Winner	2.01	2.60	2.34	3.88	1.78	2.04	2.73
Yudal	3.92	2.28	1.99	3.79	1.31	1.83	2.59
Mean	**2.96**	**2.21**	**2.08**	**3.12**	**2.22**	**2.13**	**3.49**

Appendix 4

Table 3, averaged **Fe** concentration (µg/g DW) in seven tissue types among 14 genotypes of *B.napus* at GS 6.2/6.3.

Variety	L.root	T.root B	T.root T	Stem B	Stem M	Stem T	Seeds
Canberra	190.7	91.4	67.3	9.6	28.9	26.0	56.0
Darmor	136.7	110.2	87.5	28.7	25.8	88.5	50.1
FD502	146.6	147.4	88.7	27.4	32.2	85.6	61.3
Grizzly	130.2	95.2	66.5	21.0	26.1	23.7	61.8
Lioness	144.1	131.1	111.6	19.9	28.8	26.6	54.6
NK Bravour	71.2	167.2	135.6	18.8	41.2	28.2	56.0
Ningyou 7	145.8	139.9	91.6	49.2	15.6	41.5	51.4
PR45-D01	141.9	100.6	73.9	13.6	24.3	29.1	54.5
Royal	139.5	122.4	104.8	15.8	38.4	32.4	60.8
Sun	63.9	143.7	105.3	10.1	27.6	23.1	60.7
Tapidor ADAS	148.7	160.6	98.6	22.2	76.3	24.0	56.0
Tapidor DH	202.9	120.6	116.9	22.4	35.2	26.7	48.9
Winner	171.4	138.4	70.9	15.7	30.9	26.7	52.0
Yudal	128.6	93.3	98.6	24.4	23.7	41.7	51.6
mean	**140.2**	**125.9**	**94.1**	**21.3**	**32.5**	**37.4**	**55.4**

Table 4, averaged **Mn** concentration (µg/g DW) in seven tissue types among 14 genotypes of *B.napus* at GS 6.2/6.3.

Variety	L.root	T.root B	T.root T	Stem B	Stem M	Stem T	Seeds
Canberra	14.94	7.64	7.07	0.66	9.21	11.09	25.90
Darmor	9.93	5.53	5.42	0.70	4.94	9.85	23.60
FD502	11.76	6.76	5.64	0.50	7.14	17.56	29.34
Grizzly	10.28	5.46	3.94	0.53	5.29	8.04	24.07
Lioness	9.82	9.45	8.21	0.47	7.43	10.69	28.44
NK Bravour	7.58	7.05	7.70	0.53	9.05	11.23	28.19
Ningyou 7	11.37	7.07	5.27	0.53	4.23	6.48	23.09
PR45-D01	8.50	4.82	4.05	0.48	4.12	5.07	23.18
Royal	18.25	10.79	8.67	0.57	10.26	14.85	25.14
Sun	10.44	8.05	7.63	0.47	6.96	10.79	27.24
Tapidor ADAS	10.40	8.23	8.37	0.38	8.94	12.38	29.90
Tapidor DH	11.53	9.74	7.02	0.62	9.78	8.80	25.99
Winner	13.85	8.27	7.04	0.62	8.30	8.58	27.28
Yudal	21.86	9.54	10.79	0.57	5.62	11.09	29.67
mean	**12.18**	**7.74**	**6.92**	**0.54**	**7.23**	**10.46**	**26.50**

Appendix 4

Table 5, averaged **Zn** concentration (µg/g DW) in seven tissue types among 14 genotypes of *B.napus* at GS 6.2/6.3.

Variety	L.root	T.root B	T.root T	Stem B	Stem M	Stem T	Seeds
Canberra	11.65	8.34	6.63	8.96	8.76	8.54	36.60
Darmor	12.13	8.45	5.10	14.68	12.16	8.67	34.94
FD502	8.95	7.11	4.01	6.51	6.07	23.26	43.02
Grizzly	8.62	6.84	4.09	7.66	8.70	11.47	46.77
Lioness	11.00	6.78	5.44	7.78	6.81	8.84	38.79
NK Bravour	6.69	7.12	5.21	8.15	7.98	11.16	43.76
Ningyou 7	13.95	11.44	9.09	8.19	5.09	8.99	45.20
PR45-D01	7.90	5.97	4.05	7.10	5.72	5.61	33.59
Royal	8.76	8.64	5.97	8.61	9.26	11.58	42.94
Sun	9.85	7.23	5.29	20.34	4.94	7.23	42.21
Tapidor ADAS	9.36	7.68	5.79	6.03	6.46	8.05	41.33
Tapidor DH	13.76	11.61	9.07	16.22	13.94	13.15	51.33
Winner	8.32	6.76	6.10	2.37	4.28	7.31	30.13
Yudal	9.49	6.20	6.15	9.53	7.44	6.83	33.69
mean	**10.03**	**7.87**	**5.86**	**9.44**	**7.69**	**10.05**	**40.31**

Appendix 5 Analysis of variance of all mineral nutrients at harvest

Table 1, ANOVA tables for six macronutrients; P, K, Mg, Ca, S and Na with proportion of partial and total variance reported as ω^2_p and ω^2, respectively. The colon represents interaction between treatment factors.

P							
Source of variation	**df**	**SS**	**MS**	**F value**	**P value**	**ω²p**	**ω²**
Croptype	2	0.1315	0.0657	20.764	1.6E-09	0.037	0.002
Tissue	6	60.657	10.110	3193.5	0.0E+00	0.949	0.868
Croptype:Variety	27	1.4865	0.0551	17.392	2.0E-63	0.299	0.020
Croptype:Tissue	12	1.3815	0.1151	36.367	4.0E-68	0.290	0.019
Croptype:Variety:Tissue	161	3.5507	0.0221	6.9667	2.0E-80	0.481	0.044
Residuals	828	2.6211	0.0032				
Total	1036	69.8					
K							
Croptype	2	11.218	5.6090	50.217	2.6E-21	0.087	0.029
Tissue	6	149.78	24.964	223.50	2.4E-169	0.563	0.387
Croptype:Variety	27	50.122	1.8564	16.620	1.1E-60	0.289	0.122
Croptype:Tissue	12	11.364	0.9470	8.4786	2.7E-15	0.080	0.026
Croptype:Variety:Tissue	161	70.300	0.4366	3.9092	6.1E-38	0.311	0.136
Residuals	828	92.484	0.1117				
Total	1036	385.3					
Mg							
Croptype	2	0.0723	0.0361	103.20	9.7E-41	0.165	0.017
Tissue	6	3.2406	0.5401	1541.9	0.0E+00	0.899	0.752
Croptype:Variety	27	0.1312	0.0049	13.869	1.5E-50	0.251	0.028
Croptype:Tissue	12	0.1699	0.0142	40.432	8.8E-75	0.313	0.039
Croptype:Variety:Tissue	161	0.4002	0.0025	7.0959	4.7E-82	0.486	0.080
Residuals	828	0.2900	0.0004				
Total	1036	4.3					
Ca							
Croptype	2	4.6553	2.3276	102.41	1.8E-40	0.164	0.069
Tissue	6	15.838	2.6397	116.14	2.9E-106	0.400	0.234
Croptype:Variety	27	6.5287	0.2418	10.639	5.0E-38	0.201	0.088
Croptype:Tissue	12	6.5531	0.5461	24.026	2.4E-46	0.210	0.094
Croptype:Variety:Tissue	161	14.545	0.0903	3.9748	6.5E-39	0.316	0.163
Residuals	828	18.820	0.0227				
Total	1036	66.9					

Appendix 5

Table 2, Continued

	df	SS	MS	F value	P value	ω²p	ω²
S							
Croptype	2	0.9728	0.4864	189.49	1.7E-68	0.267	0.040
Tissue	6	9.3067	1.5511	604.23	1.8E-298	0.777	0.389
Croptype:Variety	27	3.3992	0.1259	49.043	1.6E-151	0.556	0.139
Croptype:Tissue	12	1.5186	0.1266	49.298	1.6E-88	0.359	0.062
Croptype:Variety:Tissue	161	6.5803	0.0409	15.92	1.4E-170	0.698	0.258
Residuals	828	2.1255	0.0026				
Total	1036	23.9					
Na							
Croptype	2	0.2911	0.1455	26.627	6.2E-12	0.047	0.013
Tissue	6	5.1391	0.8565	156.70	9.5E-133	0.474	0.234
Croptype:Variety	27	6.4588	0.2392	43.764	1.9E-139	0.527	0.289
Croptype:Tissue	12	1.2269	0.1022	18.705	3.6E-36	0.170	0.053
Croptype:Variety:Tissue	161	4.1730	0.0259	4.7419	3.7E-50	0.367	0.151
Residuals	828	4.5259	0.0055				
Total	1036	21.8					

Appendix 5

Table 2, ANOVA tables for five micronutrients; B, Cu, Fe, Mn and Zn with proportion of partial and total variance reported as ω^2_p and ω^2, respectively. The colon represents interaction between factors.

			B				
Source of variation	**df**	**SS**	**MS**	**F value**	**P value**	**ω²p**	**ω²**
Croptype	2	90.963	45.4814	25.562	1.7E-11	0.045	0.006
Tissue	6	2804.6	467.43	262.70	8.2E-188	0.602	0.195
Croptype:Variety	27	6421.5	237.83	133.67	4.2E-280	0.775	0.444
Croptype:Tissue	12	809.45	67.454	37.910	1.1E-70	0.299	0.055
Croptype:Variety:Tissue	161	2753.0	17.099	9.6103	1.2E-111	0.572	0.172
Residuals	828	1473.3	1.7793				
Total	1036	14352.7					
			Cu				
Croptype	2	55.669	27.8344	90.702	2.4E-36	0.147	0.046
Tissue	6	371.39	61.898	201.70	3.3E-158	0.537	0.311
Croptype:Variety	27	178.38	6.6067	21.529	1.4E-77	0.348	0.143
Croptype:Tissue	12	89.621	7.4684	24.337	6.3E-47	0.213	0.072
Croptype:Variety:Tissue	161	238.62	1.4821	4.8296	2.0E-51	0.373	0.159
Residuals	828	254.10	0.3069				
Total	1036	1187.8					
			Fe				
Croptype	2	76192.09	38096.05	25.214	2.3E-11	0.045	0.008
Tissue	6	6903284	1150547	761.48	0.0E+00	0.815	0.713
Croptype:Variety	27	328266.4	12158.02	8.0467	1.6E-27	0.155	0.030
Croptype:Tissue	12	209892.7	17491.06	11.576	9.0E-22	0.109	0.020
Croptype:Variety:Tissue	161	895746	5563.639	3.6822	1.5E-34	0.294	0.068
Residuals	828	1251057	1510.938				
Total	1036	9664439					
			Mn				
Croptype	2	128.975	64.4874	2.8595	5.8E-02	0.004	6.1E-04
Tissue	6	86891.4	14481.9	642.17	2.1E-307	0.788	0.632
Croptype:Variety	27	10926.8	404.695	17.945	2.2E-65	0.306	0.075
Croptype:Tissue	12	6139.68	511.640	22.687	7.8E-44	0.201	0.043
Croptype:Variety:Tissue	161	14501.3	90.0701	3.9939	3.4E-39	0.317	0.079
Residuals	828	18672.8	22.5516				
Total	1036	137260.8					
			Zn				
Croptype	2	31.898	15.9488	1.8584	1.6E-01	0.002	1.3E-04
Tissue	6	85375.6	14229.3	1658.0	0.0E+00	0.906	0.739
Croptype:Variety	27	10898.3	403.641	47.033	5.0E-147	0.545	0.092
Croptype:Tissue	12	2153.10	179.425	20.907	1.9E-40	0.187	0.018
Croptype:Variety:Tissue	161	9916.8	61.5949	7.1771	4.4E-83	0.490	0.074
Residuals	828	7106.0	8.5821				
Total	1036	115481.6					

Appendix 6 Macronutrient concentrations at harvest.

Table 1, averaged **P** concentration (%DW) in seven tissue types among three crop types and 30 genotypes of *B.napus* at harvest.

Croptype	Variety	L.root	T.root B	T.root T	Stem B	Stem M	Stem T	Seeds
Spring OSR	**Cubs Root DH1**	0.132	0.137	0.204	0.081	0.043	0.066	0.727
Spring OSR	**Drakkar**	0.144	0.186	0.257	0.101	0.108	0.053	0.892
Spring OSR	**Regina II DH1**	0.148	0.230	0.289	0.057	0.031	0.027	1.147
Spring OSR	**Stellar DH**	0.145	0.142	0.154	0.076	0.028	0.020	0.944
Spring OSR	**Yudal**	0.126	0.091	0.065	0.114	0.151	0.072	0.757
Spring OSR	**mean**	**0.139**	**0.157**	**0.194**	**0.086**	**0.072**	**0.047**	**0.893**
Swede	**Best of All**	0.311	0.231	0.226	0.062	0.029	0.030	0.762
Swede	**Drummonds PT**	0.143	0.101	0.176	0.059	0.049	0.042	0.885
Swede	**Jaune**	0.275	0.218	0.278	0.093	0.061	0.060	0.981
Swede	**Petranova**	0.165	0.150	0.165	0.099	0.047	0.028	0.874
Swede	**Turnip Hybrid**	0.227	0.175	0.232	0.081	0.060	0.058	1.017
Swede	**Vige DH1**	*NA*	0.309	0.659	0.082	0.055	0.064	0.857
Swede	**mean**	**0.224**	**0.197**	**0.289**	**0.080**	**0.050**	**0.047**	**0.896**
Winter OSR	**Canberra**	0.223	0.192	0.167	0.197	0.137	0.090	0.660
Winter OSR	**Darmor**	0.132	0.108	0.076	0.106	0.038	0.046	0.651
Winter OSR	**English Giant DH1**	0.425	0.273	0.247	0.134	0.093	0.076	0.824
Winter OSR	**FD502**	0.201	0.132	0.106	0.164	0.160	0.099	0.622
Winter OSR	**Grizzly**	0.146	0.126	0.132	0.130	0.083	0.049	0.618
Winter OSR	**Lioness**	0.180	0.118	0.130	0.191	0.107	0.045	0.878
Winter OSR	**NK Bravour**	0.309	0.261	0.212	0.227	0.203	0.118	0.765
Winter OSR	**Ningyou 7**	0.306	0.223	0.239	0.144	0.087	0.095	0.718
Winter OSR	**PI271452**	0.090	0.089	0.058	0.048	0.039	0.045	0.891
Winter OSR	**PR45-D01**	0.219	0.150	0.141	0.102	0.056	0.045	0.863
Winter OSR	**Red Russian**	0.255	0.162	0.184	0.074	0.057	0.065	1.069
Winter OSR	**Royal**	0.200	0.109	0.112	0.164	0.108	0.052	0.806
Winter OSR	**Sun**	0.246	0.182	0.201	0.263	0.136	0.089	0.734
Winter OSR	**TN145**	0.186	0.024	0.087	0.184	0.122	0.050	0.621
Winter OSR	**TN172**	0.133	0.137	0.132	0.116	0.046	0.039	0.599
Winter OSR	**Tapidor ADAS**	0.207	0.135	0.138	0.251	0.126	0.078	0.832
Winter OSR	**Tapidor DH**	0.111	0.158	0.137	0.163	0.060	0.038	0.831
Winter OSR	**Temple**	0.192	0.115	0.138	0.129	0.076	0.041	0.736
Winter OSR	**Winner**	0.262	0.213	0.183	0.192	0.126	0.075	0.728
Winter OSR	**mean**	**0.212**	**0.153**	**0.148**	**0.157**	**0.098**	**0.065**	**0.760**
Overall mean		**0.201**	**0.163**	**0.184**	**0.129**	**0.084**	**0.059**	**0.810**

Appendix 6

Table 2, averaged **K** concentration (%DW) in seven tissue types among three crop types and 30 genotypes of *B.napus* at harvest.

Croptype	Variety	L.root	T.root B	T.root T	Stem B	Stem M	Stem T	Seeds
Spring OSR	**Cubs Root DH1**	0.763	0.411	0.376	1.082	1.186	0.850	0.519
Spring OSR	**Drakkar**	1.058	0.950	0.731	1.953	1.593	1.264	0.532
Spring OSR	**Regina II DH1**	0.299	0.177	0.212	2.059	1.801	1.225	0.977
Spring OSR	**Stellar DH**	0.525	0.428	0.421	1.829	1.682	1.424	0.607
Spring OSR	**Yudal**	0.187	0.097	0.120	0.534	1.083	1.449	0.503
Spring OSR	**mean**	**0.566**	**0.413**	**0.372**	**1.491**	**1.469**	**1.243**	**0.628**
Swede	**Best of All**	1.993	1.738	1.901	1.682	1.133	1.014	0.603
Swede	**Drummonds PT**	0.436	0.240	0.333	1.282	1.610	1.574	0.636
Swede	**Jaune**	1.861	1.474	0.858	2.019	1.972	2.114	0.627
Swede	**Petranova**	0.652	0.460	0.409	1.710	2.116	1.834	0.738
Swede	**Turnip Hybrid**	1.799	1.490	1.344	1.770	1.459	1.108	0.646
Swede	**Vige DH1**	*NA*	0.356	0.809	1.317	0.671	0.356	0.650
Swede	**mean**	**1.348**	**0.959**	**0.942**	**1.630**	**1.494**	**1.333**	**0.650**
Winter OSR	**Canberra**	1.057	1.032	0.938	1.945	1.686	1.253	0.535
Winter OSR	**Darmor**	1.180	1.082	0.830	1.858	1.293	1.121	0.570
Winter OSR	**English Giant DH1**	1.310	1.260	1.225	2.024	1.502	1.158	0.648
Winter OSR	**FD502**	1.055	0.969	0.933	1.881	1.854	1.307	0.509
Winter OSR	**Grizzly**	1.149	1.078	0.863	1.811	1.548	1.070	0.540
Winter OSR	**Lioness**	1.288	1.123	1.014	2.298	1.666	0.967	0.544
Winter OSR	**NK Bravour**	1.070	1.095	0.859	1.899	1.764	1.246	0.548
Winter OSR	**Ningyou 7**	1.223	1.128	0.905	1.204	1.520	1.380	0.603
Winter OSR	**PI271452**	0.840	0.769	0.566	0.808	0.607	0.391	0.736
Winter OSR	**PR45-D01**	1.092	0.773	0.713	0.998	0.937	0.828	0.674
Winter OSR	**Red Russian**	0.970	0.791	0.676	1.684	1.890	1.334	0.641
Winter OSR	**Royal**	1.018	0.793	0.725	2.142	2.036	1.427	0.629
Winter OSR	**Sun**	1.485	1.294	1.393	2.143	1.734	1.296	0.515
Winter OSR	**TN145**	1.244	0.250	0.655	2.110	1.644	1.120	0.575
Winter OSR	**TN172**	0.961	0.732	0.567	1.312	1.245	1.197	0.511
Winter OSR	**Tapidor ADAS**	1.688	1.199	1.024	2.719	2.263	1.390	0.611
Winter OSR	**Tapidor DH**	1.120	0.823	0.700	1.837	1.972	1.535	0.528
Winter OSR	**Temple**	1.093	0.746	0.712	1.572	1.321	0.912	0.388
Winter OSR	**Winner**	1.088	1.104	0.877	1.808	1.990	1.243	0.612
Winter OSR	**mean**	**1.154**	**0.950**	**0.851**	**1.792**	**1.604**	**1.167**	**0.575**
Overall mean		**1.086**	**0.862**	**0.790**	**1.710**	**1.559**	**1.213**	**0.599**

Appendix 6

Table 3, averaged **Mg** concentration (%DW) in seven tissue types among three crop types and 30 genotypes of *B.napus* at harvest.

Croptype	Variety	L.root	T.root B	T.root T	Stem B	Stem M	Stem T	Seeds
Spring OSR	**Cubs Root DH1**	0.064	0.030	0.049	0.083	0.041	0.055	0.211
Spring OSR	**Drakkar**	0.052	0.050	0.044	0.056	0.056	0.041	0.233
Spring OSR	**Regina II DH1**	0.043	0.042	0.049	0.100	0.051	0.030	0.272
Spring OSR	**Stellar DH**	0.059	0.047	0.038	0.058	0.021	0.027	0.216
Spring OSR	**Yudal**	0.033	0.020	0.027	0.066	0.070	0.057	0.188
Spring OSR	**mean**	**0.050**	**0.038**	**0.041**	**0.073**	**0.048**	**0.042**	**0.224**
Swede	**Best of All**	0.169	0.096	0.090	0.061	0.042	0.048	0.228
Swede	**Drummonds PT**	0.034	0.035	0.056	0.074	0.049	0.042	0.253
Swede	**Jaune**	0.168	0.139	0.148	0.086	0.050	0.054	0.238
Swede	**Petranova**	0.062	0.054	0.042	0.100	0.055	0.040	0.233
Swede	**Turnip Hybrid**	0.148	0.112	0.122	0.078	0.053	0.069	0.258
Swede	**Vige DH1**	*NA*	0.101	0.236	0.041	0.018	0.021	0.180
Swede	**mean**	**0.116**	**0.090**	**0.116**	**0.073**	**0.044**	**0.046**	**0.232**
Winter OSR	**Canberra**	0.094	0.086	0.064	0.135	0.090	0.076	0.208
Winter OSR	**Darmor**	0.047	0.042	0.025	0.118	0.072	0.043	0.192
Winter OSR	**English Giant DH1**	0.089	0.046	0.043	0.080	0.043	0.041	0.209
Winter OSR	**FD502**	0.082	0.083	0.040	0.112	0.069	0.063	0.185
Winter OSR	**Grizzly**	0.035	0.049	0.049	0.084	0.054	0.053	0.179
Winter OSR	**Lioness**	0.050	0.048	0.039	0.106	0.057	0.037	0.241
Winter OSR	**NK Bravour**	0.083	0.067	0.029	0.064	0.037	0.024	0.217
Winter OSR	**Ningyou 7**	0.105	0.095	0.053	0.080	0.077	0.081	0.190
Winter OSR	**PI271452**	0.073	0.047	0.026	0.091	0.067	0.074	0.246
Winter OSR	**PR45-D01**	0.090	0.056	0.046	0.084	0.055	0.045	0.235
Winter OSR	**Red Russian**	0.126	0.081	0.061	0.085	0.041	0.036	0.259
Winter OSR	**Royal**	0.069	0.042	0.039	0.092	0.063	0.047	0.241
Winter OSR	**Sun**	0.066	0.083	0.054	0.099	0.053	0.038	0.233
Winter OSR	**TN145**	0.087	0.014	0.037	0.103	0.048	0.032	0.181
Winter OSR	**TN172**	0.066	0.053	0.035	0.089	0.058	0.056	0.176
Winter OSR	**Tapidor ADAS**	0.071	0.068	0.048	0.122	0.066	0.056	0.241
Winter OSR	**Tapidor DH**	0.066	0.074	0.063	0.104	0.060	0.056	0.236
Winter OSR	**Temple**	0.083	0.057	0.056	0.105	0.061	0.066	0.211
Winter OSR	**Winner**	0.086	0.082	0.050	0.086	0.062	0.037	0.201
Winter OSR	**mean**	**0.077**	**0.062**	**0.045**	**0.097**	**0.060**	**0.051**	**0.215**
Overall mean		**0.079**	**0.063**	**0.059**	**0.088**	**0.055**	**0.048**	**0.220**

Appendix 6

Table 4, averaged **Ca** concentration (%DW) in seven tissue types among three crop types and 30 genotypes of *B.napus* at harvest.

Croptype	Variety	L.root	T.root B	T.root T	Stem B	Stem M	Stem T	Seeds
Spring OSR	**Cubs Root DH1**	0.587	0.603	0.717	0.893	0.709	0.982	0.452
Spring OSR	**Drakkar**	0.507	0.461	0.511	0.727	0.756	0.515	0.462
Spring OSR	**Regina II DH1**	0.678	0.834	0.894	0.820	0.663	0.520	0.427
Spring OSR	**Stellar DH**	0.757	0.605	0.498	0.694	0.462	0.506	0.471
Spring OSR	**Yudal**	0.557	0.458	0.347	0.765	0.733	0.628	0.495
Spring OSR	**mean**	**0.617**	**0.592**	**0.593**	**0.780**	**0.665**	**0.630**	**0.461**
Swede	**Best of All**	1.213	0.546	0.626	0.850	0.709	0.886	0.426
Swede	**Drummonds PT**	0.698	0.489	0.693	0.826	0.747	0.768	0.507
Swede	**Jaune**	0.946	0.608	0.976	0.841	0.682	0.763	0.489
Swede	**Petranova**	0.691	0.580	0.518	0.795	0.657	0.622	0.319
Swede	**Turnip Hybrid**	0.767	0.569	0.724	0.760	0.666	0.762	0.506
Swede	**Vige DH1**	*NA*	1.166	2.159	0.745	0.590	0.736	0.467
Swede	**mean**	**0.863**	**0.659**	**0.949**	**0.803**	**0.675**	**0.756**	**0.452**
Winter OSR	**Canberra**	0.566	0.451	0.444	0.903	0.788	0.666	0.393
Winter OSR	**Darmor**	0.542	0.433	0.364	0.906	0.669	0.528	0.392
Winter OSR	**English Giant DH1**	0.625	0.354	0.346	0.695	0.573	0.531	0.371
Winter OSR	**FD502**	0.585	0.477	0.419	1.010	0.844	0.684	0.387
Winter OSR	**Grizzly**	0.357	0.308	0.353	0.753	0.569	0.479	0.405
Winter OSR	**Lioness**	0.529	0.421	0.384	0.870	0.647	0.531	0.475
Winter OSR	**NK Bravour**	0.500	0.369	0.322	0.768	0.608	0.518	0.429
Winter OSR	**Ningyou 7**	0.793	0.584	0.579	0.825	0.843	1.077	0.442
Winter OSR	**PI271452**	0.561	0.460	0.333	0.832	0.632	0.768	0.431
Winter OSR	**PR45-D01**	0.505	0.341	0.317	0.743	0.548	0.506	0.438
Winter OSR	**Red Russian**	0.810	0.554	0.548	0.890	0.507	0.639	0.449
Winter OSR	**Royal**	0.452	0.300	0.307	0.832	0.662	0.572	0.391
Winter OSR	**Sun**	0.468	0.457	0.360	0.892	0.622	0.671	0.388
Winter OSR	**TN145**	0.575	0.076	0.240	0.917	0.553	0.464	0.326
Winter OSR	**TN172**	0.577	0.474	0.405	0.928	0.580	0.694	0.335
Winter OSR	**Tapidor ADAS**	0.581	0.521	0.353	1.024	0.664	0.567	0.463
Winter OSR	**Tapidor DH**	0.527	0.593	0.476	0.822	0.589	0.536	0.517
Winter OSR	**Temple**	0.684	0.420	0.391	0.967	0.682	0.674	0.421
Winter OSR	**Winner**	0.511	0.395	0.384	0.816	0.536	0.560	0.391
Winter OSR	**mean**	**0.566**	**0.420**	**0.386**	**0.863**	**0.638**	**0.614**	**0.413**
Overall mean		**0.626**	**0.497**	**0.533**	**0.837**	**0.650**	**0.645**	**0.429**

Appendix 6

Table 5, averaged **S** concentration (%DW) in seven tissue types among three crop types and 30 genotypes of *B.napus* at harvest.

Croptype	Variety	L.root	T.root B	T.root T	Stem B	Stem M	Stem T	Seeds
Spring OSR	**Cubs Root DH1**	0.246	0.191	0.232	0.235	0.274	0.384	0.419
Spring OSR	**Drakkar**	0.190	0.156	0.155	0.193	0.209	0.165	0.290
Spring OSR	**Regina II DH1**	0.179	0.201	0.188	0.270	0.284	0.215	0.964
Spring OSR	**Stellar DH**	0.143	0.136	0.138	0.216	0.254	0.320	0.243
Spring OSR	**Yudal**	0.144	0.111	0.103	0.171	0.258	0.355	0.625
Spring OSR	**mean**	**0.181**	**0.159**	**0.163**	**0.217**	**0.256**	**0.288**	**0.509**
Swede	**Best of All**	0.425	0.190	0.195	0.174	0.165	0.193	0.592
Swede	**Drummonds PT**	0.164	0.126	0.208	0.180	0.194	0.196	0.689
Swede	**Jaune**	0.482	0.338	0.262	0.304	0.264	0.387	0.480
Swede	**Petranova**	0.236	0.191	0.168	0.212	0.195	0.228	0.674
Swede	**Turnip Hybrid**	0.214	0.225	0.195	0.169	0.169	0.182	0.697
Swede	**Vige DH1**	*NA*	0.200	0.408	0.149	0.107	0.100	0.591
Swede	**mean**	**0.304**	**0.212**	**0.239**	**0.198**	**0.182**	**0.214**	**0.621**
Winter OSR	**Canberra**	0.134	0.106	0.088	0.250	0.222	0.201	0.294
Winter OSR	**Darmor**	0.131	0.123	0.124	0.322	0.236	0.186	0.465
Winter OSR	**English Giant DH1**	0.222	0.164	0.151	0.245	0.220	0.228	0.942
Winter OSR	**FD502**	0.132	0.104	0.098	0.244	0.259	0.220	0.323
Winter OSR	**Grizzly**	0.109	0.082	0.078	0.246	0.210	0.175	0.295
Winter OSR	**Lioness**	0.126	0.090	0.104	0.295	0.263	0.219	0.232
Winter OSR	**NK Bravour**	0.098	0.079	0.066	0.158	0.155	0.142	0.200
Winter OSR	**Ningyou 7**	0.268	0.262	0.224	0.279	0.277	0.419	0.518
Winter OSR	**PI271452**	0.220	0.176	0.184	0.192	0.163	0.216	0.259
Winter OSR	**PR45-D01**	0.148	0.087	0.070	0.158	0.134	0.143	0.250
Winter OSR	**Red Russian**	0.299	0.318	0.309	0.305	0.223	0.240	1.040
Winter OSR	**Royal**	0.144	0.095	0.089	0.242	0.243	0.219	0.261
Winter OSR	**Sun**	0.158	0.126	0.107	0.260	0.224	0.210	0.240
Winter OSR	**TN145**	0.156	0.114	0.099	0.215	0.182	0.183	0.295
Winter OSR	**TN172**	0.127	0.123	0.105	0.168	0.183	0.262	0.356
Winter OSR	**Tapidor ADAS**	0.158	0.112	0.113	0.255	0.285	0.249	0.263
Winter OSR	**Tapidor DH**	0.094	0.104	0.100	0.141	0.163	0.199	0.514
Winter OSR	**Temple**	0.182	0.121	0.112	0.191	0.163	0.151	0.236
Winter OSR	**Winner**	0.130	0.117	0.102	0.192	0.181	0.175	0.217
Winter OSR	**mean**	**0.160**	**0.132**	**0.122**	**0.229**	**0.210**	**0.212**	**0.379**
Overall mean		**0.188**	**0.152**	**0.152**	**0.221**	**0.212**	**0.225**	**0.449**

Appendix 6

Table 6, averaged **Na** concentration (%DW) in seven tissue types among three crop types and 30 genotypes of *B.napus* at harvest.

Croptype	Variety	L.root	T.root B	T.root T	Stem B	Stem M	Stem T	Seeds
Spring OSR	**Cubs Root DH1**	0.281	0.225	0.166	0.343	0.384	0.259	0.0023
Spring OSR	**Drakkar**	0.149	0.123	0.113	0.288	0.232	0.158	0.0043
Spring OSR	**Regina II DH1**	0.149	0.076	0.095	0.701	0.668	0.390	0.0076
Spring OSR	**Stellar DH**	0.132	0.115	0.121	0.224	0.243	0.159	0.0061
Spring OSR	**Yudal**	0.070	0.042	0.044	0.163	0.198	0.264	0.0049
Spring OSR	**mean**	**0.156**	**0.116**	**0.108**	**0.344**	**0.345**	**0.246**	**0.0051**
Swede	**Best of All**	0.278	0.171	0.157	0.104	0.049	0.037	0.0027
Swede	**Drummonds PT**	0.151	0.094	0.132	0.348	0.342	0.302	0.0050
Swede	**Jaune**	0.191	0.232	0.154	0.113	0.063	0.047	0.0042
Swede	**Petranova**	0.301	0.262	0.185	0.667	0.586	0.487	0.0051
Swede	**Turnip Hybrid**	0.208	0.213	0.245	0.157	0.106	0.085	0.0023
Swede	**Vige DH1**	*NA*	0.113	0.172	0.125	0.053	0.024	0.0052
Swede	**mean**	**0.226**	**0.181**	**0.174**	**0.252**	**0.200**	**0.164**	**0.0041**
Winter OSR	**Canberra**	0.090	0.114	0.111	0.162	0.085	0.047	0.0024
Winter OSR	**Darmor**	0.223	0.260	0.199	0.314	0.224	0.175	0.0025
Winter OSR	**English Giant DH1**	0.076	0.128	0.120	0.120	0.052	0.029	0.0025
Winter OSR	**FD502**	0.158	0.151	0.119	0.178	0.126	0.093	0.0024
Winter OSR	**Grizzly**	0.125	0.123	0.120	0.161	0.120	0.060	0.0022
Winter OSR	**Lioness**	0.136	0.167	0.162	0.192	0.139	0.089	0.0041
Winter OSR	**NK Bravour**	0.140	0.156	0.151	0.171	0.118	0.074	0.0041
Winter OSR	**Ningyou 7**	0.193	0.239	0.193	0.238	0.210	0.174	0.0026
Winter OSR	**PI271452**	0.365	0.342	0.298	0.565	0.378	0.318	0.0045
Winter OSR	**PR45-D01**	0.154	0.156	0.178	0.207	0.132	0.096	0.0045
Winter OSR	**Red Russian**	0.297	0.290	0.277	0.467	0.309	0.260	0.0045
Winter OSR	**Royal**	0.231	0.226	0.228	0.369	0.266	0.186	0.0046
Winter OSR	**Sun**	0.066	0.072	0.069	0.046	0.036	0.029	0.0043
Winter OSR	**TN145**	0.105	0.029	0.081	0.130	0.075	0.043	0.0024
Winter OSR	**TN172**	0.128	0.143	0.115	0.142	0.093	0.122	0.0022
Winter OSR	**Tapidor ADAS**	0.142	0.217	0.170	0.206	0.123	0.084	0.0041
Winter OSR	**Tapidor DH**	0.379	0.323	0.319	0.363	0.312	0.220	0.0023
Winter OSR	**Temple**	0.125	0.151	0.135	0.171	0.099	0.068	0.0041
Winter OSR	**Winner**	0.074	0.088	0.083	0.077	0.061	0.034	0.0044
Winter OSR	**mean**	**0.169**	**0.178**	**0.165**	**0.225**	**0.156**	**0.116**	**0.0034**
Overall mean		**0.176**	**0.168**	**0.157**	**0.250**	**0.196**	**0.147**	**0.0038**

Appendix 7 Micronutrient concentrations at harvest

Table 1, averaged **B** concentration (µg/g DW) in seven tissue types among 30 genotypes of *B.napus* at harvest.

Croptype	Variety	L.root	T.root B	T.root T	Stem B	Stem M	Stem T	Seeds
Spring OSR	**Cubs Root DH1**	10.87	7.42	7.49	9.17	8.75	9.61	8.08
Spring OSR	**Drakkar**	10.93	8.25	6.87	12.17	11.51	10.04	8.22
Spring OSR	**Regina II DH1**	7.06	7.95	7.02	11.72	10.51	10.04	8.60
Spring OSR	**Stellar DH**	9.87	7.67	6.77	12.90	10.29	9.95	8.47
Spring OSR	**Yudal**	16.68	11.97	11.98	23.41	22.92	15.98	8.46
Spring OSR	**mean**	**11.08**	**8.65**	**8.03**	**13.87**	**12.79**	**11.12**	**8.37**
Swede	**Best of All**	26.27	13.34	13.52	12.87	11.26	10.15	8.84
Swede	**Drummonds PT**	10.00	8.62	10.17	11.00	9.97	9.82	8.98
Swede	**Jaune**	16.58	11.46	15.36	12.50	10.42	9.93	7.23
Swede	**Petranova**	11.35	7.84	6.91	11.97	11.38	10.57	8.63
Swede	**Turnip Hybrid**	15.33	12.44	13.58	13.18	10.58	9.75	6.06
Swede	**Vige DH1**	*NA*	12.90	19.84	14.20	12.78	12.52	9.56
Swede	**mean**	**15.90**	**11.10**	**13.23**	**12.62**	**11.06**	**10.46**	**8.22**
Winter OSR	**Canberra**	11.84	9.41	8.99	14.84	14.04	13.08	7.57
Winter OSR	**Darmor**	15.13	12.25	12.68	17.37	15.96	12.69	8.39
Winter OSR	**English Giant DH1**	11.09	8.19	8.25	13.09	12.09	11.93	5.23
Winter OSR	**FD502**	12.10	8.99	9.44	14.02	12.78	12.27	7.99
Winter OSR	**Grizzly**	11.29	7.92	8.23	12.46	10.33	9.45	8.74
Winter OSR	**Lioness**	14.00	8.78	9.50	13.35	11.81	10.59	9.90
Winter OSR	**NK Bravour**	8.92	7.54	7.41	11.69	10.30	8.99	8.36
Winter OSR	**Ningyou 7**	13.60	11.75	12.38	14.22	15.23	14.83	7.89
Winter OSR	**PI271452**	10.54	7.62	10.38	10.58	8.53	11.25	10.69
Winter OSR	**PR45-D01**	13.99	10.00	7.78	11.14	10.84	10.16	9.56
Winter OSR	**Red Russian**	11.06	8.31	7.91	12.82	11.75	11.21	9.63
Winter OSR	**Royal**	10.28	8.40	8.17	12.18	12.05	11.09	9.25
Winter OSR	**Sun**	11.76	7.73	8.08	14.12	11.63	9.83	8.47
Winter OSR	**TN145**	10.92	6.83	6.60	11.76	10.02	8.91	8.29
Winter OSR	**TN172**	10.39	7.92	6.94	10.47	10.05	9.84	8.89
Winter OSR	**Tapidor ADAS**	13.33	10.44	9.09	14.07	12.85	10.96	10.47
Winter OSR	**Tapidor DH**	25.70	22.72	22.19	23.05	24.06	22.99	8.19
Winter OSR	**Temple**	9.72	7.78	7.17	12.40	10.94	9.89	8.19
Winter OSR	**Winner**	10.50	9.71	8.39	14.20	11.53	10.73	9.54
Winter OSR	**mean**	**12.43**	**9.59**	**9.45**	**13.57**	**12.46**	**11.62**	**8.70**
Overall mean		**12.80**	**9.74**	**9.97**	**13.43**	**12.24**	**11.30**	**8.55**

Appendix 7

Table 2, averaged **Cu** concentration (µg/g DW) in seven tissue types among 30 genotypes of *B.napus* at harvest.

Croptype	Variety	L.root	T.root B	T.root T	Stem B	Stem M	Stem T	Seeds
Spring OSR	**Cubs Root DH1**	3.74	2.42	2.97	1.77	1.57	1.44	2.09
Spring OSR	**Drakkar**	4.36	2.98	2.13	1.61	2.06	1.45	2.99
Spring OSR	**Regina II DH1**	1.53	2.98	2.31	1.81	2.09	2.14	4.96
Spring OSR	**Stellar DH**	3.68	2.12	1.91	1.13	1.11	1.11	2.78
Spring OSR	**Yudal**	4.42	2.39	1.91	0.87	0.88	1.30	2.34
Spring OSR	**mean**	**3.54**	**2.58**	**2.24**	**1.44**	**1.54**	**1.49**	**3.03**
Swede	**Best of All**	9.32	3.42	4.60	2.11	2.45	2.48	1.80
Swede	**Drummonds PT**	5.09	2.99	2.59	1.70	1.51	2.01	2.52
Swede	**Jaune**	4.54	1.93	1.65	2.06	1.96	1.47	2.12
Swede	**Petranova**	5.29	3.42	3.04	2.26	3.02	2.30	3.50
Swede	**Turnip Hybrid**	4.24	2.31	2.24	1.59	1.82	2.12	1.52
Swede	**Vige DH1**	*NA*	3.18	2.54	3.50	1.66	1.50	2.19
Swede	**mean**	**5.70**	**2.87**	**2.78**	**2.20**	**2.07**	**1.98**	**2.28**
Winter OSR	**Canberra**	2.96	2.54	1.48	1.25	1.72	1.37	1.97
Winter OSR	**Darmor**	2.51	1.63	2.16	1.61	1.30	1.23	2.39
Winter OSR	**English Giant DH1**	3.38	2.49	2.30	1.89	1.89	2.21	1.48
Winter OSR	**FD502**	2.88	1.95	1.18	1.49	1.08	1.48	1.75
Winter OSR	**Grizzly**	3.40	1.97	2.28	1.83	1.83	1.61	2.30
Winter OSR	**Lioness**	3.77	2.63	1.97	1.56	1.65	1.89	3.13
Winter OSR	**NK Bravour**	2.19	1.95	1.48	1.15	1.03	1.26	2.90
Winter OSR	**Ningyou 7**	4.50	3.60	3.25	2.18	1.94	2.03	1.67
Winter OSR	**PI271452**	4.89	3.13	2.80	3.02	2.83	2.54	3.07
Winter OSR	**PR45-D01**	2.81	2.19	1.73	1.17	1.29	1.44	2.75
Winter OSR	**Red Russian**	3.35	2.36	2.36	2.84	2.90	2.11	2.29
Winter OSR	**Royal**	1.60	1.30	1.40	0.58	0.86	1.09	2.89
Winter OSR	**Sun**	3.62	1.77	1.38	1.03	0.86	1.08	3.25
Winter OSR	**TN145**	1.95	1.81	1.48	1.36	1.00	1.12	2.41
Winter OSR	**TN172**	3.12	2.49	2.37	1.62	1.83	1.80	2.57
Winter OSR	**Tapidor ADAS**	2.61	2.72	2.21	1.66	1.58	1.57	3.11
Winter OSR	**Tapidor DH**	2.13	1.76	1.61	1.33	1.16	1.01	2.43
Winter OSR	**Temple**	2.35	1.95	2.17	1.73	2.03	2.00	2.58
Winter OSR	**Winner**	3.15	2.70	2.25	1.98	1.93	1.52	2.59
Winter OSR	**mean**	**3.01**	**2.26**	**1.99**	**1.65**	**1.62**	**1.60**	**2.50**
Overall mean		**3.56**	**2.44**	**2.19**	**1.72**	**1.69**	**1.66**	**2.54**

Appendix 7

Table 3, averaged **Fe** concentration (µg/g DW) in seven tissue types among 30 genotypes of *B.napus* at harvest.

Croptype	Variety	L.root	T.root B	T.root T	Stem B	Stem M	Stem T	Seeds
Spring OSR	**Cubs Root DH1**	278.2	179.5	160.5	25.72	24.07	26.33	55.17
Spring OSR	**Drakkar**	256.4	144.4	89.0	22.79	22.60	19.75	42.65
Spring OSR	**Regina II DH1**	388.9	296.9	246.3	30.25	22.28	21.15	59.22
Spring OSR	**Stellar DH**	281.5	257.8	124.2	28.52	22.71	23.70	48.09
Spring OSR	**Yudal**	278.8	107.6	103.8	17.37	14.70	19.45	38.31
Spring OSR	**mean**	**296.8**	**197.2**	**144.8**	**24.93**	**21.27**	**22.08**	**48.69**
Swede	**Best of All**	336.8	181.9	120.1	17.69	10.54	15.01	45.31
Swede	**Drummonds PT**	312.3	227.0	140.8	15.08	10.08	11.04	48.87
Swede	**Jaune**	323.2	108.1	73.9	20.76	13.56	17.01	55.36
Swede	**Petranova**	267.5	137.1	119.4	20.44	10.97	16.19	52.84
Swede	**Turnip Hybrid**	265.8	242.5	175.5	28.88	18.56	23.85	62.12
Swede	**Vige DH1**	*NA*	327.3	157.3	21.58	19.01	23.95	44.41
Swede	**mean**	**301.1**	**204.0**	**131.2**	**20.74**	**13.79**	**17.84**	**51.48**
Winter OSR	**Canberra**	265.9	180.5	78.9	28.84	21.34	22.09	61.93
Winter OSR	**Darmor**	170.2	100.1	92.5	25.95	14.55	20.50	47.23
Winter OSR	**English Giant DH1**	146.2	118.5	142.3	19.81	16.28	17.75	53.16
Winter OSR	**FD502**	236.2	142.5	86.3	24.88	20.85	20.55	51.51
Winter OSR	**Grizzly**	191.3	97.1	75.6	24.68	15.93	14.88	52.54
Winter OSR	**Lioness**	262.2	117.4	99.5	20.36	17.82	14.38	57.15
Winter OSR	**NK Bravour**	115.9	107.1	74.5	17.70	12.74	14.51	59.34
Winter OSR	**Ningyou 7**	295.7	202.8	173.7	29.34	21.73	29.09	38.99
Winter OSR	**PI271452**	412.7	279.0	26.8	28.95	34.52	29.83	46.43
Winter OSR	**PR45-D01**	155.7	92.0	71.7	21.59	14.63	23.22	45.36
Winter OSR	**Red Russian**	246.7	124.7	113.8	16.67	14.59	21.15	63.18
Winter OSR	**Royal**	142.7	94.7	109.9	23.75	23.09	16.00	56.58
Winter OSR	**Sun**	300.3	145.3	91.0	28.14	20.31	23.30	58.85
Winter OSR	**TN145**	254.0	115.3	66.4	17.22	14.16	14.44	60.17
Winter OSR	**TN172**	240.5	146.4	156.4	22.91	18.41	17.52	54.40
Winter OSR	**Tapidor ADAS**	218.4	165.0	151.1	26.00	26.07	21.61	53.06
Winter OSR	**Tapidor DH**	184.8	113.2	135.9	22.51	18.78	22.98	58.75
Winter OSR	**Temple**	261.6	140.3	119.6	18.35	14.72	14.21	48.29
Winter OSR	**Winner**	222.4	212.4	115.4	33.24	21.34	30.49	47.29
Winter OSR	**mean**	**227.5**	**141.8**	**104.3**	**23.73**	**19.04**	**20.45**	**53.38**
Overall mean		**252.2**	**163.5**	**116.4**	**23.33**	**18.36**	**20.20**	**52.22**

Appendix 7

Table 4, averaged **Mn** concentration (µg/g DW) in seven tissue types among 30 genotypes of *B.napus* at harvest.

Croptype	Variety	L.root	T.root B	T.root T	Stem B	Stem M	Stem T	Seeds
Spring OSR	**Cubs Root DH1**	25.90	13.66	17.64	13.48	8.07	11.26	37.23
Spring OSR	**Drakkar**	15.58	10.50	9.16	14.18	14.29	9.17	36.62
Spring OSR	**Regina II DH1**	24.95	20.93	25.94	14.80	15.17	14.24	32.46
Spring OSR	**Stellar DH**	37.41	18.56	13.41	15.56	7.83	7.70	44.16
Spring OSR	**Yudal**	25.35	8.32	6.56	8.52	6.32	3.49	31.42
Spring OSR	**mean**	**25.84**	**14.39**	**14.54**	**13.31**	**10.33**	**9.17**	**36.38**
Swede	**Best of All**	52.59	14.09	18.67	9.79	6.79	7.70	37.85
Swede	**Drummonds PT**	24.75	12.49	23.59	3.57	3.28	3.13	40.01
Swede	**Jaune**	25.45	10.18	12.62	6.59	5.48	6.51	41.45
Swede	**Petranova**	19.04	9.56	10.35	10.82	7.32	5.06	30.64
Swede	**Turnip Hybrid**	31.29	18.48	19.74	11.71	9.71	11.61	38.99
Swede	**Vige DH1**	*NA*	29.25	28.90	5.25	3.67	4.35	37.38
Swede	**mean**	**30.63**	**15.67**	**18.98**	**7.95**	**6.04**	**6.39**	**37.72**
Winter OSR	**Canberra**	19.92	13.98	7.95	12.62	10.60	8.09	47.25
Winter OSR	**Darmor**	14.34	9.25	5.31	9.98	6.14	5.50	38.71
Winter OSR	**English Giant DH1**	14.49	9.20	9.63	11.53	8.46	8.51	31.67
Winter OSR	**FD502**	15.68	11.08	8.36	14.50	11.86	11.62	38.84
Winter OSR	**Grizzly**	12.51	15.54	8.45	11.40	8.07	6.34	34.09
Winter OSR	**Lioness**	19.73	10.50	7.62	13.31	9.28	7.07	41.31
Winter OSR	**NK Bravour**	18.82	13.49	9.12	16.37	13.44	10.65	38.08
Winter OSR	**Ningyou 7**	33.69	20.59	16.74	9.23	7.04	6.96	35.38
Winter OSR	**PI271452**	29.85	22.61	14.15	21.72	17.08	17.95	31.65
Winter OSR	**PR45-D01**	13.36	7.57	5.24	8.77	7.21	7.36	30.98
Winter OSR	**Red Russian**	19.77	10.92	9.72	7.80	6.66	10.13	32.91
Winter OSR	**Royal**	17.60	10.96	8.79	17.39	12.26	9.95	40.64
Winter OSR	**Sun**	25.52	21.27	14.80	31.53	23.32	20.25	36.61
Winter OSR	**TN145**	20.69	2.54	7.24	19.25	15.92	12.41	40.41
Winter OSR	**TN172**	17.70	11.86	11.28	15.44	9.94	12.01	36.41
Winter OSR	**Tapidor ADAS**	17.67	15.14	7.99	16.61	11.25	9.59	43.00
Winter OSR	**Tapidor DH**	29.00	23.31	18.81	31.16	14.66	11.85	35.71
Winter OSR	**Temple**	17.87	10.48	10.47	12.21	8.87	8.44	36.08
Winter OSR	**Winner**	15.96	12.24	7.91	12.36	6.55	6.80	33.68
Winter OSR	**mean**	**19.69**	**13.29**	**9.98**	**15.43**	**10.98**	**10.08**	**37.02**
Overall mean		**22.64**	**13.95**	**12.54**	**13.58**	**9.89**	**9.19**	**37.05**

Appendix 7

Table 5, averaged **Zn** concentration (µg/g DW) in seven tissue types among 30 genotypes of *B.napus* at harvest.

Croptype	Variety	L.root	T.root B	T.root T	Stem B	Stem M	Stem T	Seeds
Spring OSR	**Cubs Root DH1**	19.13	10.24	10.29	13.71	16.29	15.55	42.92
Spring OSR	**Drakkar**	20.74	9.75	7.25	7.25	7.20	5.04	30.35
Spring OSR	**Regina II DH1**	14.97	11.86	10.15	10.52	7.80	6.11	42.65
Spring OSR	**Stellar DH**	17.24	9.19	6.52	9.87	6.25	4.89	30.21
Spring OSR	**Yudal**	15.60	6.84	5.06	7.10	6.43	6.44	23.68
Spring OSR	**mean**	**17.53**	**9.57**	**7.85**	**9.69**	**8.79**	**7.61**	**33.96**
Swede	**Best of All**	52.75	11.94	10.01	6.54	4.46	3.54	31.12
Swede	**Drummonds PT**	17.51	7.33	7.80	6.23	4.98	4.56	37.15
Swede	**Jaune**	19.58	7.77	8.12	9.27	5.32	3.70	33.16
Swede	**Petranova**	18.19	8.95	7.56	6.82	5.35	4.47	32.57
Swede	**Turnip Hybrid**	31.36	15.15	12.37	14.33	11.31	8.31	35.89
Swede	**Vige DH1**	*NA*	12.10	15.40	9.64	7.73	5.21	29.66
Swede	**mean**	**27.88**	**10.54**	**10.21**	**8.81**	**6.52**	**4.96**	**33.26**
Winter OSR	**Canberra**	13.89	9.21	6.21	8.19	6.27	5.41	34.55
Winter OSR	**Darmor**	13.19	11.22	6.23	9.74	5.25	3.82	33.12
Winter OSR	**English Giant DH1**	16.06	8.81	7.90	11.92	10.97	8.90	52.76
Winter OSR	**FD502**	15.29	9.61	4.86	7.01	5.16	5.27	37.22
Winter OSR	**Grizzly**	17.17	10.28	8.50	12.46	8.69	7.98	40.11
Winter OSR	**Lioness**	15.17	7.96	6.52	9.74	6.95	4.82	30.91
Winter OSR	**NK Bravour**	9.99	8.66	5.63	6.30	3.85	3.64	30.63
Winter OSR	**Ningyou 7**	21.83	13.99	11.83	13.85	10.08	10.12	34.21
Winter OSR	**PI271452**	24.38	15.29	23.18	24.43	13.74	22.84	26.85
Winter OSR	**PR45-D01**	16.15	8.82	5.05	6.56	5.13	4.94	27.11
Winter OSR	**Red Russian**	19.17	9.25	7.84	6.79	6.94	7.07	37.88
Winter OSR	**Royal**	14.59	8.30	6.45	15.02	11.46	8.46	32.16
Winter OSR	**Sun**	18.58	10.14	8.04	10.73	5.53	4.10	32.30
Winter OSR	**TN145**	16.07	8.58	6.80	9.21	7.86	7.98	41.05
Winter OSR	**TN172**	20.09	13.31	10.48	19.76	14.37	10.13	38.44
Winter OSR	**Tapidor ADAS**	16.48	13.34	9.33	13.54	10.90	8.90	32.88
Winter OSR	**Tapidor DH**	23.21	16.74	14.82	20.19	15.95	13.77	48.51
Winter OSR	**Temple**	14.43	7.17	5.44	6.54	4.31	2.85	25.80
Winter OSR	**Winner**	10.88	7.66	5.00	8.00	3.96	3.65	26.73
Winter OSR	**mean**	**16.66**	**10.44**	**8.43**	**11.58**	**8.28**	**7.61**	**34.90**
Overall mean		**18.75**	**10.31**	**8.69**	**10.71**	**8.02**	**7.08**	**34.42**

Appendix 8 Analysis of variance of all mineral elements at two growth stages

Tables 1, ANOVA tables for six macronutrients (P, K, Mg, Ca, S, and Na) and five micronutrients (B, Cu, Fe, Mn and Zn) with proportion of partial and total variance reported as ω^2_p and ω^2, respectively. The colon represents interaction between treatment factors.

P							
Source of variation	**df**	**SS**	**MS**	**F value**	**P value**	**ω²p**	**ω²**
Stage	1	4.8928	4.8928	954.93	2.8E-125	0.549	0.067
Tissue	6	36.871	6.1451	1199.3	0.0E+00	0.902	0.508
Variety	13	0.5330	0.0410	8.0025	7.3E-15	0.104	0.006
Stage:Tissue	6	23.008	3.8347	748.42	1.8E-271	0.851	0.317
Stage:Variety	13	0.8128	0.0625	12.202	9.5E-24	0.157	0.010
Tissue:Variety	78	1.6389	0.0210	4.1007	3.7E-23	0.236	0.017
Stage:Tissue:Variety	78	1.7332	0.0222	4.3369	3.9E-25	0.249	0.018
Residuals	588	3.0128	0.0051				
Total	783	72.502					
K							
Stage	1	5.8086	5.8086	65.416	3.5E-15	0.076	0.022
Tissue	6	73.755	12.293	138.44	5.3E-109	0.513	0.278
Variety	13	19.652	1.5117	17.025	1.9E-33	0.210	0.070
Stage:Tissue	6	70.722	11.787	132.75	6.6E-106	0.502	0.267
Stage:Variety	13	10.038	0.7722	8.6960	2.4E-16	0.113	0.034
Tissue:Variety	78	16.936	0.2171	2.4453	1.8E-09	0.126	0.038
Stage:Tissue:Variety	78	13.957	0.1789	2.0152	3.0E-06	0.092	0.027
Residuals	588	52.211	0.0888				
Total	783	263.08					
Mg							
Stage	1	0.0572	0.0572	180.02	5.3E-36	0.186	0.017
Tissue	6	2.7247	0.4541	1428.5	0.0E+00	0.916	0.810
Variety	13	0.0768	0.0059	18.576	1.9E-36	0.226	0.022
Stage:Tissue	6	0.0782	0.0130	40.979	9.5E-42	0.234	0.023
Stage:Variety	13	0.0209	0.0016	5.0641	1.5E-08	0.063	0.005
Tissue:Variety	78	0.1327	0.0017	5.3504	1.7E-33	0.302	0.032
Stage:Tissue:Variety	78	0.0846	0.0011	3.4116	2.3E-17	0.194	0.018
Residuals	588	0.1869	0.0003				
Total	783	3.3620					
Ca							
Stage	1	773.88	773.88	2479.5	4.4E-213	0.760	0.084
Tissue	6	3215.7	535.95	1717.2	0.0E+00	0.929	0.351
Variety	13	20.424	1.5711	5.0337	1.8E-08	0.063	0.002
Stage:Tissue	6	4726.8	787.81	2524.1	0.0E+00	0.951	0.516
Stage:Variety	13	25.795	1.9843	6.3575	2.6E-11	0.082	0.002
Tissue:Variety	78	80.561	1.0328	3.3092	1.6E-16	0.187	0.006
Stage:Tissue:Variety	78	136.89	1.7550	5.6230	1.0E-35	0.315	0.012
Residuals	588	183.52	0.3121				
Total	783	9163.6					

Source of variation	df	SS	MS	F value	P value	ω²p	ω²
S							
Stage	1	0.0156	0.0156	7.3153	7.0E-03	0.008	0.001
Tissue	6	5.6988	0.9498	444.68	8.5E-215	0.772	0.503
Variety	13	1.6108	0.1239	58.014	2.5E-96	0.486	0.140
Stage:Tissue	6	0.5968	0.0995	46.569	1.0E-46	0.259	0.052
Stage:Variety	13	0.1560	0.0120	5.6184	1.0E-09	0.071	0.011
Tissue:Variety	78	1.5474	0.0198	9.2882	7.0E-63	0.452	0.122
Stage:Tissue:Variety	78	0.4309	0.0055	2.5866	1.4E-10	0.136	0.023
Residuals	588	1.2559	0.0021				
Total	783	11.312					
Na							
Stage	1	0.0359	0.0359	9.8326	1.8E-03	0.011	0.003
Tissue	6	3.6876	0.6146	168.21	4.5E-124	0.561	0.361
Variety	13	1.5353	0.1181	32.322	1.7E-60	0.342	0.146
Stage:Tissue	6	0.3894	0.0649	17.763	5.7E-19	0.114	0.036
Stage:Variety	13	0.8839	0.0680	18.608	1.7E-36	0.226	0.082
Tissue:Variety	78	0.8133	0.0104	2.8535	9.7E-13	0.156	0.052
Stage:Tissue:Variety	78	0.6708	0.0086	2.3536	9.2E-09	0.119	0.038
Residuals	588	2.1485	0.0037				
Total	783	10.165					
B							
Stage	1	1757.1	1757.1	1005.9	1.9E-129	0.562	0.140
Tissue	6	1833.6	305.60	174.96	2.9E-127	0.571	0.146
Variety	13	3644.7	280.36	160.51	1.4E-183	0.726	0.290
Stage:Tissue	6	1110.2	185.03	105.93	3.2E-90	0.445	0.088
Stage:Variety	13	1231.9	94.761	54.251	1.2E-91	0.469	0.097
Tissue:Variety	78	1215.9	15.589	8.9248	2.2E-60	0.441	0.086
Stage:Tissue:Variety	78	680.64	8.7261	4.9957	1.3E-30	0.284	0.044
Residuals	588	1027.1	1.7467				
Total	783	12501.0					
Cu							
Stage	1	70.700	70.700	378.57	1.8E-65	0.325	0.100
Tissue	6	195.14	32.523	174.15	6.9E-127	0.570	0.276
Variety	13	68.421	5.2632	28.182	1.1E-53	0.311	0.094
Stage:Tissue	6	64.117	10.686	57.220	1.1E-55	0.301	0.089
Stage:Variety	13	8.8589	0.6815	3.6489	1.4E-05	0.042	0.009
Tissue:Variety	78	116.16	1.4892	7.9740	1.2E-53	0.410	0.144
Stage:Tissue:Variety	78	70.542	0.9044	4.8426	2.4E-29	0.277	0.080
Residuals	588	109.81	0.1868				
Total	783	703.8					

Fe							
Source of variation	**df**	**SS**	**MS**	**F value**	**P value**	**ω²p**	**ω²**
Stage	1	15881.18	15881.18	16.35	6.0E-05	0.019	0.004
Tissue	6	2753711.3	458951.9	472.44	3.7E-221	0.783	0.682
Variety	13	90003.81	6923.37	7.127	5.6E-13	0.092	0.019
Stage:Tissue	6	156940.8	26156.8	26.926	2.1E-28	0.166	0.037
Stage:Variety	13	46708.21	3592.94	3.6986	1.1E-05	0.043	0.008
Tissue:Variety	78	241280.0	3093.33	3.1843	1.8E-15	0.179	0.041
Stage:Tissue:Variety	78	154513.1	1980.94	2.0392	2.0E-06	0.094	0.020
Residuals	588	571208.1	971.442				
Total	783	4030246.5					
Mn							
Stage	1	7274.9	7274.9	774.19	2.3E-109	0.497	0.085
Tissue	6	53912.1	8985.3	956.22	1.7E-299	0.880	0.629
Variety	13	4878.5	375.27	39.936	3.5E-72	0.392	0.056
Stage:Tissue	6	4691.7	781.95	83.215	3.0E-75	0.386	0.054
Stage:Variety	13	2550.4	196.19	20.878	8.9E-41	0.248	0.028
Tissue:Variety	78	4426.8	56.753	6.0397	5.0E-39	0.334	0.043
Stage:Tissue:Variety	78	2361.2	30.272	3.2215	8.9E-16	0.181	0.019
Residuals	588	5525.3	9.3968				
Total	783	85620.9					
Zn							
Stage	1	4.6E-05	4.6E-05	6.8E-06	0.998	-0.001	-7.7E-05
Tissue	6	71361.3	11893.6	1751.14	0.0E+00	0.931	0.805
Variety	13	5697.42	438.263	64.5273	4.9E-104	0.513	0.063
Stage:Tissue	6	2801.47	466.911	68.7453	1.0E-64	0.341	0.031
Stage:Variety	13	622.937	47.9182	7.05520	8.0E-13	0.091	0.006
Tissue:Variety	78	2634.99	33.7820	4.97386	2.0E-30	0.283	0.024
Stage:Tissue:Variety	78	1436.70	18.4192	2.71194	1.4E-11	0.146	0.010
Residuals	588	3993.64	6.79190				
Total	783	88548.5					

Appendix 9 Mineral nutrient concentration between two growth stages

Figure 1, Mg concentration across seven tissues between two growth stages (GS 6.2/6.3 and harvest) among 14 *Brassica napus* genotypes. Data are genotype mean ± SEM (n=3 and n=5 at GS 6.2/6.3 and harvest, respectively).

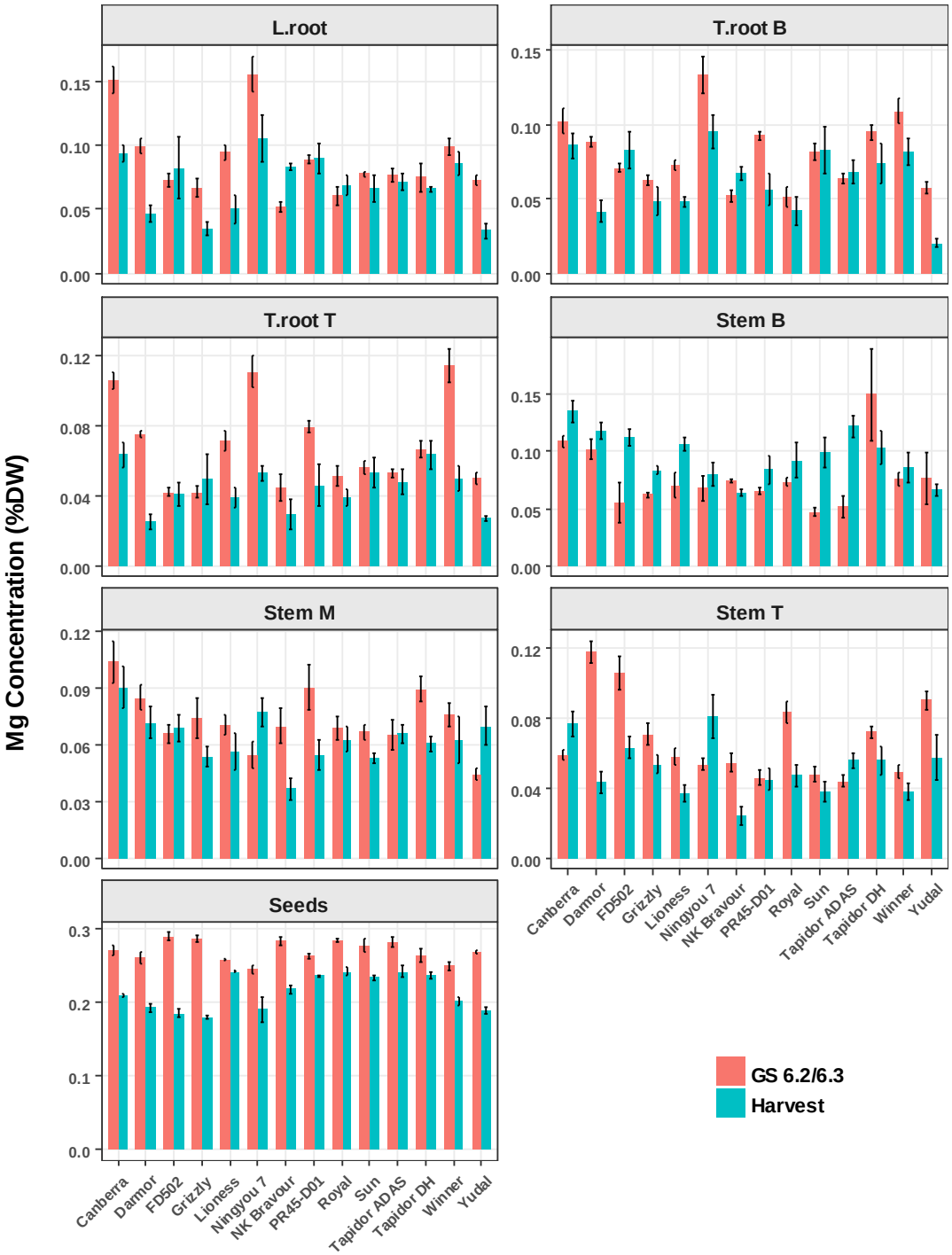

Appendix 9

Figure 2, S concentration across seven tissues between two growth stages (GS 6.2/6.3 and harvest) among 14 *Brassica napus* genotypes. Data are genotype mean ± SEM (n=3 and n=5 at GS 6.2/6.3 and harvest, respectively).

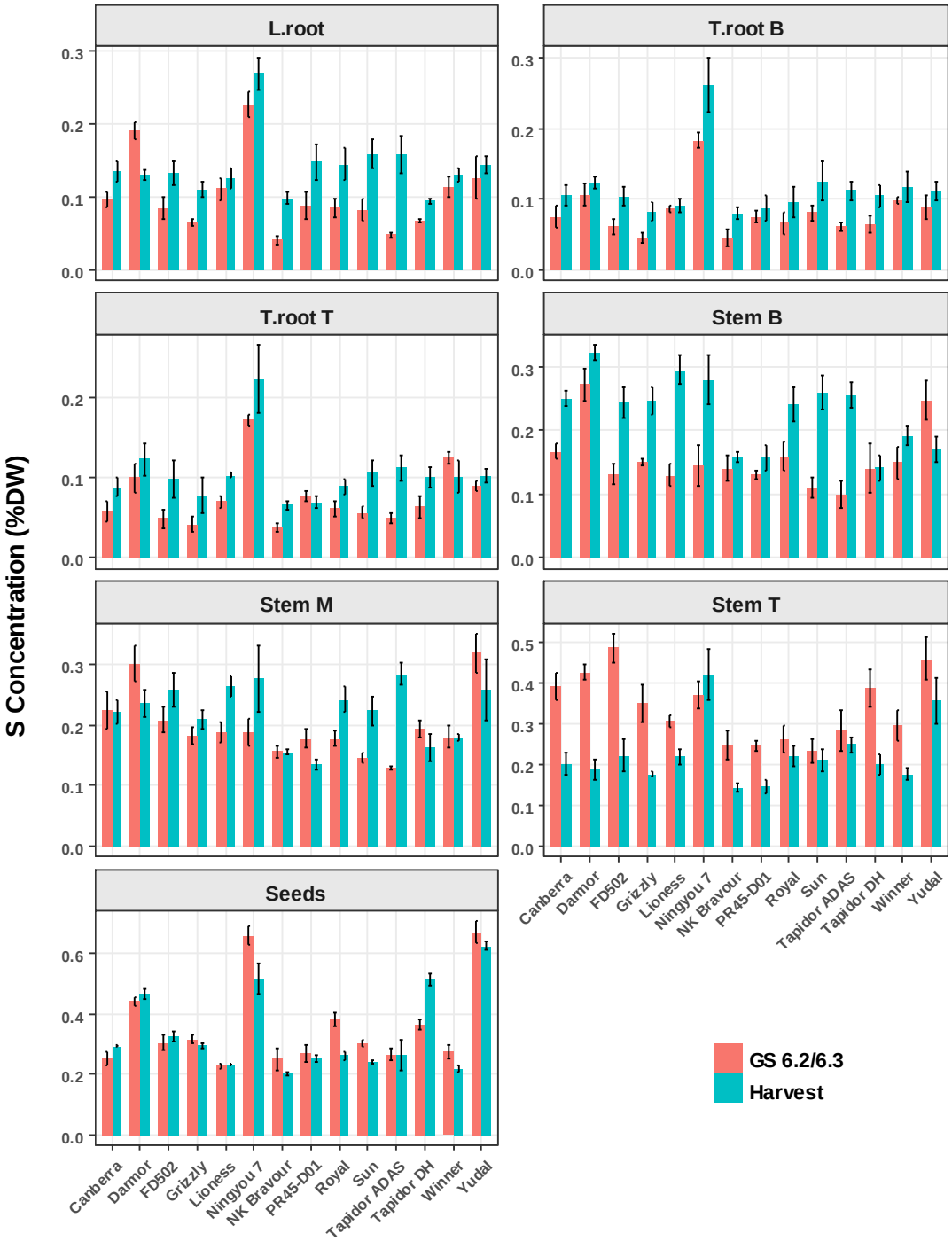

Appendix 9

Figure 3, Na concentration across seven tissues between two growth stages (GS 6.2/6.3 and harvest) among 14 *Brassica napus* genotypes. Data are genotype mean ± SEM (n=3 and n=5 at GS 6.2/6.3 and harvest, respectively).

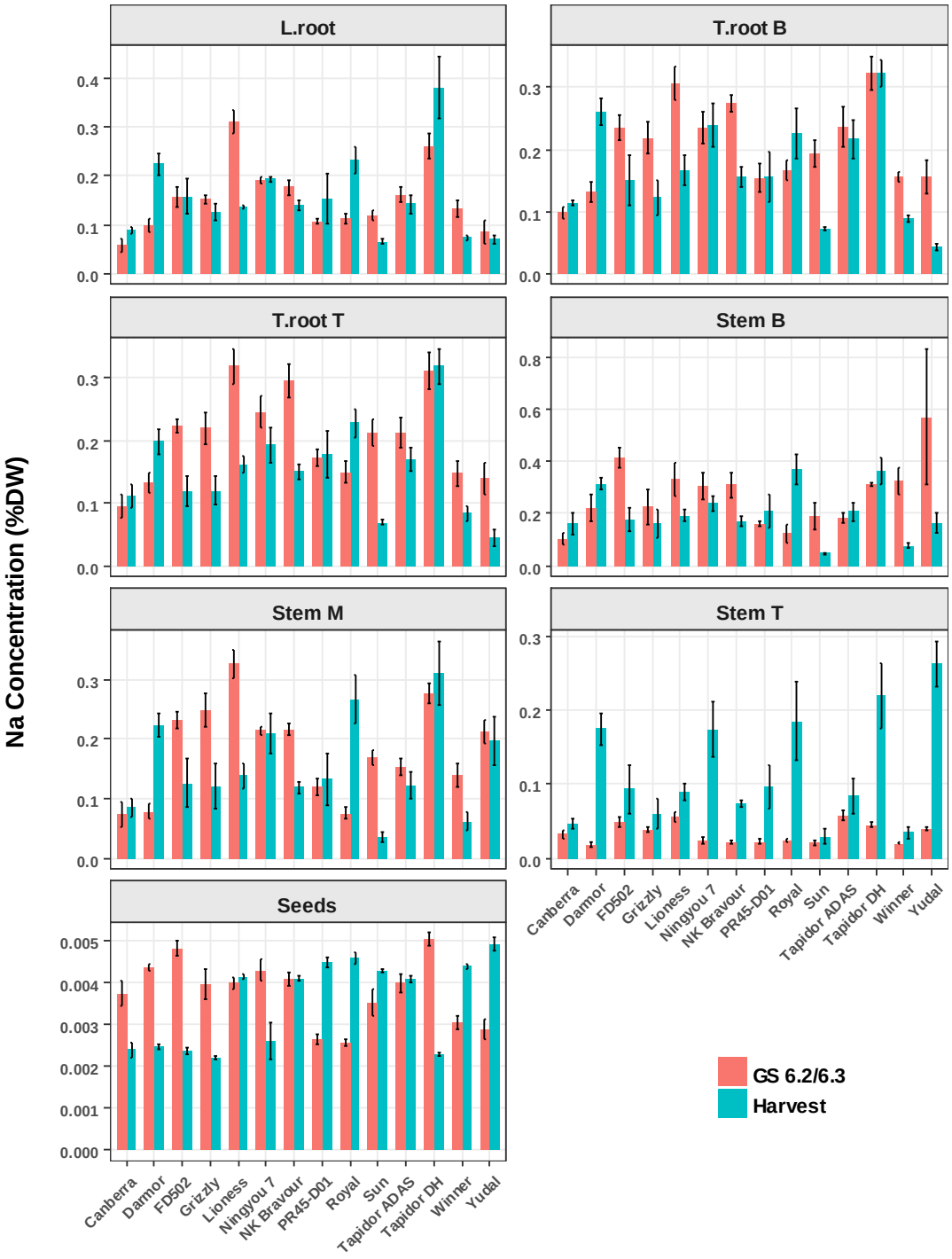

Appendix 9

Figure 4, Cu concentration across seven tissues between two growth stages (GS 6.2/6.3 and harvest) among 14 *Brassica napus* genotypes. Data are genotype mean ± SEM (n=3 and n=5 at GS 6.2/6.3 and harvest, respectively).

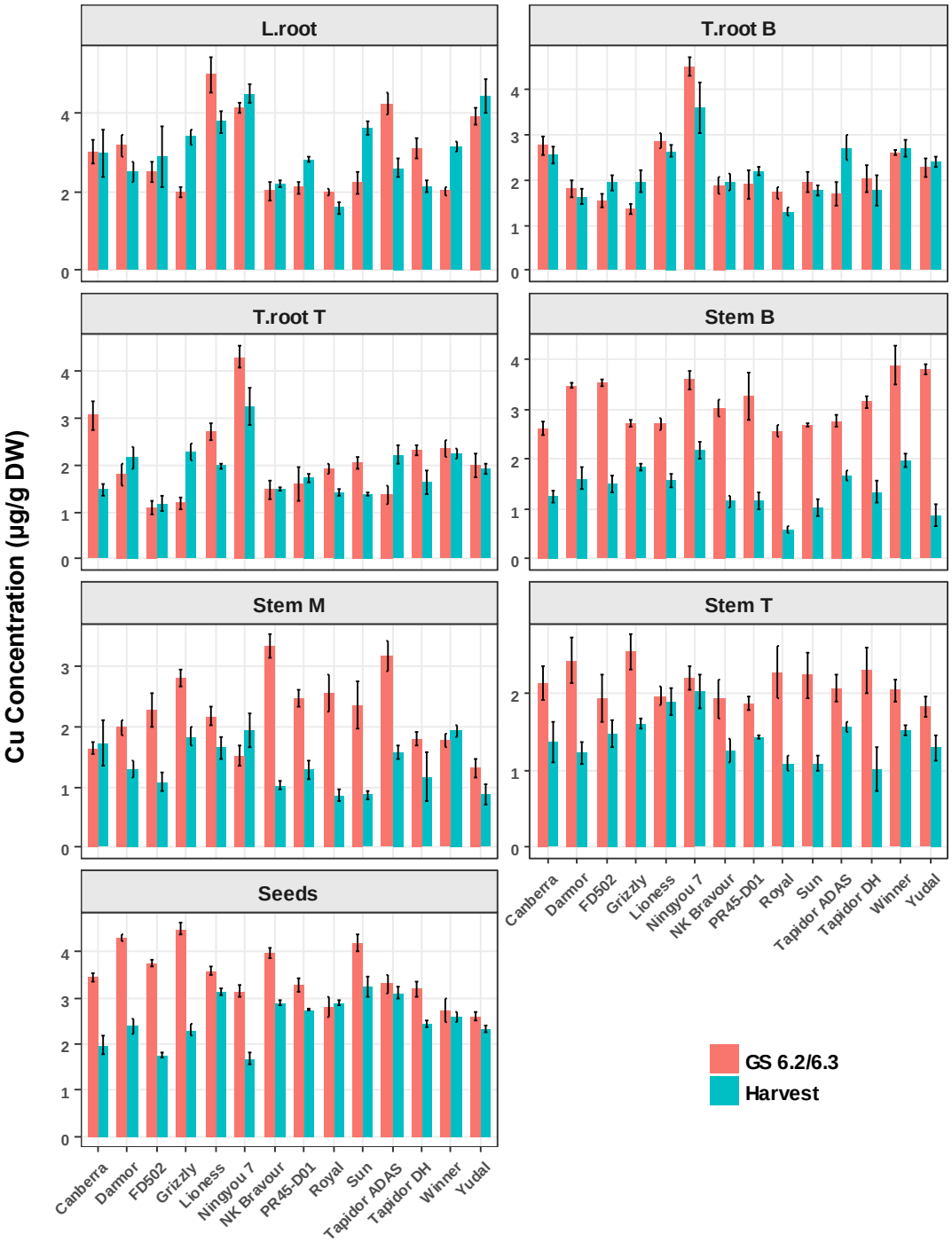

Appendix 9

Figure 5, Fe concentration across seven tissues between two growth stages (GS 6.2/6.3 and harvest) among 14 *Brassica napus* genotypes. Data are genotype mean ± SEM (n=3 and n=5 at GS 6.2/6.3 and harvest, respectively).

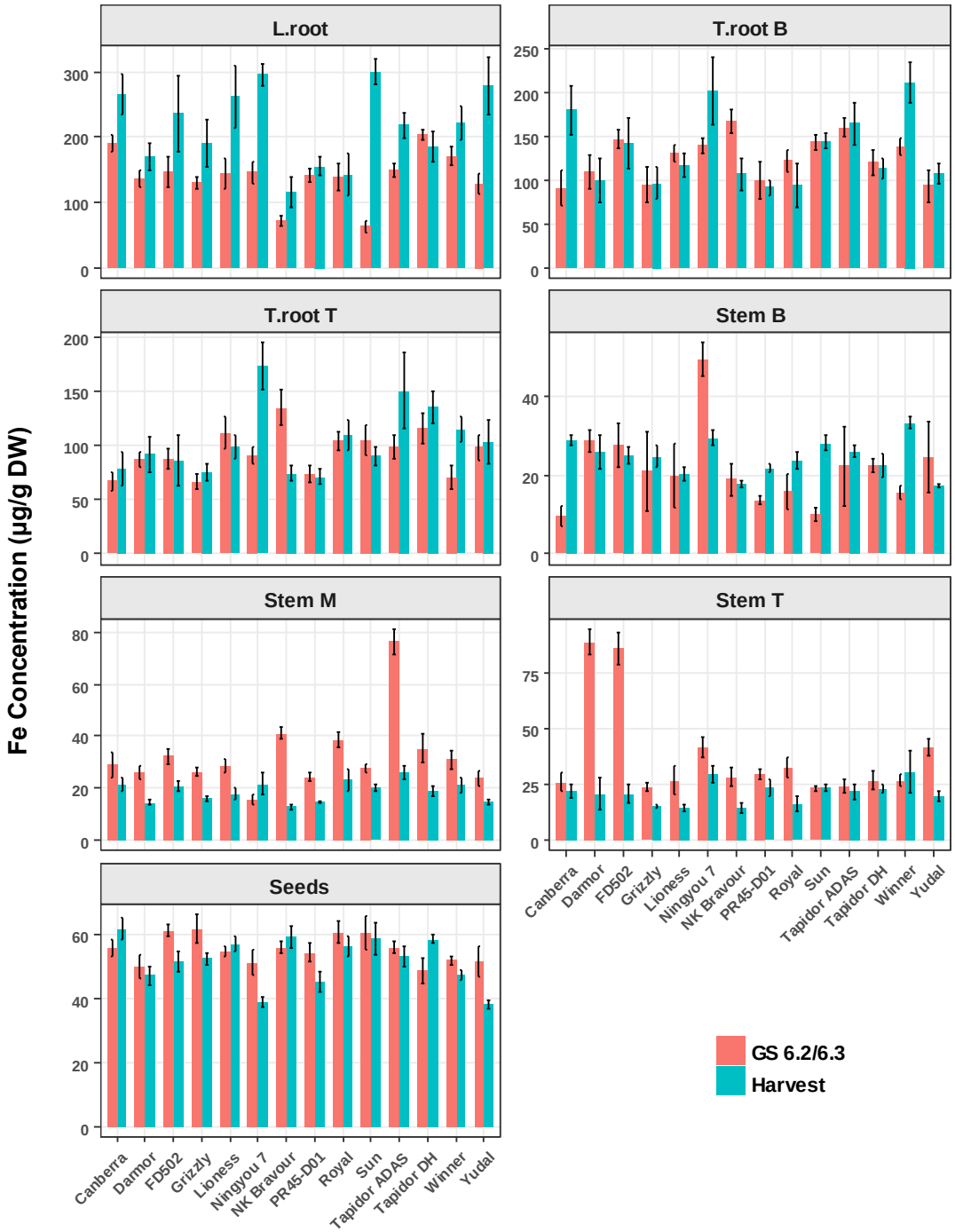

Appendix 9

Figure 6, Zn concentration across seven tissues between two growth stages (GS 6.2/6.3 and harvest) among 14 *Brassica napus* genotypes. Data are genotype mean ± SEM (n=3 and n=5 at GS 6.2/6.3 and harvest, respectively).